WOOD STRUCTURE AND COATINGS
AN ELECTRON MICROSCOPE STUDY OF
Dacrydium cupressinum,
Podocarpus dacrydioides and *Pinus radiata*
WEATHERBOARD SUBSTRATES.

A thesis

submitted in the fulfilment of

the requirements for the Degree

of

Doctor of Philosophy in Botany

in the

Department of Plant & Microbial Sciences

University of Canterbury, New Zealand

by

TINA MARIA MIDDLETON B.A; B.Sc; M.Sc (First Class Honours).

University of Canterbury

1990

TABLE OF CONTENTS

CHAPTER 5

PAGE

DETAILED STUDY OF TiO_2 TAGGED WATTYL ESTAPOL ON TRANSVERSE, TANGENTIAL AND RADIAL SECTIONS OF *D. cupressinum*, *P. dacrydioides* AND *P. radiata* WEATHERBOARDS.

CHAPTER 6

A STUDY OF WEATHERED COATING/SUBSTRATES

CHAPTER 7

LIST OF FIGURES

LIST OF TABLES

LIST OF APPENDICES

ABSTRACT

A scanning electron and transmission electron microscope study of wood substrate anatomy and ultrastructure, involving over one thousand micrographs, was made on weatherboards of two endemic timbers of New Zealand and one exotic timber, to determine their response to eight different coating systems currently recommended for exterior use.

Dacrydium cupressinum Lamb. (rimu), *Podocarpus dacrydioides* A. Rich. (kahikatea) and *Pinus radiata* D.Don. (radiata pine) were the taxa chosen and three water based primer systems, four solvent based primer systems and a specially formulated TiO_2 tagged alkyd novel coating system were used to demonstrate wood/coating relationships.

The key elements present in the coatings were detected by energy dispersive X-ray analysis and used for tracing coating penetration in the weatherboards.

The primer coated weatherboards were studied in transverse section. Penetration limit of the seven primers was three cells deep.

TiO_2 tagged alkyd coated weatherboards were also examined longitudinally as they exhibited much deeper substrate penetration than the primers. The essence of this thesis is therefore the behaviour of this substrate coating system.

The entire cross-sectional length of each weatherboard was photographed under the microscope and quantitative information on the diverse nature of the coating was obtained by counting the number of filled cells along rows of tracheids inwards from the coating interface, measuring the slope of the tracheid lengths relative to the board surface, determining the influence of the tracheid cell growth directions and cut of board as seen in profile view. Statistical analyses showed that with reference to combination comparisons of the two types of mounted weatherboard profiles, namely, 'u'-type and 'n'-type cuts, the mean gross coating penetration depth was significantly different among the three taxa. The maximum gross coating penetration limit recorded along the top surface for *D. cupressinum* 'u' and 'n'-type boards is nine cells; and for *P. dacrydioides* it is six cells in 'u'-type and thirteen cells in 'n'-type boards. Coating penetration appears shallower for *P. radiata*, with the maximum depth being eight cells for 'u'-type and four cells for 'n'-type boards. Extreme maximum penetration occurred along the sides of coated weatherboards. The mean angle made by the tracheid cell length and the substrate face is greater in 'u'-type boards than 'n'-type boards.

The performance of the TiO_2 tagged alkyd coating and the wood substrates were tested using accelerated weathering techniques involving the Xenon-arc Weather-Ometer. Coated and uncoated boards were weathered for one thousand, two thousand and three thousand hours. Coating durability and substrate behaviour were qualitatively assessed microscopically. Spectrocolorimetric and spectroscopic techniques including the L *a* b* and chromaticity colour systems, fourier transform infrared and attenuated total reflectance methods were used to obtain supplementary quantitative information.

Theories on observed coating/substrate behaviour are discussed.

ABBREVIATIONS AND SYMBOLS USED IN THE ILLUSTRATIVE MICROGRAPHS

A - aspirated pit
ap - axial parenchyma
Br - Biseriate Ray
bp - bordered pit
bpp - bordered pit pair
BSEI - Backscattered Electron Image
cc - cell corner
ccml - cell corner middle lamella
cpp - crossfield pitting
ch - checks
cml - compound middle lamella
cp - cupressoid pitting
ec - epithelial cell
EDXA - Energy Dispersive X-ray Analysis
EDAX - Energy Dispersive Analysis of X-rays (see above)
el - empty lumen
Ew - Earlywood
ew - end wall
f - fibrils
FS - Flat Sawn
FT - Fibre Tracheid
GR - Growth Ring
gRB - growth Ring Boundary
hbp - half-bordered pit pair
Hw - Heartwood
(i+P) - intercellular layer + Primary wall
IS - Intercellular Space
ICC - Intercellular layer of Cell Corner
IPA - Inner pit Aperture
L - Lumen / cell lumen
LM - Light Micrograph
Lw - Latewood
m - margo
mc - microscopic checks
mf - microfibrils
ml - middle lamella (e)
/um - micron
nm - nanometer
OPA - Outer Pit Aperture
P - Primary wall
p+i - Primary wall + intercellular layer
p - pit
pb - pit border
pc - pit cavity
pca - pit canel
pch - pit chamber

pf - pit field
pm - pit membrane
pp - pit pair
QS - Quarter Sawn
R - Ray
Rc - Resin canal
Rd - Resin duct
RLF - Radial Longitudinal Face
RLS - Radial Longitudinal Section
Rp - Ray parenchyma
RT - Ray Tracheid
S_1 - outer layer of the secondary wall
S_2 - middle layer of the secondary wall
S_3 - inner most layer of the secondary wall
s.b. - solvent based
SEI - Secondary Electron Image
SEM - Scanning Electron Image
sp - simple pit
spp - simple pit pair
sT - strand Tracheid
STEM - Scanning Transmission Electron Microscope
Sw - Sapwood
2yw - secondary wall
T - Tracheid
t - torus
Ti - Titanium dioxide (rutile form)
TE - Tracheary Elements
TEM - Transmission Electron Microscope
TF - Transverse Face
TLF - Tangential Longitudinal Face
TLS - Tangentail Longitudinal Section
TS - Transverse Section
UC - Uncoated wood
uRc - upright Ray cell
UR - Uniseriate Ray
W - Wart
w.b. - water base
Wl - Warty layer

\+ - coating filled area

* - coating devoid area

CHAPTER 1

Introduction

"...Aegyptii sex milibus annorum aput ipsos inventam, priusquam in Graeciam transiret,..."
...(The Egyptians declare that 'painting' was invented among themselves six thousand years ago before it passed over into Greece...)

"...quibusdam pulpa sine venis mero stamine et tenui constat; haec maxime fissilia..."
...(some timbers have fibre without veins, consisting of thin filaments merely, these are easiest to split.")

"...Apud nos materiae finduntur aliquae sponte; ob id architecti eas fimo inlitas siccari iubent ut adflatus non noceant..."
...(We have in our country [Rome] some timbers liable to split of their own accord, and architects consequently recommend that they should be smeared with dung and then dried, so as to make them proof against the action of the atmosphere.)

.....[Pliny, first century A.D.]

Pliny's works are one of our earliest written evidence that wood was not only painted for decorative purposes but that the architects recognised the need for surface protection of timber.

For centuries it has been known that wood is a naturally durable material and yet it is one of the most variable of substrates. Within a single board major variations in density are apparent. Worldwide each country has its own history of the use of timber; influenced by the distribution and availability of timber species.

"...scandula e robore aptissima,...facillima ex omnibus quae resinam ferunt,...e pino..."
...(the most suitable roof shingles [in Rome] are got from the hard oak...those most easily obtained are cut from all the trees that produce resin,...the pine...)

.....[Pliny, ibid]

Cladding (weatherboards), as defined by the Timber Development Association of Australia (1968), is the outer covering of the external walls of a framed building. Weatherboards produced in New Zealand prior to 1940 were from native gymnosperms. Since then there has been a shift to the use of exotic softwoods in particular radiata pine timber because it had been used successfully overseas. Angiosperms (hardwoods) are not commonly used in New Zealand on the exteriors of structures and hence are not dealt with in this study.

The traditional use of wood has been affected by the innovation of man-made substitutes for building material but many homeowners still prefer to replace old weatherboards with new ones. Since the 1960's the timber industry of New Zealand (Kerr, 1965) was urged to produce and market a product that would be maintenance free for at least 10-20 years. Not only did the development of wood substitutes affect the timber industry but it in turn put pressure on the paint industry to manufacture new improved coatings. Reconstituted wood products are used in many exterior situations in the building industry today but the use of natural timber is by no means obsolete.

The topic of wood structure and coatings has been approached by various scientists particularly in the paint chemistry, physics and engineering fields but a greater understanding was required and this is where the wood anatomists view point was deemed necessary. Côté (1983) wrote "...In spite of its obvious importance as a substrate for coatings, wood as a material is not well understood. Yet, if more effective coating systems are to be produced for use on wood, it is essential that its unique properties be considered..."

1.1 AIMS OF INVESTIGATION

Dacrydium cupressinum Lamb. (rimu), and *Podocarpus dacrydioides* A.Rich. (kahikatea), both native New Zealand timbers; and *Pinus radiata* D.Don. (radiata pine) an exotic species, are the three most readily available species from timber merchants in the South Island. Hence, these three species were chosen to form the basis of the study of substrate/coating relationships.

Some questions that are currently being asked are:-

...to what degree is depth of interfacial zone-penetration a critical factor in the durability of wood-coating systems?

and

...will a coating that assumes the final form of a film anchored into the fine structure of a cell wall either directly or through an intermediate layer (rather than resting on the surface or interlocked one to two cells deep) be a means of securing long term performance or will it pose a whole new range of technical problems?

There are 2 types of wood/coating interactions:

GROSS PENETRATION - where the coating fills the cell lumens

and

CELL WALL PENETRATION - where the components of the coating fill the inter-microfibrillar areas of the cell walls and possibly the amorphous regions within the cellulose microfibrals.

If the film composition remains constant throughout the entire level of penetration into the wood then its performance at any point is dependent on its formulation.

If a preferential migration of certain components of the coating exists to a specific part of the film or the wood substrate then the dependence of the original coating to performance is limited.

This thesis is presented in three parts.

PART (A)

This section is devoted to a survey of the relationship of eight coating systems on the three softwood taxa. Seven of the coatings are either water or solvent based primers, all available on the New Zealand market and the eighth coating is an alkyd marketed as a exterior clear coating but for the purpose of this study is TiO_2 tagged.

Primers were chosen for study because they are the coating system in immediate contact with the substrate.

The coatings studied are:-

Dulux primercryl 100% acrylic
Epiglass water based wood primer
Taubmans premium fast coat wood primer
Dulux wunderprime
Epiglass 1st coat wood primer
Epiglass G.P.182 oil based alkyd primer
Taubmans wood primer

The first three primers are water based, the latter four are solvent based. The remainder coating is TiO_2 tagged Wattyl Estapol alkyd.

The objective of this investigation was to determine microscopically whether coating penetration differs among taxa and which coating system exhibits the greatest penetration.

This preliminary examination was made on transverse sections of the weatherboards only. Because the longitudinal face of the boards were coated the degree of penetration in terms of cell rows is best viewed on the transverse face.

The other two parts of this thesis evolved from a detailed study of the coating which showed the greatest penetration, namely the TiO_2 tagged Wattyl Estapol.

PART (B)

This section contains a detailed study of the TiO_2 tagged Wattyl Estapol on flat and quarter sawn *Dacrydium cupressinum*, *Pinus radiata* and *Podocarpus dacrydioides* weatherboards viewed microscopically on the transverse, tangential and radial sections. The aims were to detect the presence of the coating in the wood qualitatively using X-ray techniques. To determine the extent of penetration in terms of cells deep and whether it was intercellular or intracellular. To investigate the role of board "mounting" presentation, gross wood morphology, specific wood anatomy and wood ultrastructure in the coating/substrate relationship. All quantitative statistical analyses are accompanied by an interpretation of the results in each section.

PART (C)

This section is concerned with evaluating the effect of accelerated weathering on uncoated weatherboards representing the three taxa and on coating performance. In order to assess the durability of the TiO_2 tagged Wattyl Estapol and the influence of wood structure on coating behaviour the coating was weathered for a determined period of time and the wood substrate underneath compared with unweathered and weathered uncoated boards. Analytical methods including spectrocolorimetry and spectroscopy were used to supplement microscopic interpretation of the results.

1.2 COATING CLASSIFICATIONS.

The bewildering variety of products available today has resulted in very complex coating classifications. Coatings have been classified various ways.

There are two main types of coatings:-

(1) CONVERTIBLE COATINGS.

(2) NON-CONVERTIBLE COATINGS.

Unlike a non-convertible coating, a convertible coating cannot be redissolved in the solvent from which it was originally deposited (OCCA, 1966). Convertible coatings can be classified into types based on film formation and curing mechanisms; for example, oxidation reaction between two film components, polymerization by heat, or polymerization by irradiation.

Another type of classification is based on the order of application; that is, **PRIMERS, UNDERCOATS** and **FINISHES/TOP COATS.**

The TiO_2 tagged Wattyl Estapol is marketed as a clear finish. Traditionally, the term **FINISH** refers to the final coat in a painting system but sometimes it refers to the entire coating system including properties affecting appearance.

Banov (1978) classified coatings into three main types:-

(i) **PAINTS**, (ii) **VARNISHES** and (iii) **LACQUERS.**

The modern coating formulator tends to refer to systems rather than to products. The Timber Development Association of Australia (1968) classified paints into two categories : **WATER THINNED** and **SOLVENT THINNED SYSTEMS.**

In **WATER THINNED** paints a continuous film is formed when the solid dispersed resin binders are freed of water by evaporation.

The thinner or **SOLVENT** can be classified into three types:

(i) **TRUE** or **ACTIVE SOLVENTS**, such as the lower alcohols, ketones and ethers.

(ii) **LATENT** or **CO-SOLVENTS** such as isopropanol, n-butanol and secondary butanol.

(iii) **DILUENTS** which are added for the purpose of increasing the solvent power of the solvent mixture for other solids present; for example, the aromatic and alophatic hydrocarbons.

1.3 COATING TERMINOLOGY

The O.C.C.A. (1984) defines **PAINT** as "...a pigmented liquid composition which is converted to a relatively opaque film after application as a thin layer..."

A **FILM FORMER** is a polymeric organic compound which when applied to its intended substrate forms a continuous film.

PIGMENTS are the fine solid particles insoluble in the vehicle. The liquid portion of the paint including the film former and volatile solvent is termed the **VEHICLE**.

The **BINDER** or film former is the "...non-volatile portion of the coating vehicle which is in the film forming ingredient used to bind the pigment particles..." (O.C.C.A. 1984) and enables the film to adhere to the substrate.

ALKYDS are excellent binders due to their ability to "wet" and disperse pigments.
Alkyds are classified as:

(i) Long-oil

(ii) Medium-oil

(iii) Short-oil

The oil length is the oil to resin ratio present. Long oil alkyds have a greater ratio of oil to resin and a high percentage of fatty acids. An increase in oil length causes an increase in film flexibility. Long and medium oil length alkyds are solu ble in both aliphatic and aromatic hydrocarbons and turpentine (OCCA, 1969). For example, the length in the TiO_2 tagged Wattyl Estapol alkyd is approximately 65% , therefore it is classified as a long oil alkyd.

PAINTS consist of **PIGMENT, BINDER, THINNER** and a range of **ADDITIVES** which may include anti-microbials, anti-foaming agents, anti-freeze, coalescing agents, driers, anti-skinning agents, anti-gelling agents, freeze-thaw stabilizers, pigment suspension aids, pigment wetting aids, thixotropic agents, viscosity control agents and preservatives.

PAINT DRIERS are the most important group of paint additives. O.C.C.A. (1984) defines DRIER as "...a material that promotes or accelerates the drying, curing or hardening of oxidizable coating vehicles..."

The metal soaps of a monocarboxylic acid dissolved in a hydrocarbon solvent and standardized to an acceptable metal content are the main types of material used. Cobalt and manganese are more active driers than lead soaps. Zirconium in the form of zirconyl soap is also used.

1.4 PRIMERS

A primer is the first coat of paint applied to timber. The main aim of priming seasoned timber is to protect it from weathering during storage. In order to move sympathetically with the timber substrate primers need a degree of hydroplasticity. Primers are not intended to act as fillers. Primers prevent oils and resins being sucked out of subsequent coats of paint. The pigment volume concentration (P.V.C.) of a primer is between 30-45% (O.C.C.A. 1974); that is 55-70% by volume of the dry coating is binder. This should be sufficient to form a flat surface which will not affect the wetting ability of subsequent coats, nor cause adhesion problems and is still porous enough to permit moisture-vapour transmission.

1.5 PIGMENTS

The function of pigment in a coating is to hide the substrate, to decorate and enhance it. Hiding pigments are capable of altering transparency or translucency. Rutile -titanium dioxide, anatase-titanium dioxide, zinc sulphide, lithopone, zinc oxide, aqueous calcium molybdate, antimony oxide, oil based calcium molybdate, basic carbonate white lead and basic silicate white lead are some of the white pigments that have been used in the paint industry for hiding purposes.

Titanium dioxide became sought after as a white pigment in the 1930's as it is resistant to heat and the media and solvents associated with paint manufacture. It is predominantly chemically stable. There are two structural forms of titanium dioxide, both of which are used in the paint industry. Rutile-titanium dioxide has increased in importance at the expense of anatase-titanium dioxide because of its non-chalking and better hiding power as well as for economic reasons. The rutile form, with mean particle size 0.2-0.3μm and refractive index 2.71, is used in undercoats and in emulsion paints. By comparison, the anatase form with a smaller mean particle size range of 0.18-0.23μm and lower R.I (2.55) is used for finishes.

EXTENDER PIGMENTS form another group of pigments. They are defined as "...generally colourless, transparent pigments used either to lower the cost of a coating or impart a special property to it..." (O.C.C.A.,1974). Extender pigments provide bulk and body to the surface coating. They can be grouped into four classes: (i) silicates, (ii) calcium sulphate, (iii) calcium carbonate and (iv) barium sulphate.

1.6 WEATHERBOARDS.

There are two main types of horizontal weatherboarding lying flat against the studs without sheathing underneath that are used in New Zealand:
(a) **BEVEL-BACK WEATHERBOARDING** and (b) **RUSTICATED WEATHERBOARDS.**

VERTICAL BOARDING is also used in exterior situations; these include **SQUARE EDGED** boards with covering battens, **TONGUED-and- GROVED** boards and **SHIP LAP** patterned boards.

Weatherboards may be **FLAT SAWN** or **QUARTER SAWN.** When timber is sawn so that the annual growth rings as viewed on the end section of a piece of weatherboard, form an angle of less than 30^{O} with the board face it is called **FLAT SAWN (SLASH GRAIN** or **PLAIN SAWN)** wood. **QUARTER SAWN** refers to timber that is sawn so that the annual growth rings form an angle of more than 60^{O} with the board face. Quarter sawn timber exhibits edge grain.

Weatherboards can be mounted two different ways; either with the pith side exposed (referred in this study as 'u'-type growth ring patterned boards) or with the outer sapwood [bark] side exposed (referred in this study as 'n'-type growth ring patterned boards). The latter is considered the correct mounting, however the weatherboards sold in New Zealand exhibit random mounting due to economic reasons with regard to timber use.

Good quality, dressed, preservative treated, new, bevel-back weatherboards were prepared for coating as outlined in the 1978 New Zealand Paint Manufacturers Association guidelines.

Each unthinned coating type was brush applied to either flat or quarter sawn board surfaces including the arris. The backs and end grains of panels used in the weathering trials were also coated. These panels were not preservative treated.

CHAPTER 2

Methods

2.1 BULK ANALYSIS OF PAINT/COATING AND BULK ANALYSIS OF WEATHERBOARD BLOCKS USING THE CAMBRIDGE STEREOSCAN MARK 250 SCANNING ELECTRON MICROSCOPE AND ENERGY DISPERSIVE X-RAY ANALYSIS (EDXA) TECHNIQUES.

Fresh paint/coating was applied to graphite blocks which were mounted onto aluminium stubs with carbon conductive paint and coated with a thin conductive layer of carbon by vacuum deposition. In the case of weatherboard bulk analysis, blocks of wood were mounted onto graphite blocks and carbon coated as described above.

The Cambridge Stereoscan mark 250 was fitted with an EDAX SW 9100/40 system and Dec PDP 11 computer with software supplied by EDAX.

Specimen magnification has no effect on the analysis since all magnification occurs after the specimen has been irradiated, however a magnification of 100 times was chosen for convenience for all bulk analyses.

Once the specimen region for analysis was chosen the electron beam was focused onto the region and the detector set to collect the emitted X-rays. In bulk specimens the electrons are totally stopped by the sample and none of the incident electrons can reach the far surface. Dead time is the period when an X-ray is being received by the detector and it is 'dead' to other incoming X-ray photons. To compensate for this loss analyses are performed in the 'live-time' mode. Spot size was adjusted to give a count rate of 3000-3500 counts per second. The energy range was set between 1-20 keV. Each analysis was performed during 60 live seconds.

Analytical data were expressed as the intensity (CPS), background (CPS) and as peak height to background (P/B) ratios. The elements were corrected for atomic number (Z), absorption (A), and fluorescence (F) effects. K refers to the standard constant. The ZAF corrections were performed by computer methods within the analyser itself. P/B ratios were not converted into weight percent. Note the 'bremsstrahlung', 'continuum' or 'white radiation' forms the majority of the X-ray background upon which characteristic lines are superimposed.

2.2 BULK ANALYSIS OF PAINT/COATING USING THE JEOL SCANNING ELECTRON MICROSCOPE AND LINK EDXA TECHNIQUES.

Elements lighter than atomic number 10 are unable to be detected with this system. Fresh paint/coating was applied to carbon blocks which were mounted onto aluminium stubs with carbon conductive paint and carbon coated to provide electrical conductivity without introducing extraneous X-ray peaks.

The JEOL JSM-35 S.E.M. fitted with a LINK 290 Energy Dispersive X-ray Analyser (EDXA) was operated with an accelerating voltage of 15 kV and a beam current of the order of 0.5×10^{-9} Amps to give a count rate of the order of 1500 counts per sec. The specimen tilting angle of 0^{o} and the take off angle of the detector of 35^{o} were held constant throughout. The S.E.M. was operated at 15 KeV to allow for +ve identification of certain possible overlapping k and l characteristic lines.

2.3 CONSTRUCTION OF THE GRAPHITE ROD SPECIMEN HOLDER.

A pure graphite rod was cut into a 1 cm length and a tiny hole drilled in the centre of the rod using a twist drill (SKF) size 80; 0.0135 ins diameter. The depth of the hole was approximately ten times the diameter. The carbon block was placed hole uppermost onto an aluminium stub and mounted with carbon conductive paint. The carbon block was examined using S.E.M./ E.D.X.A. The focused beam was positioned in the centre of the hole to check that the X-rays were undetectable indicating that the hole was deep enough.

2.4 PREPARATION OF WOOD FOR SCANNING ELECTRON MICROSCOPY (SECONDARY ELECTRON AND BACKSCATTERED ELECTRON IMAGES).

Small blocks of 'painted' dry weatherboard were cut into cubes and the desired area selected for trimming. The cubes were clamped in a vice and screwed into position on a Reichert stereomicroscope. The transverse face was shaved smooth with a sharp razor blade taking care not to disturb the coated side. The trimmed block was then cut diagonally so as to produce two 45^{o} faces as described by Exley *et al* (1973,1977). The specimens were mounted onto metal stubs. Conductive carbon paint was smeared onto the stubs. The specimens were carbon coated on an Edwards High Vacuum coater and examined under the Cambridge Stereoscan 250 mark 2 in conjunction with the Robinson backscatter detector.

The backscatter detector provides atomic number contrast, thus elements of high atomic number emit more backscattered electrons than those of lower atomic number. Because the coating is a region of higher mean atomic number than the wood it appears brighter.

2.5 PREPARATION OF THIN SECTIONS FOR LIGHT MICROSCOPY.

Small sample blocks of wood were sawn out of the coated weatherboards. The blocks were then cut into match stick sized pieces and the transverse section of the wood carefully trimmed with a sharp razor blade into a short column of cells, taking care that the coated side remained intact. The unembedded wood was then sectioned in the transverse plane using an LKB 2128 Ultrotome IV (Bromma Ultramicrotome system). 1 µm thin sections were cut using glass knives. The knife cutting angle was set at 5^{o}. Sections were floated off onto the knife and then transferred to ethanol cleaned microscope slides and heat fixed to the slide, stained with Toluidine Blue and mounted in Depex. Toluidine Blue stains unlignified cells purple and lignified cells blue-green. The sections were photographed with the Leitz Wetzlar orthoplan microscope.

2.6 L.R.WHITE EMBEDDING TECHNIQUE

Coated wood samples were cut into small pieces with a sharp razor blade taking care to cut the transverse sections as required ready for orientation for embedding. The air dried specimens were dehydrated in two changes of 100% ethanol (absolute ethanol 1 hr each at room temperature) before infiltrating with 100% London resin (L.R.White - medium grade). The low viscosity of London resin enables short infiltration times depending on the tissue size; when infiltrated the tissue turns translucent and sinks to the bottom of the vial. The specimens were subsequently embedded

in London resin using plastic embedding moulds which were sealed, as oxygen inhibits polymerization. The resin was thermal cured at 70^{oc} for a minimum of 24 hours. Some specimens were polymerized in a nitrogen environment. Embedding moulds containing specimens in L.R.White were transferred to a bell jar which was filled with nitrogen. The bell jar was placed in the oven and left for 24 hours at 70^{oc}.

2.7 SPURR'S RESIN EMBEDDING TECHNIQUE

Coated wood samples were cut into small pieces with a sharp razor blade taking care to cut the transverse sections as required ready for orientation for embedding. The air dried specimens were then oven dried. Several methods of embedding were tried in order to determine the best technique for coated wood. The procedures were as follows:-

PROCEDURE A.

Specimens were dehydrated in 100% ethanol and evacuated for 10 minutes, then embedded in 100% Spurr's resin and polymerised overnight at 70^{oc}.

PROCEDURE B.

Specimens were dehydrated in 100% ethanol and evacuated for 10 minutes then infiltrated in 50/50 ethanol/Spurr's for 10 minutes prior to embedding in 100% Spurr's and polymerized overnight at 70^{oc}.

PROCEDURE C.

Oven dried specimens (1 hr at 70^{oc}) were embedded directly in 100% Spurr's and polymerised overnight at 70^{oc}.

This last method proved most successful and was the quickest to perform.

2.8 PREPARATION OF ULTRA-THIN SECTIONS FROM SPURR'S EMBEDDED BLOCKS FOR TRANSMISSION ELECTRONMICROSCOPY.

Spurr's embedded specimens were glued onto already prepared capsules made of the embedding medium. The capsule was secured on a chuck on an LKB Pyramitome and the surface of the block manually trimmed using glass knives. Survey sections were cut prior to ultra-thin sectioning. The block was then trimmed into a trapezium using a sharp razor blade. The block was further trimmed on the Pyramitome using glass knives. The corner of the knife was positioned to shave a few μm off the edge of the block. The specimen block was then rotated through 90^{o} and the next side trimmed. All four sides were trimmed in a similar manner to produce a "mesa".

Some of the mesas were sectioned on the LKB Ultrotome Type 4801 A in conjunction with control unit 4802 A. Ultra-thin sections 80 nm thick were cut using glass knives and floated out onto distilled water. The distilled water was contained in a trough made from adhesive vinyl tape wrapped around the knife from one side to the other. A syringe with hypodermic needle was used for maintaining the correct height of the water in the trough. Filter paper soaked in chloroform was held above the sections to induce unrolling. The ribbons of cut sections were picked up on formvar coated grids by gripping the edge of the grid with forceps and lowering the coated side of the grid down onto the trough containing the floating sections. 100 mesh copper grids were used. The sections were placed face up onto filter paper lining labelled petri dishes.

Some Spurr's embedded specimens were cut with a diamond knife on the LKB 2128 Ultrotome IV (Bromma ultramicrotome system). The diamond knife cutting angle was set at 3^{O} and 70 nm section thickness was selected. The suitability of various staining techniques for thin sections is discussed by Nunn (1970), Hayat (1975), Reid (1975) and Roland (1978).

2.9 URANYL ACETATE STAINING OF ULTRA-THIN SECTIONS FOR TRANSMISSION ELECTRON MICROSCOPY.

Uranyl acetate UO_2 (CH_3 CO O_2) . 2 H_2O is a useful stain for electron microscopy because uranium has an atomic number of 92 and uranyl ions contain an atom of sufficiently high atomic weight to be effective in scattering electrons. Uranyl acetate produces high contrast and is suitable for high resolution work. Uranyl acetate is very slow to dissolve in water and its solubility increases at higher temperatures and in alcoholic solutions. Research (Lewis & Knight, 1977) has shown that uranyl acetate stain penetrates ultra-thin sections completely. 1% uranyl acetate in 50% ethanol was used.

Using a pipette drops of uranyl acetate were placed onto a marked and labelled sheet of wax parafilm lining a glass petri dish. Each mounted grid was in turn picked up with forceps and placed face down onto a drop of stain and left for 15 minutes at room temperature. The grids were then washed thoroughly in ethanol. Using forceps each grid was immersed into a beaker of ethanol for 5 seconds, blotted dry and then dipped into two changes of distilled water and blotted dry.

2.10 LEAD CITRATE STAINING OF ULTRA-THIN SECTIONS FOR TRANSMISSION ELECTRON MICROSCOPY.

The uranyl acetate stained grids were stained in Sato's lead citrate which was prepared following Hayat's (1975) schedule. Lead has an atomic number of 82 and it is generally agreed that sections stained with lead citrate are penetrated completely.

Glass petri dishes were lined with wax parafilm sheets and prepared in a similar manner as for uranyl acetate staining. Pipetted drops of lead citrate were placed on the wax sheet and each grid was placed face down onto the lead stain. The dish was covered and sections left to stain for 10 minutes. When the staining time had expired each grid was removed in turn and held in forceps and washed in two changes of distilled water and blotted dry. The grids were placed section face up on clean dry filter paper lining a petri dish and labelled.

2.11 EXAMINATION OF ULTRA-THIN URANYL ACETATE-LEAD CITRATE STAINED SPECIMENS USING THE TRANSMISSION ELECTRON MICROSCOPE.

The JEOL 1200 EX T.E.M. was operated with an accelerating voltage of 80 kV; the spot size was set at 2. All photographs were taken on a 35 mm film with the shutter speed set at 0.5 seconds.

2.12 EXAMINATION & MICROANALYSIS OF ULTRA-THIN UNSTAINED SECTIONS USING THE JEOL TRANSMISSION ELECTRON MICROSCOPE IEM 1200/2000 - ASID 10/20 AND ENERGY DISPERSIVE SYSTEM (STEM/EDXA).

Information on the location and distribution of elements in tracheid cell walls can be obtained using ultra-thin sections (< 0.2μm thick) and the transmission electron microscope adjusted to STEM mode (scanning transmission mode). In ultra-thin sections X-ray intensity is reduced in comparison with a bulk specimen. Ultra-thin samples are those in which almost no effects of inelastic electron scattering or X-ray absorption occur although a little energy is imparted to the specimen to produce X-rays. Lateral diffusion of the electron beam is negligible. In ultra-thin sections the improved image resolution and increased contrast and magnification allow placement of the electron beam with greater accuracy.

Ultra-thin unstained sections were analysed. The data collected for a particular analysis of 1 element in a given period of time is related to the total number of atoms of that element in the

specimen region analysed. The TEM was operated at 80 kV. One solution to the problem of extraneous background which occurs when operating at high accelerating voltages in STEM mode was to reduce the uncollimated radiation by using grids with a large mesh size (Ryan et al, 1984). An EM-SR graphite specimen retainer was used with the SM-SCSH common specimen holder. For ultra-thin sections the ZAF correction is much smaller compared with bulk samples. When using ultra-thin sections the production of X-ray signals is very low. For photographic purposes the analysis time was increased in order to accumulate sufficient X-ray counts in a mapping display. This method is purely qualitative. Peak height ratios do not represent elemental ratios for the X-rays generated may be differentially absorbed before reaching the detector.

2.13 MEASUREMENT OF CONTACT ANGLES OF COATINGS ON SUBSTRATES.

Coating contact angle measurements have been used to characterize liquids, solids and substrates. The technique involves placing a drop of coating using either a pipette or pointed rod onto a glass slide and measuring the contact angle.

A schematic diagram and definition of the contact angle interfacial tension between solid, liquid and vapour are discussed by Pierce and Schoff (1988). The only type of surface tension that can be directly measured is the surface tension of the liquid drop/vapour interface. Angle Θ is the contact angle. A drop diameter of 2-4mm is the accepted size for contact angle measurement studies (Pierce and Scoff, 1988).

The angle of contact was measured with the aid of an Olympus light microscope and camera lucida.

2.14 ACCELERATED WEATHERING TESTS ON COATED WEATHERBOARDS.

EXPOSURE APPARATUS-ATLAS XENON ARC WEATHER-O-METER.

Model Ci 65

CONTROLLED IRRADIANCE EXPOSURE SYSTEM

(ASTM-American Society for Testing Materials)

TEST METHOD-ASTM G 26-83.

LIGHT SOURCE-Long arc water cooled xenon lamp rated at

6500 watts, but operated at around 6000 watts.

METHOD USED TO REGULATE WATTAGE TO LAMP-Automatic irradiance.

OPTICAL FILTERS-Borosilicate glass inner and outer filters.

SPECTRAL IRRADIANCE-0.55 W/m^2 at 340 nm when operated at 6000 watts.

RELATIVE HUMIDITY-Controlled through the use of a wet bulb depression circuit.

CONDITIONED WATER-17^{oc}.

AIR TEMPERATURE-34^{oc}.

SPECIMEN SPRAY WATER TYPE-Distilled water. (Maximum flow rate 18 litres per hour).

SPECIMEN SPRAY UNIT-4 nozzles which are in close proximity to the xenon lamp and the light sensor and sprays water on the specimens. (Nozzle type F-80).

SPECIMEN RACK ROTATION DURING EXPOSURE-1 ±0.1 rpm (revolutions per minute).

CYCLE-18 minutes continuous light and spray followed by 102 minutes of light.

WEATHERBOARD ANGLE-Vertical.

2.15 COLOUR SYSTEMS FOR MEASURING THE REFLECTIVE COLOURS OF SURFACES

The Hunter Labscan Spectrocolorimeter and the Minolta Chroma-Meter CR200, tristimulus colour analysers for measuring reflective colours of surfaces, were used to make absolute chromatic measurements on uncoated, coated, unweathered and weathered weatherboards.

Their spectral response closely approximates the Commission Internationale l'Eclairage (CIE) Standard Observer curves ($x_2\bar{}$, $y\bar{}$ and $z\bar{}$).

The following four different colour systems for measuring absolute chromaticity were used:

$L^*a^*b^*$, $L^*C^*H^o$, CIE Yxy

and colorimetric densities Dx Dy Dz.

For two colours to match, the tristimulus values X,Y, and Z (as determined by the CIE (1931)) must be identical. X, Y and Z are the three quantities defining the colours. Colour as perceived has three dimensions: lightness,hue and chroma. The metric lightness factor (L) is included to identify a sample colour precisely because the two chromaticity coordinates (a* b* ie hue and chroma) are unable to describe a colour completely.

The CIE L* a* b* colour system most closely represents the human sensitivity to colour. Equal distances in the CIE L* a* b* system approximately resemble perceived colour differences.

The L* a* b* defining equations are:

$$L^* = 116\left(\frac{Y}{Yo}\right)^{1/3} - 16$$

$$a^* = 500\left(\frac{X}{Xo}\right)^{1/3} - \left(\frac{Y}{Yo}\right)^{1/3}$$

$$b^* = 200\left(\frac{Y}{Yo}\right)^{1/3} - \left(\frac{Z}{Zo}\right)^{1/3}$$

where Xo, Yo and Zo are the tristimulus values of the illuminant used.

In the CIE L*C*H* colour system L* is the metric lightness factor, C* is the metric chroma and Ho is the metric hue angle.

In the CIE Yxy colour system the lightness factor Y is the percentage reflectance while x and y are the chromaticity coordinates.

The defining equations are:

$$x = \frac{X}{X + Y + Z}$$

$$y = \frac{Y}{X + Y + Z}$$

and the tristimulus values X, Y and Z can be calculated from the Y, and x and y values where

$$X = Y\,(x/y),\quad Y = Y,\ \text{and}\ Z = Y\left(\frac{1-x-y}{y}\right)$$

1 All samples were measured on the Hunter Labscan Spectrocolorimeter and three measurements were made on the surface of each sample and the averages obtained. Each measurement was made on a 44mm diameter area.

Colour terms used here are derived from CIE (1970). The illuminant condition chosen was the CIE Standard Illuminant D_{65} (which is intended to represent overcast sky daylight with a component of ultraviolet radiation). The correlated colour temperature of the light source was approximately 6500 kelvin units. The CIE (1964) ten degree standard observer was selected. The Hunter Labscan Spectrocolorimeter uses $0^o/45^o$ geometry i.e. the sample is illuminated along the normal and viewed (detected) at an angle of 45^o from the normal to its surface through a ring of 16 fiber optic receptor stations.

2 The same samples were also measured on the portable Minolta Chroma-Meter CR200. Three measurements were made on the surface of each sample and the averages obtained. Each measurement was made on a 8mm diameter area. The Chroma-Meter CR200 uses diffuse $/0^o$ geometry. The sample was illuminated with diffuse light from all directions and a detector measures the light reflected along the normal to the sample.

2.16 FOURIER TRANSFORM INFRARED (FTIR) TECHNIQUE

In all spectroscopic techniques a polychromatic beam of radiation is acted upon such that each frequency of the radiation is differentiated from all the other frequencies in such a way that the resolution element (intensity of each frequency) can be measured.

An interferogram contains information on the intensity of each frequency in the spectrum; it utilizes a mathematical operation known as the Fourier Transformation. Interferometry is also known as fourier transform spectroscopy. Because the FTIR scans up to 100 microns in depth the surface detail, as detected by the ATR method, may be undetected.

A Biorad Digilab FTS 60 was used to produce FTIR spectra of unweathered and weathered boards coated with TiO_2 tagged Wattyl Estapol. For each sample 1 mg of scraped off coating was chopped into tiny pieces and the sample mixed with 100 mg dry potassium bromide (KBr) powder and ground into a fine powder in a mortar. KBr was used as a matrix because it has no infrared spectrum. The KBr-sample mixture was placed in the nut cell holder portion of a mini pellet press with the bottom bolt screwed in place. The top bolt was subsequently introduced. Pressure was applied by tightening the bolts. The mixture was pressed in vacuo to form the transparent pellet.

2.17 ATTENUATED TOTAL REFLECTANCE (ATR) TECHNIQUE.

(also known as multiple internal reflectance or internal reflection spectroscopy)

In the ATR technique a beam of light that is internally reflected from the surface of a transmitting medium travels a few microns beyond the reflecting boundary and is returned to the transmitting medium as a part of the process of reflection. The ATR method produces a reflection spectrum from the interface of a high refractive index transmitting prism and the sample substrate (i.e. when the absorbing sample which has a lower refractive index than the transmitting medium is brought into contact with the reflecting interface of the prism part of the incident radiation will be absorbed and the total reflection will be attenuated).

A Biorad Digilab FTS 60 was used to produce ATR spectra of unweathered and weathered boards coated with TiO_2 tagged Wattyl Estapol. For each sample two thin 1 cm square shavings of the coating were pressed against both sides of a crystal and clamped between rubber backed aluminium foil. The prism used in ATR was KRS-5 since this crystal has a large depth of penetration and can produce infrared spectra over the entire mid-IR 4000-400 cm^{-1}. The ATR scans up to 5 microns in depth. A 45^{o} crystal geometry was used and the spectra were recorded at 4 cm^{-1} resolution. The abscissa scales are presented as wavenumbers (cm^{-1}).

CHAPTER 3

3.1 GROSS WOOD STRUCTURE

Dacrydium cupressinum and *Podocarpus dacrydioides* are both members of the Podocarpaceae family. *Pinus radiata* belongs to the Pinaceae family and on the basis of its wood anatomy is placed in the Ponderosa group of conifers.

For trees growing in temperate regions the annual growth increment is visible as a series of concentric rings. However, characteristic notable variation in growth ring patterns occur within genera and can be used to distinguish species. Patel (1967) noted from detailed studies of the anatomical features of the secondary xylem of the Podocarpaceae, that *D. cupressinum* differs from the other species of *Dacrydium* in that the growth rings are indistinct microscopically irrespective of the ring width. Orman and Reid (1946) deduced that *D. cupressinum* shows greater anatomical similarity to the *Podocarpus* species than to the *Dacrydium* species. *P. dacrydioides* also has indistinct growth rings. By contrast to the two endemic taxa, *P. radiata* has distinct growth rings.

3.2 WOOD ANATOMY

Tracheids and parenchyma are the major cell types in all three taxa. Axial parenchyma is abundant in *D. cupressinum* and *P. dacrydioides* but sparse in *P. radiata*. The lengths and diameters of stem and root early wood tracheids were measured by Patel (1967, 1970) and Donaldson (1983). They recorded *D. cupressinum* has an average tracheid length of 3.38 mm and 3.63 mm respectively, compared to 3.19 mm and 2.67 mm, the figures they obtained for *P. dacrydioides*. The tracheids of *P. radiata* are much longer and wider in root wood than in stem wood. The average values recorded by Patel (ibid) were 2.72 mm for stem wood and 4.52 mm for root wood. The tangential diameter for stem wood tracheids as presented by Patel (ibid) are 38.35 μm, 31.75 μm and 29.43 μm for *P. radiata*, *D. cupressinum* and *P. dacrydioides* respectively.

Tracheid walls are pierced by a variety of pit types. The pits may be paired with adjacent tracheids, axial parenchyma cells, ray parenchyma cells or ray tracheids. Intertracheid pits are bordered, possess a torus and margo and are present in the earlywood radial walls of all three taxa. The bordered pits are usually uniseriate. Biseriate bordered pits are infrequent but if present are arranged oppositely. Tangential pits on the tracheid walls are rare.

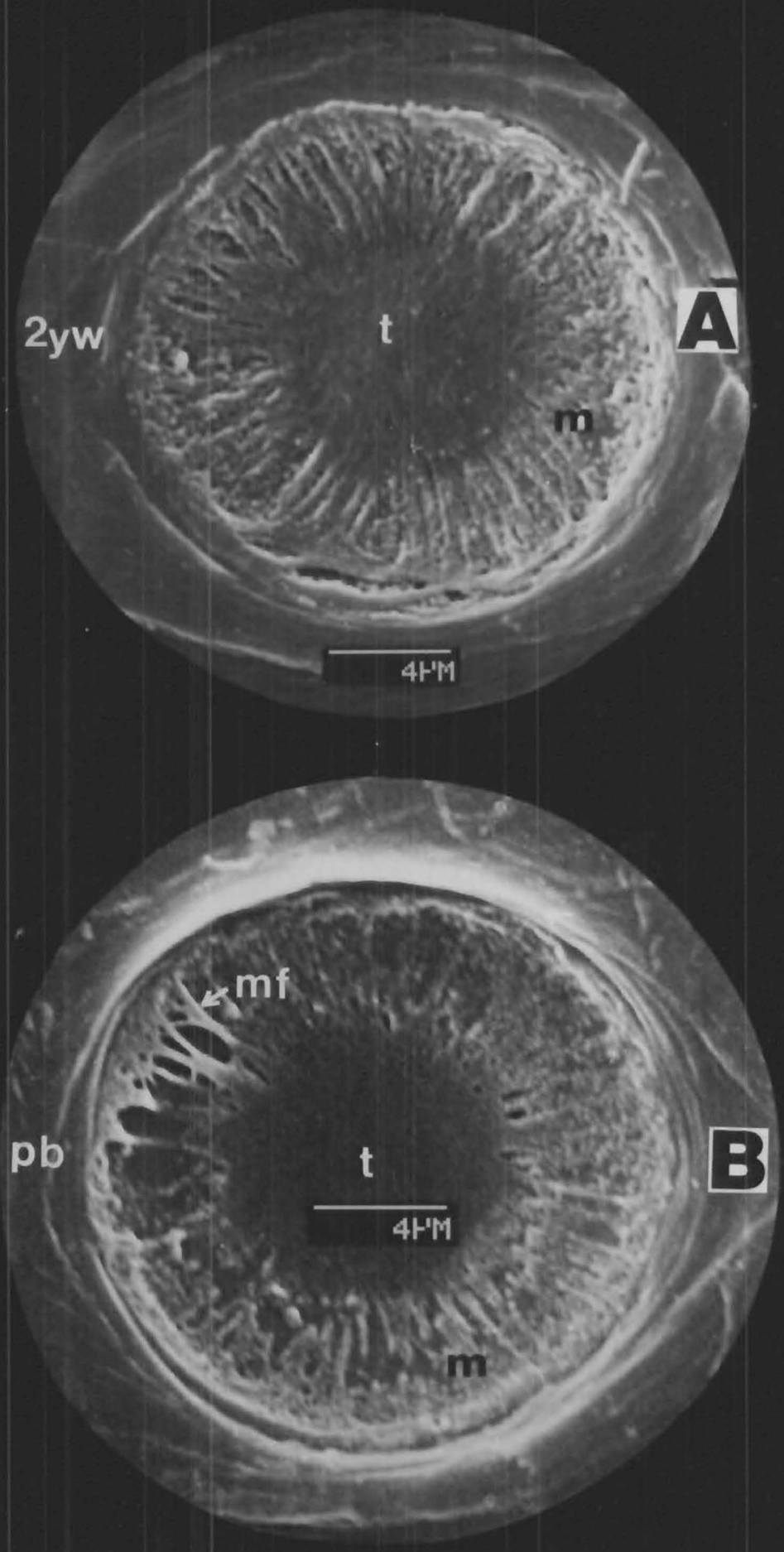

FIGURE 1

(R.L.F.) Conifer bordered pit-pair membranes in (A) *D.cupressinum* (rimu) and (B) *P.radiata*. (SEM)

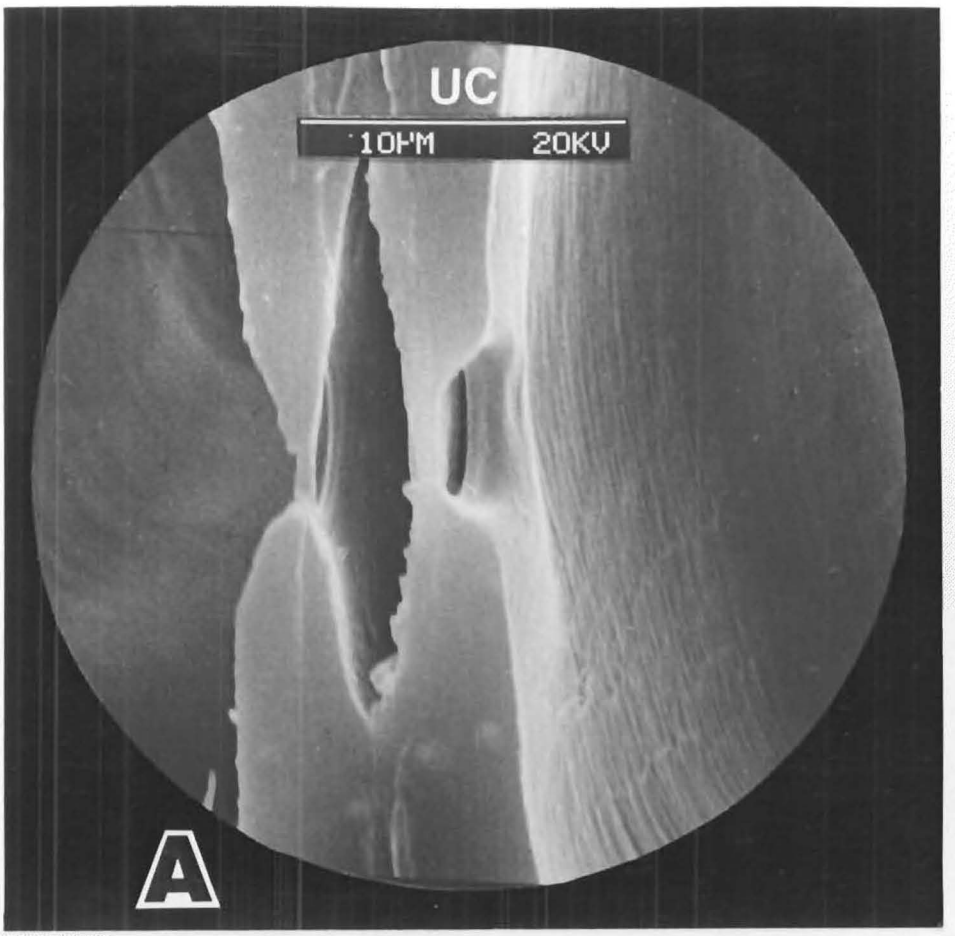

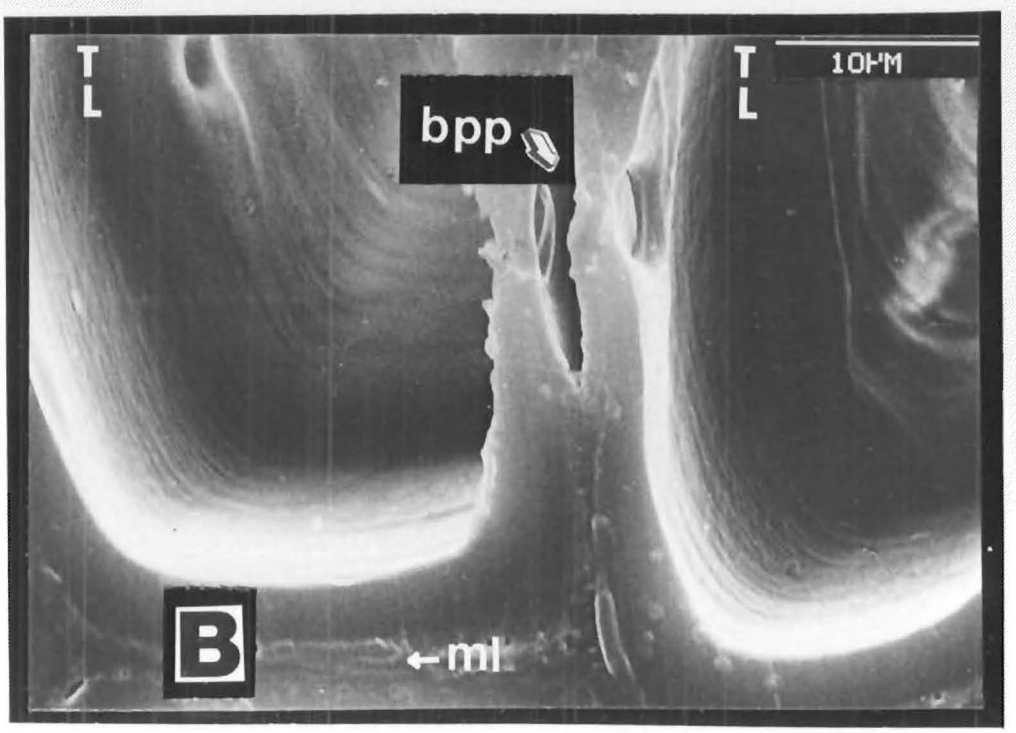

FIGURE 2

(T.F.) A & B Longitudinal cut through the walls of two contiguous tracheids, in *D.cupressinum* (rimu), showing the pit - pair (SEM).

Figures 1 and 2 show different views of bordered pits. A range of pit types is featured in figure 3. Pits connecting tracheids to axial parenchyma lack borders, torus and margo. Pits in the tracheid walls leading to ray parenchyma have borders overarching simple pit membranes (figure 4) and form prominent cross-fields. In *D. cupressinum* the cross-field pits are cupressoid, taxodioid and piceoid; the former two types often exhibit large apertures. *P. dacrydioides* also possesses cupressoid cross-field pits but these are small; taxodioid and piceoid types are sometimes present, (Kaeiser, 1954). There are generally one to two pits per cross-field in both *D. cupressinum* and *P. dacrydioides*. The pits leading to ray parenchyma in *P. radiata* are the pinoid type; the pits are variable in shape and size and there may be up to four pits per cross-field.

Strand tracheids associated with resin ducts occur in *P.radiata*. Axial parenchyma is sparse in *P. radiata* but abundant in both *D. cupressinum* and *P. dacrydioides*. The pits on the radial walls are simple or sieve-like.

The rays in all three taxa are predominantly uniseriate although part-biseriate and biseriate rays have been observed. The horizontal walls of ray parenchyma in both *D. cupressinum* and *P. dacrydioides* are thin and generally unpitted although Patel (ibid) found some evidence of weakly pitted areas in *D. cupressinum*. There are two types of horizontal ray walls in *P. radiata* (a) thin and unpitted and (b) thicker and pitted walls. Ray tracheids are present in *P. radiata* and are dentate.

The genus *Pinus* is separated from all other conifers by the presence of resin ducts and associated thin walled epithelial cells. In *P. radiata* short and long parenchyma cells partly or completely surround the epithelial lining.

3.3 WOOD ULTRASTRUCTURE

3.3.1 TRACHEID CELL WALL STRUCTURE

In the last half century scientists made significant contributions to the field of wood ultrastructure with the aid of the transmission electron microscope. These included major discoveries by Harada, Wardrop, Liese and co-workers of the 1950's era. Technical improvement both in technique and instrumentation led to a tendency to refine and confirm existing concepts. Literature on the structure and composition of the tracheid cell wall is extensive. It is well known that coniferous wood cell walls consist of cellulose (the framework substance) in the form of long crystalline microfibrils embedded in hemicellulose (the matrix substance) and bound together by lignin.

Earlywood tracheid wall thickness in stem wood was measured from transverse sections by Patel (1967, 1970); the values given for *D. cupressinum*, *P. dacrydioides* and *P. radiata* were 2.76μm, 3.01μm and 3.45μm respectively. The tracheid cell walls of *D. cupressinum*, *P. dacrydioides* and *P. radiata* consist of both primary and secondary walls and exhibit the typical structure of conifer normal

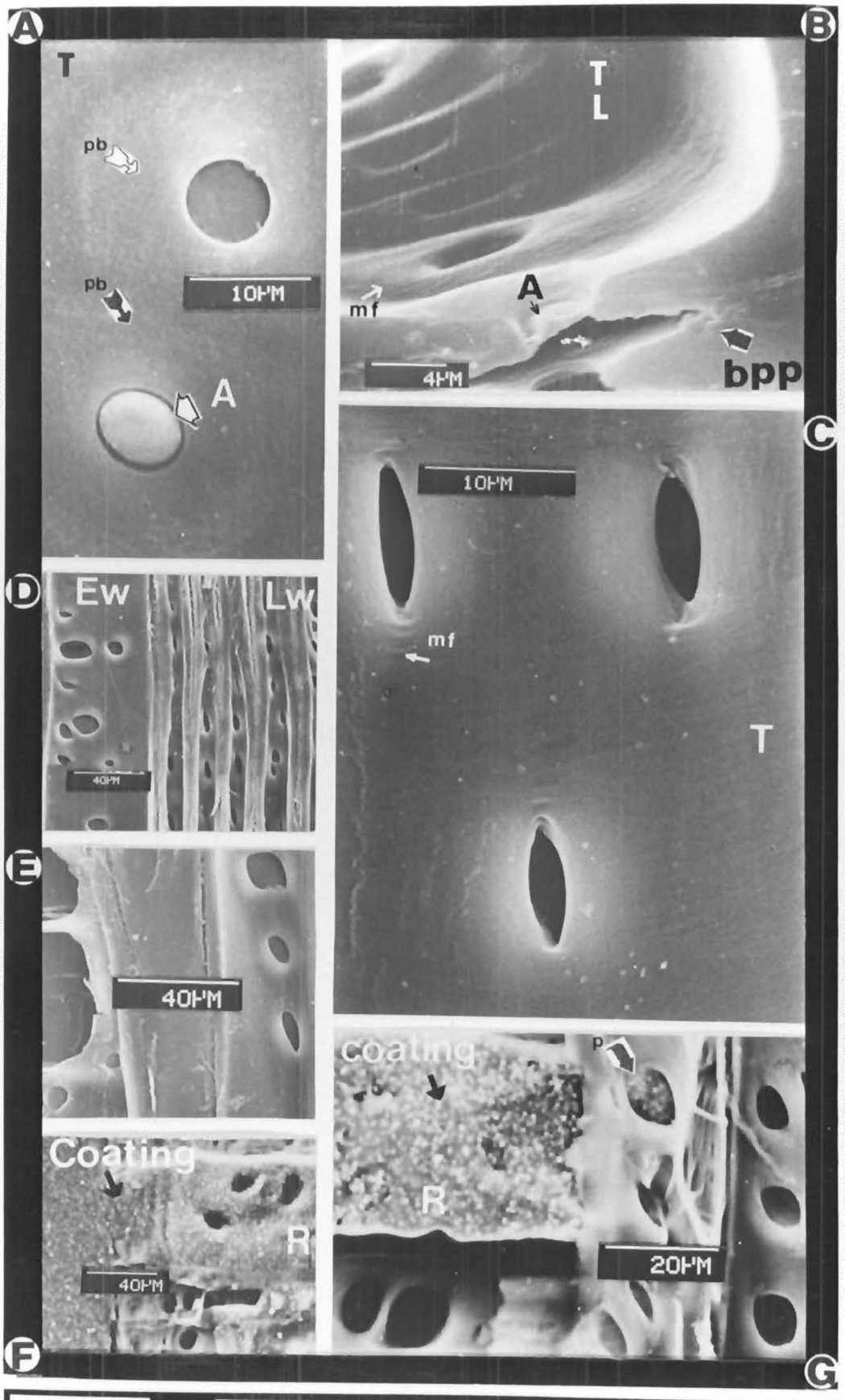

FIGURE 3

CELL WALL PITTING

A. (R.L.F.) Conifer bordered pit-pairs in *P.radiata* latewood.
B. (T.F.) Conifer bordered pit-pairs in *D.cupressinum* (rimu).
C. (R.L.F.) Bordered pits in *P.radiata*.
D-G. (R.L.F.) Tracheid to ray cross-field pitting in *P.radiata*. Note the coating filled cells in figures F & G. (SEM).

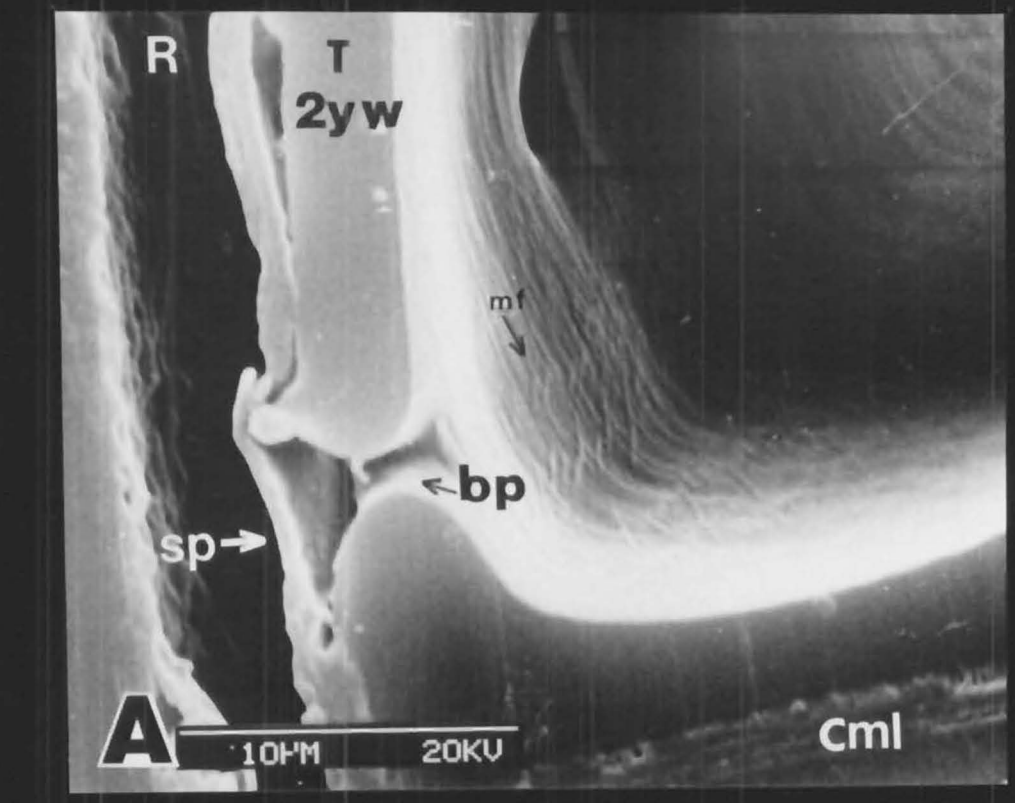

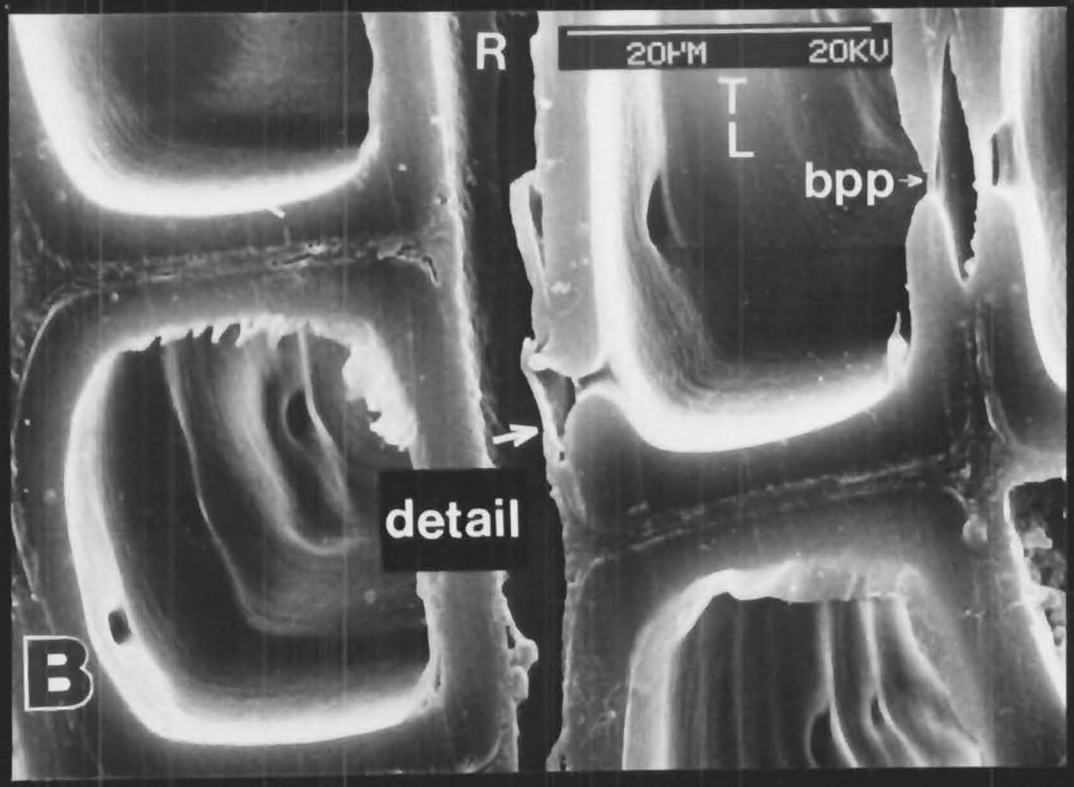

FIGURE 4

(T.F.) A simple pit in a ray cell of *D.cupressinum* (rimu) forming a half-bordered pit pair with the adjacent tracheid pits. Fig. A. detail of Fig. B. (SEM).

wood as described by Wardrop (1954), and Wardrop & Dadswell (1957). A thin network of irregularly arranged microfibrils make up the primary wall. The middle lamella connects individual tracheids to surrounding tracheid cells. The three layers, designated S_1, S_2 and S_3 of the secondary wall are easily distinguished in all three taxa. Page (1976) and Ruel et al (1978) believed that each of the three secondary wall layers consist of lamellae of polysaccharide and lignin and that each lamella of polysaccharide consists of a single layer of parallel cellulose microfibrils sheathed in a monomolecular layer of hemicelluloses. Kerr & Goring (1975) proposed that part of the hemicellulose in the secondary walls forms a thin coating on the cellulose microfibrils. The microfibrils of the outer S_1 layer are orientated in a nearly transverse direction to the long side of the cells. The S_2 consists of microfibrils orientated at a small angle to the long axis of the cell, and the innermost S_3 layer consists of nearly transverse orientated microfibrils.

Wall sculpturing may be present on the lumen face. A warty layer is very obvious on the walls of *P. radiata*. Figure 5 shows the warty layer lining a pit chamber. Very fine helical thickening and callitrisoid thickening may be seen on the tracheid walls of some specimens of *D. cupressinum* and helical thickening is occasionally observed in *P. radiata*.

3.3.2 CELL WALL POROSITY

Controversy still exists on the subject of the nature of the organization of the cellulose micromolecules of the cell wall within a microfibril due to insufficient TEM evidence and different preparation techniques employed. Two main schools of thought are the 'chain folding' and the 'spiral arrangement' theories as reviewed by Côté (1981). Regarding the dimension of the cellulose fibrils in mature cells it is generally held that the diameters are between 20 nm to 40 nm. (Côté [ibid]).

Various experiments have demonstrated cell wall porosity in *P. radiata* and will be discussed in more detail later. However it is notable here that Wardrop and Davies (1961) deduced that the middle lamella, primary wall and outer S_1 layers are regions of low packing density and relatively high porosity; capillaries in the middle lamella appeared smaller than those of other regions of the cell wall; and the number of penetrable capillaries was greater in the S_1 and S_3 layers than in the S_2 layer.

3.3.3 CELL WALL PITTING

The fine structure of conifer pits has intrigued scientists for decades.

In the last twenty years detailed descriptions of the formation and development of the pit membrane and border include those by Liese (1965); Côté (1965), Thomas (1968, 1970); Murmanis & Sachs (1969); Parham & Baird (1973); Imamura et al (1974); and Barnett & Harris (1975). Figure 5 depicts a series of micrographs illustrating the ultrastructure of intertracheid pitting in *P. radiata*. The torus is defined as the central thicker part of a pit membrane (IAWA, 1964) of a

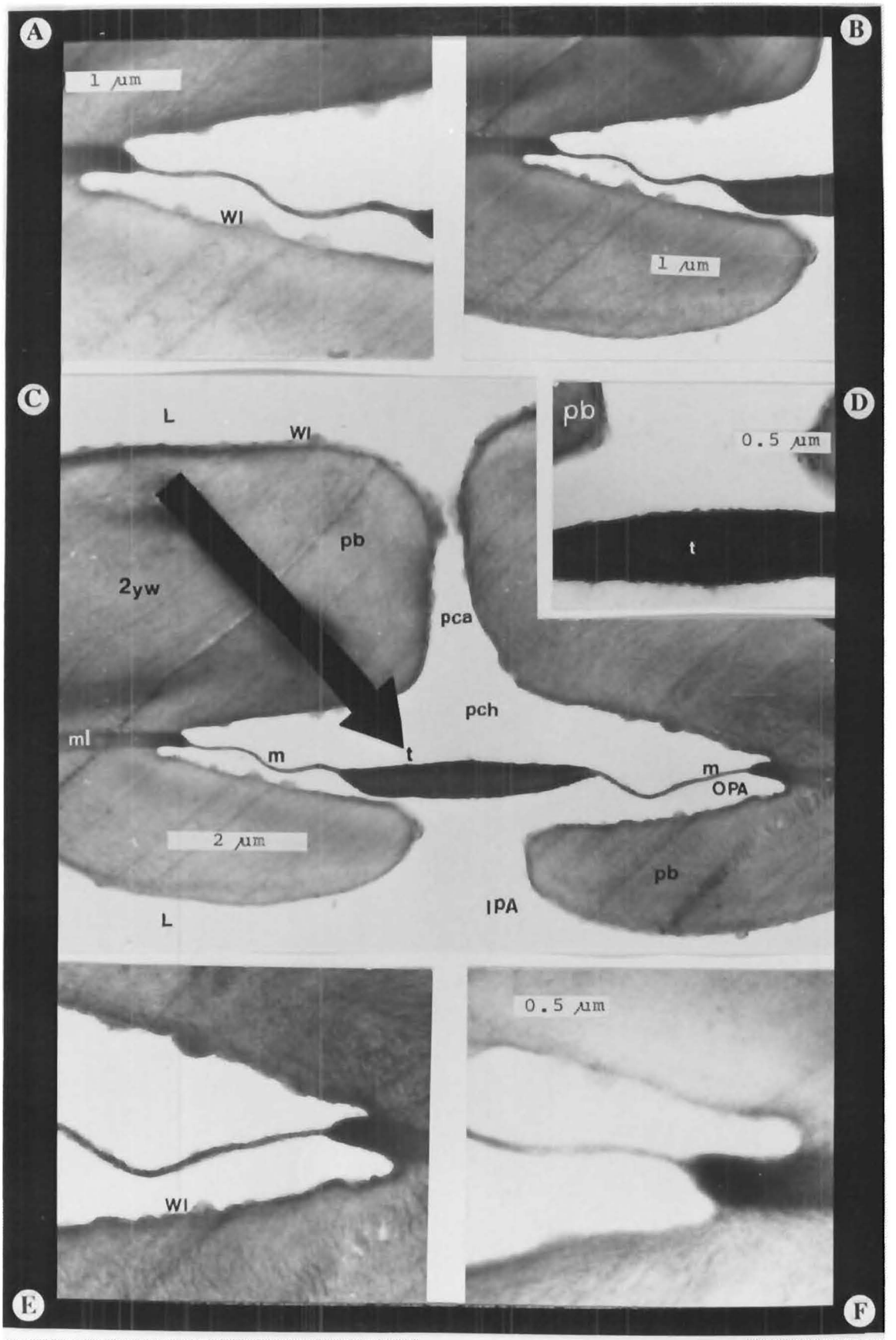

FIGURE 5 (T.S.). RADIATA PINE.
A - F. Details of the inter-tracheid pit pair in fig.C.

bordered pit in earlywood tracheids and it is surrounded by a margo of cellulose microfibrils. Full development of the microfibrillar structure of the torus and margo in the primary wall formation stage and the embedding of the margo throughout the differentiating zone are attributed to the general phenomena which occurs in the process of bordered pit membrane formation in tracheids (Imamura et al, 1974). Frey-Wyssling et al (1956) suggested that in *Pinus sylvestris* the large radiating microfibrils that make up the margo were formed both by aggregation of the existing small microfibrils and the addition of new radial microfibrils. They believed a central ring of microfibrils was set off from the remainder of the membrane to form the torus while the microfibrils of the margo were formed by the aggregation of smaller microfibrils and subsequently as each microfibril diameter increased with age the number of strands decreased. Their work led to several schools of thought on the subject. From a study of the differentiating longitudinal tracheids in Southern Yellow Pines, Thomas (1968) deduced that the margo of the bordered pit membrane was imperforate. He also obtained evidence to reject theories that microfibril formation was due to pit aspiration. He produced examples showing the characteristic radial orientation of a large number of microfibrils in pit membranes which had never been aspirated. Thomas's theory on pit membrane differentiation involved the delineation of a primary pit field which consisted of the two primary walls and the intercellular substance. The next stage involved the apposition of large radiating microfibrils onto the existing primary wall which was succeeded by torus formation. Circularly orientated microfibrils were deposited in the central region of the pit membrane. Apposition of amorphous, hydrolysis-resistant substances followed. The final stage involved enzymatic removal of bulk portion of both the primary wall and the intercellular substances within the margo as the pit membrane approached maturity.

Harada & Côté (1967) recognized two types of bordered pit membranes in coniferous tracheids. One type had circularly orientated microfibrils around the periphery of the torus and the other type had a continuous passage of microfibrils from margo to torus. The structure of the earlywood bordered pit of *D. cupressinum*, *P. dacrydioides* and *P. radiata* is very similar as seen under the scanning electron microscope (refer figures 1 and 3). It is notable that the thick latewood pit membrane in all three taxa, lacks any obvious pores in the margo. The absence of pores in the margo may also be due to the reticulate network of unseparated microfibrils (Butterfield & Meylan, 1980) and/or to the deposition of encrusting secondary material.

Imamura et al (1974) traced the development of the bordered pit in *Pinus densiflora*, *Cryptomeria japonica* and *Chamaecyparis obtusa* and reported that the pit border of the earlywood tracheid was formed by the deposition of the S_1 layer, being supplied with the simultaneous apposition of the initial pit border on the pit cavity side. During S_1 layer formation the transversely orientated microfibrils in the inner surface of the tracheid curved around the pit aperture and some extended towards the top of the pit border. They summerized pit border formation as involving successive

depositions of microlamellae of the S_1 layer around the pit aperture. Subsequently the S_2 and S_3 layers are deposited in the tracheid wall, followed by orientation of microfibrils of the S_2 layer around the pit border region. The microfibrils of the S_2 layer are arranged in a near parallel orientation in the unpitted area but sweep around the pit aperture in streamline pattern. They further emphasised that the S_2 layer did not contribute to pit border elongation. A year later new theories on the early stages of bordered pit formation in *P. radiata* were proposed by Barnett & Harris (1975). They envisaged that the rearrangement of the primary wall into thin areas enclosed by rims was stimulated by some agent which penetrated the primary wall causing weakening of the attractive forces between cellulose microfibrils and/or between microfibrils and the matrix substance. They explained the observed birefringence as the result of centrifugal movement of wall material including a few microfibrils which became orientated in a roughly circular fashion around the affected area. Earlier, Young & Service (1971) had attributed the circular pattern to a slow moving viscous flow around a circular obstruction which was possibly the raised rim around the pit field.

Booker (1989) proposed a new hypothesis to explain the characteristic appearance of aspirated pits in *P. radiata*. His "dynamic mechanism" theory incorporates many facets of currently accepted "static mechanism" theories of pit aspiration which involve a water filled tracheid on one side of the pit and air on the other side; during evaporation, the pit membrane is drawn towards the pit aperture of the water-filled tracheid. Booker postulated that the most important factor controlling pit aspiration is the maximum adhesion strength between liquid and cell wall rather than the surface tension of the liquid.

The pitting between longitudinal tracheids and ray parenchyma is half bordered and the membrane of this type of pit pair lacks the central torus and is imperforate (Côté & Krahmer, 1962). Permeability, penetration and coating deposition will be discussed in ensuing chapters with reference to *D. cupressinum*, *P. dacrydioides* and *P. radiata* cell walls and pitting.

CHAPTER 4

TRANSVERSE SECTION SURVEY OF EIGHT COATING SYSTEMS ON *Dacrydium cupressinum*, *Podocarpus dacrydioides* and *Pinus radiata* WEATHERBOARDS.

4.1 X-RAY ANALYSIS OF PAINT/COATING AND WEATHERBOARD SUBSTRATES

The basic principles of X-ray microanalysis in electron microscopy and sample preparation have been comprehensively described in the literature. Advantages and disadvantages of the various combinations of X-ray analytical systems and electron microscope types and the choice of analysis whether qualitative or quantitative; standardless or standardized; bulk, thick or ultrathin samples have been profusely discussed by Hall (1978); Chandler (1977, 1983); Nasir (1965); Robards (1978); van Steveninck (1978); Russ (1983); Roomans & Shelburne (1983). Qualitative X-ray analysis has proved very useful for the identification of the element constituents present in a sample. X-ray microanalysis is used to assist in solving biological problems, but the approach is somewhat different from that used for metal and mineral specimens because biological specimens consist of an organic matrix of elements (C, N, O and H). Elements with an atomic number lighter than ten are not detectable with conventional energy-dispersive detectors.

X-ray analysis performed in this study was primarily used for the detection of key elements and to obtain qualitative information only. No attempt was made to produce biological standards for the material used as it was deemed unnecessary. Information on the location and distribution of these elements within wood tissue is important in the understanding of coating/substrate relationships and hence great care was taken during sample preparation to avoid redistribution and loss of elements. This was most satisfactorally achieved using sections of oven dried wood that was not dehydrated through any graded series of solvent. Ryan (1986) in a study of radiata pine wood treated with metal containing preservatives stressed the importance of thin section preparation for X-ray analysis in the transmission electron microscope. Both bulk and ultrathin section analyses were performed in this study with the aid of the Cambridge and Jeol electron microscopes and EDAX and LINK X-ray systems. Operating conditions such as the distance of the X-ray detector from the specimen, the accelerating voltage; illuminating current, tilting angle of the specimen and X-ray acquisition time were held constant for each analysis. Both the scanning and the transmission electron microscopes were operated at the energy KeV (see methods) most appropriate to each type of instrument, to allow for positive identification of certain possible overlapping k and l characteristic lines. Specially constructed graphite supports or holders were used to reduce the background radiation.

FIGURE 6

EDXA SPECTRA OF THE DIFFERENT COATING TYPES

A - GRAPHITE ROD SAMPLE SUPPORT HOLDER

B - DULUX PRIMERCRYL 100% ACRYLIC w.b.

C - EPIGLASS WATER BASED WOOD PRIMER w.b.

D - TAUBMANS PREMIUM FAST COAT WOOD PRIMER w.b.

E - DULUX WUNDERPRIME s.b.

F - EPIGLASS 1st COAT WOOD PRIMER s.b

G - EPIGLASS G.P.182 OIL BASED ALKYD PRIMER s.b.

H - TAUBMANS WOOD PRIMER s.b.

I - TiO_2 TAGGED WATTYL ESTAPOL

* see appendix 1 for spectral details of the elements detected in the coatings.

The Cambridge Stereoscan 250 Mark 2 was used in conjunction with the Robinson backscatter detector and was equipped with an EDXA to identify the constituent elements.

Replications were made using a JEOL JSM -35 SEM fitted with a LINK 290 EDXA.


RATE: 3379CPS TIME: 60LSEC
00-20KEV: 10EV/CH PRST: OFF
A: GRAPHITE ROD B:
FS= 224 MEM: A FS= 200
00 02 04 06 08 10 12 14 16 18
CURSOR (KEV)=10.240
A
EDAX

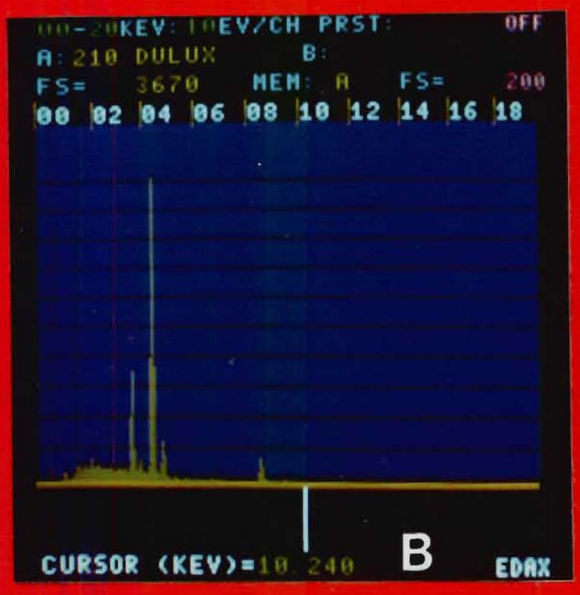
00-20KEV: 10EV/CH PRST: OFF
A: 210 DULUX B:
FS= 3670 MEM: A FS= 200
00 02 04 06 08 10 12 14 16 18
CURSOR (KEV)=10.240
B
EDAX

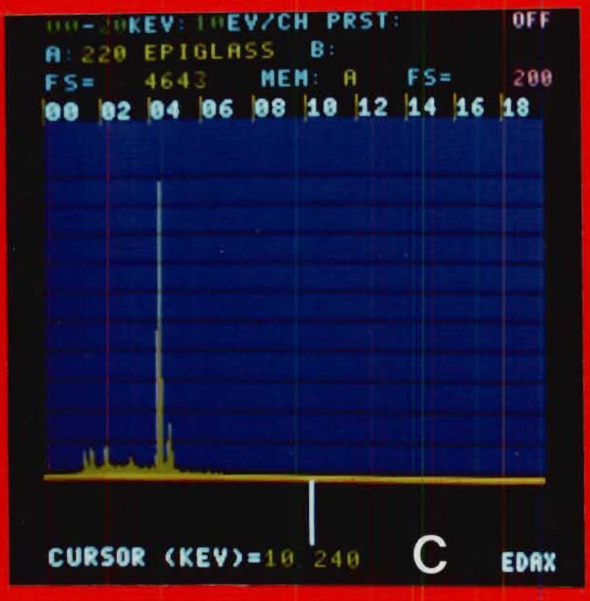
00-20KEV: 10EV/CH PRST: OFF
A: 220 EPIGLASS B:
FS= 4643 MEM: A FS= 200
00 02 04 06 08 10 12 14 16 18
CURSOR (KEV)=10.240
C
EDAX

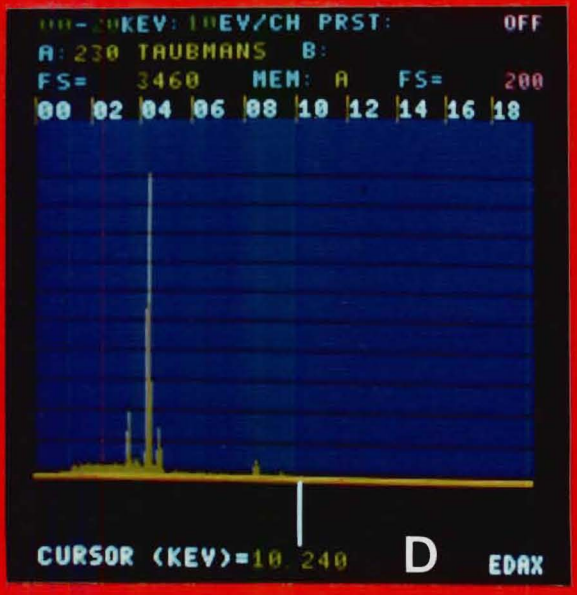
00-20KEV: 10EV/CH PRST: OFF
A: 230 TAUBMANS B:
FS= 3460 MEM: A FS= 200
00 02 04 06 08 10 12 14 16 18
CURSOR (KEV)=10.240
D
EDAX

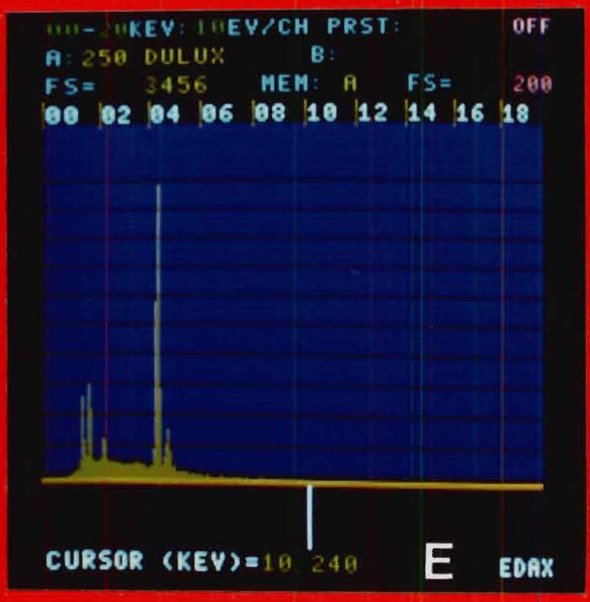
00-20KEV: 10EV/CH PRST: OFF
A: 250 DULUX B:
FS= 3456 MEM: A FS= 200
00 02 04 06 08 10 12 14 16 18
CURSOR (KEV)=10.240
E
EDAX

fig 6

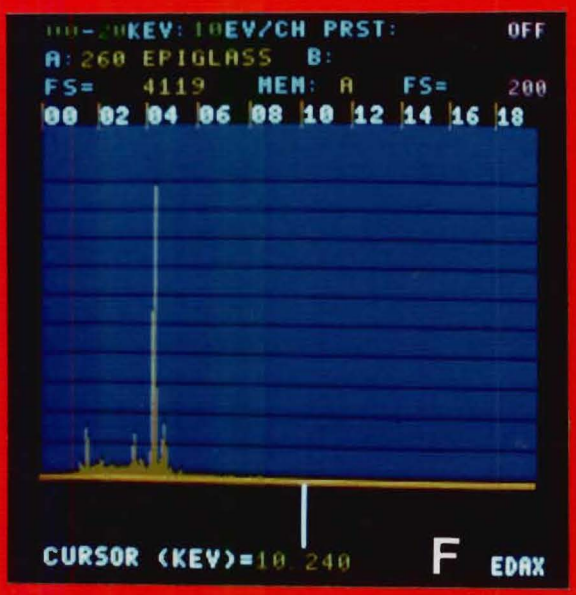
00-20KEV: 10EV/CH PRST: OFF
A: 260 EPIGLASS B:
FS= 4119 MEM: A FS= 200
00 02 04 06 08 10 12 14 16 18
CURSOR (KEV)=10.240
F
EDAX

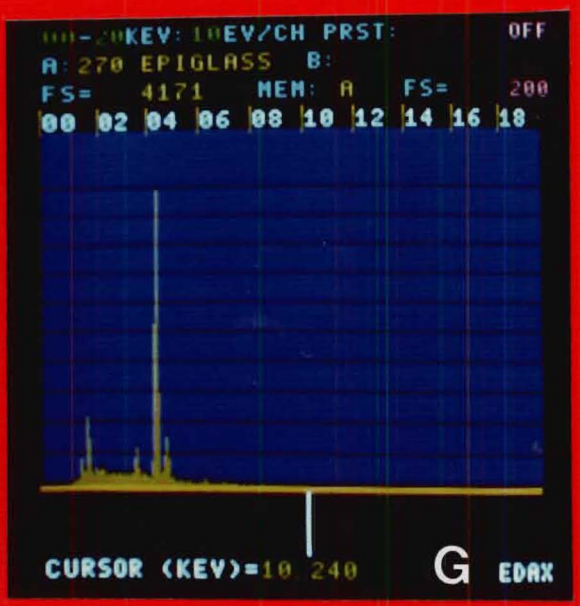
00-20KEV: 10EV/CH PRST: OFF
A: 270 EPIGLASS B:
FS= 4171 MEM: A FS= 200
00 02 04 06 08 10 12 14 16 18
CURSOR (KEV)=10.240
G
EDAX

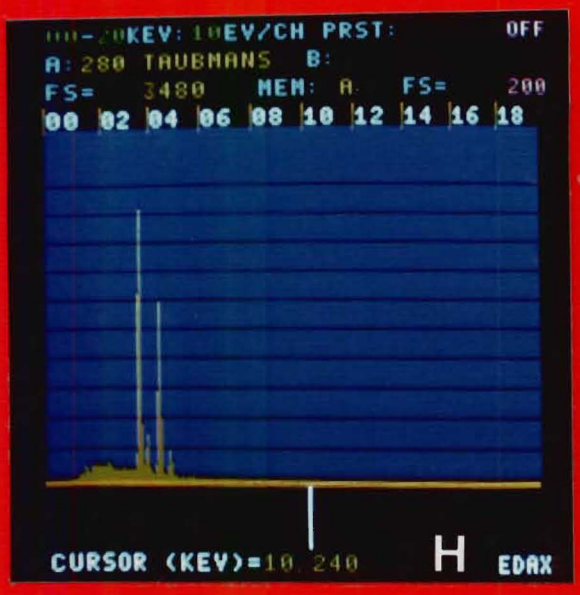
00-20KEV: 10EV/CH PRST: OFF
A: 280 TAUBMANS B:
FS= 3480 MEM: A FS= 200
00 02 04 06 08 10 12 14 16 18
CURSOR (KEV)=10.240
H
EDAX


00-20KEV: 10EV/CH PRST: OFF
A: 420 WATTYL B:
FS= 2721 MEM: A FS= 200
00 02 04 06 08 10 12 14 16 18
CURSOR (KEV)=10.240
I
EDAX

fig 6

Figure 6 shows the EDXA spectra of the eight coating types studied. Spectral details of the elements detected in the coatings are given in appendix 1. Key elements present in the three taxa are also provided. The element ratios were corrected for atomic number (Z), absorption (A) and fluorescence (F) effects (ZAF correction). The analytical data are expressed as intensity (counts per second), background (counts per second), peak/height to background (P/B), ZAF corrections and weight percent element. The P/B ratios were not converted into weight percent since the P/B ratio to element concentration is essentially linear in thin sections (Russ, 1983). Analyses performed on the Cambridge and Jeol SEM systems are shown for comparison.

In all the coatings analysed titanium dioxide is the dominant element. It is notable that when rutile-TiO_2 is made into a pigment it is often coated with Al_2O_3 and SiO_2 to give improved performance, durability and dispersibility. For example, the manufacturer's grade used in tagging the Wattyl Estapol coating was Du Pont Ti-Pure R902. Ten percent weight/weight of rutile-TiO_2 dispersion was added to the coating. This particular dispersion contains 61.6% Ti-Pure R902 which in turn contains a minimum of 91% rutile-TiO_2. The percentage of TiO_2 present in the primers is higher and the figures range from 12.5 to 22 percent. All the primers contain $CaCO_3$ in varying amounts and other extender pigments such as $CaSO_4$, $BaSO_4$ and a variety of silicates. These form the bulk of the remaining elements detected by X-ray analysis. Solvent thinned coatings contain the catalyst cobalt naphthenate which acts as a drier and this accounts for the Co detected. The paint manufacturers of Wattyl Estapol exterior clear alkyd (pers comm.) informed that this coating contains H, C, O, Fe, Mg and smaller concentrations of Ca, Pb, Co, Mn, Cl, S and N but as pointed out earlier the X-ray detector's ability to detect all elements is limited.

Bulk analysis only was carried out on the three weatherboard taxa. All possess the elements Al, Si, S, Cl, K, Ca, Fe and Zn in varying amounts. The presence of the metal-containing preservatives copper-chrome-arsenate (CCA) was detected in *P. dacrydioides* and *P. radiata.* Heartwood *D. cupressinum* is generally untreated, however preservative treatment of sapwood *D. cupressinum* is recommended by the wood preservation authority.

4.2 VISCOSITY OF COATINGS

The viscosity values of the eight coating systems studied are shown in Krebs Units (KU) in appendix 2. The ranges vary from 61-76 KU. Originally a KU value of around 100 was thought to correspond to good brushing properties of a house paint; but now days coatings are formulated to much lower KU values. (ASTM special pub.500,1972).

Liquids which behave in the manner of water or raw linseed oil are referred to as Newtonian liquids because they exhibit Newtonian flow (Morgans, 1984). If a Newtonian liquid is pigmented then the presence of solid particles will increase the viscosity. Viscosity can also be increased on

storage due to adsorption by the pigments of certain molecular weight fractions of the polymer binder or by chemical reactions between an acidic medium and basic pigments such as certain grades of rutile TiO_2. All coatings used in this study were freshly prepared products. Gray (1961) stated that coatings of lower viscosity are recommended for impermeable softwood species while high viscosity primers, which are thicker surface film formers, are more suitable for permeable species. A thixotropic system is one in which a gel forms during the resting stage but when a stress is applied a fluid results and the system flows, but immediately after the stress is removed it reverts back to the gel state. In a flocculated system the pigment particles tend to form clusters after they have been dispersed. Flocculation in highly pigmented coatings is often accompanied by thixotropy and pseudoplastic flow (Morgans, ibid). The thixotropic index of TiO_2 tagged Wattyl Estapol exterior clear is 1.01; hence it is almost Newtonian in viscosity.

4.3 CONTACT ANGLES OF COATINGS

Gray (1961) reviewed the thermodynamics of wetting and spreading of coatings on solids and concluded problems of adhesion are complex and difficult to reduce to quantitative terms. Surface tension is expressed as dynes/cm. With the aid of a horizontal microscope and goniometer eye piece, Gray measured the contact angles of glycerol and distilled water and the spreading property of selected coatings on a variety of timber species. Gray deduced that the critical surface tension for spreading is usually 42-45 dynes/cm for coatings compared to 62.8 and 72.8 dynes/cm for glycerol and distilled water. Mineral spirits has a surface tension of 24 dynes/cm (Pierce & Schoff, 1988). As the solvent evaporates from the coating, the coating surface tension increases because it is raised either by a higher rate of solvent evaporation from the edges or by conductive transport of the solvent-rich material outwards from the coating interior. The advancing contact angle is the angle measured as the drop advances across the surface and is useful to explain the spreading behaviour of the coating. The advancing and receding behaviour of coatings was not studied, however fixed (stationary) contact angles of the eight coating types on a glass substrate were measured. Glass was chosen because it is a uniform mounting medium(see method 2.13).

The means, standard deviations and ranges are tabulated in appendix 3. The total range for the coatings was between 19-34 degrees and the range among means was 20-28 degrees. Pierce and Schoff (ibid) stated that in practice good wetting and adhesion of coatings occur when contact angle is low.

The analysis of variance is shown in Table 1. The calculated F value of 7.59 for 'among coatings' is greater than the critical F values given in statistical tables for F 0.05 and F 0.01 (7,72), thus the null hypothesis is rejected. It is therefore concluded that there is significant difference 'among coatings' as statistics show that the samples come from populations with different means with a

TABLE 1

CONTACT ANGLES OF COATINGS ON A HORIZONTAL SURFACE

(refer appendix 3)

TABLE 1.1.1 ANALYSIS OF VARIANCE - ONE WAY ANOVA

SOURCE	df	SS	MS	F	P>F
AMONG COATINGS	7	481.15	68.74	7.59	0.0001
WITHIN	72	652.40	9.06		
TOTAL	79	1133.55			

TABLE 1.1.2 .

DUNCAN'S NEW MULTIPLE RANGE FOR THE COMPARISON OF MEANS AT THE P=0.05 LEVEL.

THE MEANS WHICH ARE NOT SIGNIFICANTLY DIFFERENT (n.s) ARE GROUPED TOGETHER.

THE MEANS ARE RANKED FROM HIGHEST TO LOWEST.

BRAND	COATING	DUNCAN GROUPING
DULUX	PRIMERCRYL 100% ACRYLIC	
WATTYL	TiO_2 TAGGED ESTAPOL EXTERIOR CLEAR	
TAUBMANS	PREMIUM FAST COAT WOOD PRIMER	
DULUX	WUNDERPRIME	
EPIGLASS	WATER BASED WOOD PRIMER	
TAUBMANS	WOOD PRIMER	
EPIGLASS	G.P.182 OILBASED ALKYD PRIMER	
EPIGLASS	FIRST COAT WOOD PRIMER	

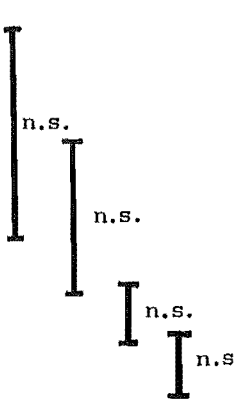

probability of obtaining such an F value by chance alone of 0.0001. The term 'among' in statistical packages is often referred to as 'treatment' and the term 'within' is synonymous with 'error or individuals' (Larkin, 1979).

Duncan's New Multiple Range test for the comparison of means is shown in Table 1.1.2. After ranking the means, this statistical treatment suggests that the contact angles of Dulux primercryl 100% acrylic, TiO_2 tagged Wattyl Estapol, Taubmans premium fast coat wood primer, Dulux wunderprime and Epiglass waterbased wood primer are not significantly different at the P=0.05 level. By contrast, Taubmans wood primer, Epiglass G.P.182 oil based alkyd primer and Epiglass 1st coat wood primer are shown as significantly different. Epiglass 1st coat wood primer has the lowest mean contact angle. These results do not uphold microscope evidence that TiO_2 tagged Wattyl Estapol exhibits deeper penetration than the primers. If contact angle alone controlled penetration depth, then the TiO_2 tagged Wattyl Estapol would be singled out in these statistical tests but as it does not, some other feature must also be involved.

This chapter deals with preliminary observations of coating/substrate interaction prior to degradation. The degree of penetration, effect of growth ring boundaries, springwood/summerwood variation, taxa control and the type of penetration is discussed here for each coating type. The concluding discussion of this section briefly reviews theories on the subject. To avoid repetitive descriptions of the coating/substrate ultrastructure the topics of permeability, penetration, diffusion and the role of the cell wall and pit membranes will be discussed in greater detail in the following chapter which is devoted to the study of just one of the coating systems selected from this survey.

Different methods of sample preparation and cutting techniques were employed to ascertain whether techniques can interfere with the coating. To prevent redistribution of elements, dry wood was preferred, although it is more difficult to section. Specimens analysed by X-ray techniques were not stained whereas those used in ultrastructural studies required staining.

Micrograph quality is controlled by the nature of each investigation. For example, to obtain backscattered images, the specimens are not gold/palladium coated but carbon coated, which means less distinct images results.

It was noted that in unembedded sections, coating-filled cells retained their shapes during sectioning whilst those with empty lumens were distorted easily.

4.4 DULUX PRIMERCRYL 100% ACRYLIC COATED WEATHERBOARDS

Figures 7 to 14 contain a selection of light micrographs, electron micrographs and X-ray maps which qualitatively demonstrate the position and location of the water based primer on *D. cupressinum*, *P. dacrydioides* and *P. radiata* weatherboards.

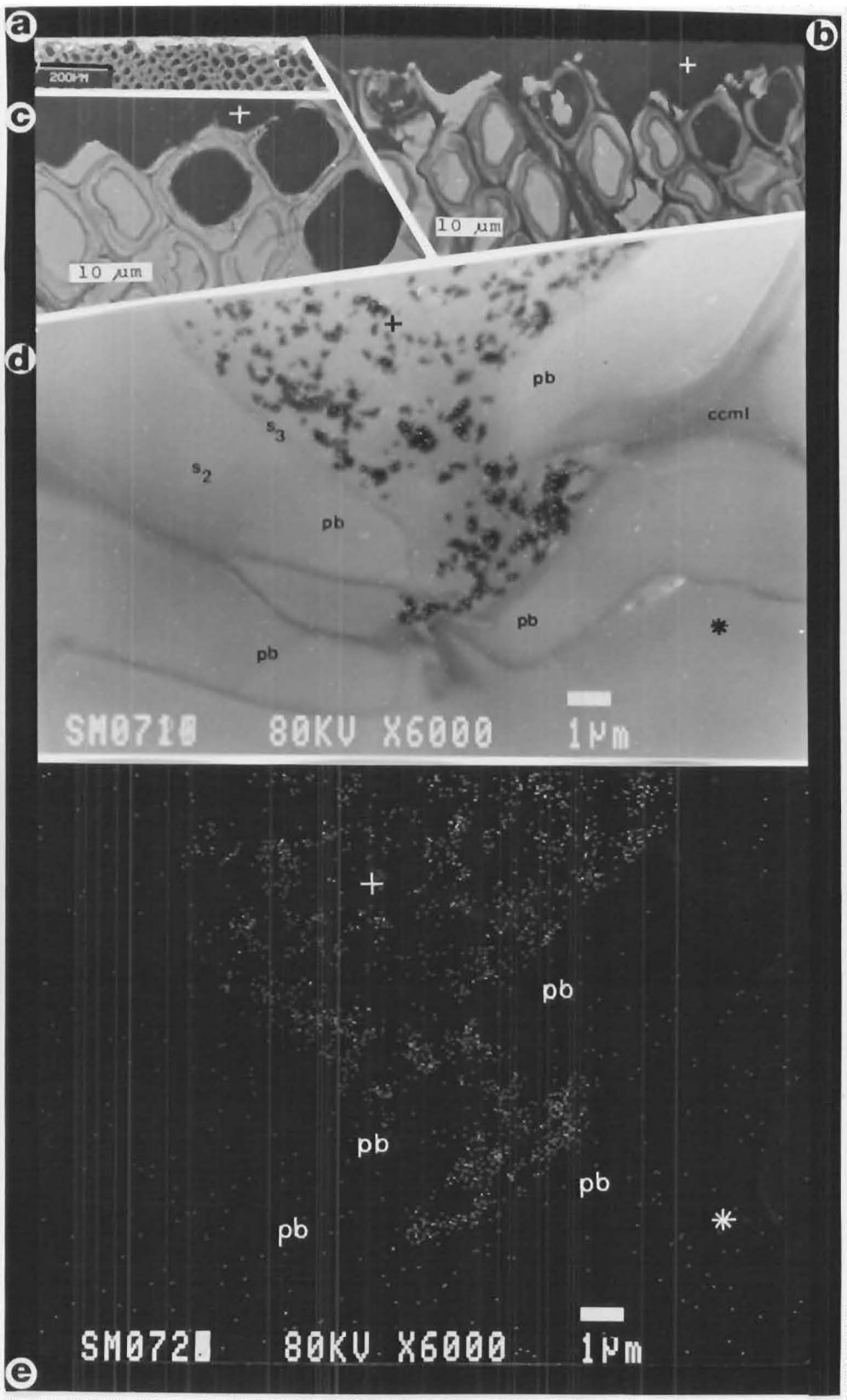

FIGURE **7** (T.F./ T.S.) RIMU COATED WITH DULUX PRIMERCRYL 100 % ACRYLIC.

A Latewood - earlywood. (BSEI /SEM).
B & C Toluidine Blue stained unembedded section.(LM).
D Ultrathin-thin, unstained section of coating / tracheid bordered pit interface.
E Corresponding EDXA element (Ti - K) X-ray map for fig.D. (STEM).

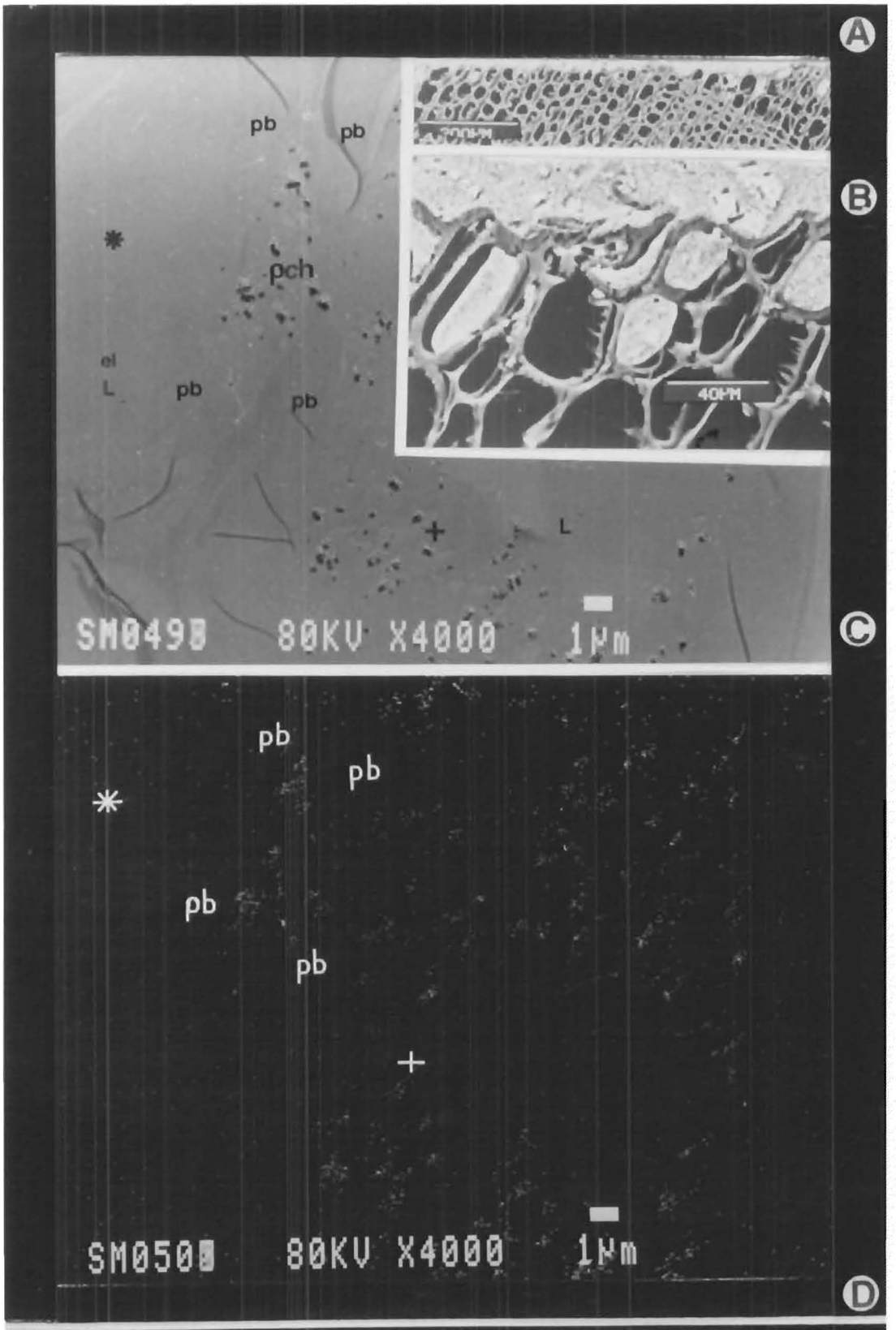

FIGURE 8 (T.F./T.S). *P.dacrydioides* COATED WITH DULUX PRIMERCRYL 100% ACRYLIC. (w.b.).

A Earlywood/latewood boundary.(BSEI/SEM).
B Detail of earlywood in fig.A.(BSEI/SEM).
C Ultra-thin,unstained section of coating / tracheid wall interfacial region. (STEM).
D Corresponding EDXA element (Ti-K) x-ray map for fig.c. (STEM).

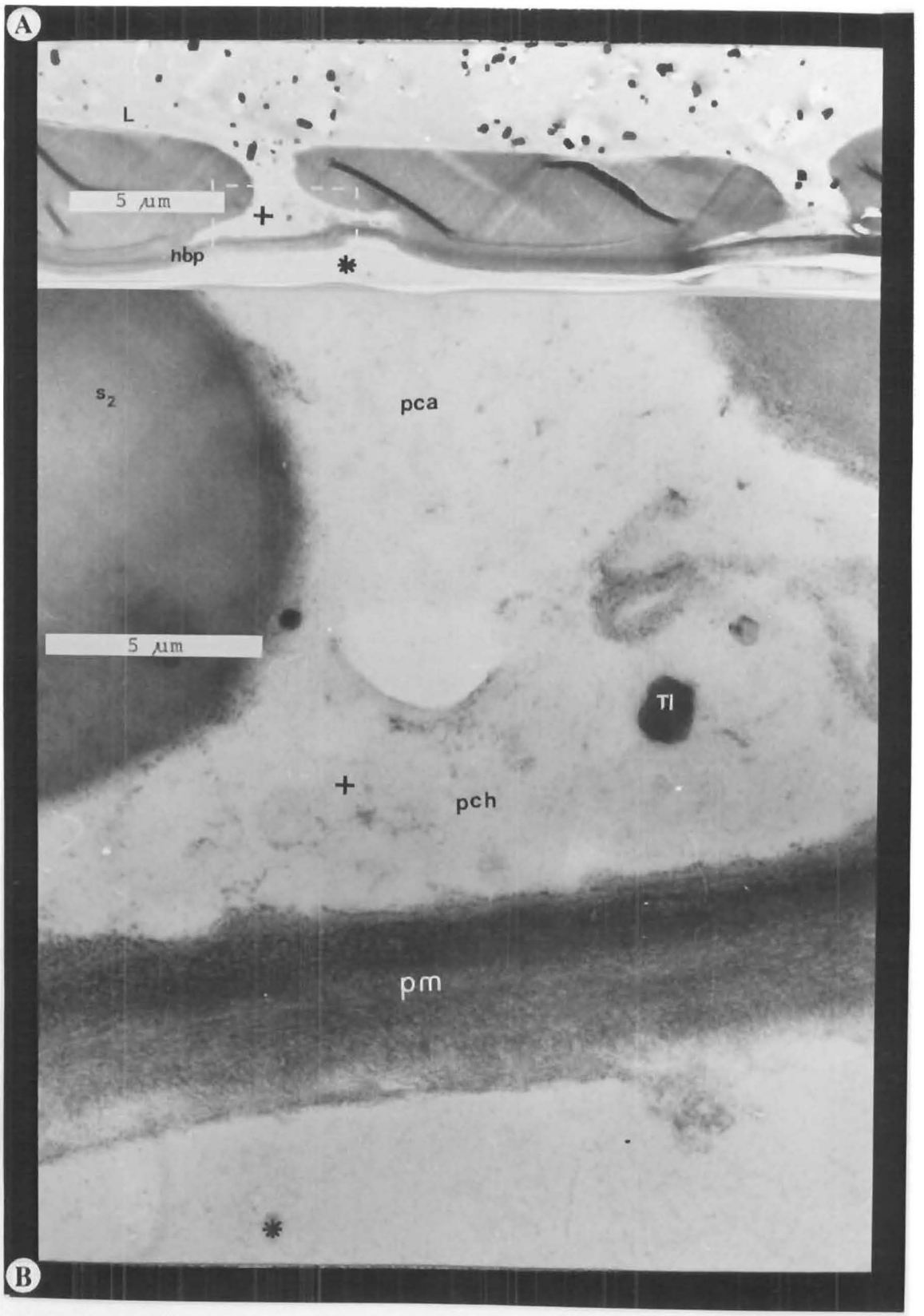

FIGURE 9 (T.S.). KAHIKATEA COATED WITH DULUX PRIMERCRYL 100% ACRYLIC (w.b.).

A Cupressoid cross-field pits between tracheid and ray parenchyma. (TEM).

B Detail of fig.A. (Earlywood).
Note the borders overaching the simple pit membranes.

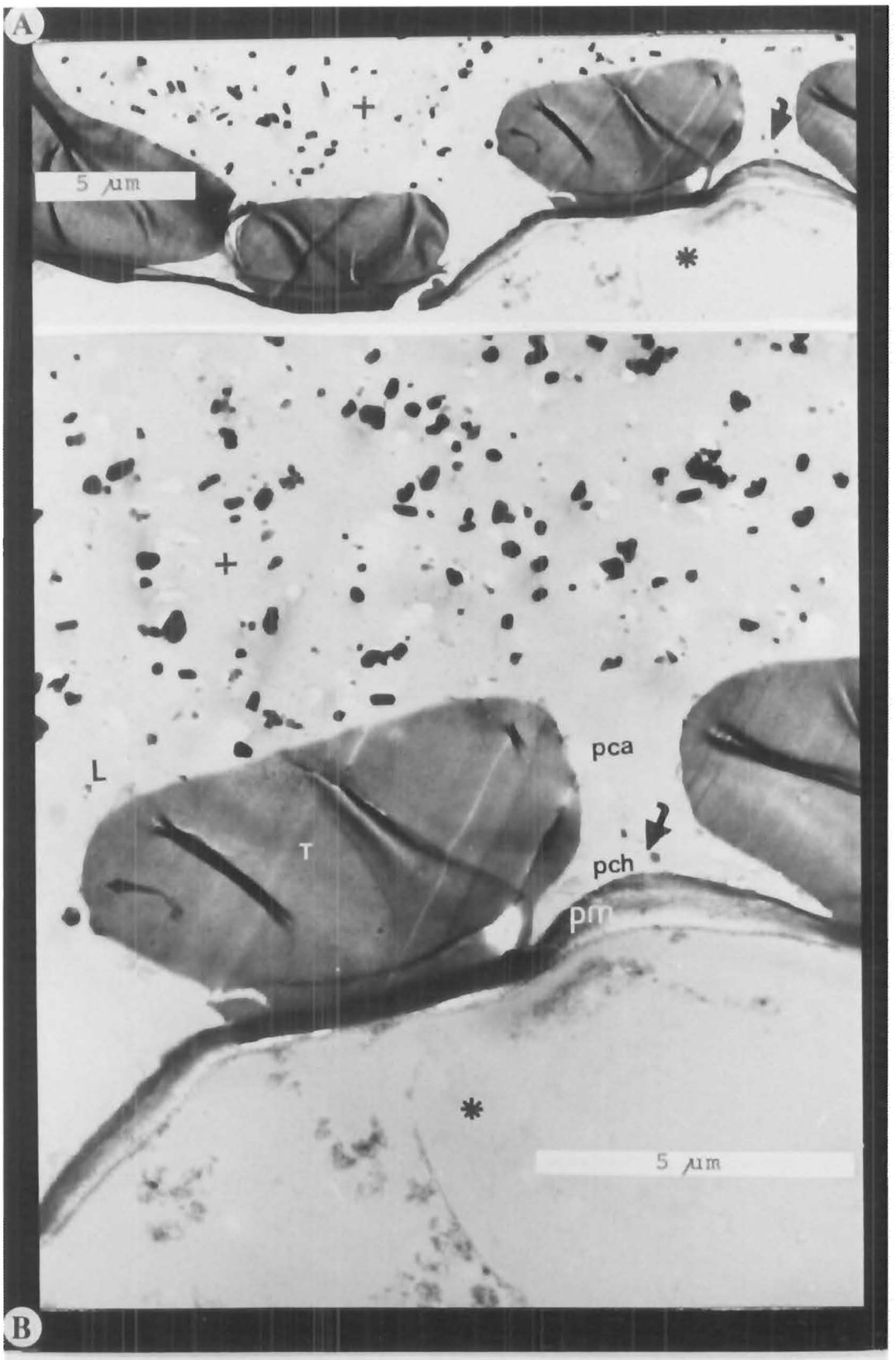

FIGURE 10 **(T.S.). *P dacrydioides* COATED WITH DULUX PRIMERCRYL 100% ACRYLIC.(w.b.).**

A Cupressoid cross-field pits between tracheid and ray parenchyma. The elliptical apertures are bordered on the two long sides. (TEM).

B Detail of fig.A. Uranyl acetate - lead citrate stained, Spurr's embedded,latewood section.(TEM).

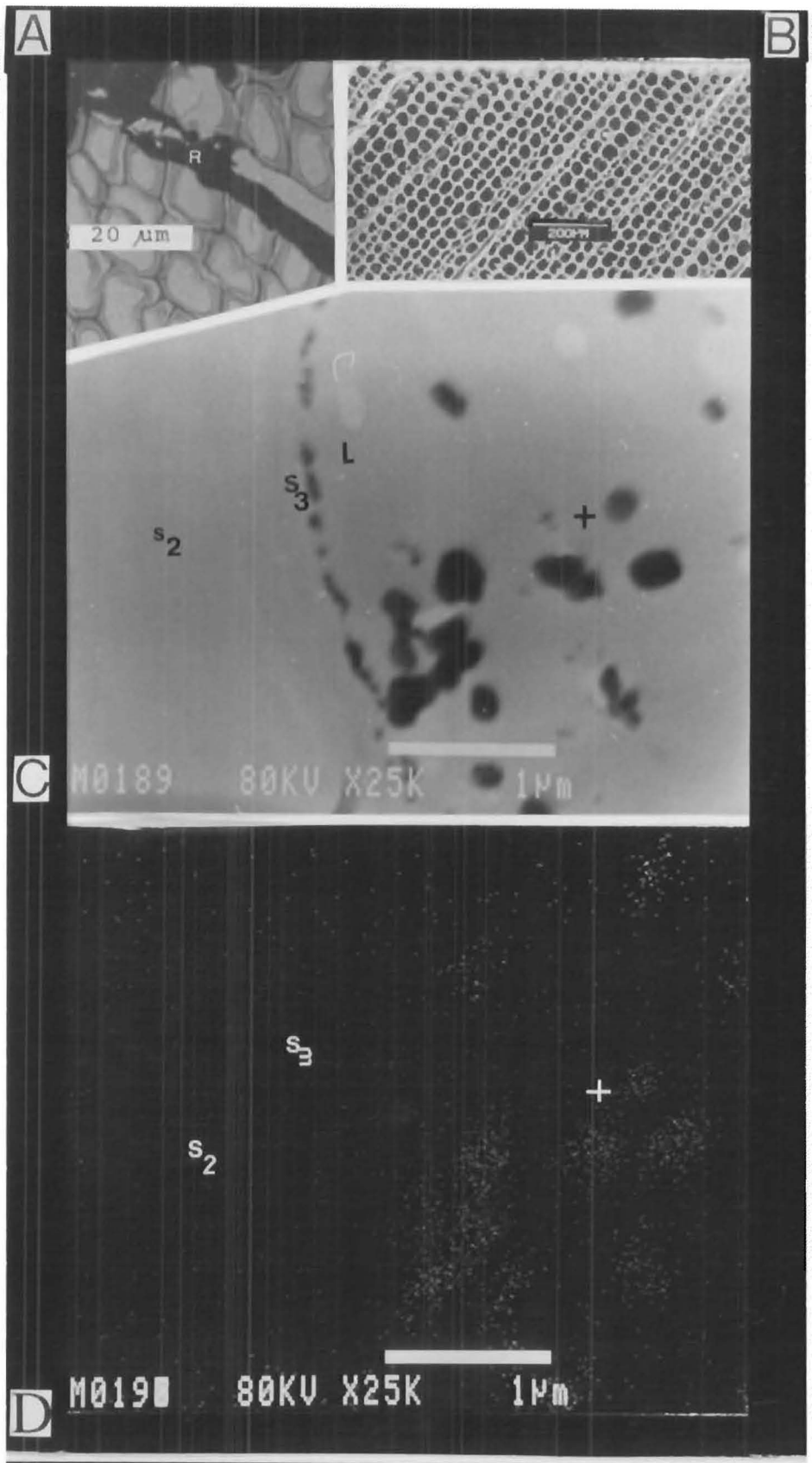

FIGURE 11 (T.F./T.S.). *P.radiata* COATED WITH DULUX PRIMERCRYL 100% ACRYLIC (w.b.).
A Toludine Blue stained unembedded section.(LM).
B Earlywood. (BSEI/SEM).
C Ultra-thin,unstained section of coating / tracheid wall interfacial region. (STEM).
D Corresponding EDXA element (Ti-K) x-ray map for fig. C. (STEM).

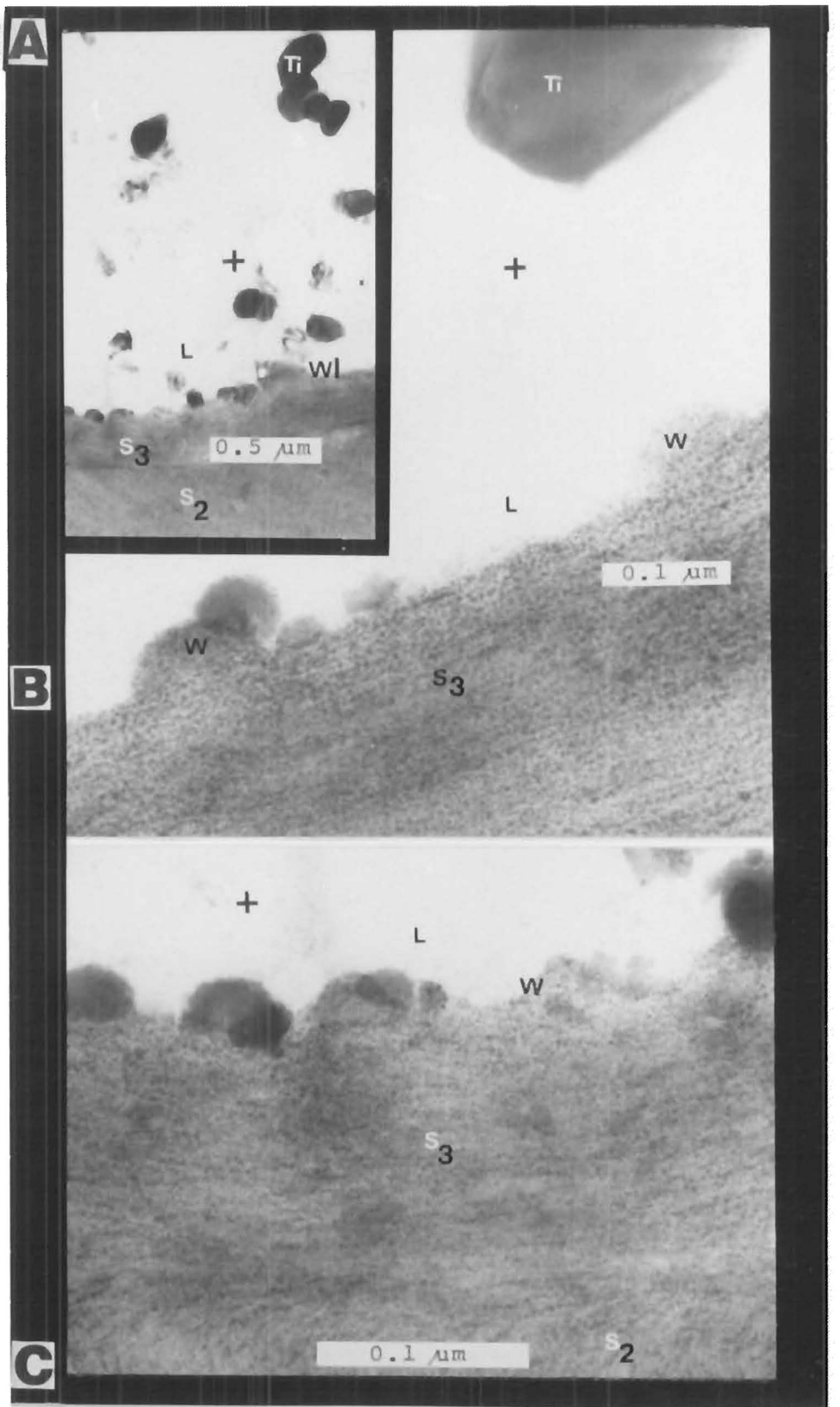

FIGURE 12 **(T.S.). *P.radiata* COATED WITH DULUX PRIMERCRYL 100% ACRYLIC (w.b.)**

A Ultra-thin,uranyl acetate - lead citrate stained, Spurr's resin embedded section showing coating / tracheid wall interface. (TEM).

B Coating / substrate interface. S_3 layer of tracheid wall. (TEM).

C Detail if fig.A. (TEM).

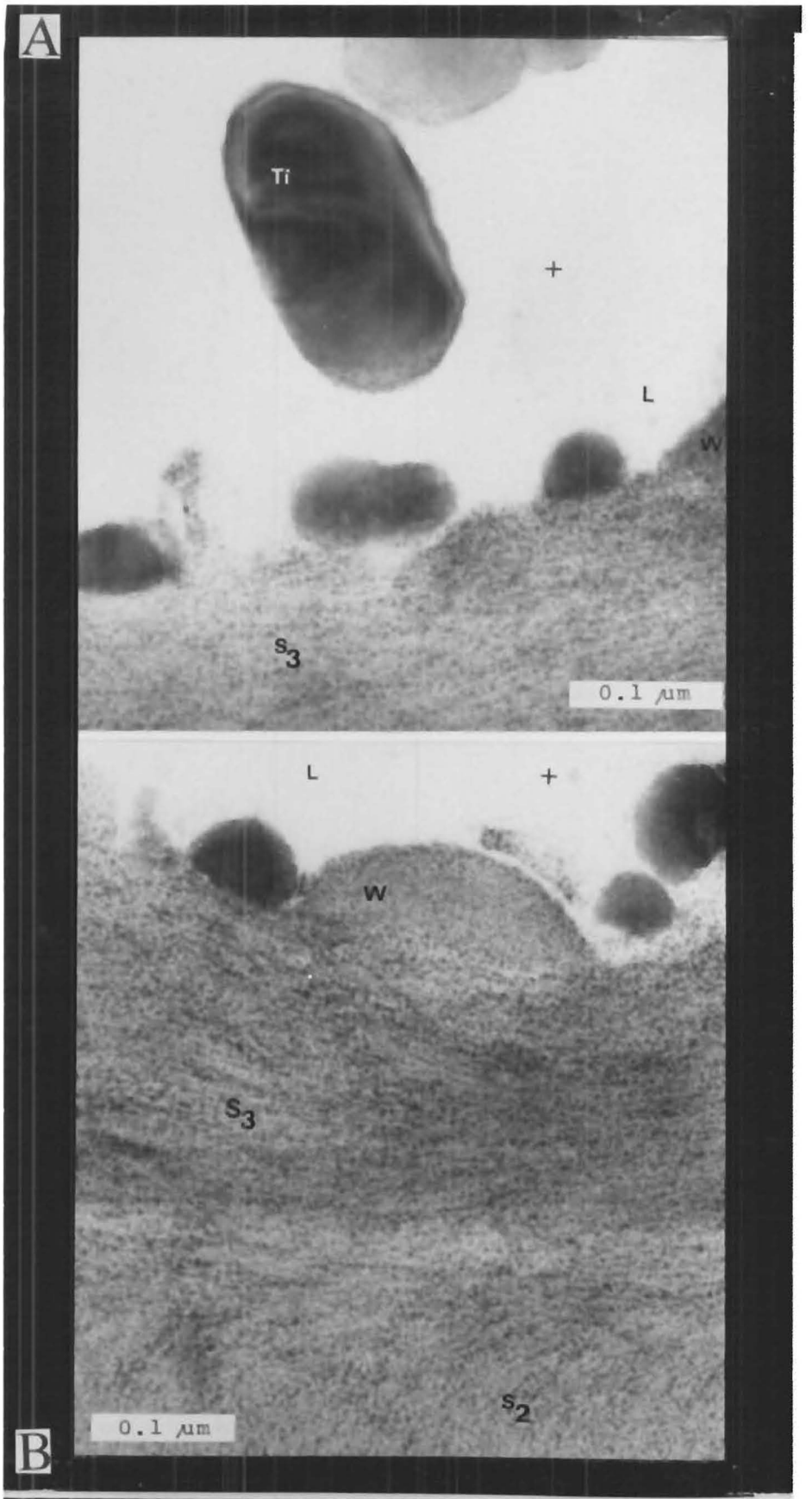

FIGURE 13 **(T.S.). *P.radiata* COATED WITH DULUX PRIMERCRYL 100% ACRYLIC (w.b.).**
A & B Ultra-thin, uranyl acetate - lead citrate stained, Spurr's resin embedded, sections showing coating / tracheid wall interface. (TEM).

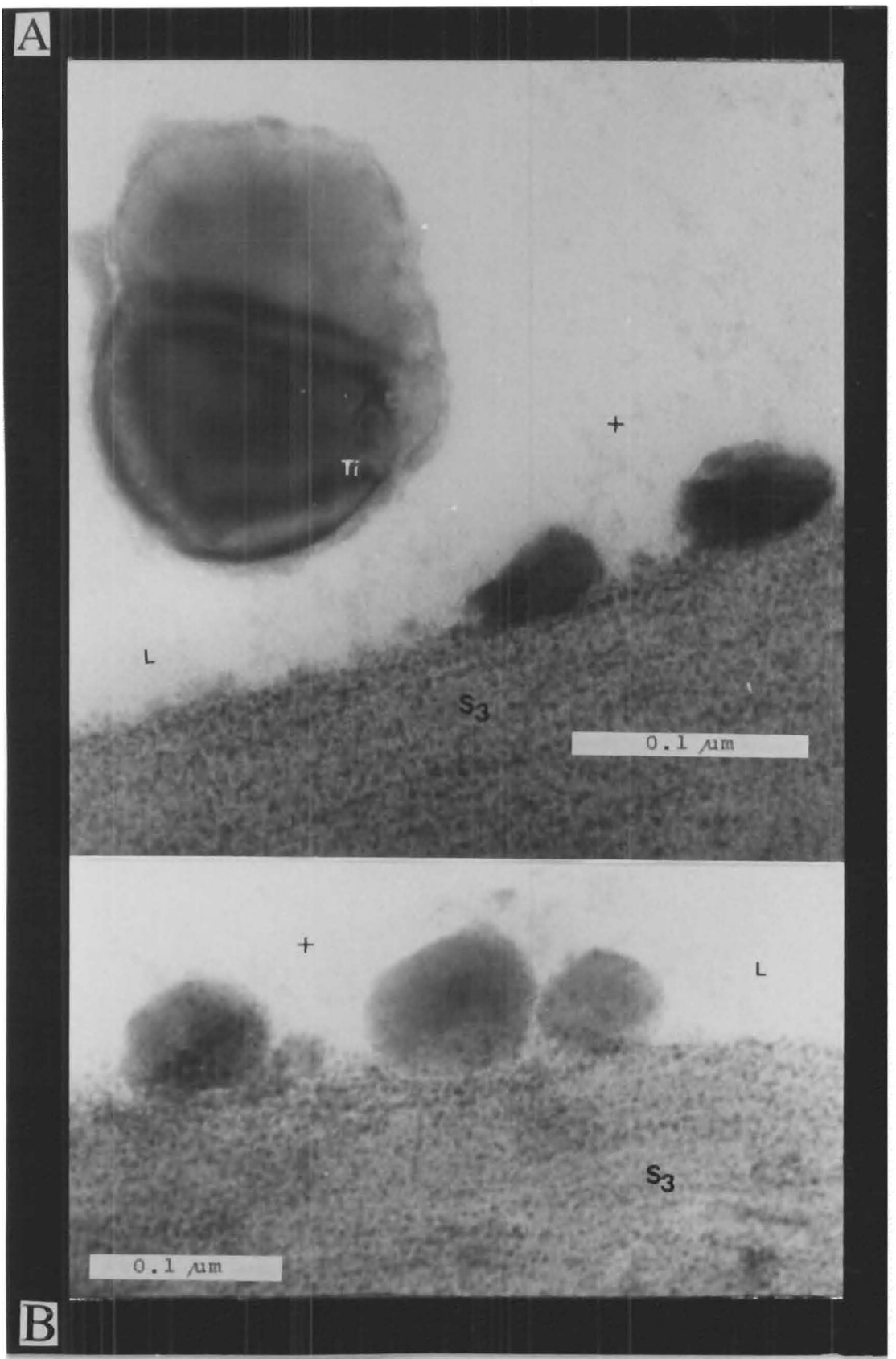

FIGURE 14 **(T.S.). *P.radiata* COATED WITH DULUX PRIMERCRYL 100% ACRYLIC (w.b.).**
A & B Ultra-thin, uranyl acetate - lead citrate stained, Spurr's resin embedded sections showing coating / tracheid wall interface. (TEM).

The backscattered electron images in figures 7, 8 and 11 indicate that in most cases coating penetration is limited to one or two cell rows deep; and occasionally three cells deep in the early springwood zone. Penetration into the lumen of the latewood is almost non existent and the coating appears to be locked only into those cells opened by machining. Some evidence of flow along ray cells exists as indicated in the Toluidine stained unembedded section in figure 11 (A).

Although weatherboards are either sold as flat sawn or quarter sawn boards; when the surface is examined under the microscope the terms flat and quarter sawn are no longer suitable. At the cellular level, tracheid rows often appear oblique to the tangential or radial direction of cut and the intertracheid pits are presented to the board surface in a variety of angular positions.

The ultrathin sections and their corresponding EDXA element maps for titanium presented in figures 7, 8 and 11 provide evidence that the titanium particles are too large to penetrate the cell walls. However they exhibit a tendency to line the cell lumen and congregate along any irregularities present in the S_3 layer of the cell wall; in particular in the vicinity of warts (refer figures 11, 12 and 13). All types of pit membrane present in the three taxa appear to act as barriers to titanium particle movement. The intertracheid aspirated pits containing a torus and margo and the simple pit membranes between ray parenchyma and tracheid cells depicted in figures 9 and 10 illustrate this phenomenon.

4.5 EPIGLASS WATER BASED WOOD PRIMER COATED WEATHERBOARDS

Figures 15 to 18 illustrate the coating behaviour of Epiglass water based primer on *D. cupressinum*, *P. dacrydioides* and *P. radiata* weatherboards.

Cell lumen penetration is restricted to one to three cells deep. The particle size of the pigments present in this coating is greater and the very coarse texture is visible in figures 15 (B), 16 (A) and 17 (A). This coating contains the greatest percentage of titanium compared with the other coating systems. The titanium particles appear abrasive on the S_2 layer of the cell wall (figure 15 [D]).

The distribution of individual titanium particles is denser in this acrylic co-polymer water based primer (figure 18 [A]) than in the Dulux primercryl 100% acrylic primer.

The wood of *P. radiata* is softer than that of the two endemic taxa and the earlywood prone to distortion during machining (figure 17 [A]). Once the cells have been burred, lumen penetration is prevented. Note the empty ray cells which have been 'sealed' over. Frequently the S_3 layer of the cell wall is destroyed during machining and the S_2 layer is exposed to the coating film. Although the linear distribution of tiny particles along the S_2 wall is easily distinguished under the electron microscope the X-ray was unable to identify the elements (figure 18 [B]).

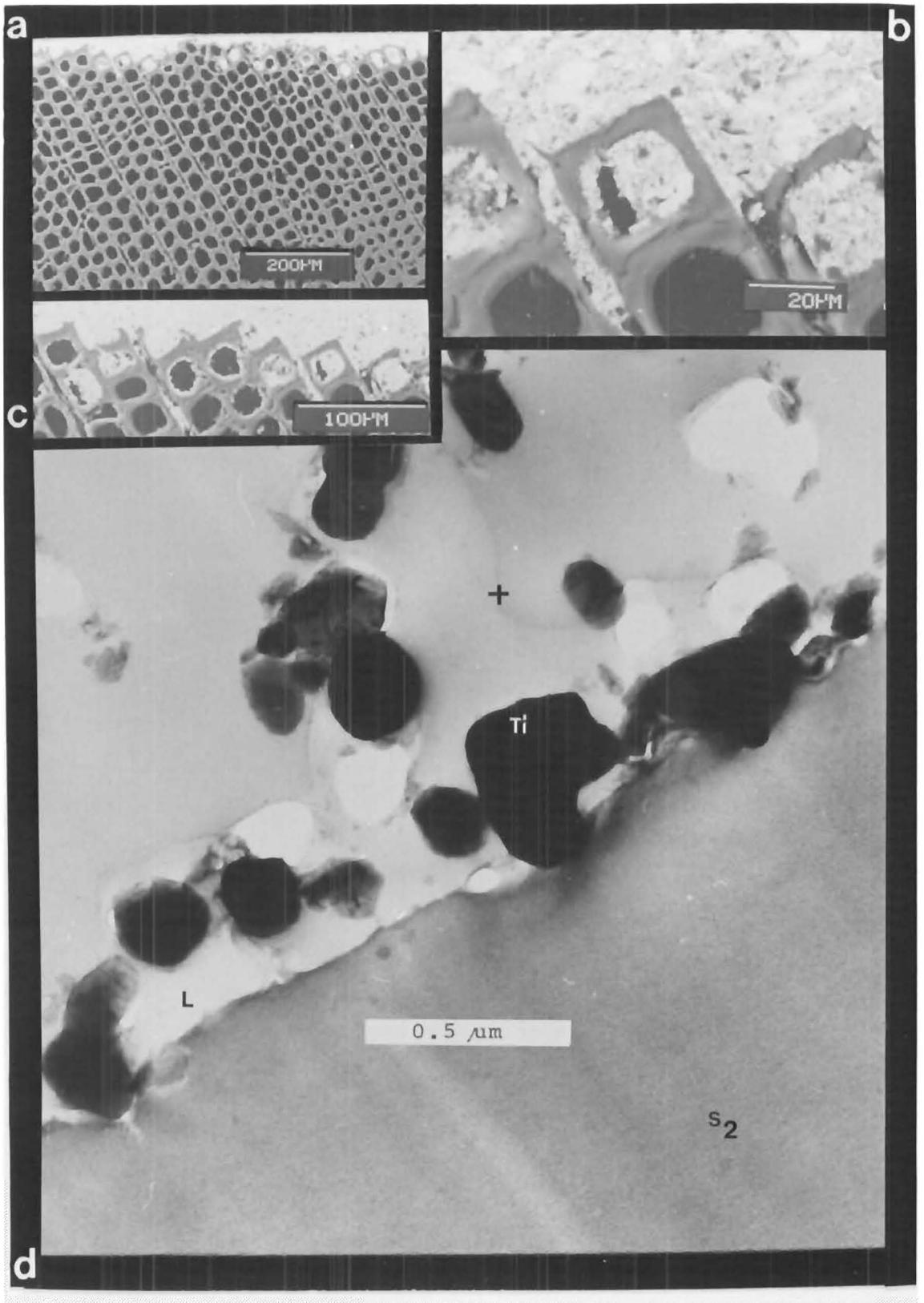

FIGURE 15 (T.F. / T.S.). RIMU COATED WITH EPIGLASS WATER BASED WOOD PRIMER.

A Earlywood → latewood. (BSEI / SEM).

B & C Details of fig. A.

D Ultra-thin, uranyl acetate - lead citrate stained Spurr's resin embedded section showing coating / tracheid wall interfacial region.
Note the titanium pigment particles lodged against the secondary wall. (TEM).

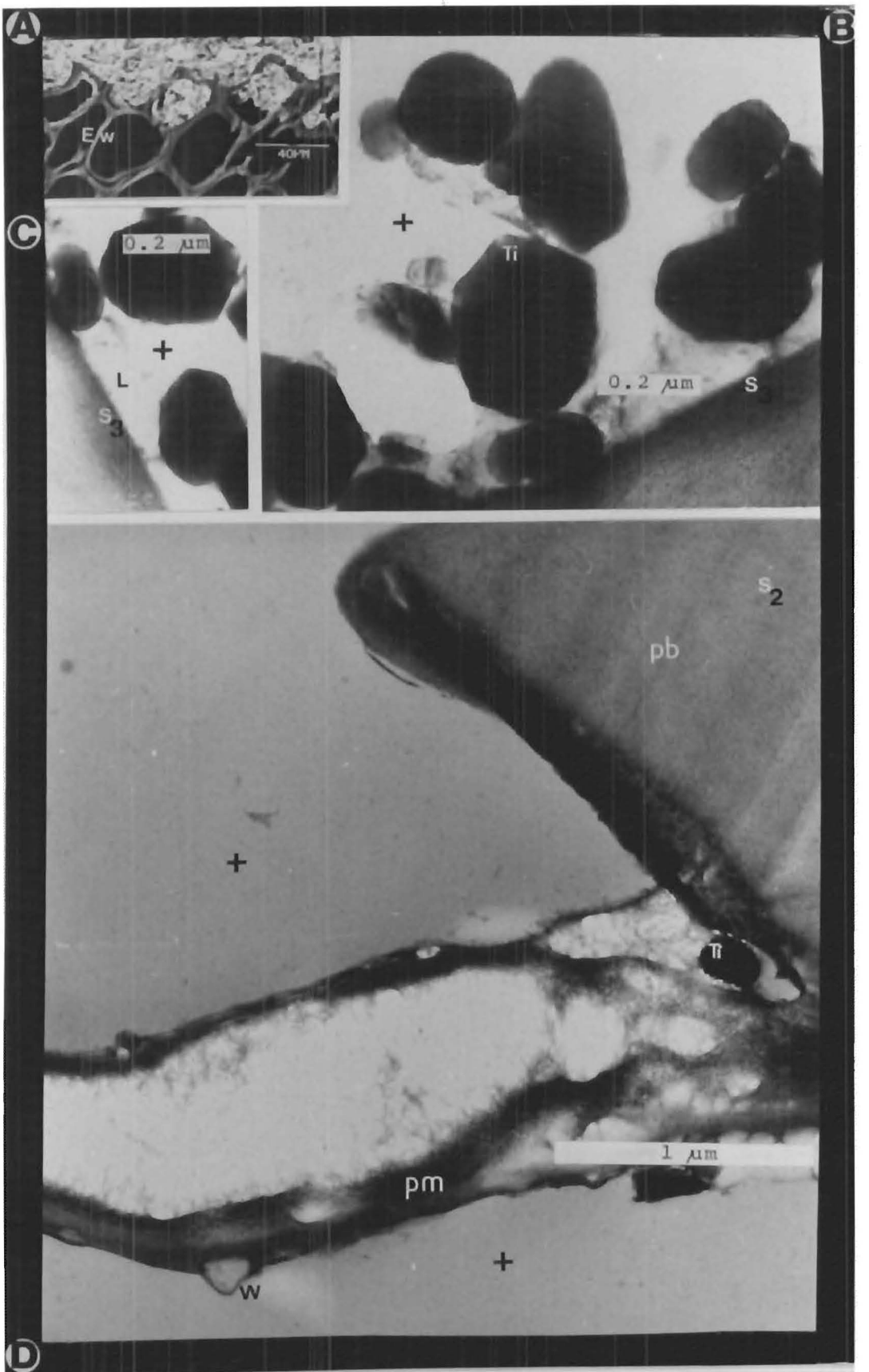

FIGURE 16 (T.F./T.S.) *P.dacrydioides* COATED WITH EPIGLASS WATER BASED WOOD PRIMER.

A Earlywood. (BSEI / SEM).

B & C Ultra-thin, uranyl acetate - lead citrate stained, Spurr's resin embedded sections showing coating / tracheid wall interface

D Titanium particle wedged in pit membrane. (TEM)

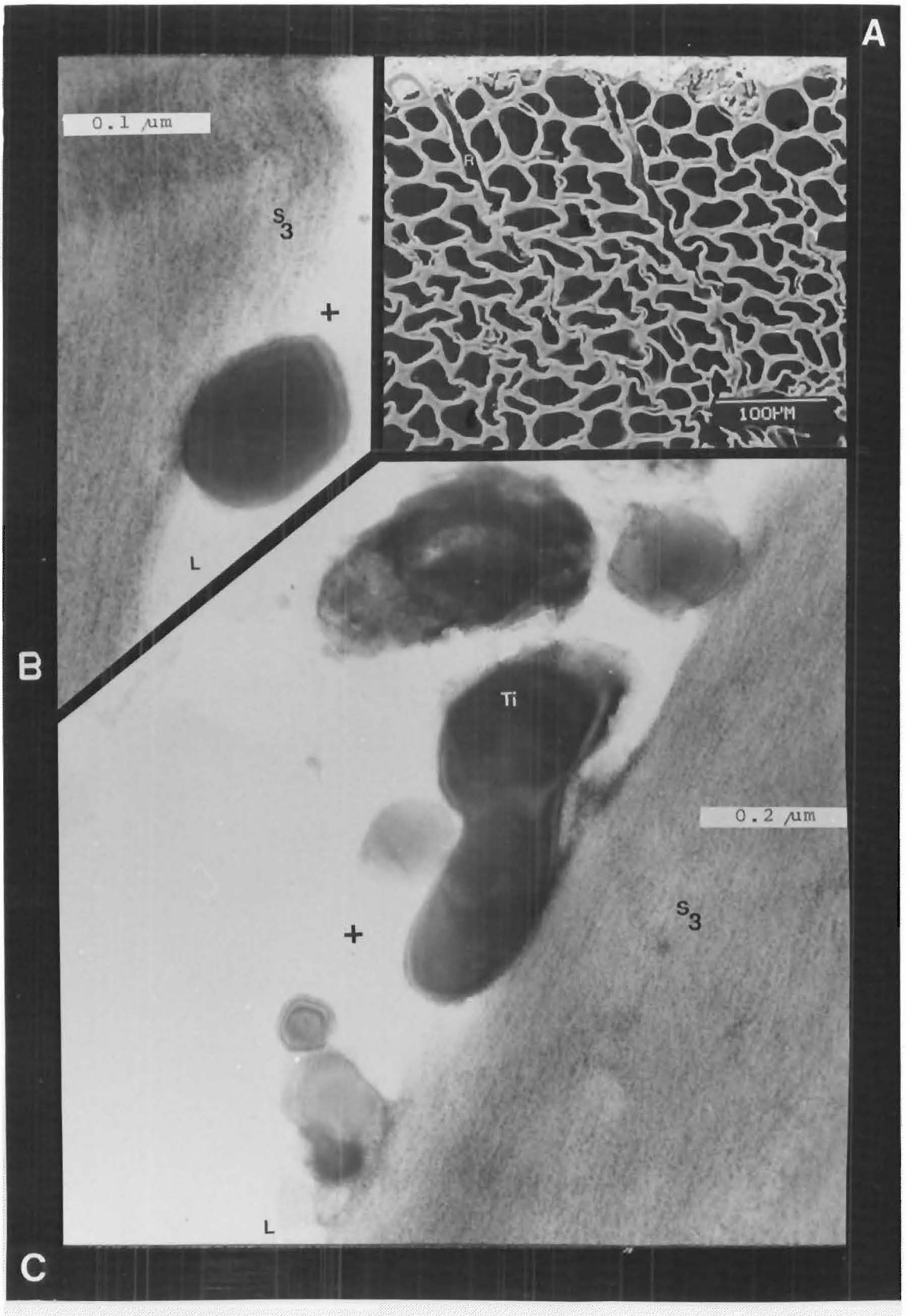

FIGURE 17 (T.F. / T.S.) RADIATA PINE COATED WITH EPIGLASS WATER BASED WOOD PRIMER.

A Earlywood. (BSEI / SEM).

B & C Ultra-thin, uranyl acetate - lead citrate stained Spurr's resin embedded sections showing coating / tracheid wall interfacial region.
Note the range of pigment sizes. (TEM).

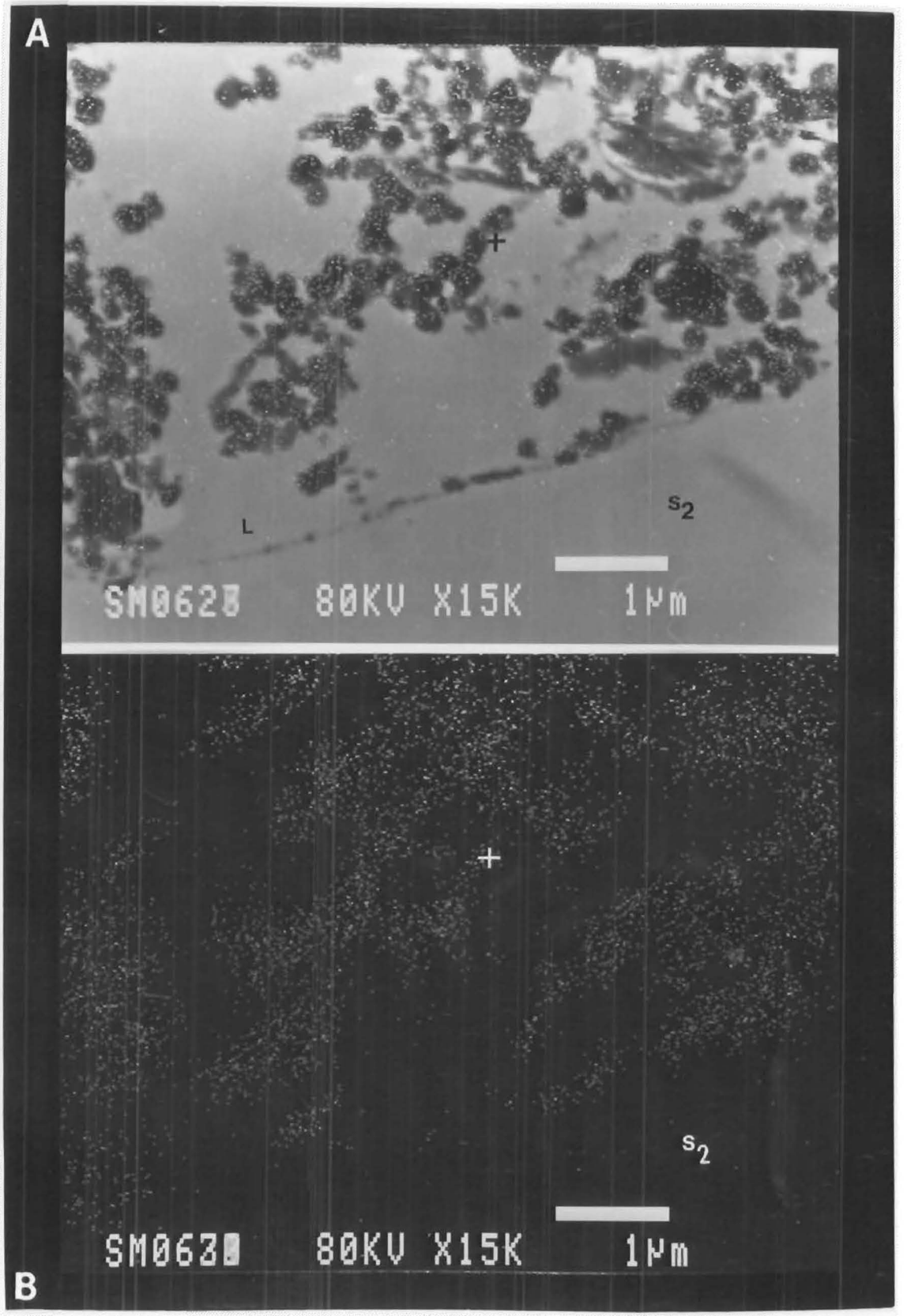

FIGURE 18 (T.S.). RADIATA PINE COATED WITH EPIGLASS WATER BASED WOOD PRIMER.

A Ultra-thin, unstained section showing coating/tracheid secondary wall interface. (STEM). Note the superimposed (Ti-K) X-ray map.

B (Ti-K) X-ray map.

4.6 TAUBMANS PREMIUM FAST COAT WOOD PRIMER COATED WEATHERBOARDS

Figures 19 to 21 show that like the other two water based primers this oil modified water based primer exhibits similar coating/substrate relationships on *D. cupressinum, P. dacrydioides* and *P. radiata* weatherboards. Penetration is one to three cells deep; influenced by machining quality and wood density.

The cell corner middle lamella region depicted in figure 20 [A] was ruptured during machining to expose the primary wall and intercellular region.

The titanium particles are easily identified but the X-ray was unable to detect the band of tiny particles seen at the lower left portion of this unstained section of *P. dacrydioides*. Given the opportunity to travel along ray cells the coating has the potential to move long distances. Figures 21 [B] and [C] shows several coating filled ray cells traversing early/latewood boundaries and the epithelial cell region surrounding a resin canal.

In, summary these three water based primers essentially show similar behavioural trends on the three weatherboard substrates although they are formulated by different paint manufacturers.

4.7 DULUX WUNDERPRIME COATED WEATHERBOARDS

Figures 22 to 26 depict the coating/substrate interface of *D. cupressinum, P. dacrydioides* and *P. radiata* weatherboards.

Penetration depth is one to two cells deep but occasionally three cells deep in the earlywood zone. The distance of ray parenchyma penetration in *P. radiata* is further than that for the two endemic taxa (figure 24 [A] and [B]).

The layered structure of the secondary cell wall is clearly delineated in figures 22 [D], 23 [F], 24 [C] and 26 [A] and there is no visual evidence of coating penetration into the unstained cell walls.

The growth rings of *P. dacrydioides* are very narrow (figure 23 [A] - [C]) and the coating appears to bridge over the thick walled small lumened latewood tracheids and fill the partly opened large thin walled earlywood tracheids.

Stained sections viewed at very high magnifications reveal the presence of tiny particles lining the S_3 wall layer in *P. radiata* (figures 24 [D], [E] and 25). These particles were too small to be identified by X-ray but are too large to be artifacts of staining so presumably are other extender pigments present in this oil based alkyd primer.

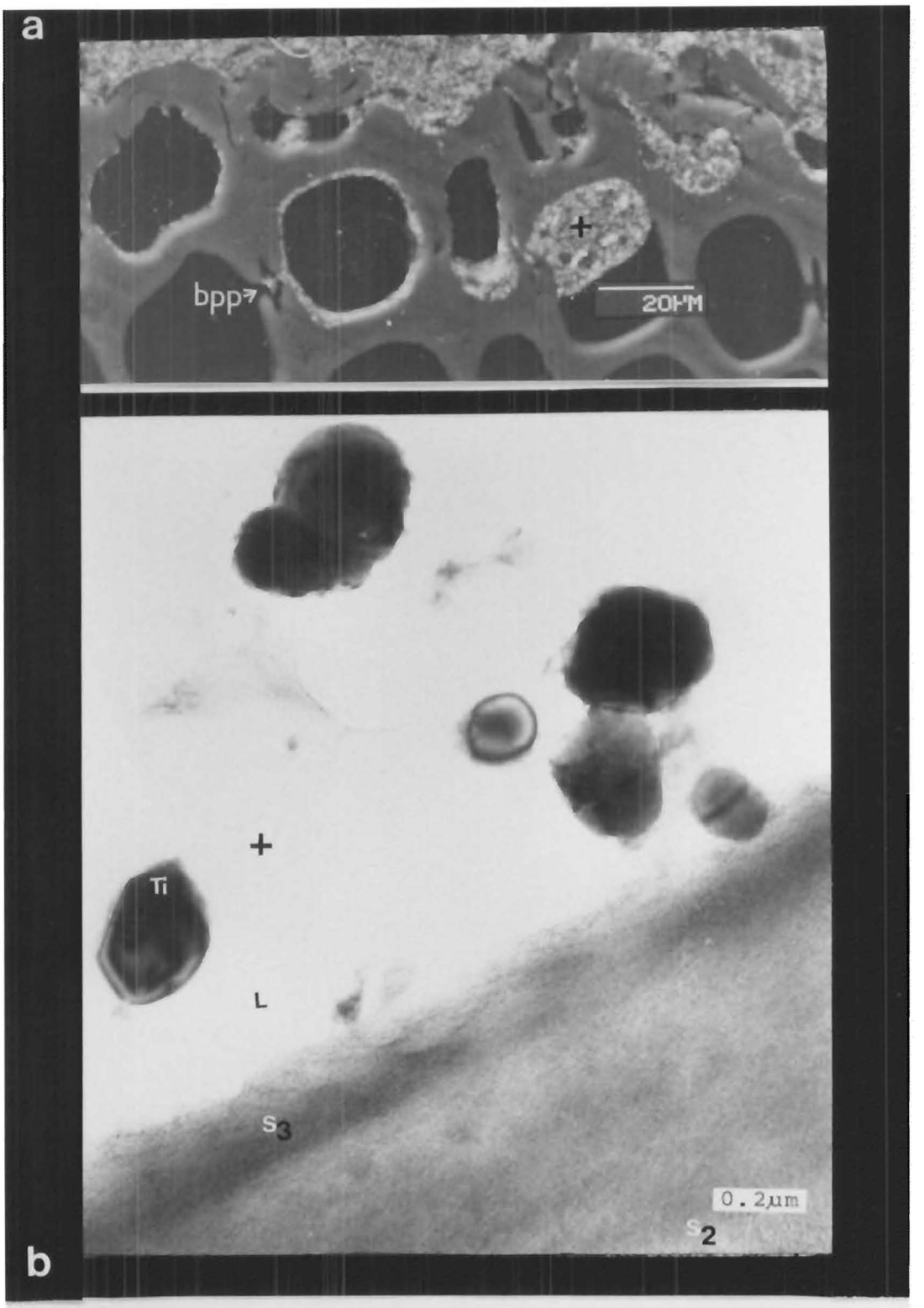

FIGURE 19 **(T.F./T.S.). *D.cupressinum* COATED WITH TAUBMANS PREMIUM FAST COAT WOOD PRIMER.**

A Note the partly filled lumens and coating in the chambers of the bordered pits.(BSEI/SEM).

B Ultra-thin, uranyl acetate - lead citrate stained, Spurr's resin embedded sections showing coating / tracheid wall interface. (TEM).

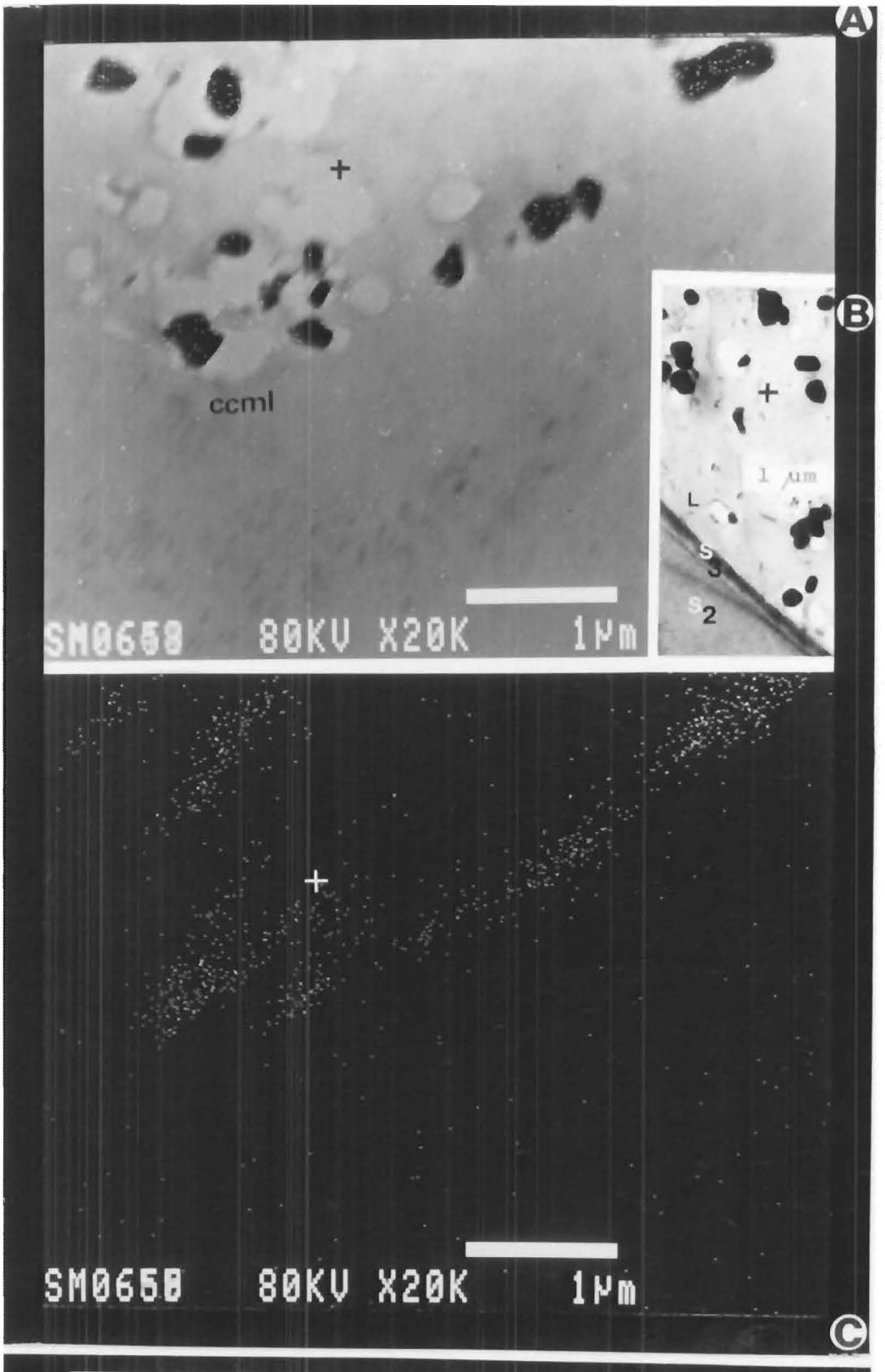

FIGURE 20 (T.F./T.S.). *P.dacrydioides* COATED WITH TAUBMANS PREMIUM FAST COAT WOOD PRIMER.(w.b.)

A Ultra-thin, uranyl acetate - lead citrate stained Spurr's resin embedded section through the middle lamella region that was exposed to machining. Note the superimposed (Ti-K) x-ray map. (STEM).

B Coating / substrate interface. (TEM).

C Corresponding EDXA element (Ti-K) x-ray map for fig.A. (STEM).

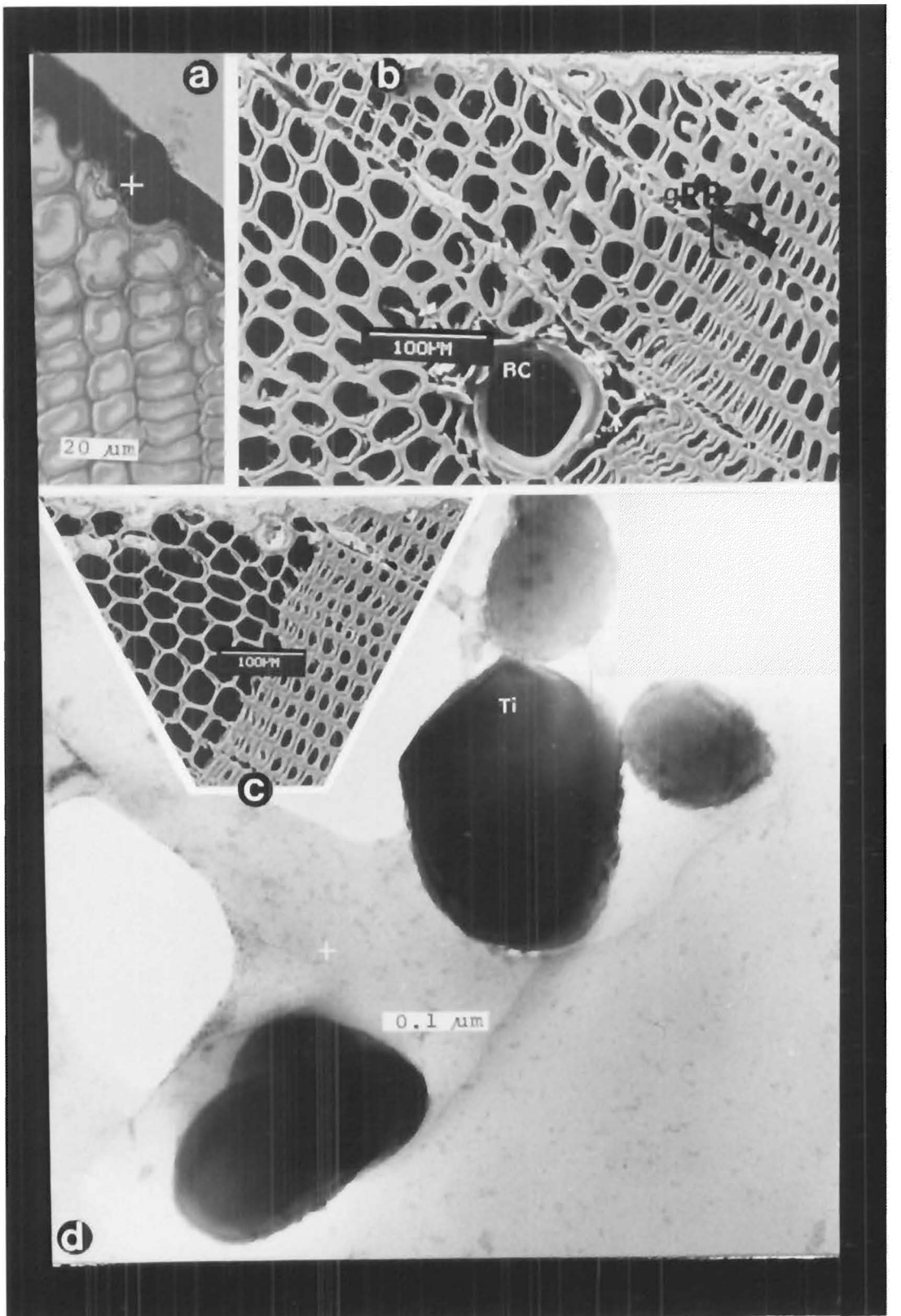

FIGURE 21 (T.F./T.S.). *P.radiata* COATED WITH TAUBMANS PREMIUM FAST COAT WOOD PRIMER.(w.b.)

A Toluidine Blue stained unembedded section through earlywood - latewood. (LM).

B & C Note the growth ring boundary and resin canal. (BSEI / SEM)

D Ultra-thin section through the coating.(TEM).

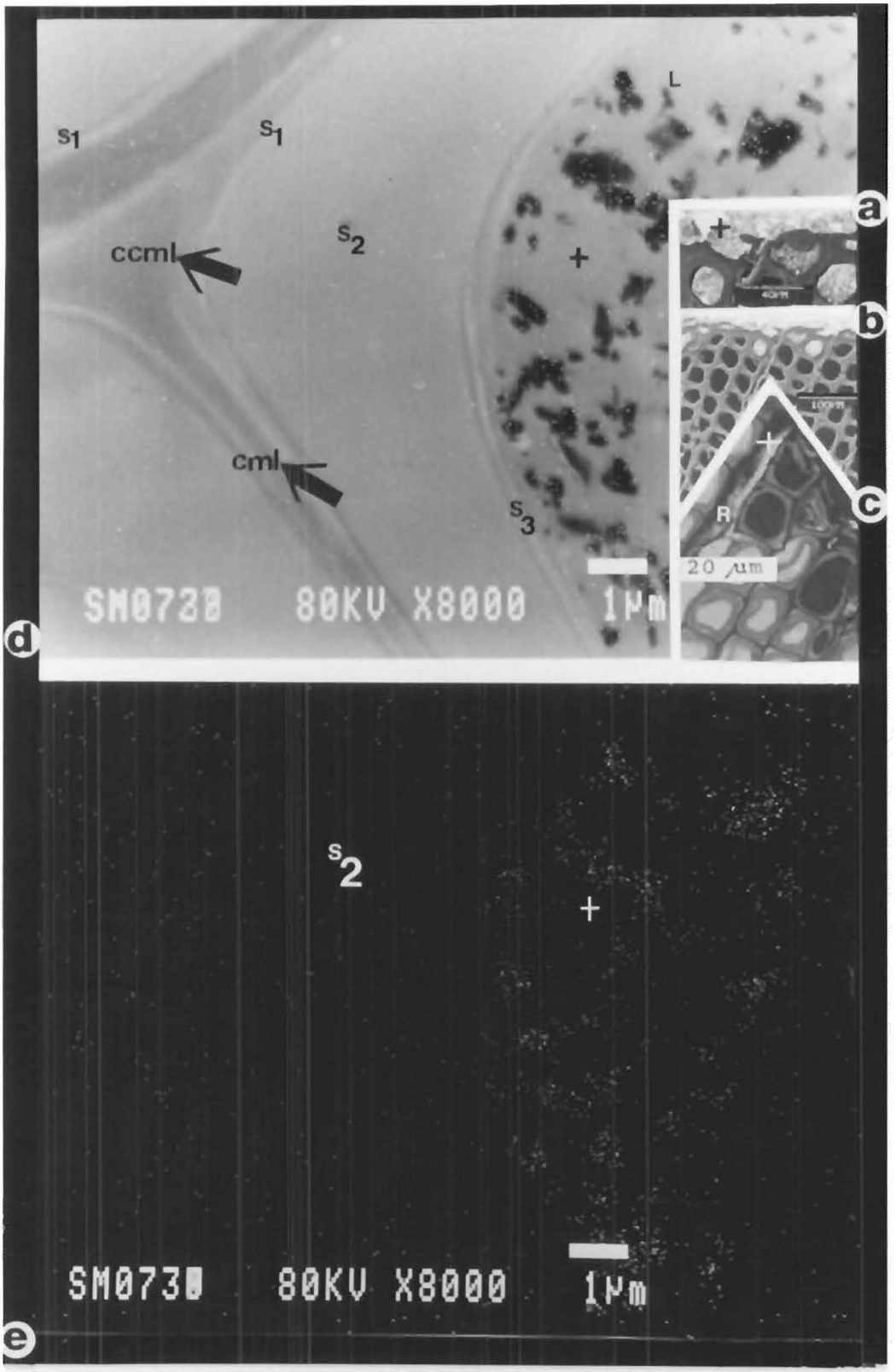

FIGURE 22 (T.F./T.S.). *D.cupressinum* COATED WITH DULUX WUNDERPRIME. (s.b.).

A & B Coating / substrate interface. (Fig.A. detail of B.) (BSEI / SEM).

C Toluidine Blue stained unembedded section through earlywood. (LM).

D Ultra-thin, unstained section of coating / tracheid wall interface. (STEM).

E Corresponding EDXA element (Ti-K) x-ray map of fig.D. (STEM)

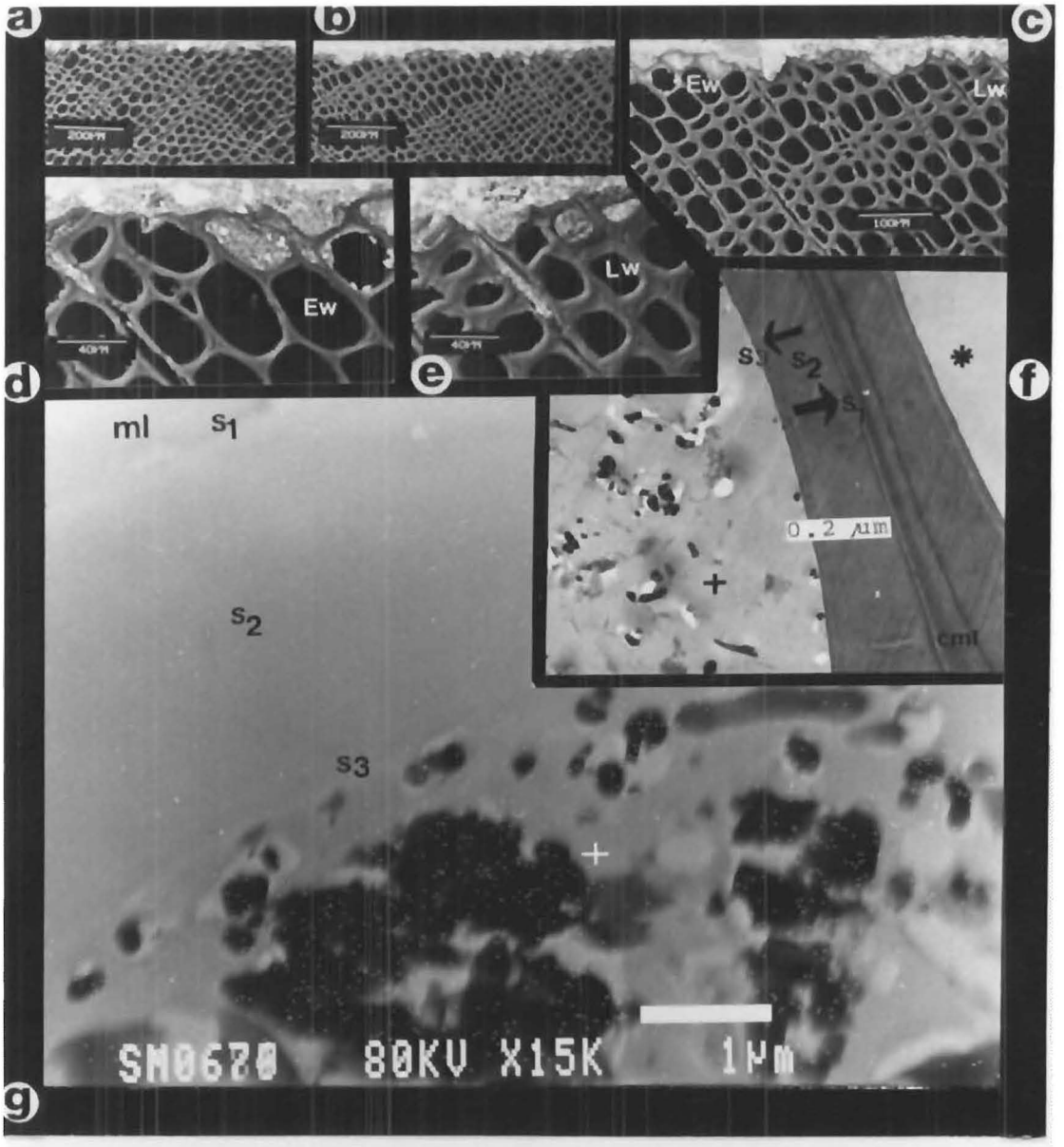

FIGURE 23 **(T.F./T.S.). *P.dacrydioides* COATED WITH DULUX WUNDERPRIME. (s.b.).**

A, B & C Sections through several growth rings. (BSEI / SEM)

D & C Earlywood and latewood details of fig.C. (BSEI / SEM)

F Ultra-thin, uranyl acetate - lead citrate stained, Spurr's resin embedded section through adjacent tracheary elements showing full and empty cell lumens. (TEM).

G Superimposed EDXA element (Ti-K) x-ray map on an unstained ultra-thin section showing the coating / tracheid cell wall interface. (STEM).

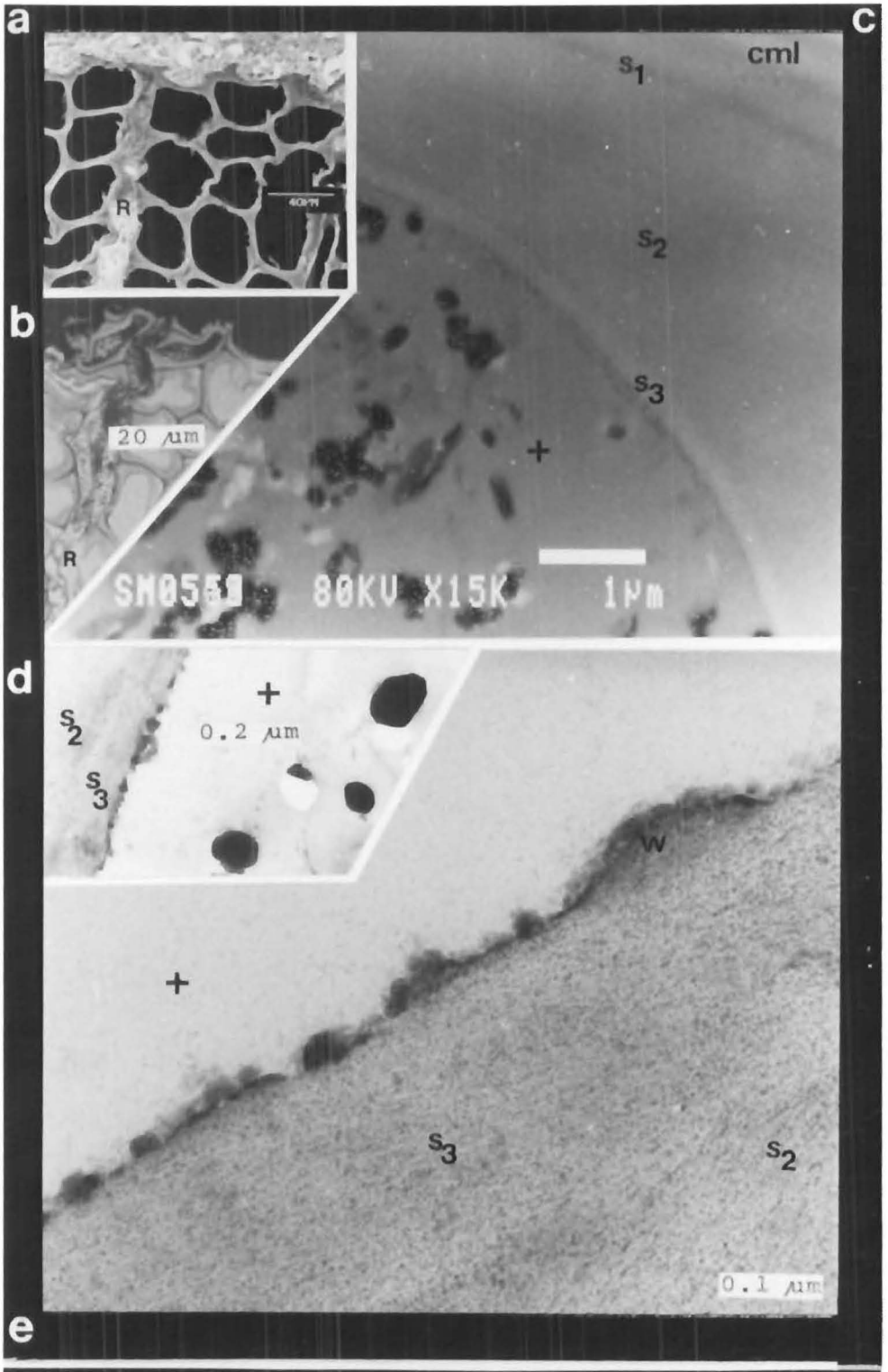

FIGURE 24 **(T.F./T.S.). *P.radiata* COATED WITH DULUX WUNDERPRIME. (s.b.).**

A Earlywood. (BSEI / SEM).

B Toluidine Blue stained, unembedded section through earlywood. (LM).

C Superimposed EDXA element (Ti-K) x-ray map on unstained ultra-thin section showing the relationship between coating and tracheid cell wall (STEM).

D & E Ultra-thin, uranyl acetate - lead citrate stained, Spurr's resin embedded sections showing coating / tracheid wall interface.(TEM).

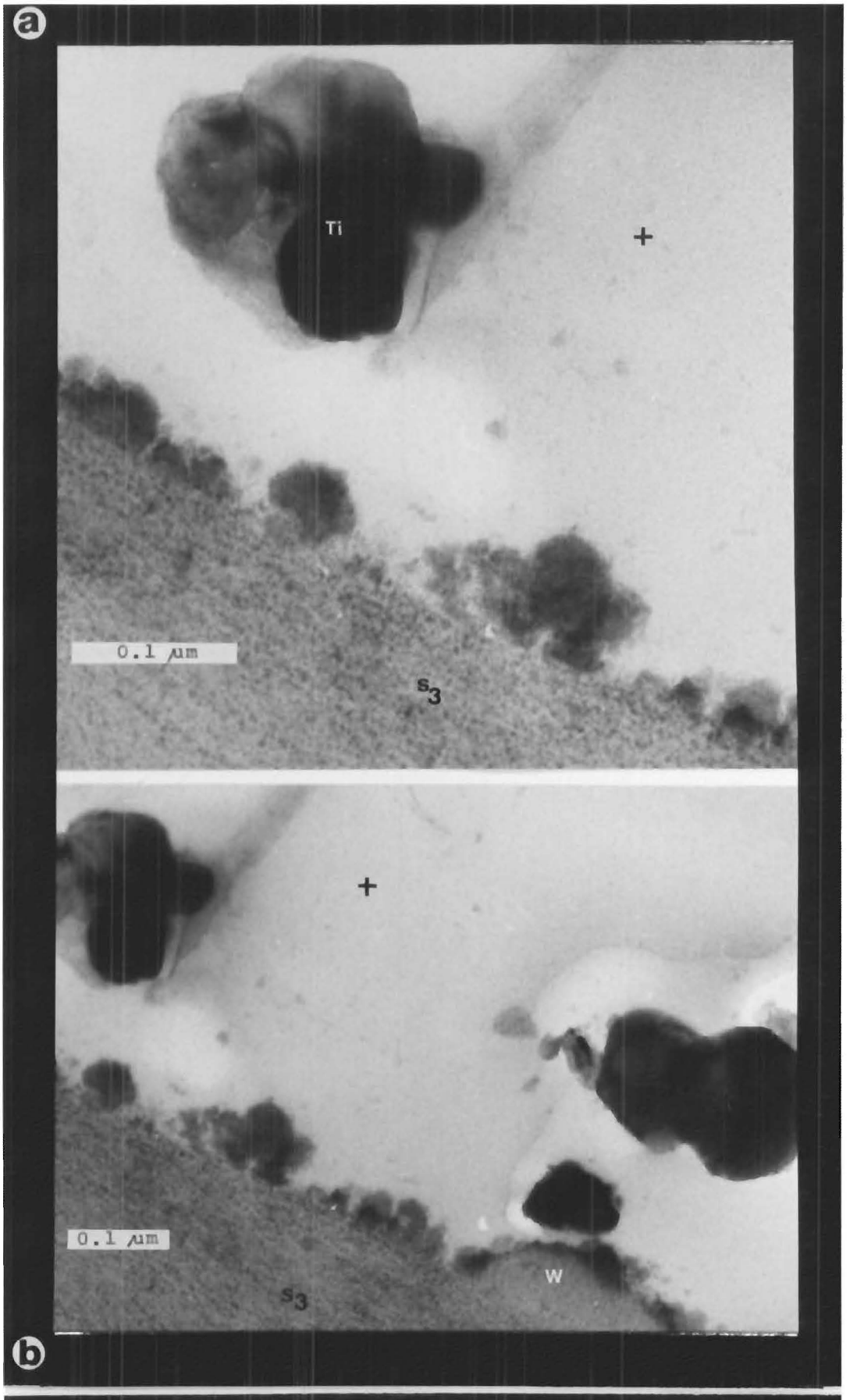

FIGURE 25 **(T.S.) *P.radiata* COATED WITH DULUX WUNDERPRIME. (s.b.).**
A & B Ultra-thin, uranyl acetate - lead citrate stained section. Coating / tracheid interface (TEM)

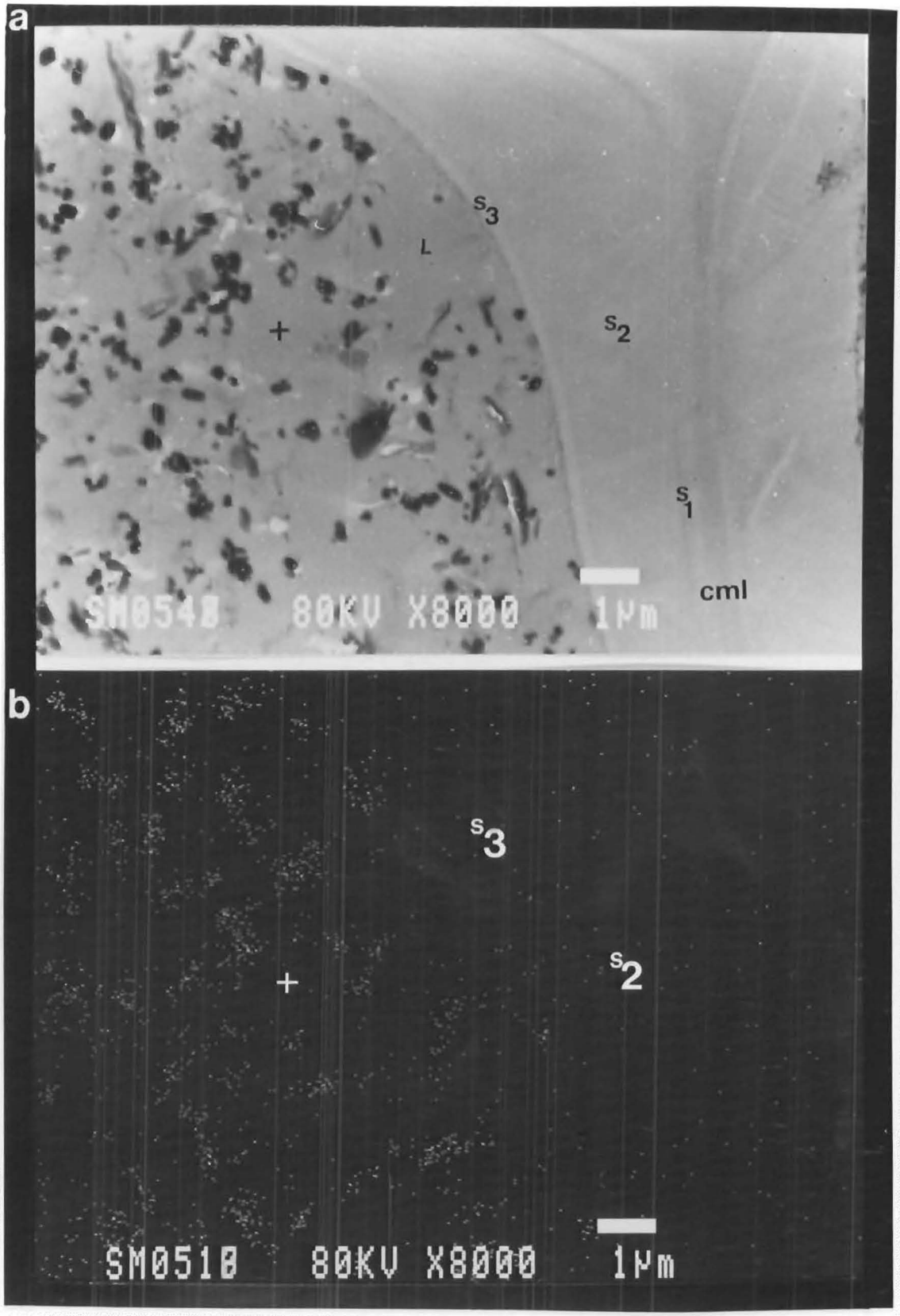

FIGURE **26** (T.S.) RADIATA PINE COATED WITH DULUX WUNDERPRIME. (s.b.).

A Ultra-thin, unstained section through coating and tracheid cell walls.
Note the superimposed (Ti-K) X-ray map.(STEM).

B Corresponding EDXA element (Ti-K) X-ray map for fig.A. (STEM).

4.8 EPIGLASS 1st COAT WOOD PRIMER ON WEATHERBOARDS

Figures 27 to 29 show gross penetration of this long oil alkyd primer into cell lumens of *D. cupressinum*, *P. dacrydioides* and *P. radiata* weatherboards.

Penetration is typically one to two cells deep but three cells have been recorded.

The extent of ray parenchyma penetration is minimal; being only as deep inwards as the third tracheid cell when viewed in transverse section. The simple pit membrane between ray parenchyma and tracheid cells prevents coating migration through the pits when it lies in the median position as in figure 27 [D] or has deflected to one side as in figure 28 [B] and [C]. The titanium particles abut the membrane but the mechanical action is not strong enough to rupture the membrane.

4.9 EPIGLASS G.P.182 OIL BASED ALKYD PRIMER ON WEATHERBOARDS

Figures 30 to 35 illustrate coating behaviour in the vicinity of bordered pits which occur in close proximity to the machined surfaces of *D. cupressinum*, *P. dacrydioides* and *P. radiata*.

Frequently the coating fills adjacent tracheid cell lumens and the pit chambers between (figures 30 [B], 34 [B] & [C] and 35). Often the coating appears to have burst through the pits but its flow was halted at some stage (figures 32 [C] & [D] and 33 [A]). Remnants of the pit membrane torn by machining may delay or arrest coating movement into surrounding cells. The pit membrane between ray parenchyma and tracheid cells is uniform and lacks the delicate structure of the margo (figure 30 [C]). Coating entry is also facilitated through fissures (figure 34 [A]).

4.10 TAUBMANS WOOD PRIMER ON WEATHERBOARDS

Figures 36 to 38 confirm the limited degree of penetration of this oil based primer on *D. cupressinum*, *P. dacrydioides* and *P. radiata* substrates.

Penetration is restricted to one or two cells deep and the behaviour of this coating is very similar to the other oil based solvent thinned primers previously reviewed. The bulk of the penetration is confined to the larger earlywood cell lumens opened by machining (figures 36 [A]-[C] and 37 [A] & [B]). As noted earlier with reference to the other primers, ray parenchyma penetration is greatest in *P. radiata* (figure 38).

The ultrathin sections reveal densely packed coating particles filling the cell lumens. X-ray maps for elements present in the coating showed no difference in particle distribution in earlywood and latewood cell lumens.

In summary, with the exception of all primers penetrating rays in *P. radiata* more deeply than in the podocarps, penetration behaviour showed negligible differences among taxa.

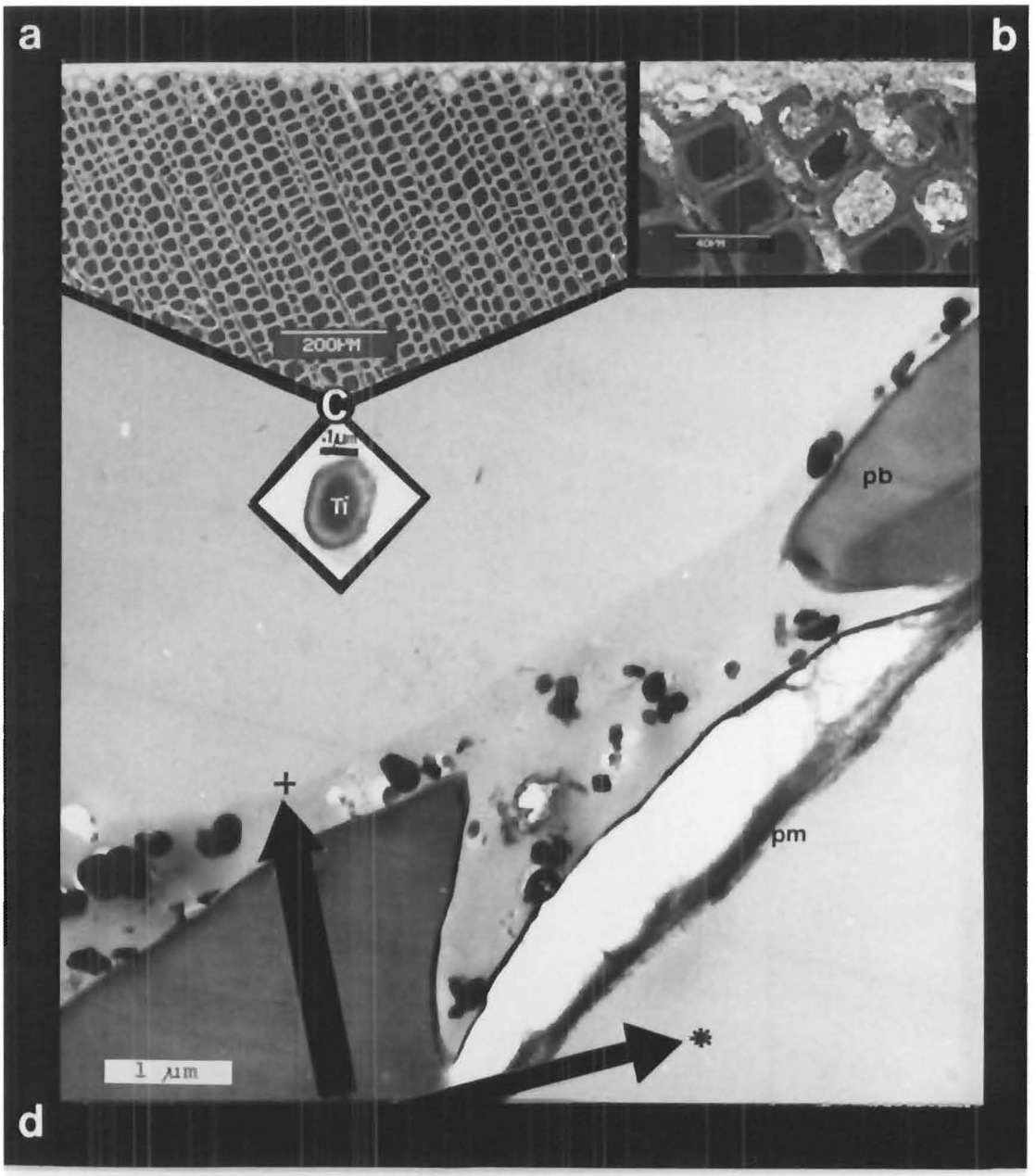

FIGURE 27 **(T.F./T.S.). *D.cupressinum* COATED WITH EPIGLASS 1st COAT WOOD PRIMER. (s.b.).**

A Latewood - earlywood. (BSEI / SEM).
B Detail of fig.A. (BSEI / SEM).
C Highly magnified Titanium particle. (TEM).
D Cupressoid cross-field pits between tracheid and ray parenchyma. Note the borders overarching the simple pit membrane and the coated and uncoated regions (arrowed). (TEM)

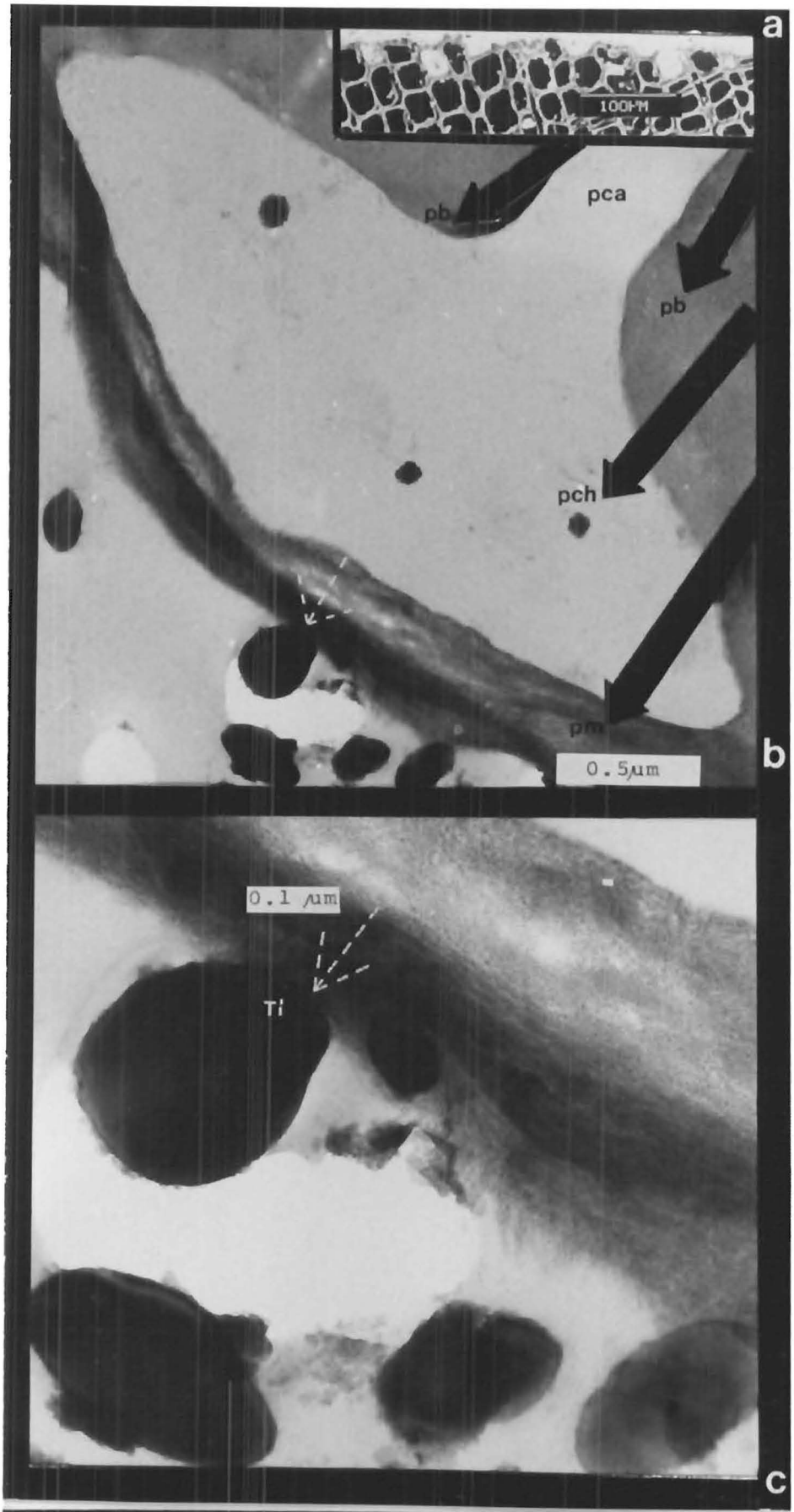

FIGURE 28 (T.F./T.S.). *P.dacrydioides* COATED WITH EPIGLASS 1st COAT WOOD PRIMER. (s.b.).
A Growth ring boundary. (BSEI / SEM).
B Ultra-thin, uranyl acetate - lead citrate stained section through a pit. C Detail of fig b

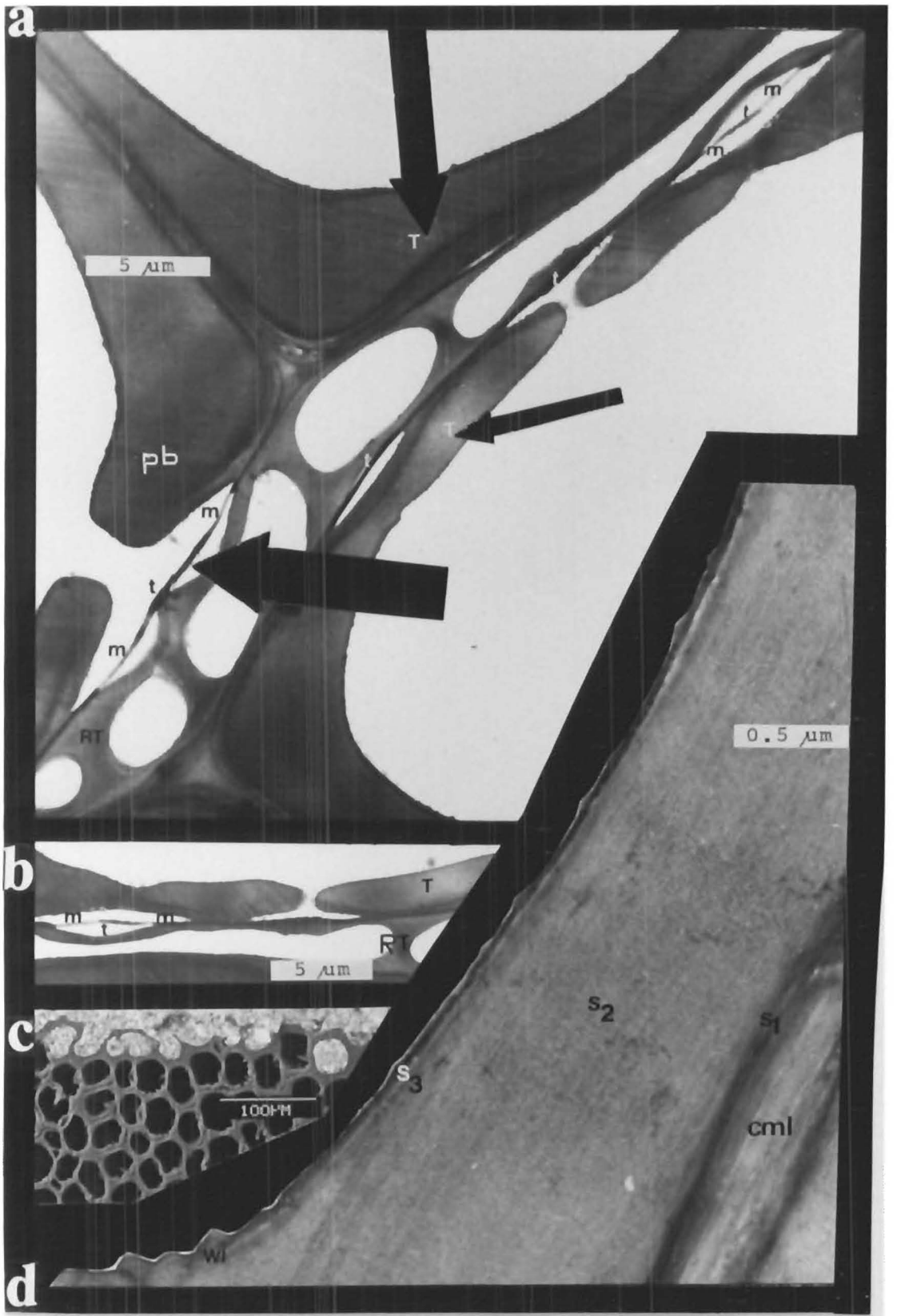

FIGURE 29 **(T.S./ T.F.) *P.radiata* COATED WITH EPIGLASS 1st COAT WOOD PRIMER.**

A & B Ultra-thin, uranyl acetate - lead citrate stained Spurr's resin embedded sections showing pits connecting tracheids to ray tracheid cells in an area beneath the coated zone. (TEM).

C Earlywood. (BSEI / SEM).

D Tracheid wall; note the warty layer. (TEM).

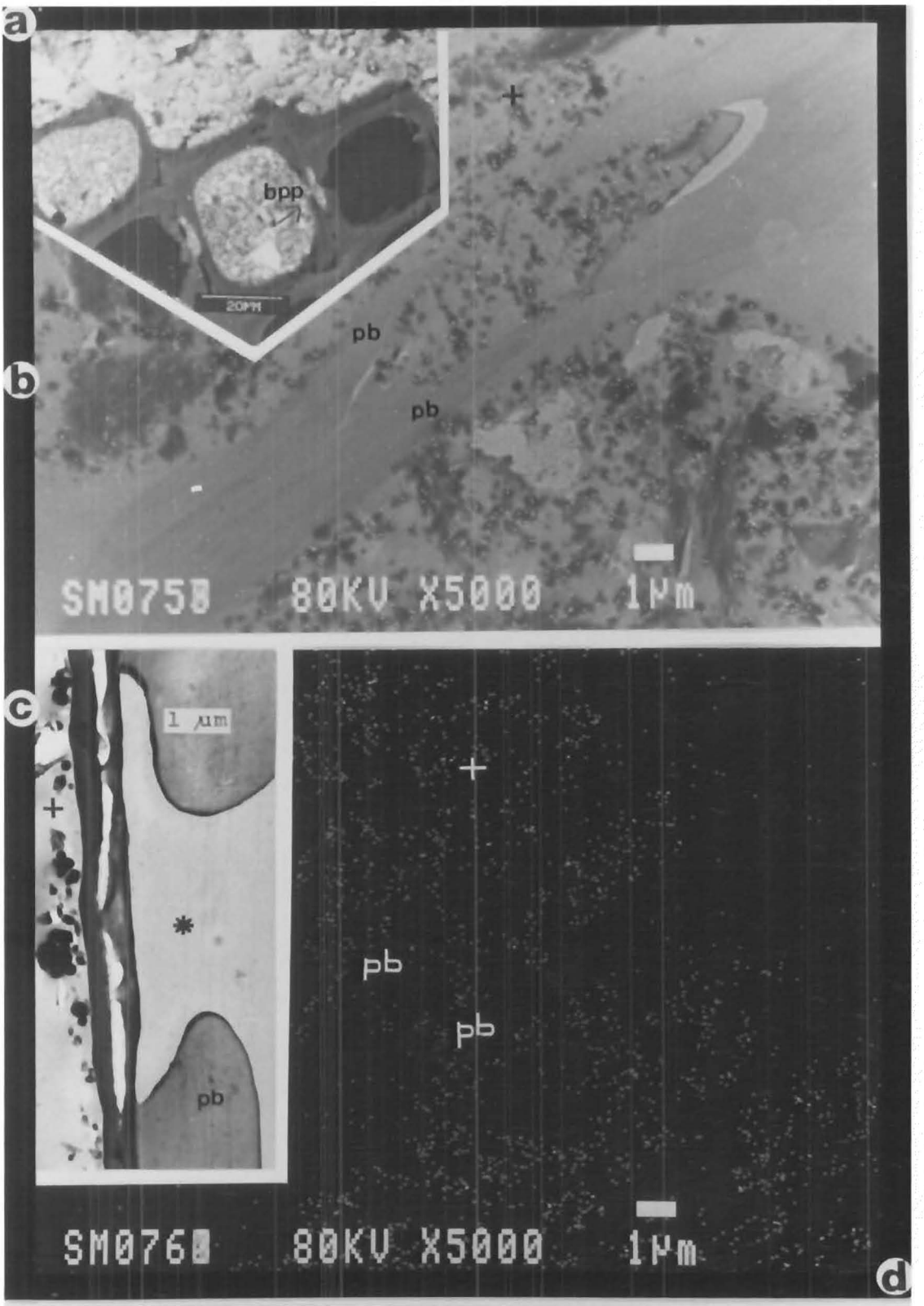

FIGURE 30 **(T.F./ T.S.) *D.cupressinum* COATED WITH EPIGLASS G.P. 182 OIL BASED ALKYD PRIMER (s.b).**

A Note the bordered pit pair between tracheary elements. (BSEI / SEM)

B Superimposed EDXA element (Ti-K) x-ray map on an ultra-thin section of a bordered pit pair.(STEM)

C Cupressoid cross-field pit between a ray parenchyma cell and a tracheid cell.

D Corresponding EDXA map (Ti-K) for fig.B.

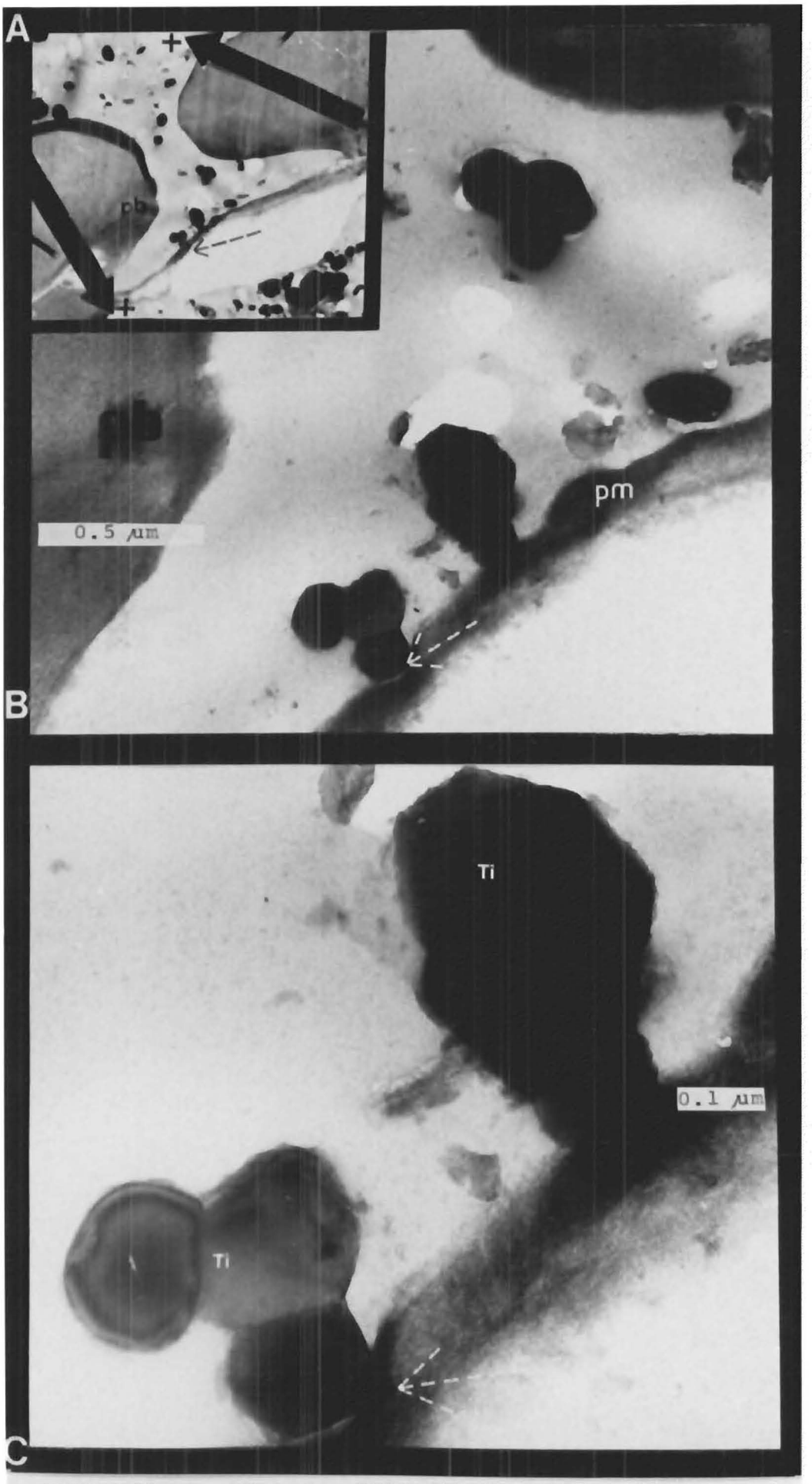

FIGURE 31 (T.S.) RIMU COATED WITH EPIGLASS G.P. 182 OIL BASED ALKYD PRIMER. (s.b.).

A,B & C Increasing magnifications of coating / pit border and membrane interface. (TEM

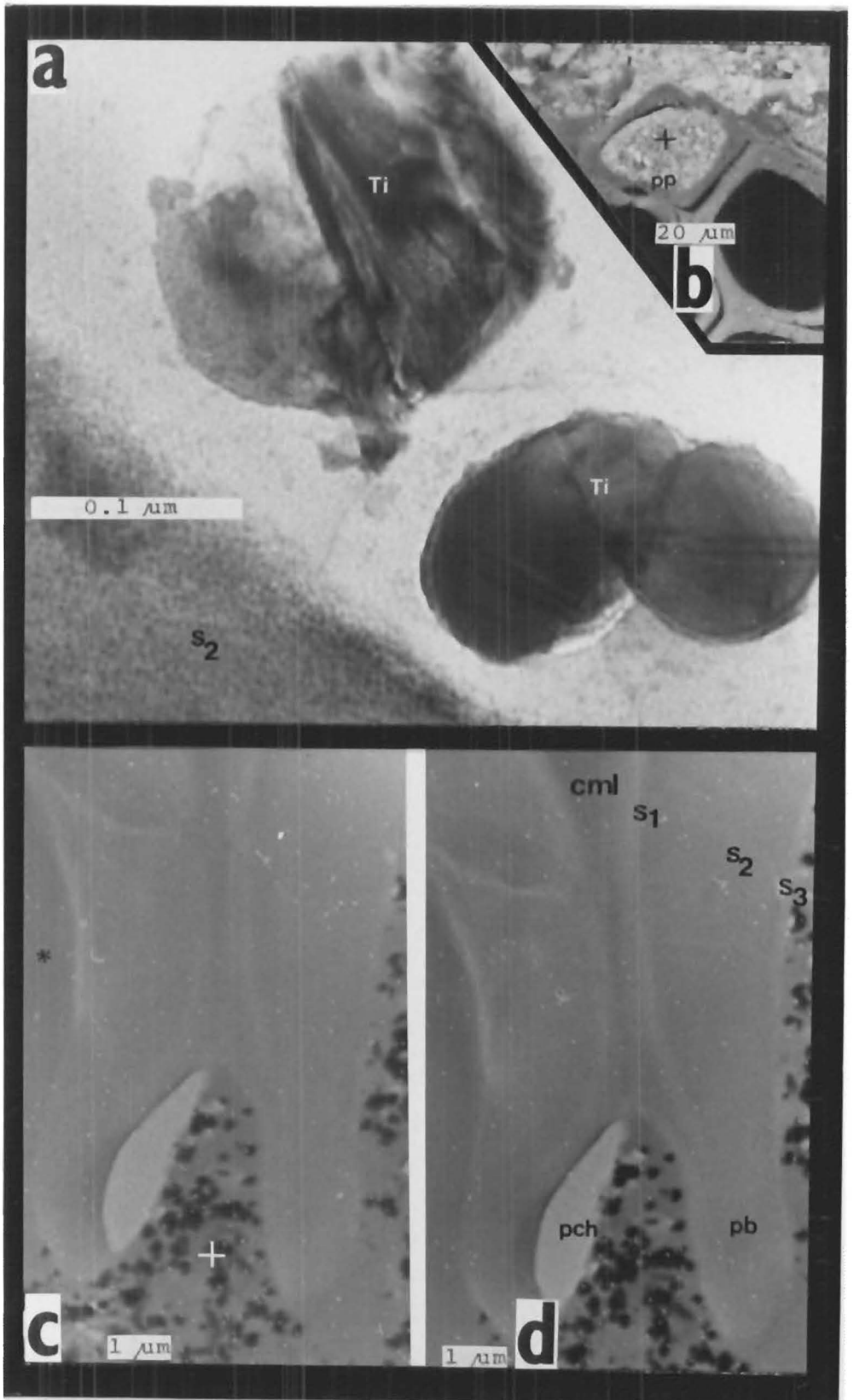

FIGURE 32 (T.F./ T.S.) *P.dacrydioides* **COATED WITH EPIGLASS G.P. 182 OIL BASED ALKYD PRIMER (s.b).**

A Note the intertracheid pits. (BSEI / SEM)

B Ultrathin, uranyl acetate - lead citrate stained embedded section through coating / wall interface.

C & D Superimposed EDXA element x-ray map of CCA treated wood. Unstained section showing intertracheid pits. Fig.C - Arsenic (AS-K); fig.D - Chrome (Cr-K).(STEM).

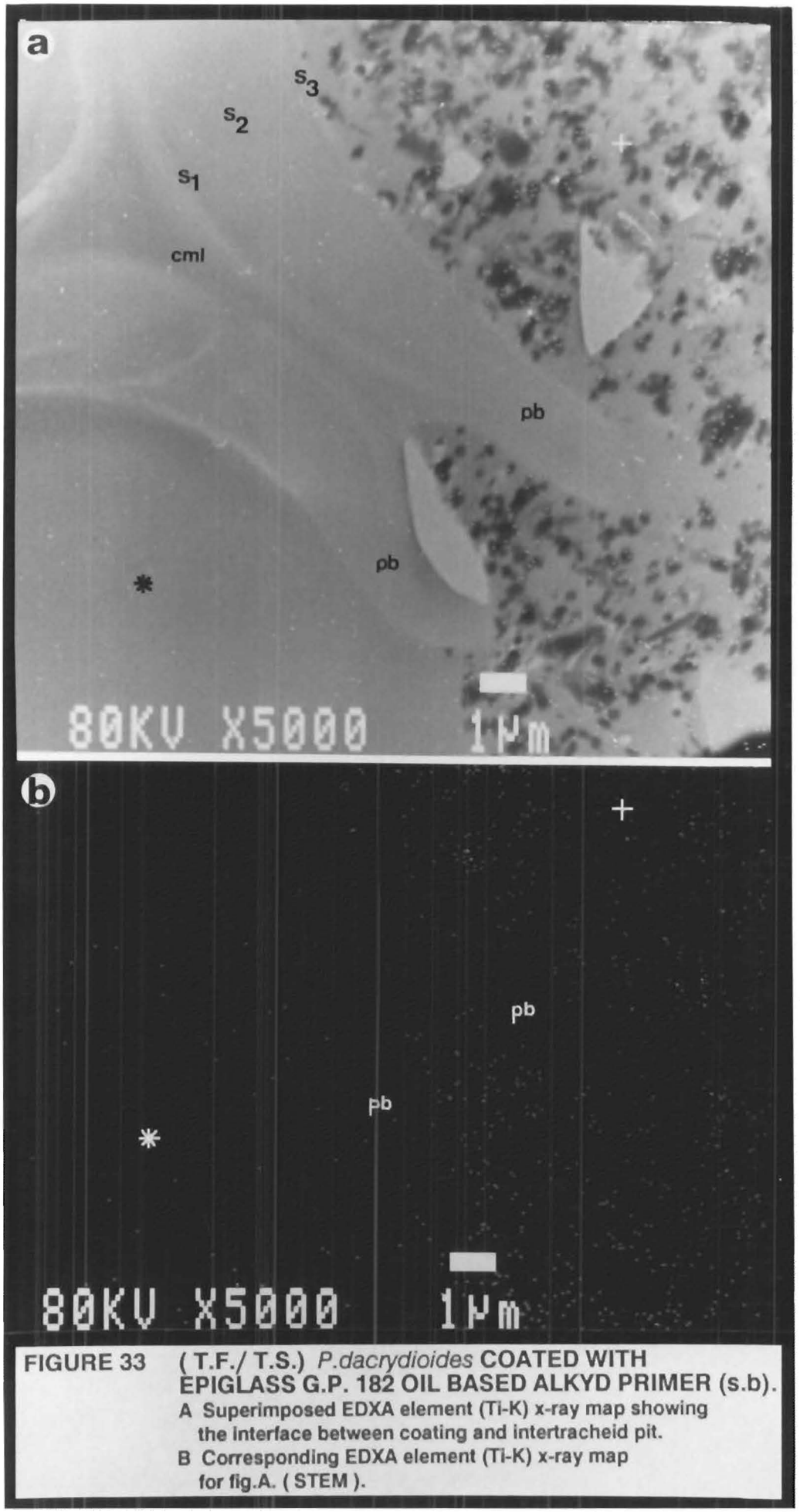

FIGURE 33 (T.F./ T.S.) *P.dacrydioides* COATED WITH EPIGLASS G.P. 182 OIL BASED ALKYD PRIMER (s.b).
A Superimposed EDXA element (Ti-K) x-ray map showing the interface between coating and intertracheid pit.
B Corresponding EDXA element (Ti-K) x-ray map for fig.A. (STEM).

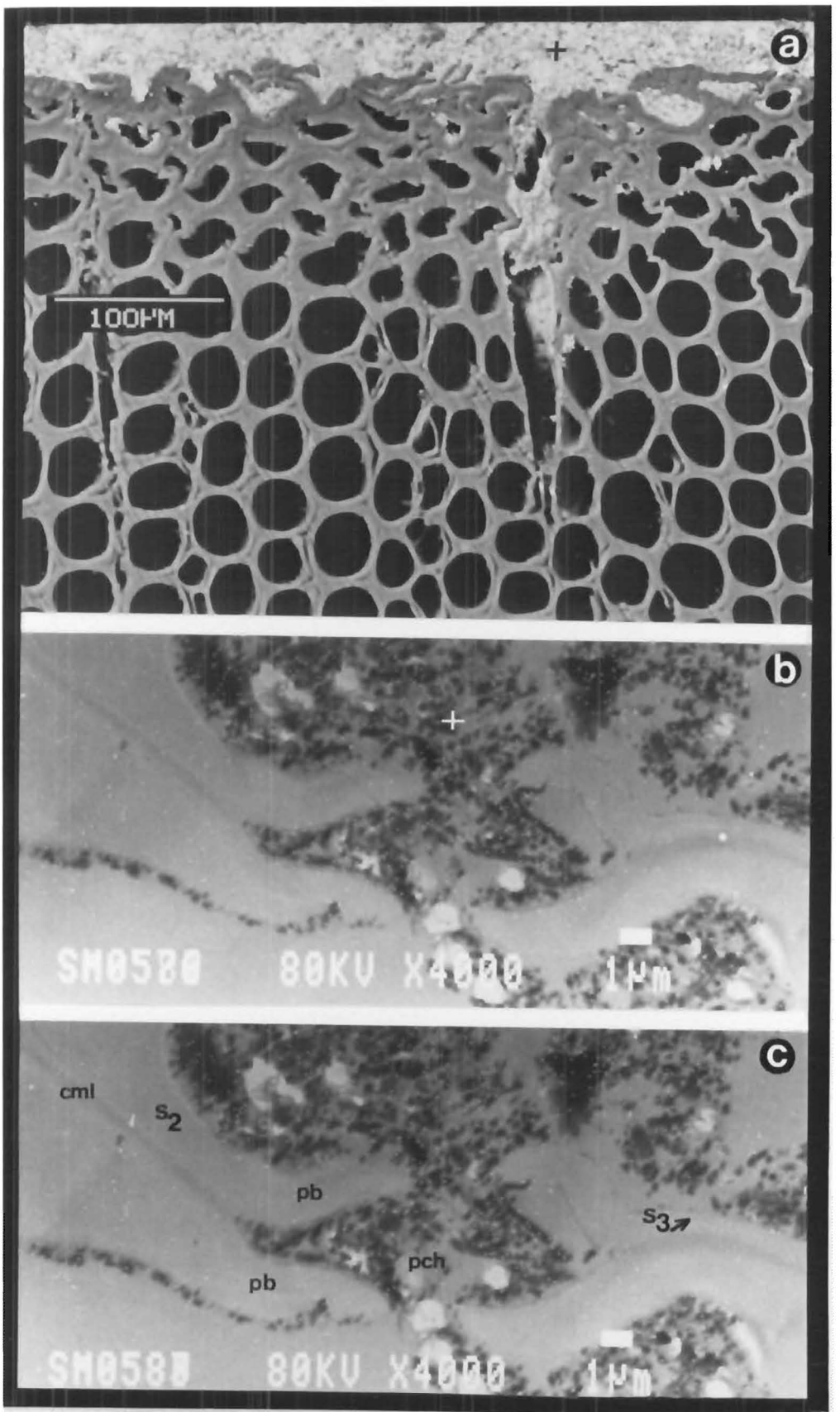

FIGURE 34 **(T.F./ T.S.) *P.radiata* COATED WITH EPIGLASS G.P.182 OIL BASED ALKYD PRIMER.(s.b.)**
A Machined surface of latewood cells.(BSEI/SEM)
B & C Superimposed EDXA element x-ray map of CCA treated wood. Unstained section. Intertracheid bordered pits.
Fig.B - Arsenic (As-K); fig.C - Chrome (Cr-K). (STEM).

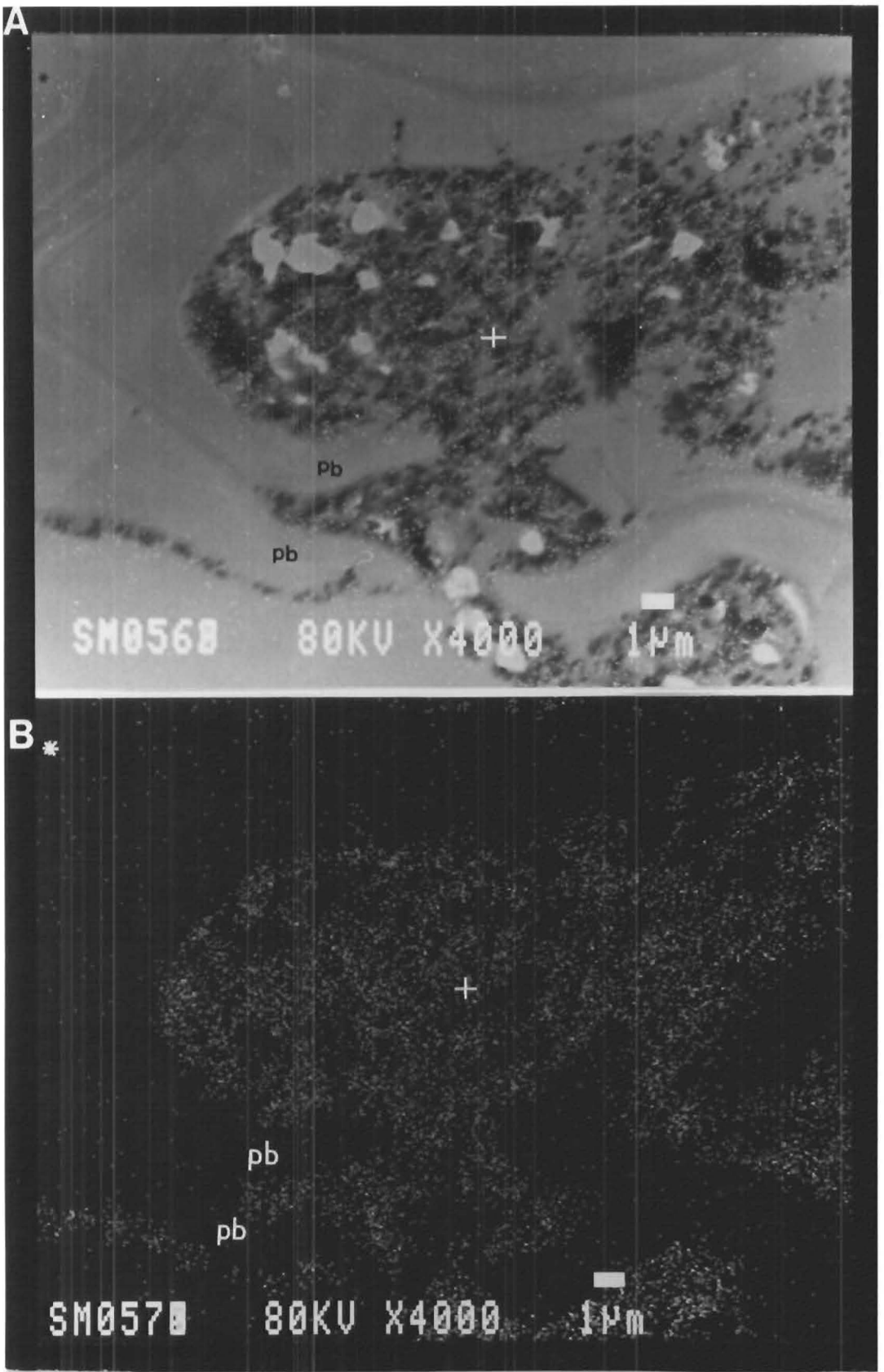

FIGURE 35 **(T.F./ T.S.) *P.radiata* COATED WITH EPIGLASS G.P.182 OIL BASED ALKYD PRIMER.(s.b.)**

A Superimposed EDXA element (Ti-K) x-ray map on ultra-thin, unstained section through intertracheid bordered pits.

B Corresponding EDXA element (Ti-K) x-ray map for fig.A. (STEM).

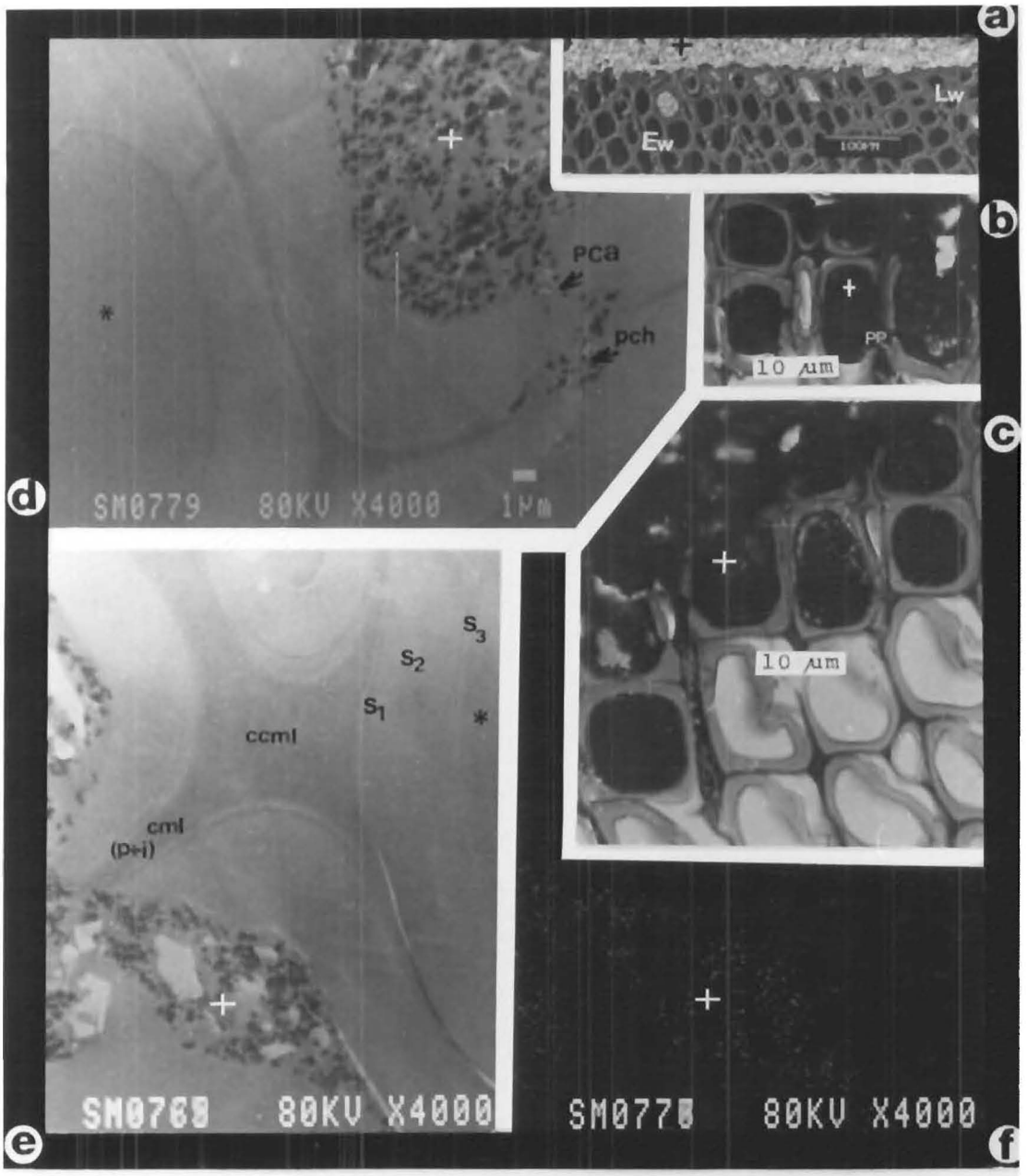

FIGURE 36 (T.F./ T.S.) *D.cupressinum* **COATED WITH TAUBMANS WOOD PRIMER. (s.b.)**

A Growth ring boundary. (BSEI / SEM).
B & C Toluidine Blue stained, unembedded sections (LM).
D & E Ultra-thin, uranyl acetate - lead citrate stained Spurr's resin embedded latewood sections showing the coating / tracheid wall interfacial region. (STEM).
F Corresponding EDXA element (TiK) x-ray map for fig.E. (STEM).

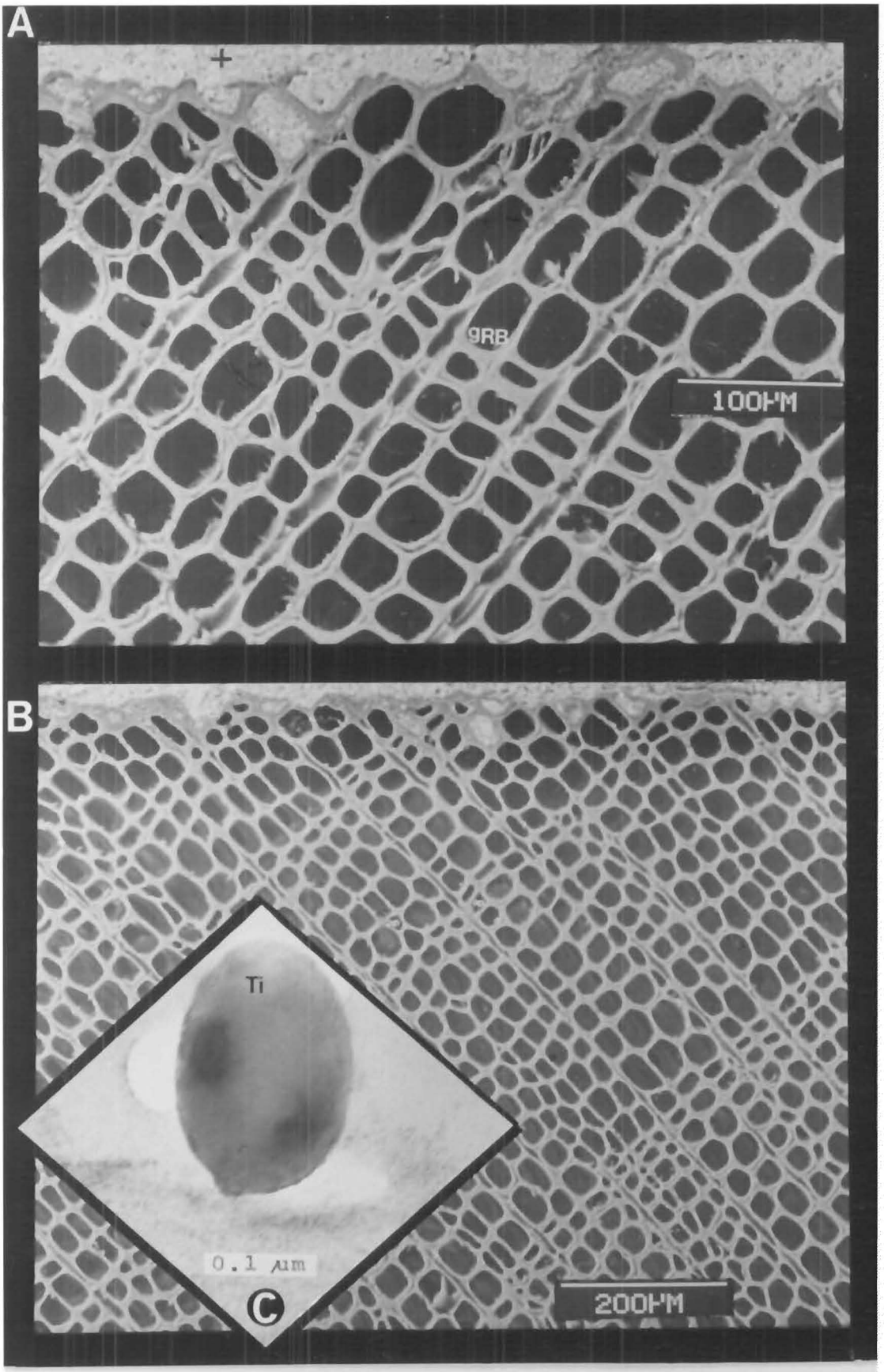

FIGURE 37 (T.F./ T.S.) *P.dacrydioides* **COATED WITH TAUBMANS WOOD PRIMER. (s.b.)**

A & B Growth rings and growth ring boundaries. (BSEI/SEM).

C A titanium pigment particle highly magnified.(TEM).

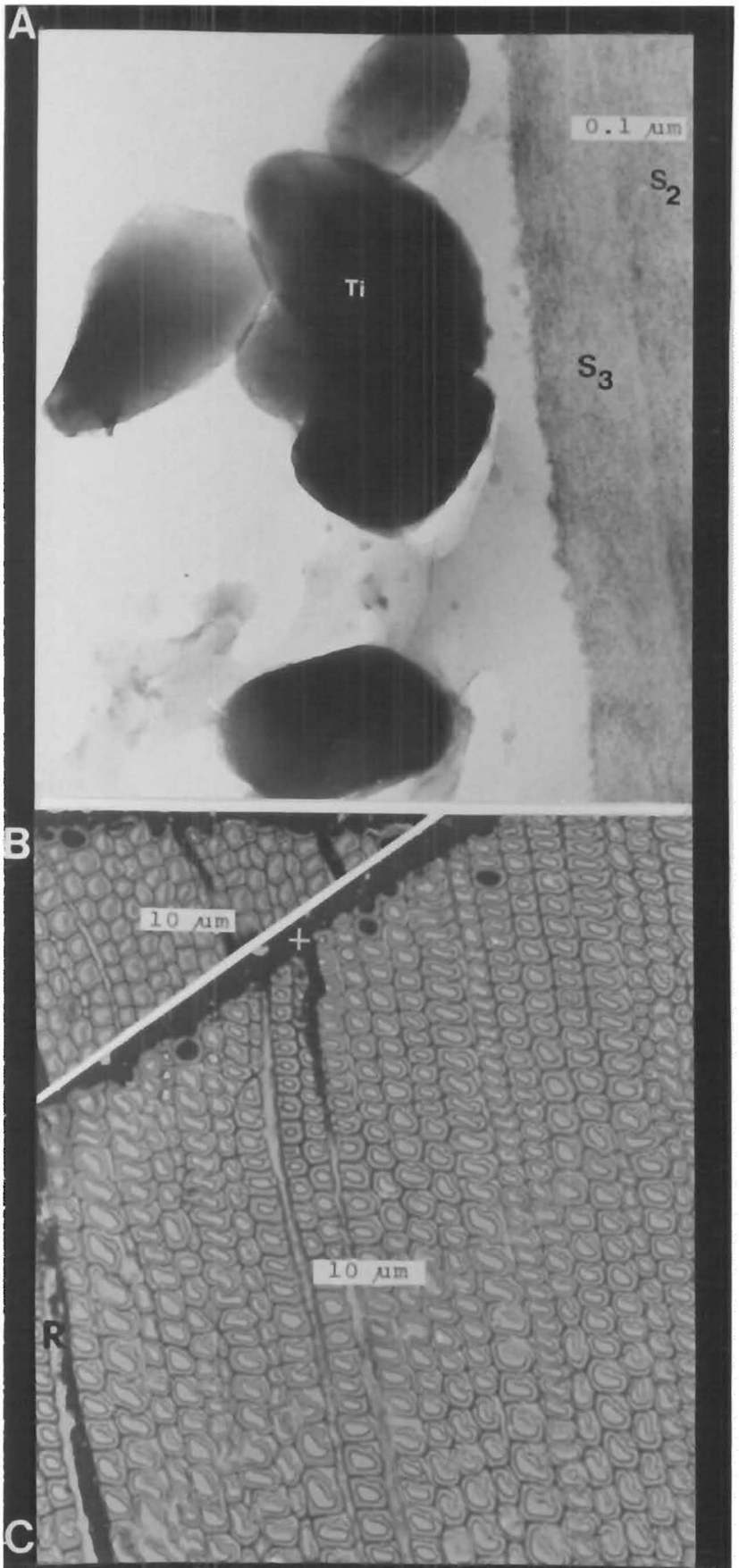

FIGURE 38 (T.F./ T.S.) *P.radiata* COATED WITH TAUBMANS WOOD PRIMER. (s.b.)

A Ultra-thin, uranyl acetate - lead citrate stained embedded section. Coating / tracheid interface. (TEM).

B & C Toluidine Blue stained unembedded sections.(LM).

It is notable that the drying times of the solvent based primers increase from one to three hours respectively in the order described in this survey. Visually drying time does not appear to control the degree of gross penetration.

4.11 TiO_2 TAGGED WATTYL ESTAPOL ON WEATHERBOARDS

Micrographic evidence (figures 39 to 44) revealed that this pigmented alkyd behaved differently to the primers. In contrast to the minimal penetration exhibited by the primers, this coating travelled into the wood several millimetres. In both *D. cupressinum* and *P. dacrydioides* there were cases of up to twenty-seven filled cells in certain boards. Chapter 5 has more detailed discussions of the results of a quantitative study of coating penetration. Figures 41 [A] and 43 [B] are typical examples illustrating the extent of coating penetration. Highly magnified unstained ultrathin sections provided evidence that the large pigment particles were contained in the cell lumens. X-ray maps of the Ti-K elements were superimposed on the electron images to confirm observations.

Pit aspiration is an irreversible process; once the pit membrane is deflected, movement of material between two tracheid cells is blocked (figure 39 [B]). Initially the centrally thickened torus and delicate margo are suspended in the middle position between the pit-pair (figure 42). These ultra-thin stained sections through bordered pit-pairs of *P. dacrydioides* show fine deposits lining and adhering to both the pit membrane and the border rims. The swollen torus in figure 42 [A] and [B] is unusual. Compare it to the typical torus magnified in figure 42 [C]-[E].

The presence of large titanium particles separated by the pit membrane suggest that the adjacent tracheids were filled by two separate flow paths. A similar interpretation can be postulated for the coating filled ray parenchyma and tracheid cells featured in figures 39 [C] and 40 [C]-[E]. Deposits of smaller particles lining the S_3 layer of the tracheid cell walls, although faintly visible in unembedded cells, are more readily seen in the stained highly magnified sections in figure 41 [C] and [D] and figure 44. These deposits have remained intact and were not dragged across the section during microtoming.

4.12 DISCUSSION

This survey showed that machining is influential on surface and sub-surface damage to cells and paint locking ability. Grit size and wood structure and density are more important factors controlling the depth and type of damage than depth of planing and feed speed (Murmanis et al , 1986 and Young, 1988). Rougher surfaces offer greater surface area for coating attachment than well planed surfaces with minimal coating adhesion. Mirams (1965) detected paint holding problems in highly planed

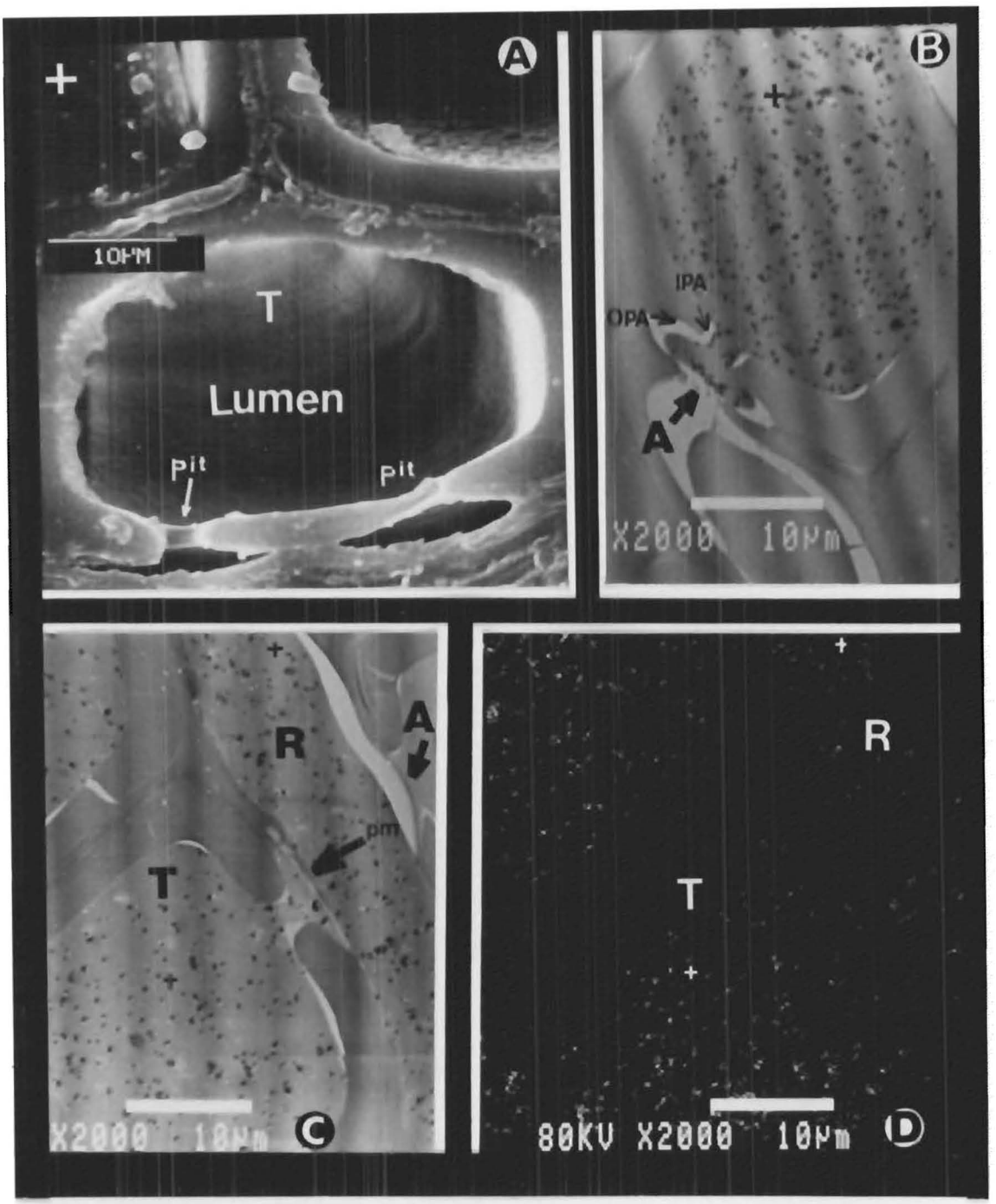

FIGURE 39

(T.F./T.S.) *D.cupressinum* RIMU COATED WITH TiO_2 TAGGED WATTYL ESTAPOL .

A. Earlywood (SEM).
B.& C. Ultra-thin, unstained section of the coating / tracheid and ray wall interfaces. Note the aspirated pit membranes. (STEM)
D. Corresponding EDXA element (Ti - K) X-ray map of figure C. (STEM).

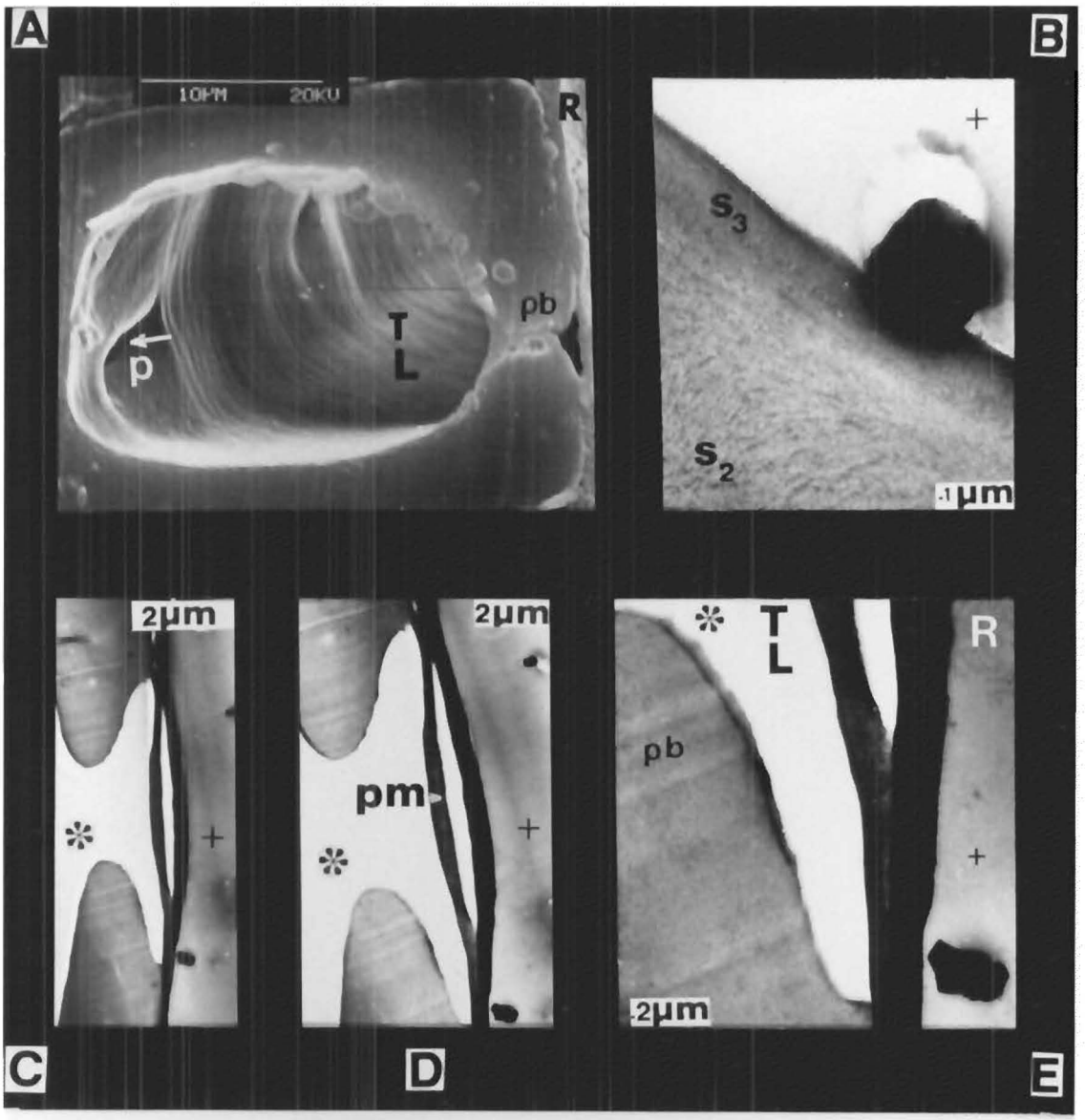

FIGURE 40

(T.F./ T.S.) *D.cupressinum* **RIMU COATED WITH TiO_2 TAGGED WATTYL ESTAPOL.**

A. A cupressoid cross-field pit between a tracheid and ray parenchyma cell. (SEM).
B. Ultra-thin, uranyl acetate - lead citrate stained, Spurr's resin embedded section showing coating / tracheid wall interface. (TEM).
C - E. Increasing magnifications of a cupressoid cross-field pit between an empty tracheid cell and a coating filled ray parenchyma cell.

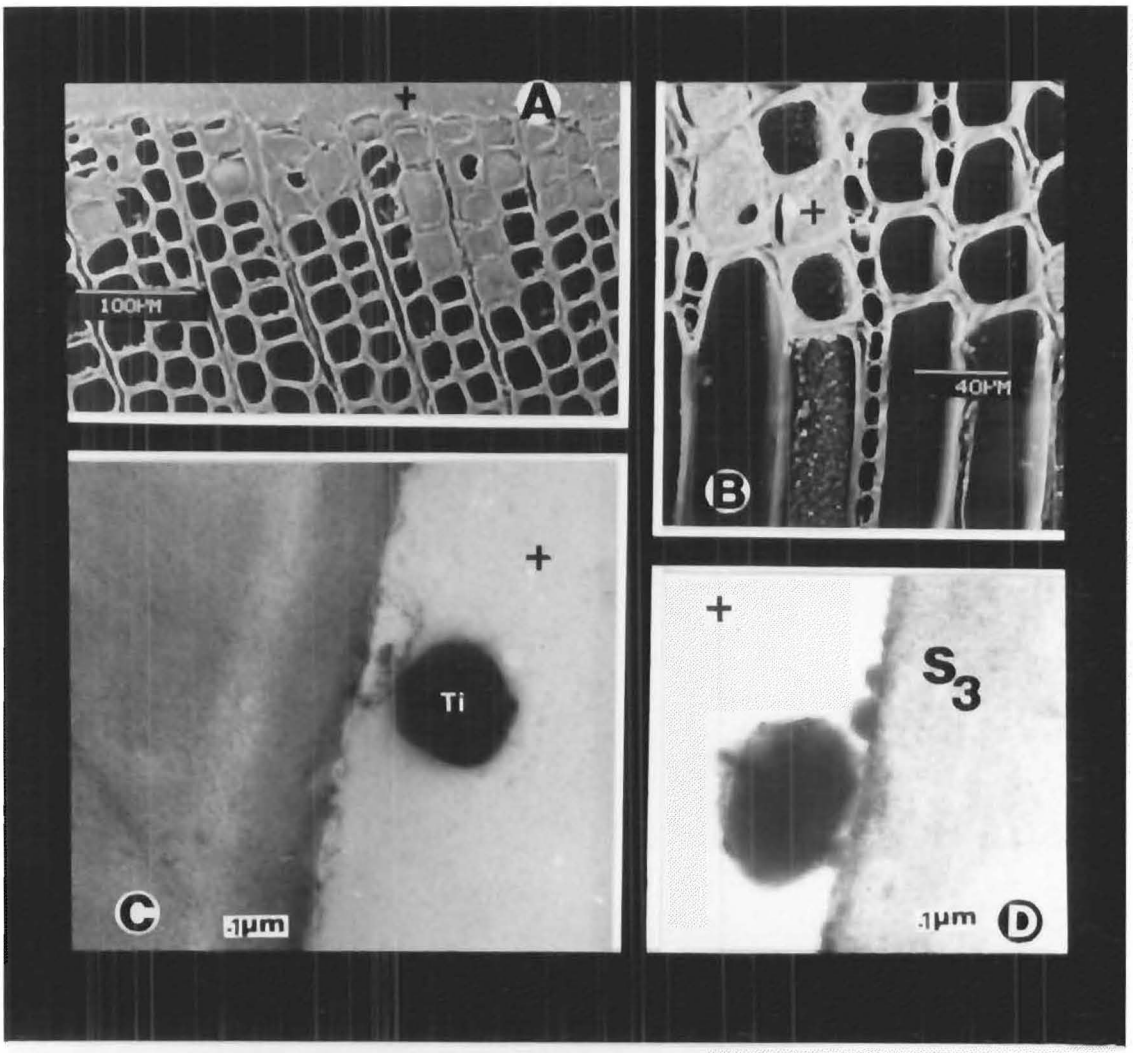

FIGURE 41

(T.F./T.S.) *P.dacrydioides* KAHIKATEA COATED WITH TiO_2 TAGGED WATTYL ESTAPOL .

A. Earlywood. (SEM).
B. (T.F./T.L.F.) Earlywood. (SEM).
C. & D. Ultra-thin, uranyl acetate-lead citrate stained Spurr's resin embedded sections showing coating / tracheid wall interface. (TEM).

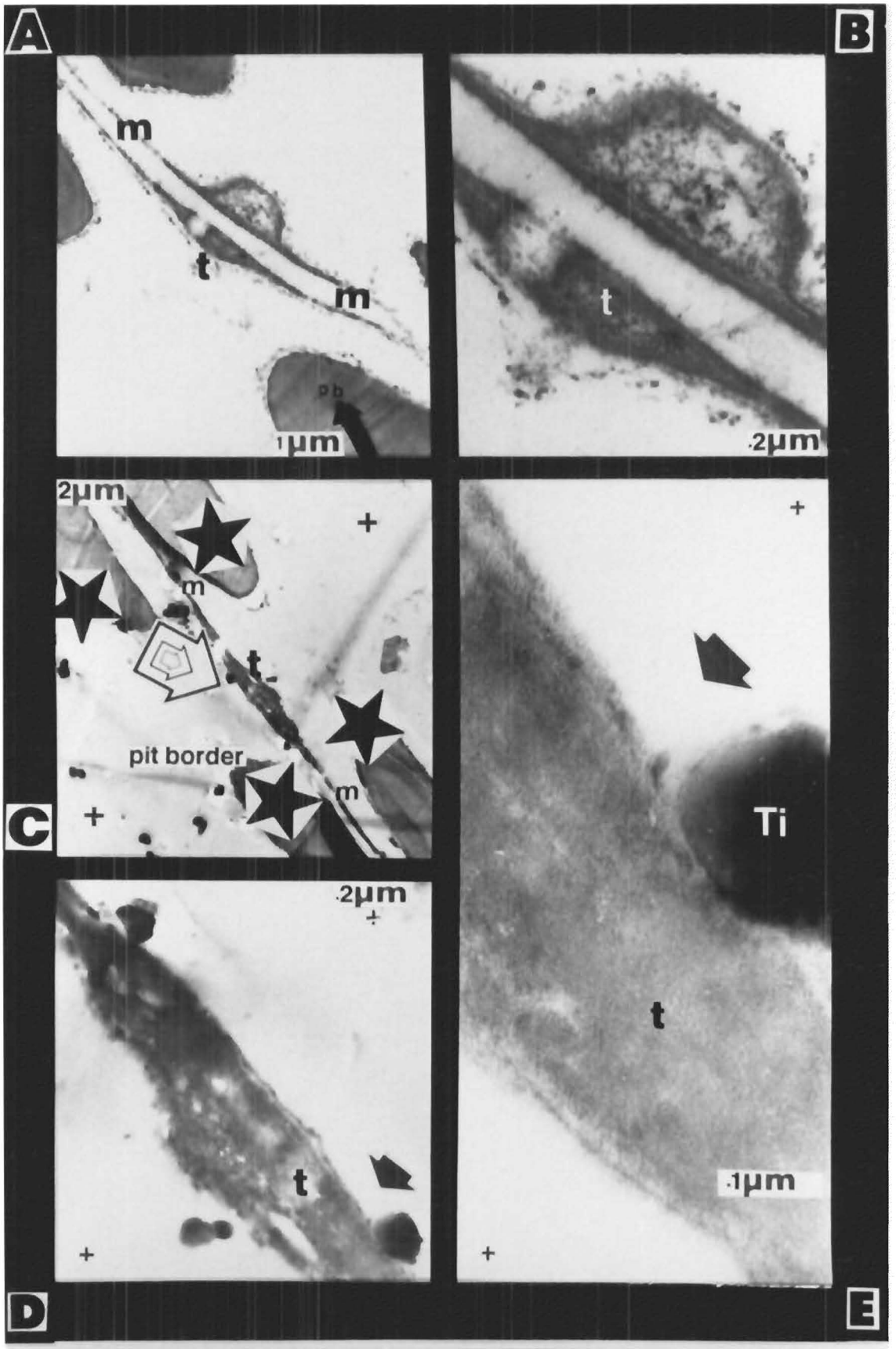

FIGURE 42

(T.S.) *P.dacrydioides* KAHIKATEA COATED WITH TiO_2 TAGGED WATTYL ESTAPOL.
A. & B. Conifer bordered pit-pair in earlywood tracheids.
C. - E. Ultra-thin, uranyl acetate-lead citrate stained, Spurr's resin embedded sections showing coating / pit membrane interface. (TEM).

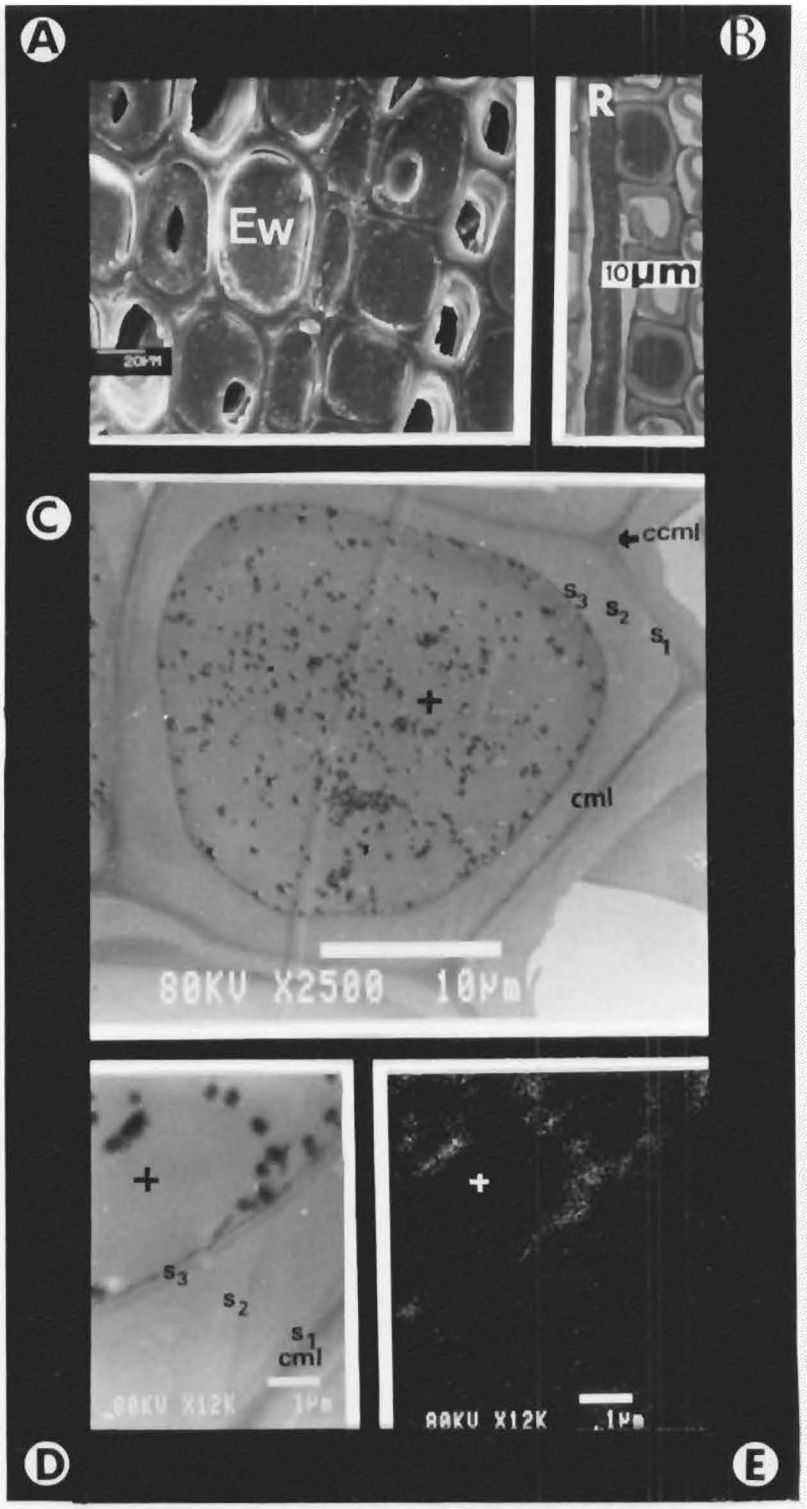

FIGURE 43

(T.F./ T.S.) P.radiata COATED WITH TiO_2 TAGGED WATTYL ESTAPOL .

A. Earlywood (SEM)

B. Note the coating filled ray cell and adjacent tracheids. Toluidine blue stained unembedded section. (L M)

C. &. D Ultra-thin, unstained sections of coating filled tracheid lumens. (STEM).

E. Corresponding EDXA element (Ti-K) Xray map of Fig.D. (STEM)

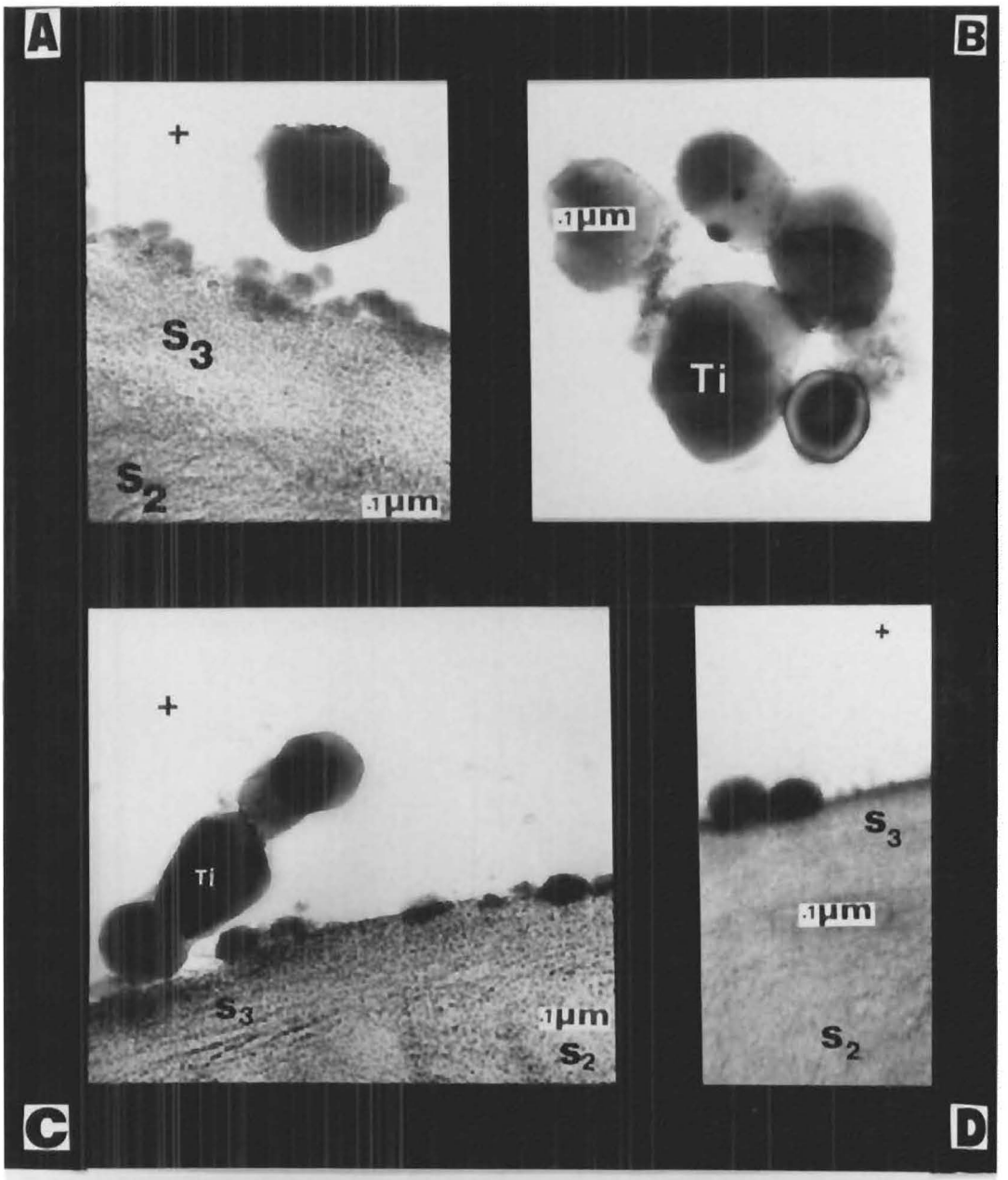

FIGURE 44

(T.S.) *P.radiata* COATED WITH TiO_2 TAGGED WATTYL ESTAPOL .

A., C. & D. Ultra-thin, uranyl acetate-lead citrate stained, Spurr's resin embedded sections showing coating / tracheid wall interface. (TEM).

B. Highly magnified titanium particles. (TEM).

boards. According to Feist (1984) the improved performance observed for rough sawn timber was due to better mechanical adhesion of the finish and the presence of more finish in the wood.

In many cases, particularly exemplified by the primers, coating penetration is limited to one to two cell rows deep which were either opened by machining or to the length of that portion of a tracheid which due to the slope of the grain ran from the surface into the wood. Fractures produced by machining open up crevices and aid coating penetration. All of the upper rows of cell lumens filled with coating would have emerged at some point on the surface of the substrate to form tubes for the conduction of liquids from the surface into the wood. When painting weatherboards, the coating is usually applied approximately parallel to the long axis of the cells. The transverse ends of weatherboards pose a different problem and are not dealt with in this study.

Quarter sawn boards are regarded as more stable than flat sawn boards because in the latter type the transition between spring and summerwood is more exposed and timber shrinks less in the radial direction. The early/latewood bands in both *D. cupressinum* and *P. dacrydioides* are indistinct but in *P. radiata* the growth rings are much broader. The wider, less dense springwood is capable of absorbing the coating to a greater degree than the narrower denser summerwood. In softwoods the volume of springwood may be as high as 80% of the air space (Miniutti, 1963). Fresh coating usually adheres firmly to both spring and summerwood but with age the weak zones will become apparent. If the summerwood bands are sufficiently narrow it is possible for the coating to remain spanned across. The summerwood cells have smaller lumens and expansion is greater in these thicker walled tracheids. Most movement occurs at the growth ring boundary. Miniutti (ibid) noted that more problems were encountered on the pith side of flat sawn boards which is the side of lowest density and that cell size decreases downwards when viewed in cross-section. Blakeney (1979) concluded that the denser the wood the poorer the paintability. Within a species, some weatherboards are superior to others.

It is known that the lower the viscosity; the lower the molecular weight but viscosity alone does not control paintability and substrate penetration. For example, the water based primer with the lowest viscosity value (Dulux primercryl 100% acrylic) did not behave differently to the Epiglass and Taubmans water based primers which are the most viscous primers studied here, indicating other factors are involved. Sinclair and Chamberlain (1959), and Sinclair (1962) deduced that the spreading rate of priming paints was not significantly different on treated and untreated *P. radiata*.

On the whole there is diverse opinion whether treated timber is amenable to painting. *P. radiata* is more easily treated than *D. cupressinum* and *P. dacrydioides* because the latter two wood species are less permeable (McQuire et al., 1979). Diffusion treatment of weatherboards with boron compounds may result in the migration out of some preservative salts onto the board surface of certain timber species (Mirams, 1965). However, Plackett and Blackeney (1987) reported that boron salts do not present painting problems. Sinclair (1965) pointed out that some water repellent treatments

were capable of promoting adhesion problems. Blackeney (1979) remarked that certain oil-based preservatives such as creosote or pentachlorophenol in oil solution impair paint adhesion but by contrast the copper-chrome-arsenate preservatives (Celure and Tanalith) actually improve adhesion. Light organic solvent preservative (LOSP) treated wood can be painted (Plackett and Blackeney, 1987).

It is well known that coatings do not adhere well to wet wood. The wood used in this study was dried to the average moisture content specified in the N.Z.Standards N.Z.S. 3602 : 1975. Water in wood is in two forms-free water that entirely or partly fills the cell cavities or bound water which is held within the cell wall structure. The permeability of wood depends on the ease with which fluids pass through under an applied pressure gradient and strongly affects the ease of preservation (Kininmonth and Williams, 1972). *P. radiata* is extremely permeable to moisture and is dimensionally unstable (Mills and McQuire, 1976). The variation in wood density of *P. radiata* throughout New Zealand is marked and thus influential in preservative retention (McQuire, 1975; McQuire et al., 1975).

X-ray maps were used in this study to provide supplementary qualitative information on the presence and location of copper-chromium-arsenic in ultrathin sections through *P. radiata* and *P. dacrydioides* tracheid walls. In order to elucidate whether these metal elements in the preservative are distributed throughout the cell wall or line the tracheid lumen walls and interfere with coating penetration, the X-ray maps were superimposed onto the electron images. The X-ray maps in figure 32 [C] & [D] and figure 34 [B] & [C] suggest a uniform distribution of the elements, but a detailed quantitative examination involving electron microprobe and spot analysis at high magnifications would really be required to confirm visual observations. Although this is beyond the scope of this study, the observations by other workers in pine and larch are worth outlining here.

Ryan (1986) observed deposits of C C A lining the lumen of *P. radiata* tracheids and Chou et al (1973) found that the inner face of the tracheid wall of Scots pine was covered by a 20-30 μm thick layer containing all the preservative elements at high concentration. In a comprehensive study of the microdistribution of CCA in the walls of tracheids impregnated with Tanalith C, Chou et al were able to discern fine deposits throughout the S_2 layer of the cell wall. The morphology of these deposits was clearly dictated by the orientation of the cellulose microfibrils. Electron dense zones alternated with clear regions. The dense lines were discontinuous and apparently composed of discrete particles. From this it was inferred that the wood cellulose contains both crystalline regions impenetrable to metal ions and non-crystalline penetrable areas. They deduced that the surface of each cellulose microfibril in the secondary wall was coated by a 1.5-20 nm thick layer of the metallic deposit.

With the aid of SEM/EDXA, Desai and Côté (1976) were able to characterize the location of components of water-based preservatives; primarily ammoniacal zinc salt solutions. They believed that once the free ammonia had evaporated the zinc-amine complex could break down and zinc oxide would precipitate from the system. Eventually some zinc would diffuse into the cell wall as a solu ble

amine complex. Morphological studies on the movement of preservatives into the cell wall, in particular the diffusion of copper, zinc and chromium compounds was carried out by Yata et al (1978, 1979. 1981, 1982 & 1983). In a cell wall the intercellular and primary layer and the S_1/S_2 boundary were the most permeable layers. They found that the copper concentration was ten times greater in the intercellular and primary layer than in the S_2 layer of the wall. Electron micrographs of ultrathin transverse sections of pre-cut cell walls of larch were used to demonstrate the permeability of various parts of the cell wall. Yata et al (1981) deduced that the diffusion depth of zinc ions into the exposed cut ends of the multilayered cell walls was uneven and always two to five times longer than that across the cell wall inwards from the lumen. A year later Yata et al (1982) produced convincing evidence that hexavalent chromium compounds used in water-borne preservatives were distributed throughout the cell walls of all cell types. They used electron micrographs to demonstrate the sequence of diffusion in both hardwood and softwood species including larch. Their results showed that the chromium concentration in the intercellular and primary layer was higher than that in the secondary wall. Chromium remained in the wall without reacting with cell wall constituents. Orientation of the chromium compounds conformed to the orientation of cellulose microfibrils of the secondary wall. Their conclusion that chromium was deposited on the surface of microfibril crystalline cores and in the encrusting materials between the microfibrils is in agreement with the findings of Chou et al (1973) for CCA.

To conclude, this survey singled out one particular coating system which showed exceptional penetration of the substrate. The remainder of this thesis investigates the observed behaviour of the TiO_2 tagged Wattyl Estapol alkyd coating.

CHAPTER 5

DETAILED STUDY OF TiO_2 TAGGED WATTYL ESTAPOL ON TRANSVERSE, TANGENTIAL AND RADIAL SECTIONS OF *D.cupressinum, P.dacrydioides* AND *P.radiata* WEATHERBOARDS

5.1 DEPTH OF COATING PENETRATION IN "u" AND "n"-TYPE BOARDS.

In order to obtain a complete picture of the diverse nature of this coating, on different cuts of weatherboard representing the three taxa, six sets of photographs are presented. Figures 45 to 50 represent typical examples of the coating on the two main types of cut. They are referred to here as "u"-type or "n"-type depending on whether the pith or bark side is exposed to the coating.

The depth of coating penetration was quantitatively determined across the entire transverse face of each weatherboard by counting the number of filled cells along rows of tracheids inwards from the coating/substrate interface. The values are tabulated in appendix 4. Statistical analyses (Sokal and Rohlf, 1981) were performed on the results in order to determine whether there was:

(i) any variation among taxa regardless of cut

(ii) any difference among the three taxa exhibiting the "u"-type cut

(iii) any difference among the three taxa exhibiting the "n"-type cut

(iv) any difference within each taxon along the 14 cm interval for both "u"-type and "n"-type cuts.

The Minitab (State College U.S.A., 1987 version) and SAS (Sas Institute Inc. U.S.A., 1987 version) packages for statistical analyses were used in conjunction with the IBM and UNISYS computer systems.

A one way analysis of variance (ANOVA) was chosen to estimate the variance of the taxa means about the grand mean and the variance of individual measurements about their means. The term 'among' is synonymous with 'treatment and effects'of statistical packages and the term 'within' may also be called 'error or individuals'.

FIGURE 45.1

A cross-section showing a "U"-type growth ring pattern cut through a Dacrydium cupressinum (rimu) weatherboard coated with TiO_2 tagged Wattyl Estapol Exterior Clear.

The entire length of this weatherboard section was photographed under the S E M and the individual micrographs pieced together such that figures 45.2 to 45.5 depict the sequence from left to right in an enlarged form.

"Left" and "right" refer to the edges of the weatherboard as presented in figure 45.1, and the white spots lettered a to n are reference markers to facilitate matching positions on figure 45.1 with figures 45.2 to 45.5.

The dashed lines point to positions on the weatherboard where magnifications to show details have been made.

fig 45.2 - left edge
fig 45.3 - top edge
fig 45.4 - top edge
fig 45.5 - right edge

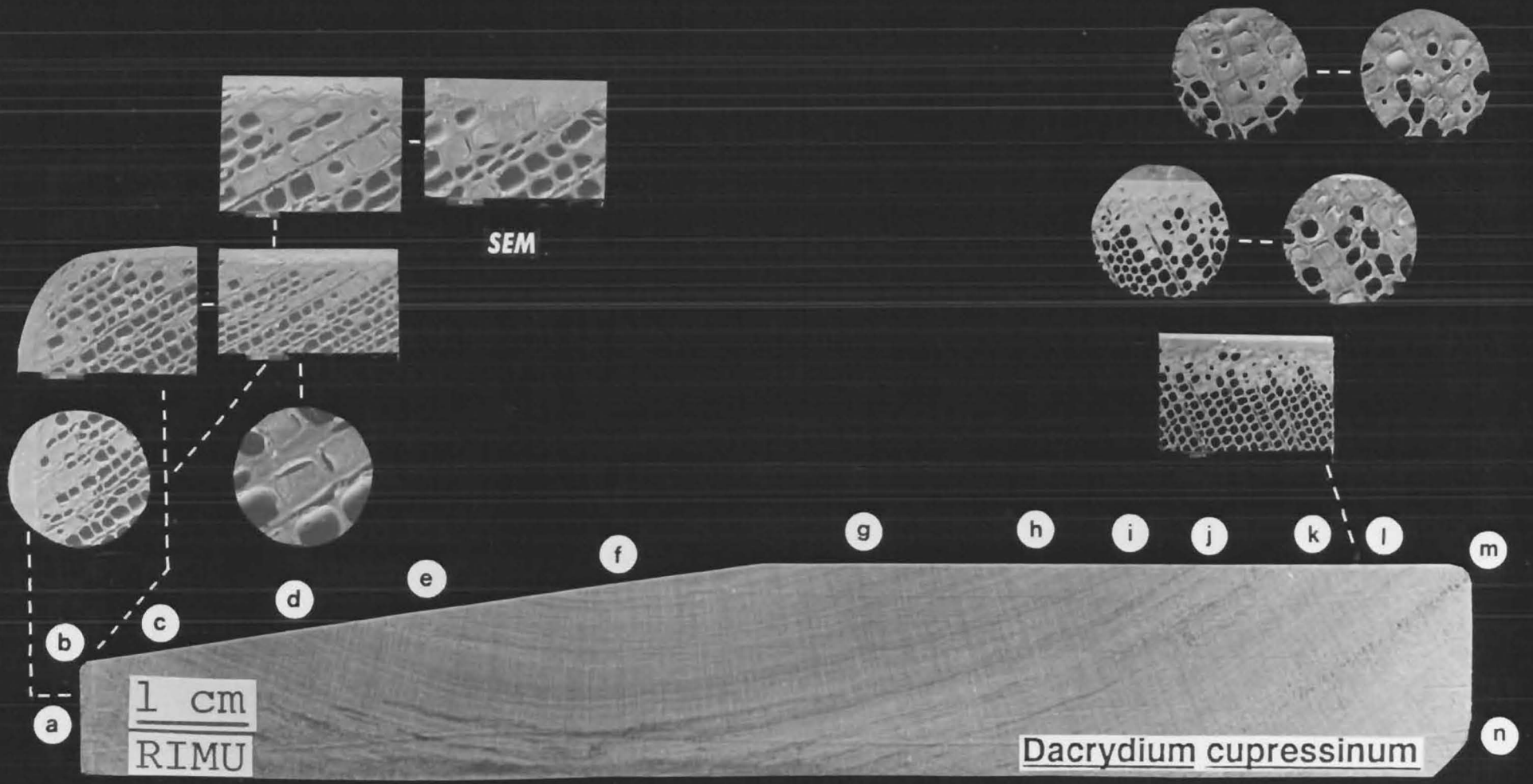

Figure 45.1

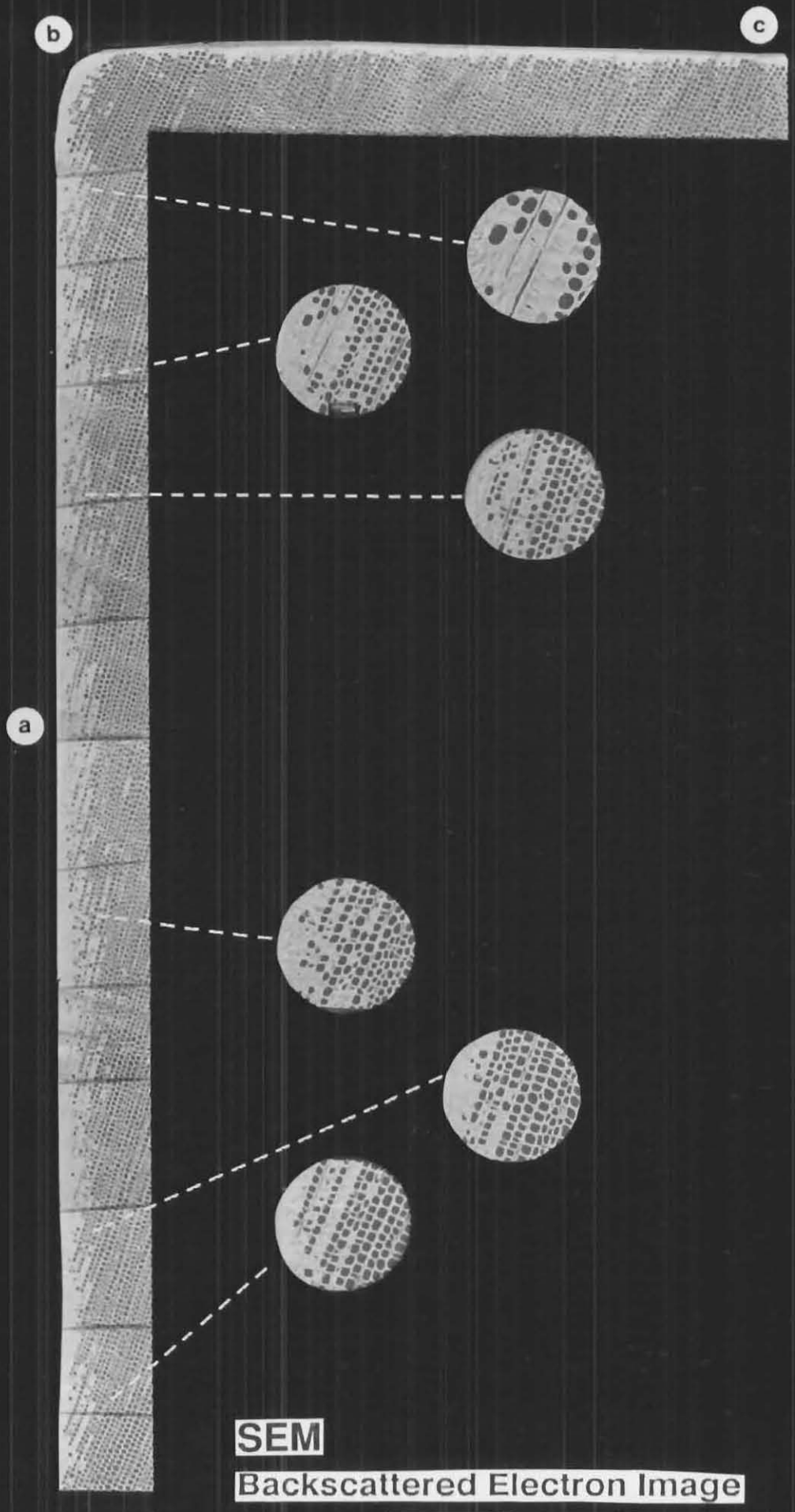

SEM

Backscattered Electron Image

Figure 45.2 Dacrydium cupressinum

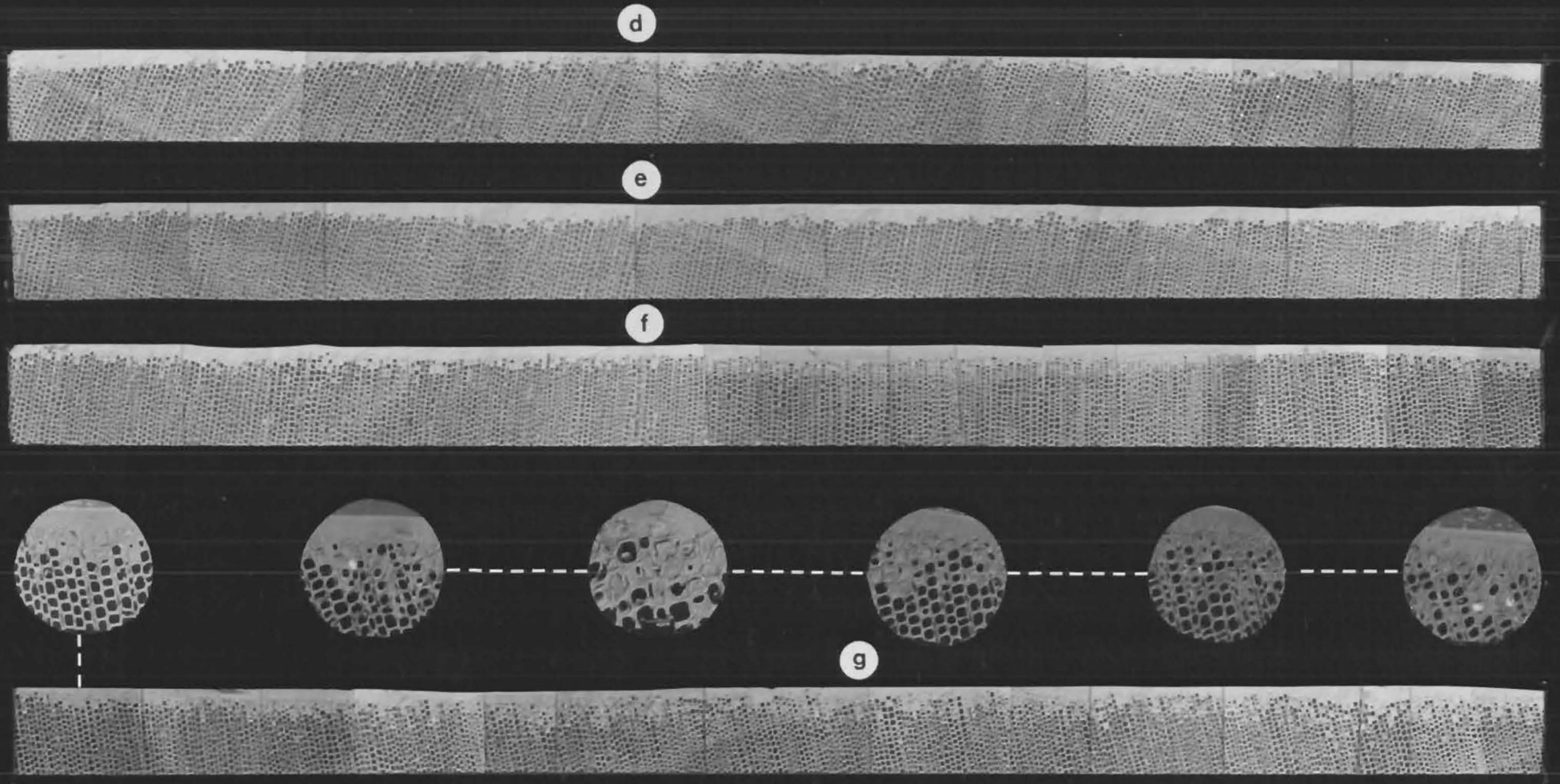

Figure 45.3 Dacrydium cupressinum

Backscattered Electron Image SEM

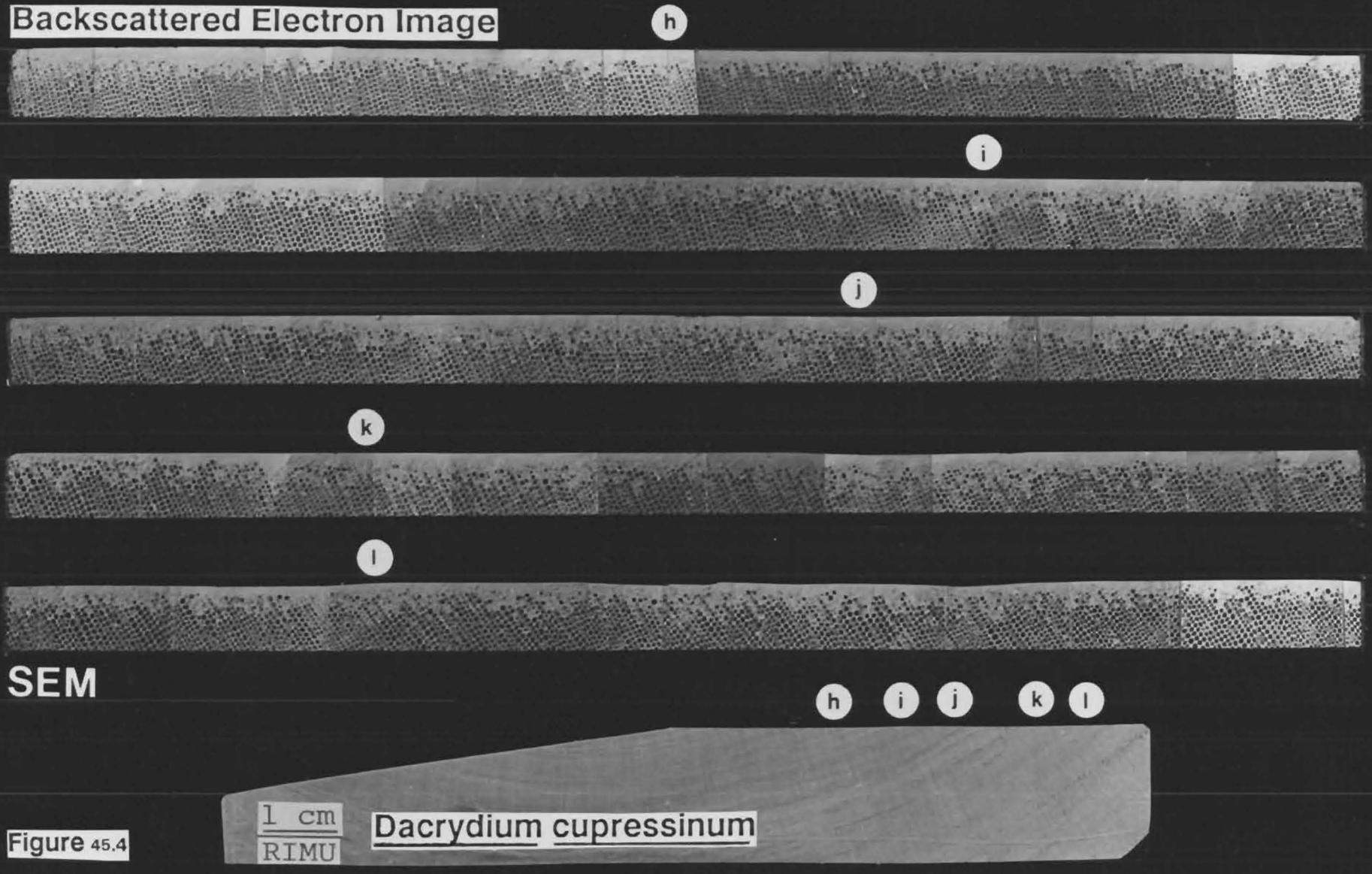
Backscattered Electron Image
h
i
j
k
l
SEM
h
i
j
k
l
1 cm
RIMU
Dacrydium cupressinum

Figure 45.4

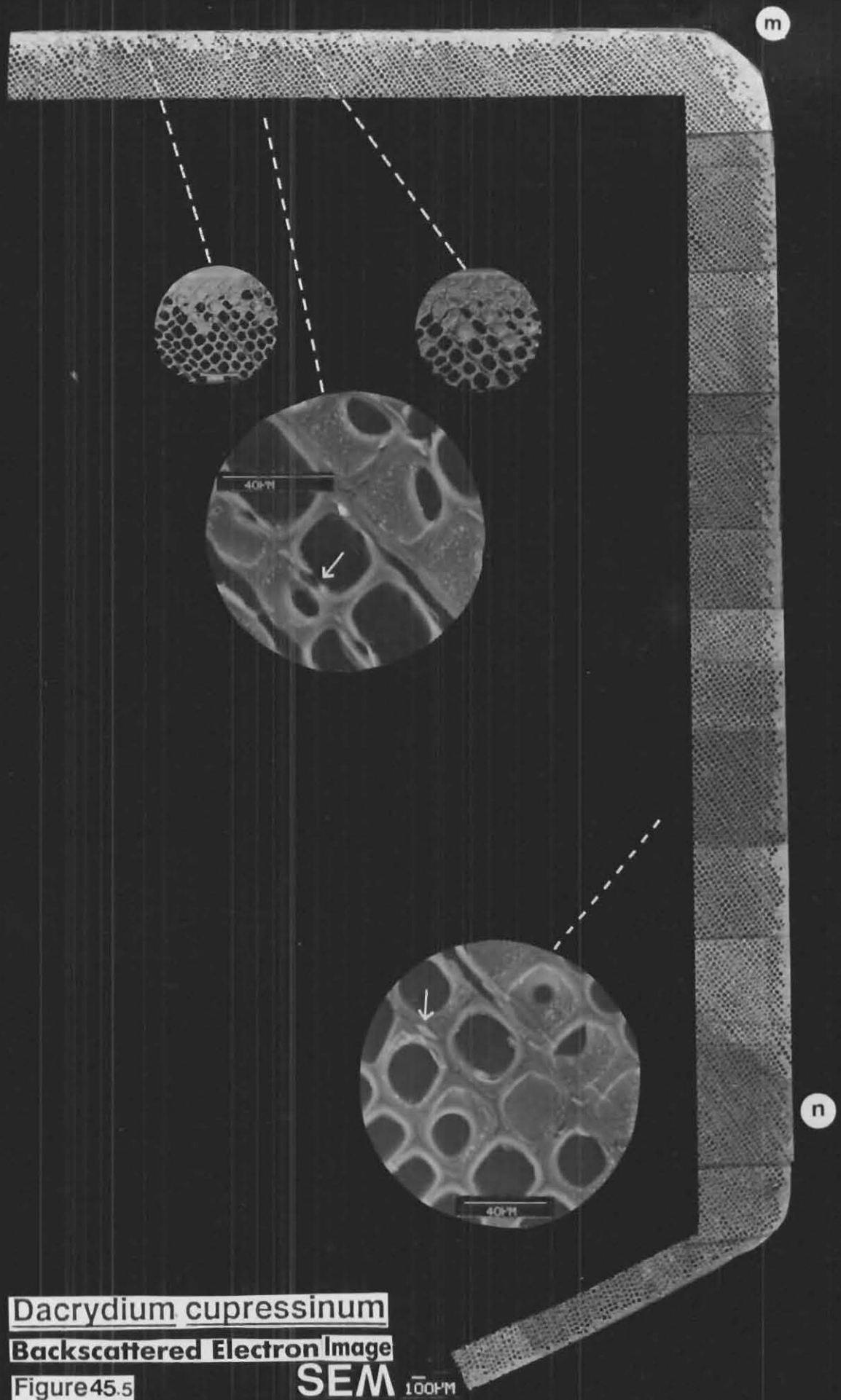

Dacrydium cupressinum

Backscattered Electron Image

Figure 45.5

SEM 100µM

FIGURE 46.1

A cross-section showing a "n"-type growth ring pattern cut through a Dacrydium cupressinum (rimu) weatherboard coated with TiO_2 tagged Wattyl Estapol Exterior Clear.

The entire length of this weatherboard section was photographed under the S E M and the individual micrographs pieced together such that figures 46.2 to 46.4 depict the sequence from left to right in an enlarged form.

"Left" and "right" refer to the edges of the weatherboard as presented in figure 46.1, and the white spots lettered a to k are reference markers to facilitate matching positions on figure 46.1 with figures 46.2 to 46.4.

The dashed lines point to positions on the weatherboard where magnifications to show details have been made.

fig 46.2 - left edge
fig 46.3 - top edge
fig 46.4 - right edge

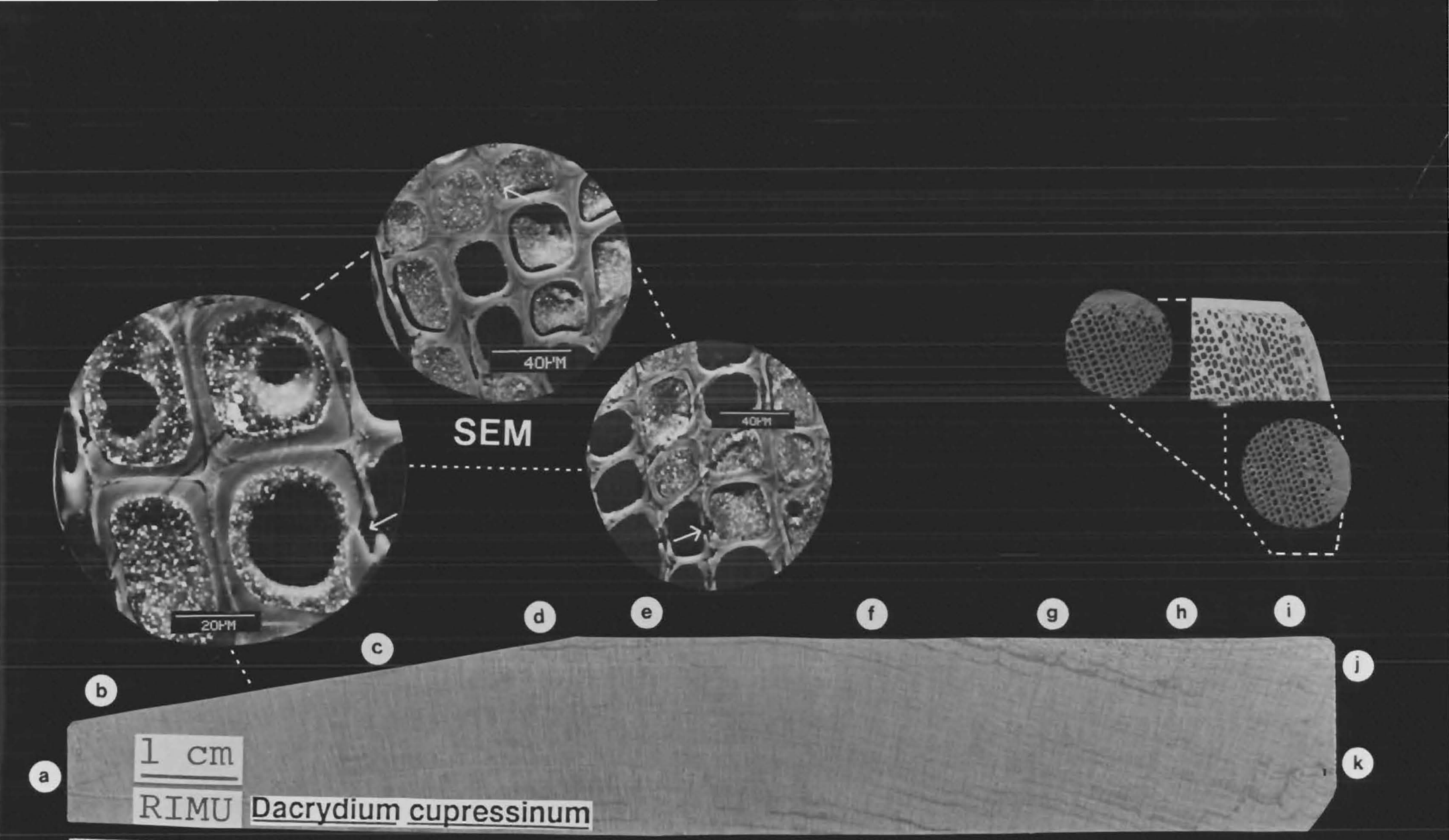
40µM
SEM
40µM
20µM
a
b
c
d
e
f
g
h
i
j
k
1 cm
RIMU Dacrydium cupressinum

Figure 46.1

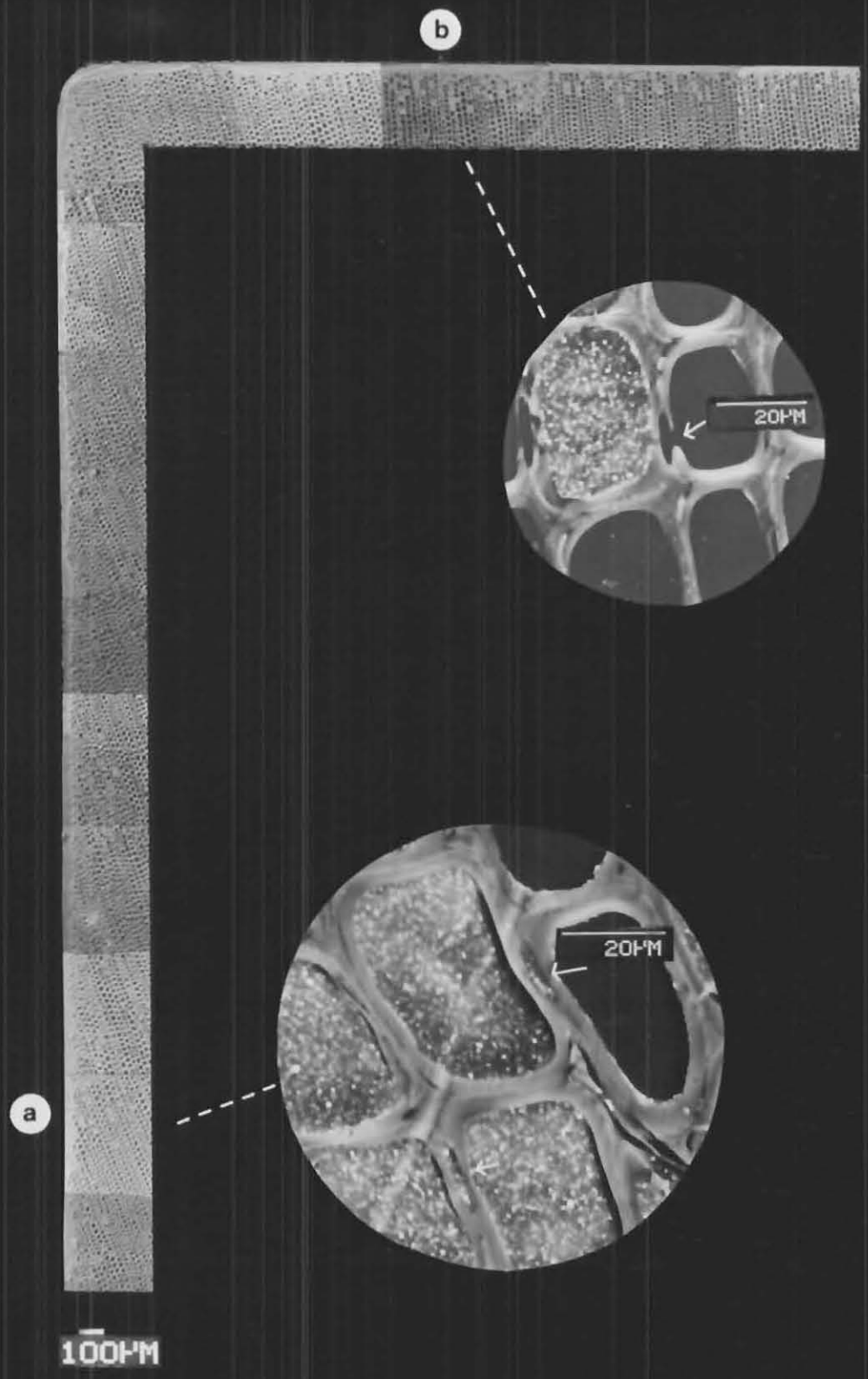

SEM

Backscattered Electron Image

Dacrydium cupressinum

Figure 46.2

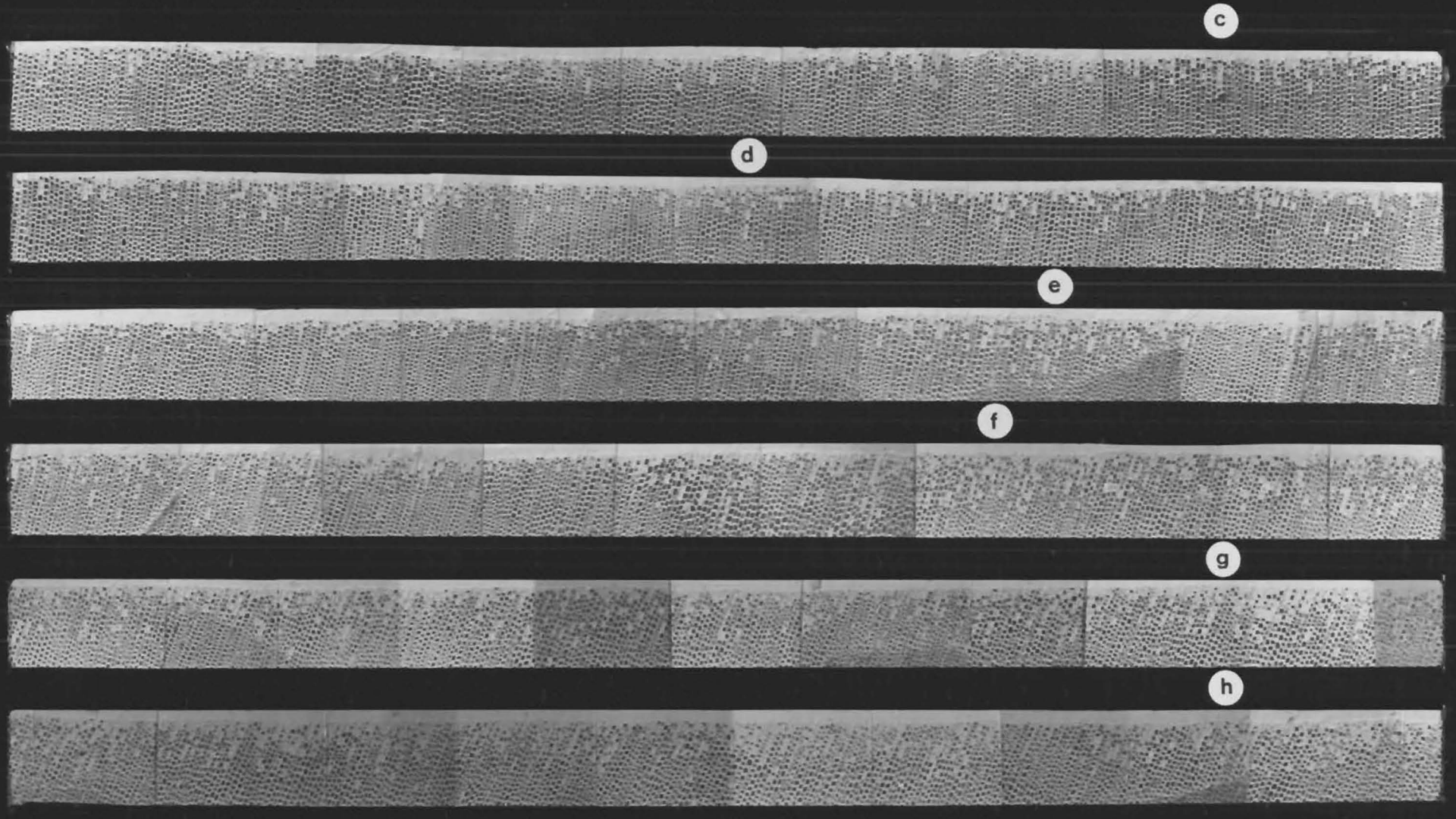

Figure 46.3 Dacrydium cupressinum

Backscattered Electron Image SEM

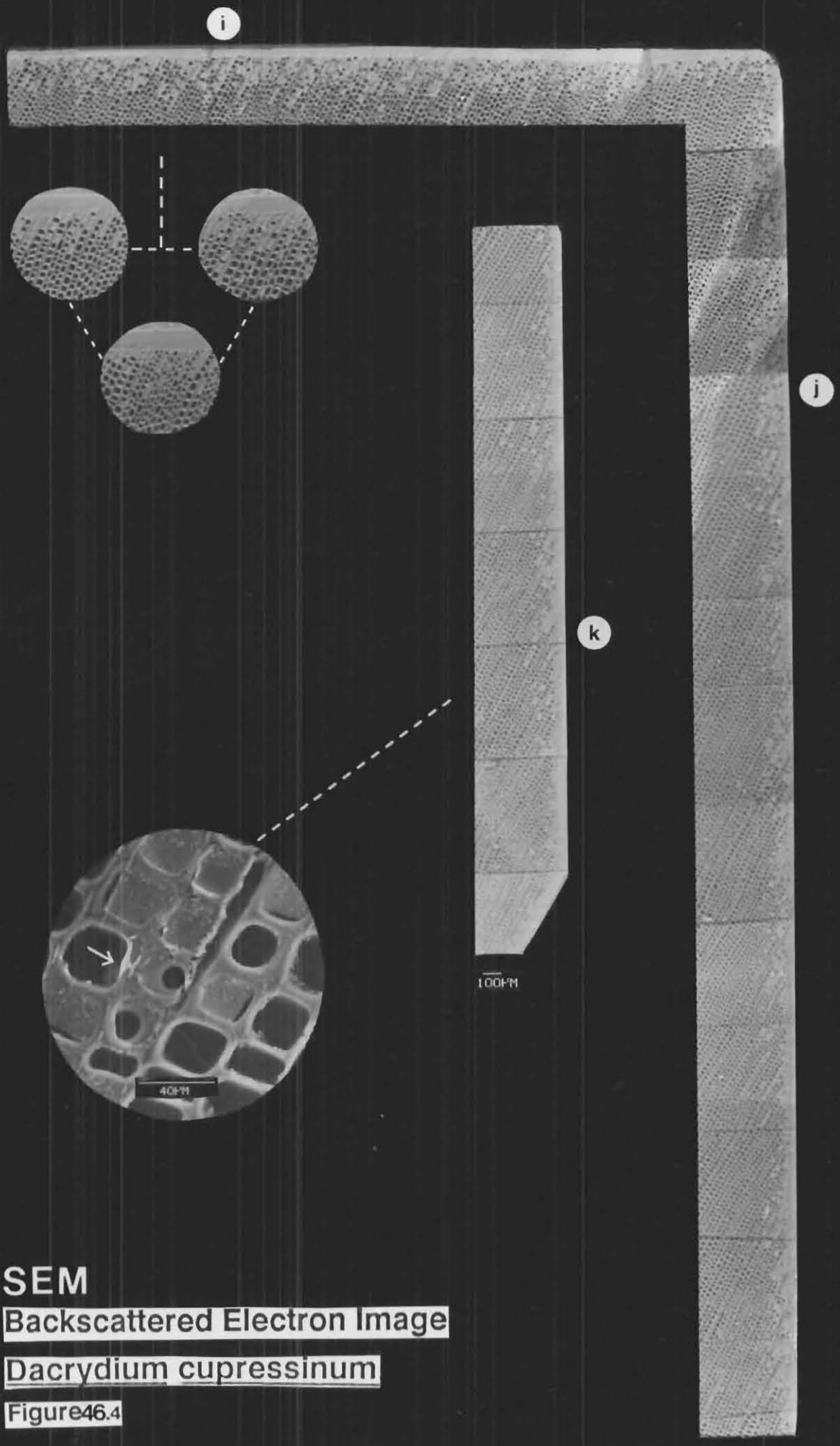

SEM

Backscattered Electron Image

Dacrydium cupressinum

Figure46.4

FIGURE 47.1

A cross-section showing a "U"-type growth ring pattern cut through a Podocarpus dacrydioides (kahikatea) weatherboard coated with TiO_2 tagged Wattyl Estapol Exterior Clear.

The entire length of this weatherboard section was photographed under the S E M and the individual micrographs pieced together such that figures 47.2 to 47.6 depict the sequence from left to right in an enlarged form.

"Left" and "right" refer to the edges of the weatherboard as presented in figure 47.1, and the white spots lettered a to p are reference markers to facilitate matching positions on figure 47.1 with figures 47.2 to 47.6.

The dashed lines point to positions on the weatherboard where magnifications to show details have been made.

fig 47.2 - left edge
fig 47.3 - top edge
fig 47.4 - top edge
fig 47.5 - top edge
fig 47.6 - right edge

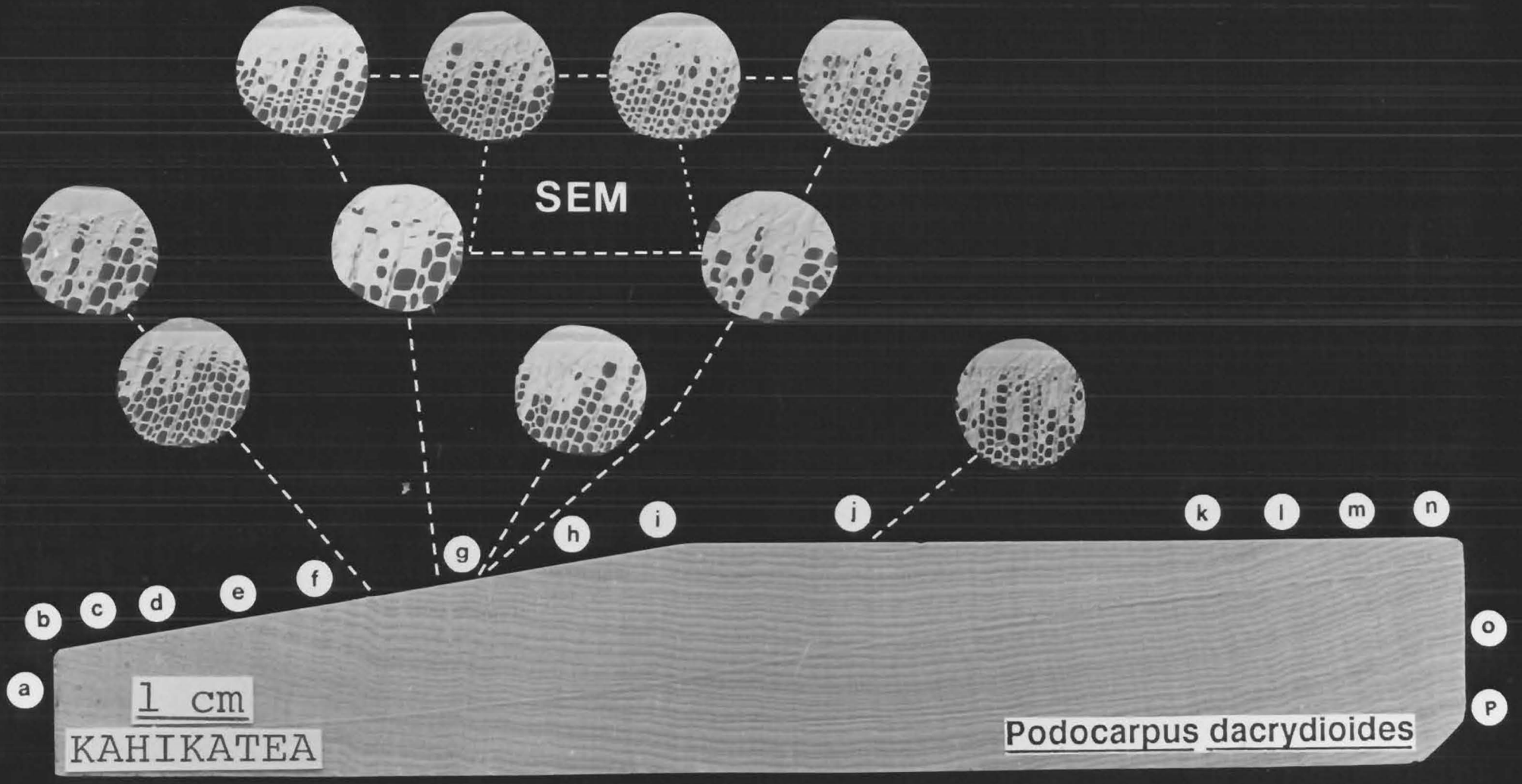
SEM
a
b
c
d
e
f
g
h
i
j
k
l
m
n
o
p
1 cm
KAHIKATEA
Podocarpus dacrydioides

Figure 47.1

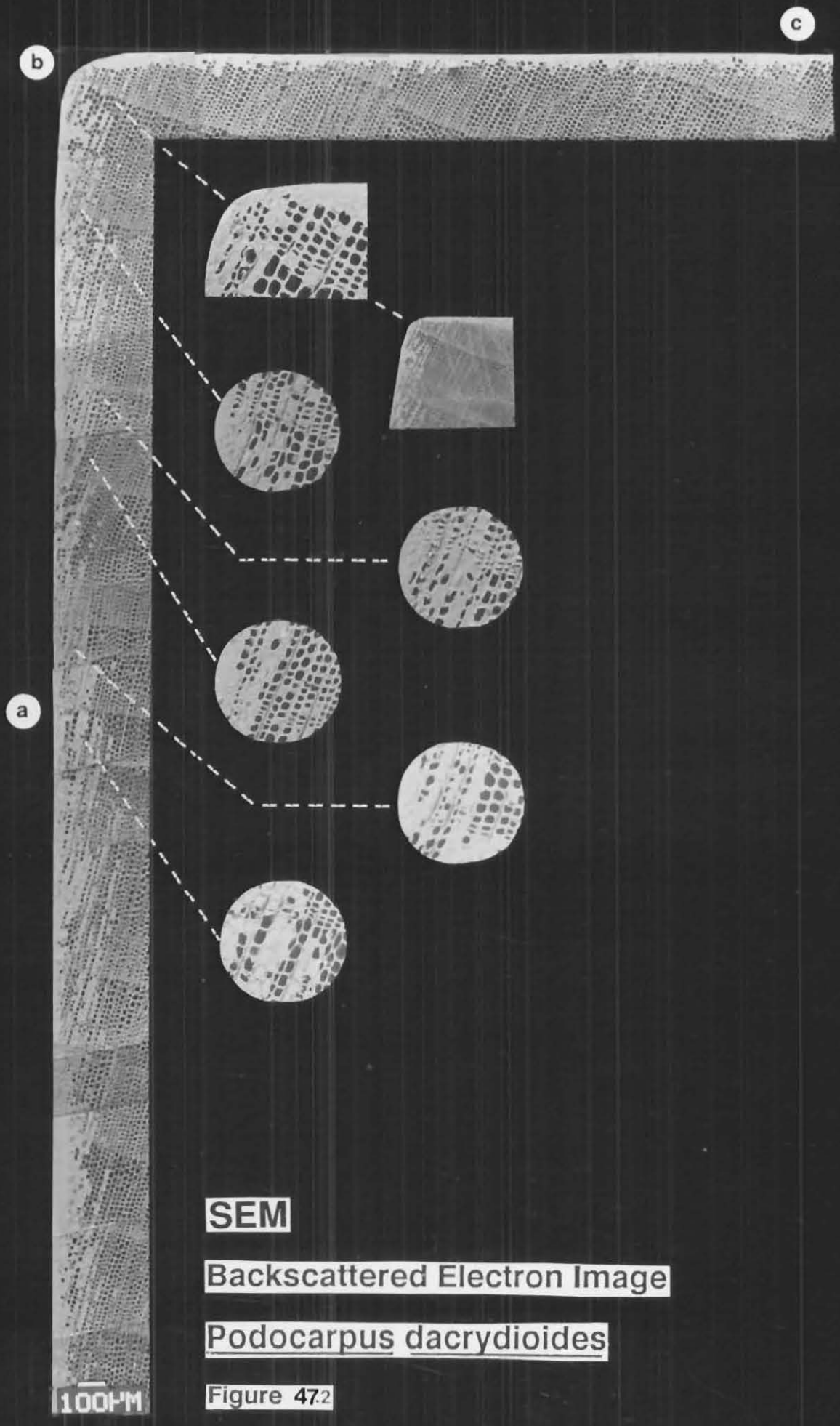

SEM

Backscattered Electron Image

Podocarpus dacrydioides

Figure 47.2

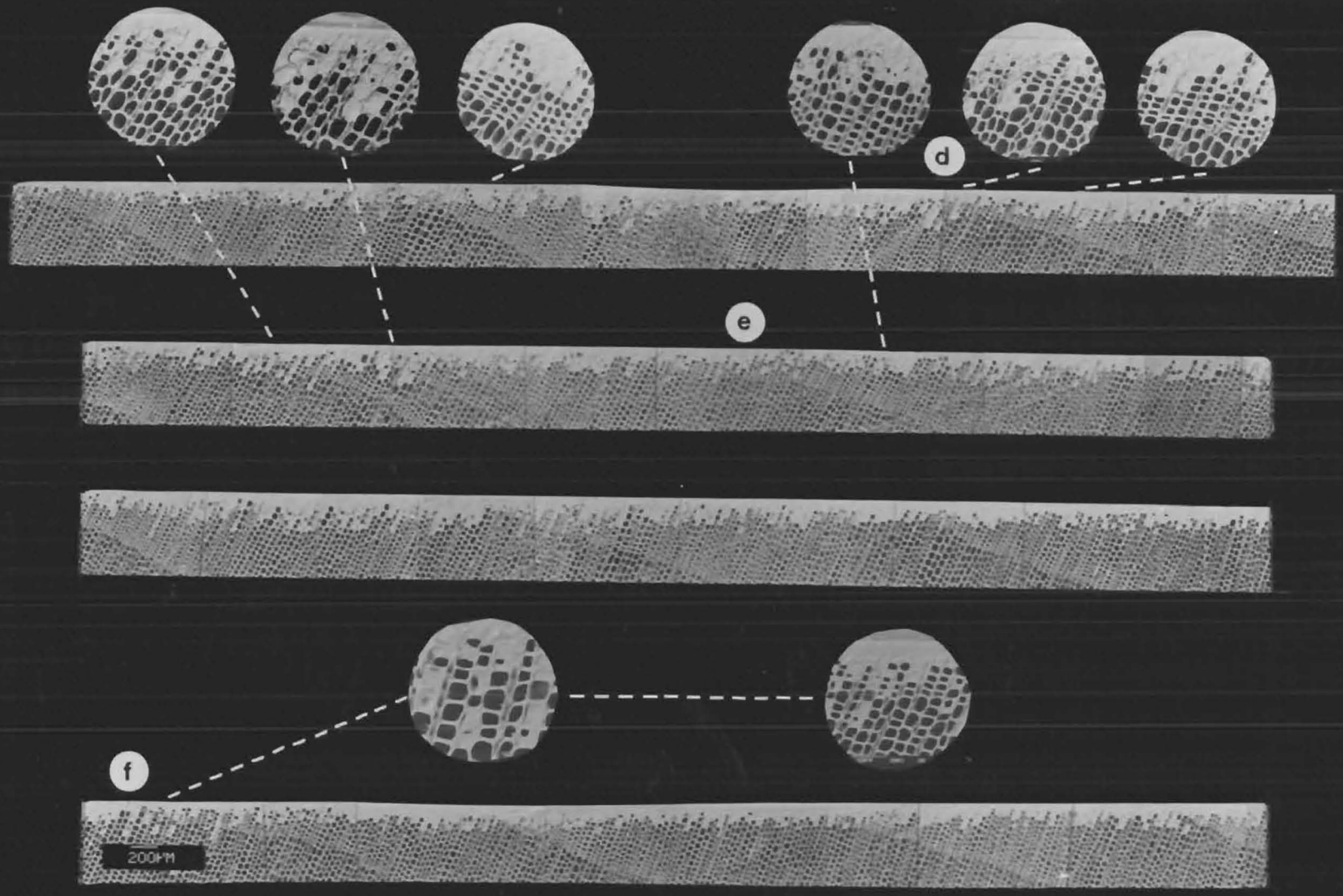

Backscattered Electron Image

SEM

Podocarpus dacrydioides

Figure 47.3

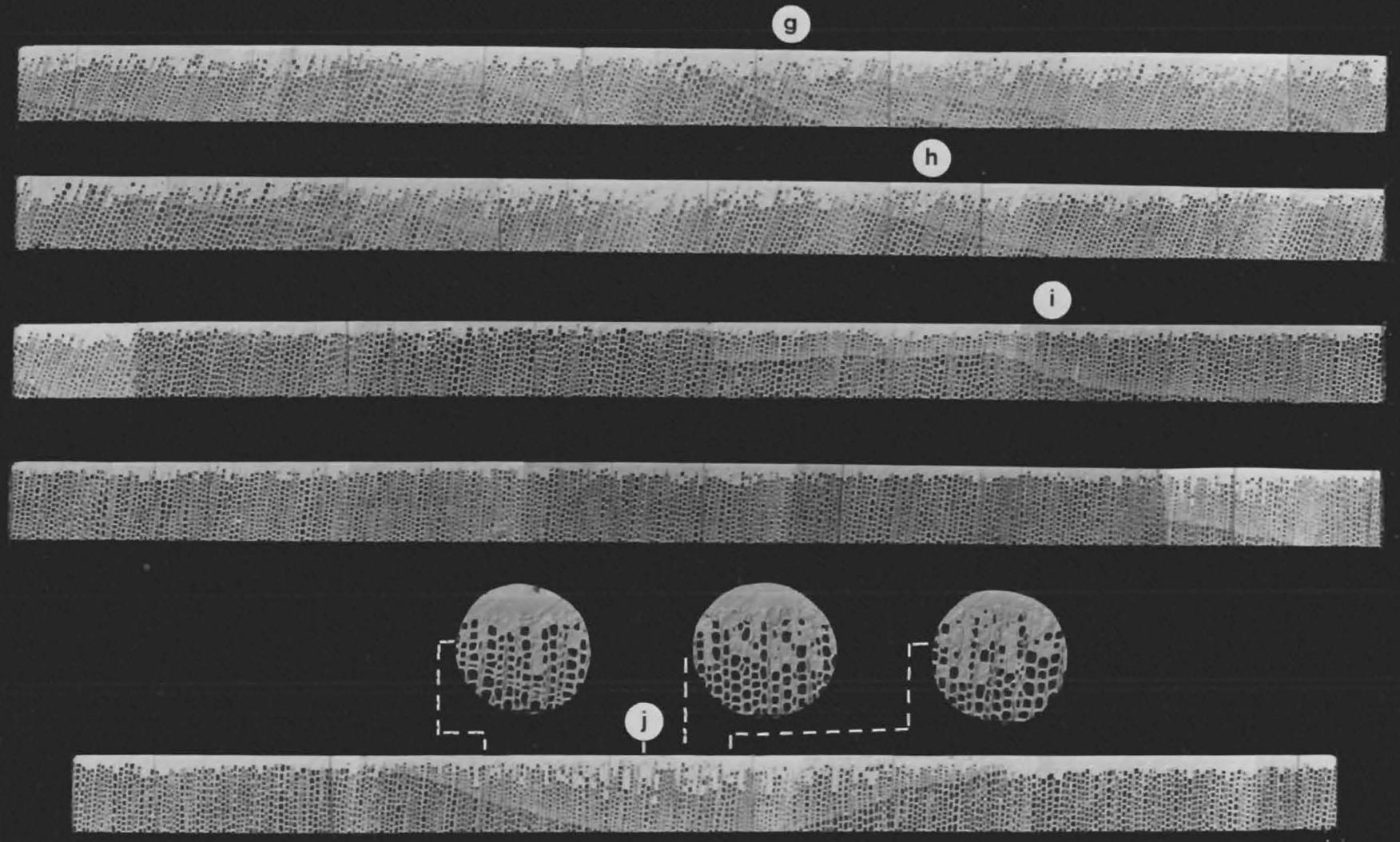

Figure 47.4 Podocarpus dacrydioides SEM Backscattered Electron Image

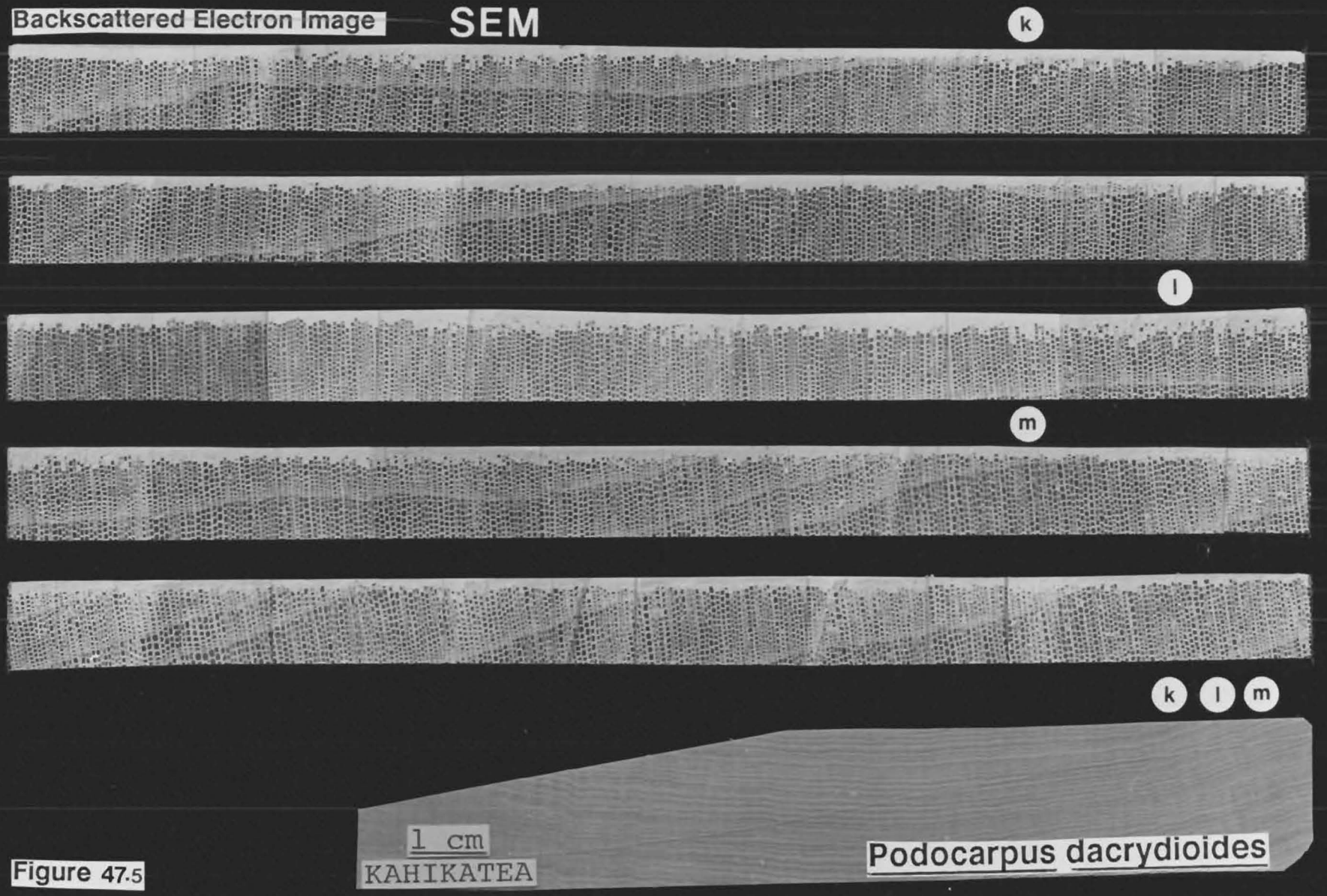
Backscattered Electron Image
SEM
k
l
m
k l m
1 cm
KAHIKATEA
Podocarpus dacrydioides

Figure 47.5

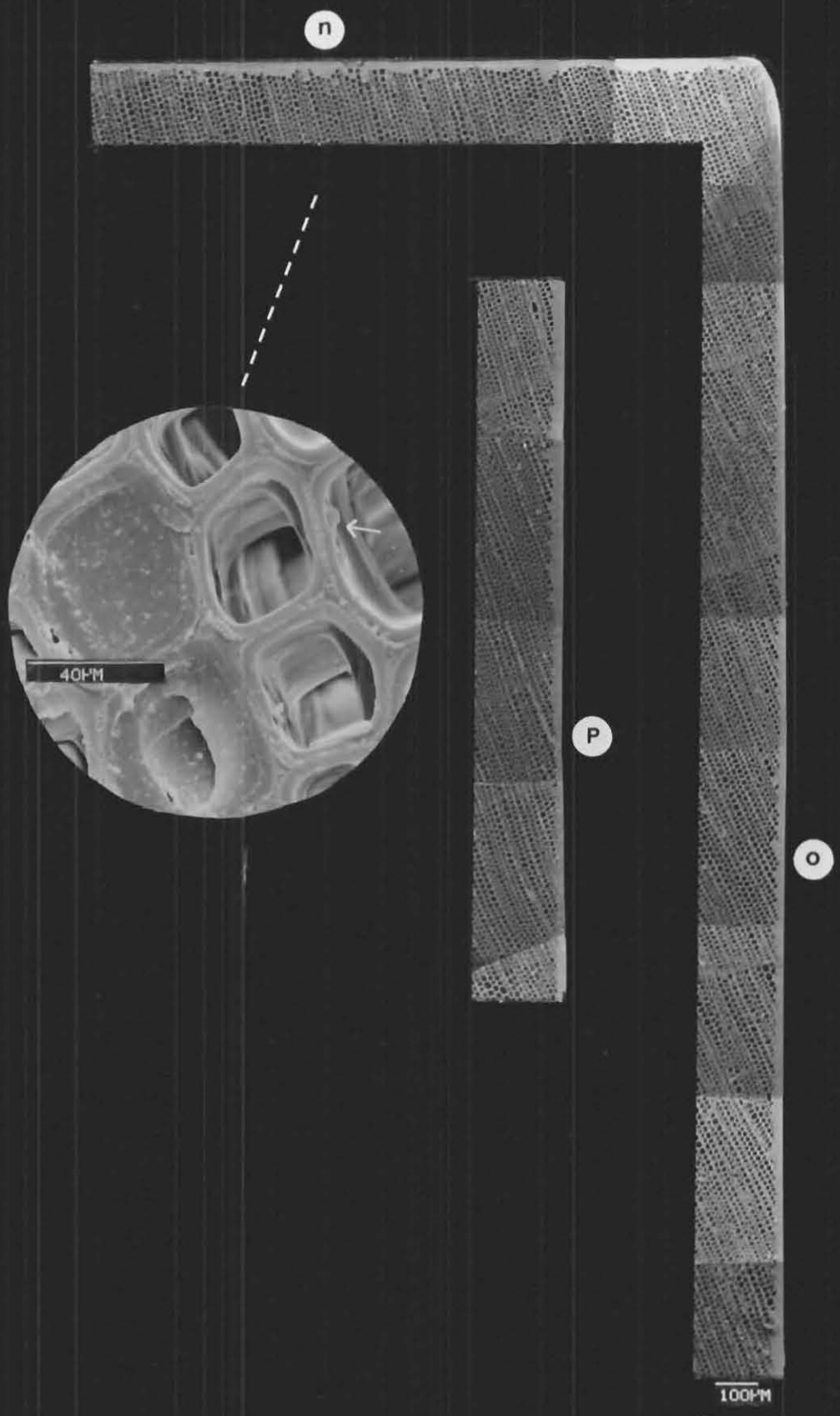

SEM

Backscattered Electron Image

Podocarpus dacrydioides

Figure 47.6

FIGURE 48.1

A cross-section showing a "n"-type growth ring pattern cut through a Podocarpus dacrydioides (kahikatea) weatherboard coated with TiO_2 tagged Wattyl Estapol Exterior Clear.

The entire length of this weatherboard section was photographed under the S E M and the individual micrographs pieced together such that figures 48.2 to 48.5 depict the sequence from left to right in an enlarged form.

"Left" and "right" refer to the edges of the weatherboard as presented in figure 48.1, and the white spots lettered a to k are reference markers to facilitate matching positions on figure 48.1 with figures 48.2 to 48.5.

The dashed lines point to positions on the weatherboard where magnifications to show details have been made.

fig 48.2 - left edge
fig 48.3 - top edge
fig 48.4 - top edge
fig 48.5 - right edge

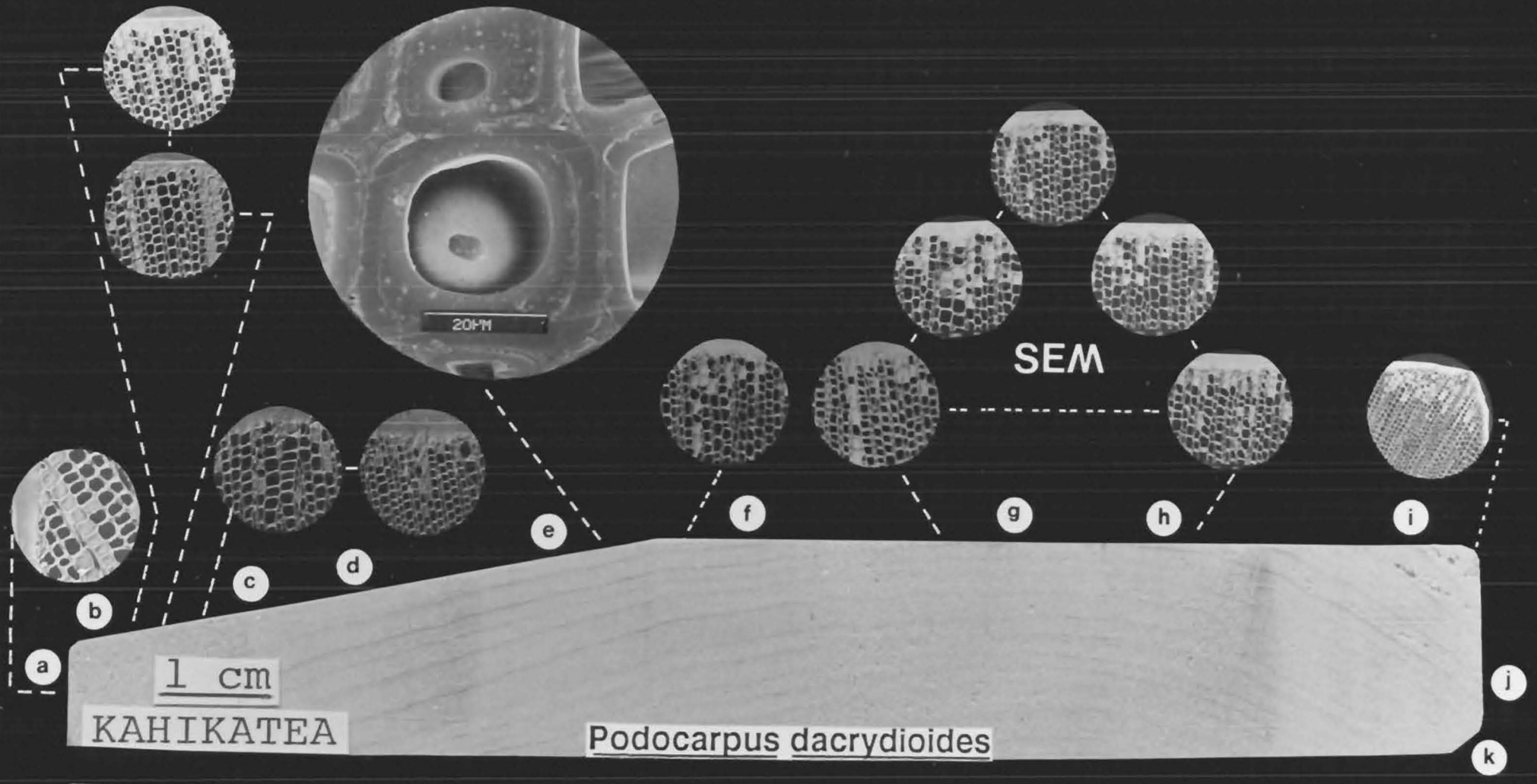
20µm
SEM
a
b
c
d
e
f
g
h
i
j
k
1 cm
KAHIKATEA
Podocarpus dacrydioides

Figure 48.1

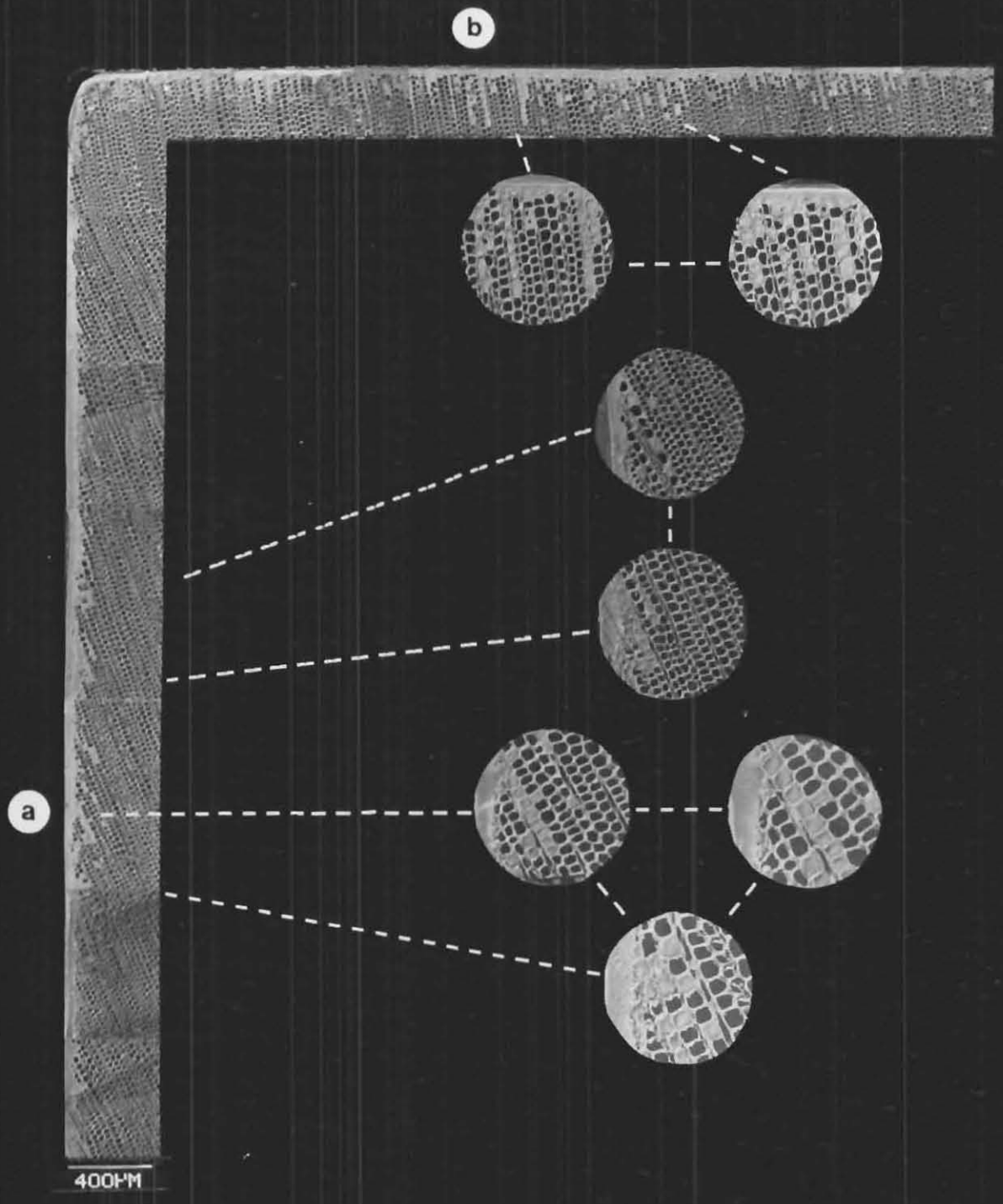

SEM

Backscattered Electron Image

Podocarpus dacrydioides

Figure 48.2

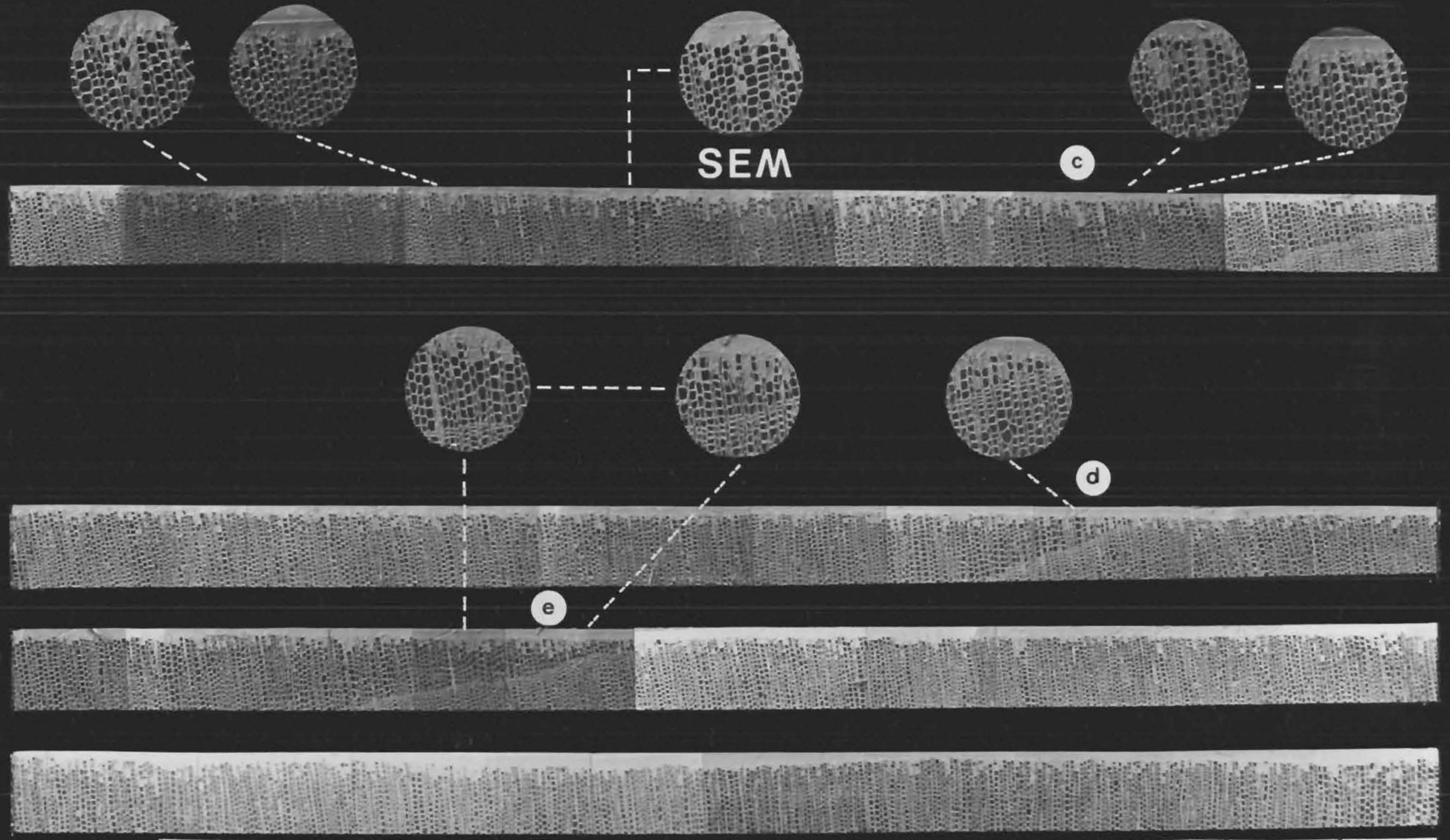

Figure 48.3 Podocarpus dacrydioides

Backscattered Electron Image

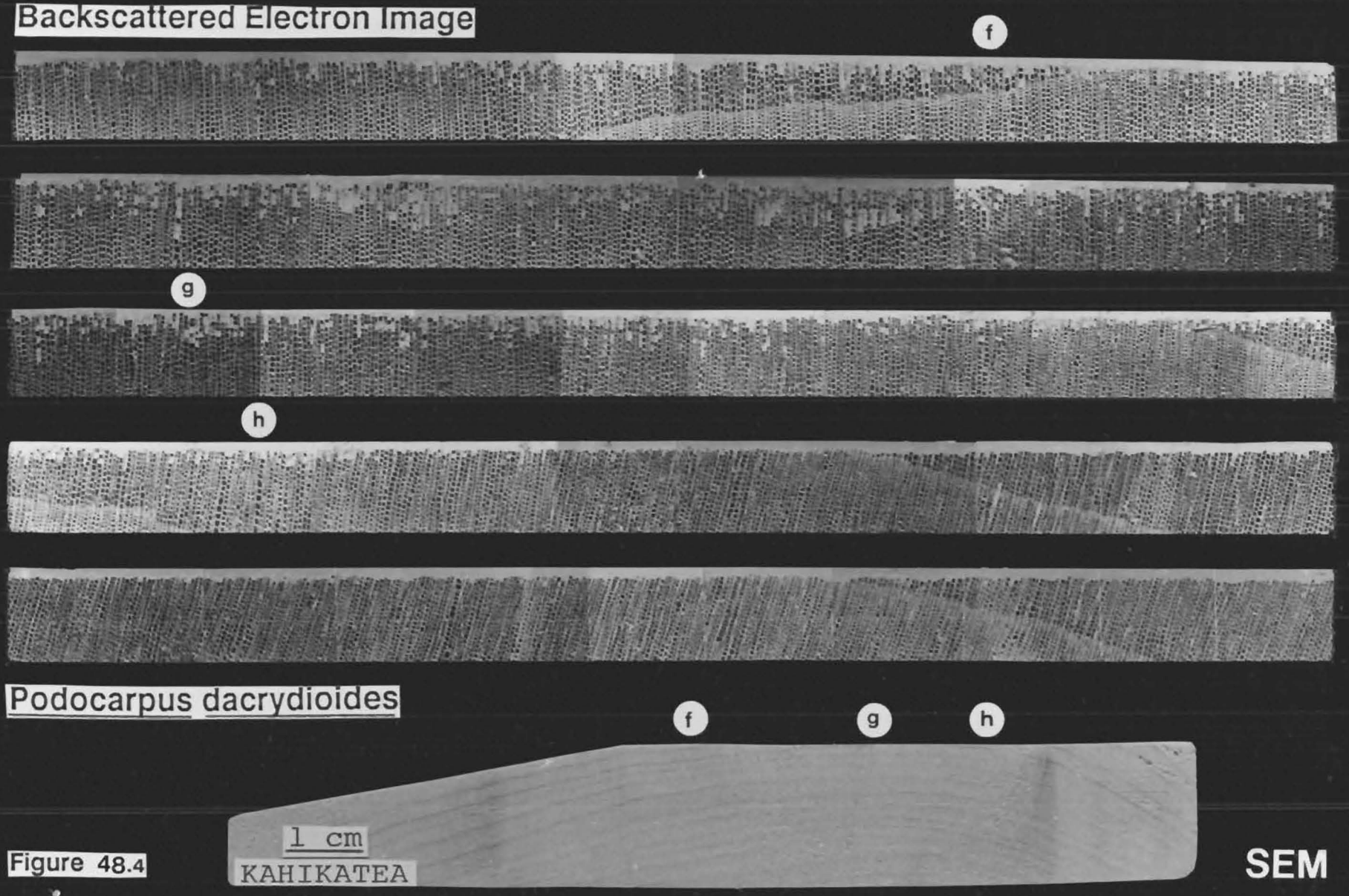
Backscattered Electron Image
f
g
h
Podocarpus dacrydioides
f
g
h
1 cm
KAHIKATEA
SEM

Figure 48.4

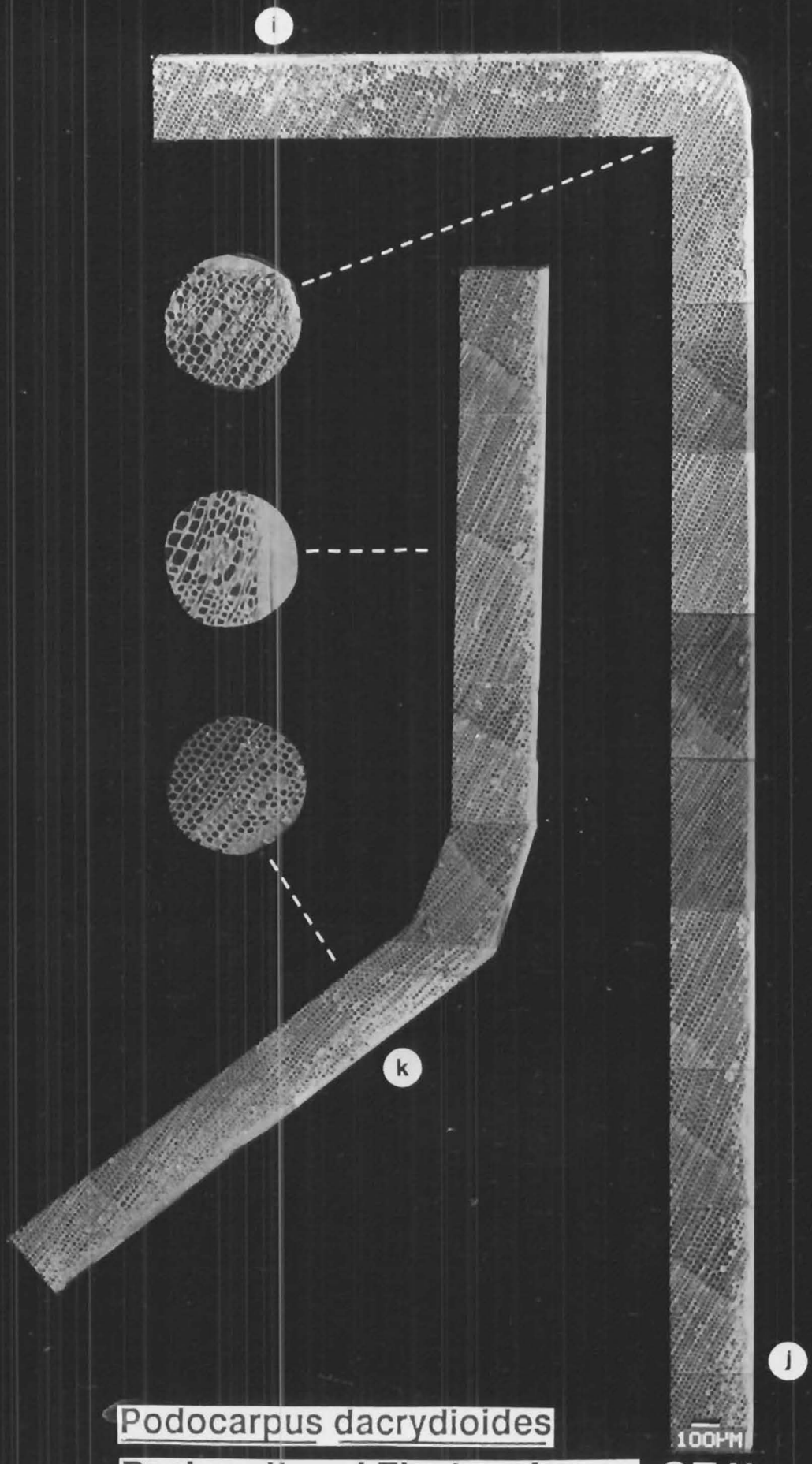

Podocarpus dacrydioides

Backscattered Electron Image SEM

Figure 48.5

FIGURE 49.1

A cross-section showing a "U"-type growth ring pattern cut through a Pinus radiata (radiata pine) weatherboard coated with TiO_2 tagged Wattyl Estapol Exterior Clear.

The entire length of this weatherboard section was photographed under the S E M and the individual micrographs pieced together such that figures 49.2 to 49.5 depict the sequence from left to right in an enlarged form.

"Left" and "right" refer to the edges of the weatherboard as presented in figure 49.1, and the white spots lettered a to j are reference markers to facilitate matching positions on figure 49.1 with figures 49.2 to 49.5.

The dashed lines point to positions on the weatherboard where magnifications to show details have been made.

fig 49.2 - left edge
fig 49.3 - top edge
fig 49.4 - top edge
fig 49.5 - right edge

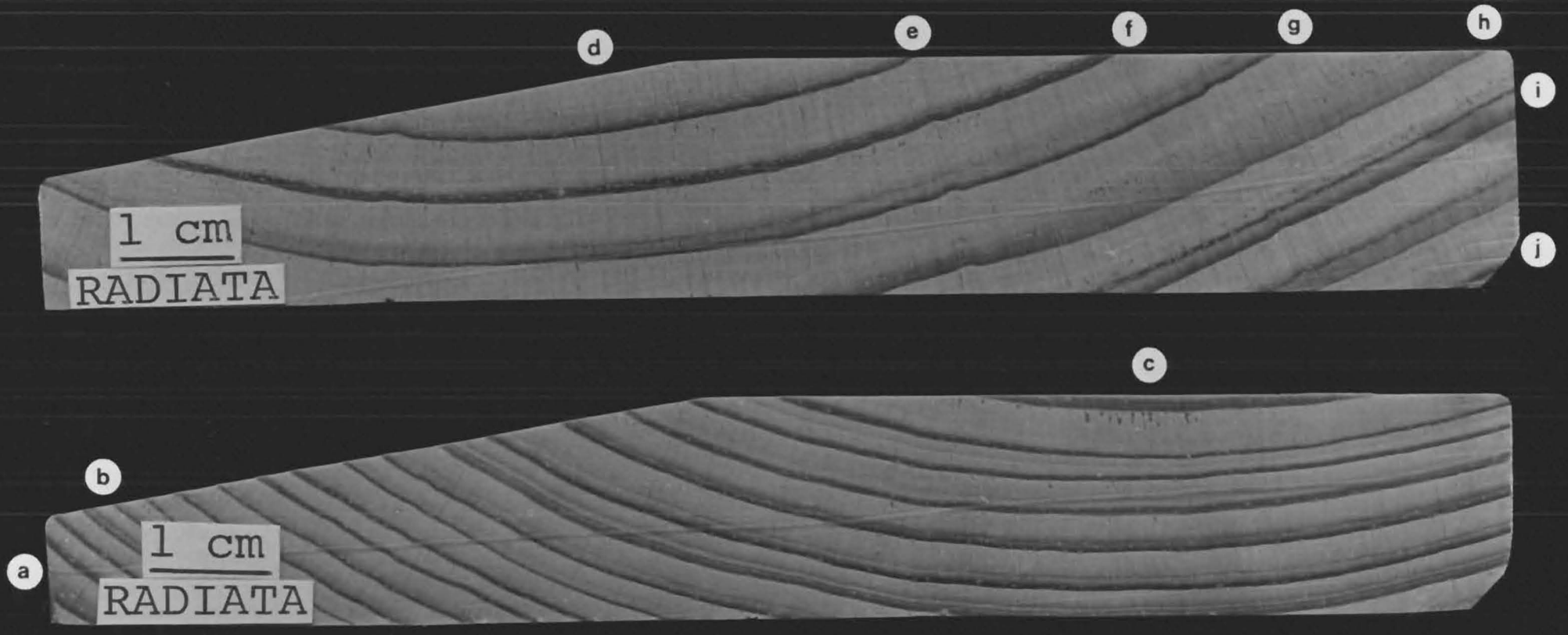

Figure 49.1 Pinus radiata

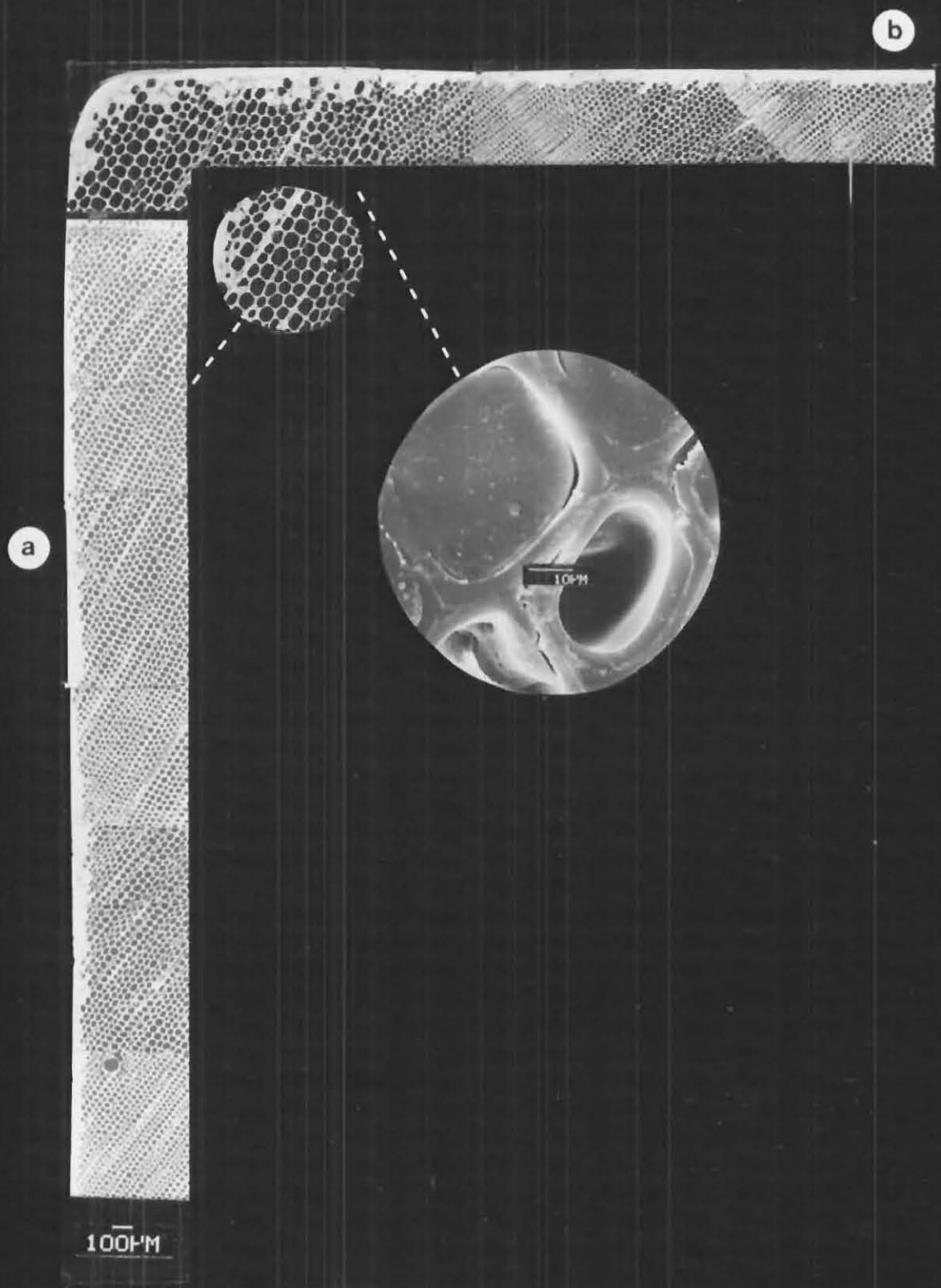

Backscattered Electron Image

Pinus radiata

Figure 49.2

SEM


Backscattered Electron Image Pinus radiata
100µM
C
SEM
C
1 cm
RADIATA

Figure 49.3

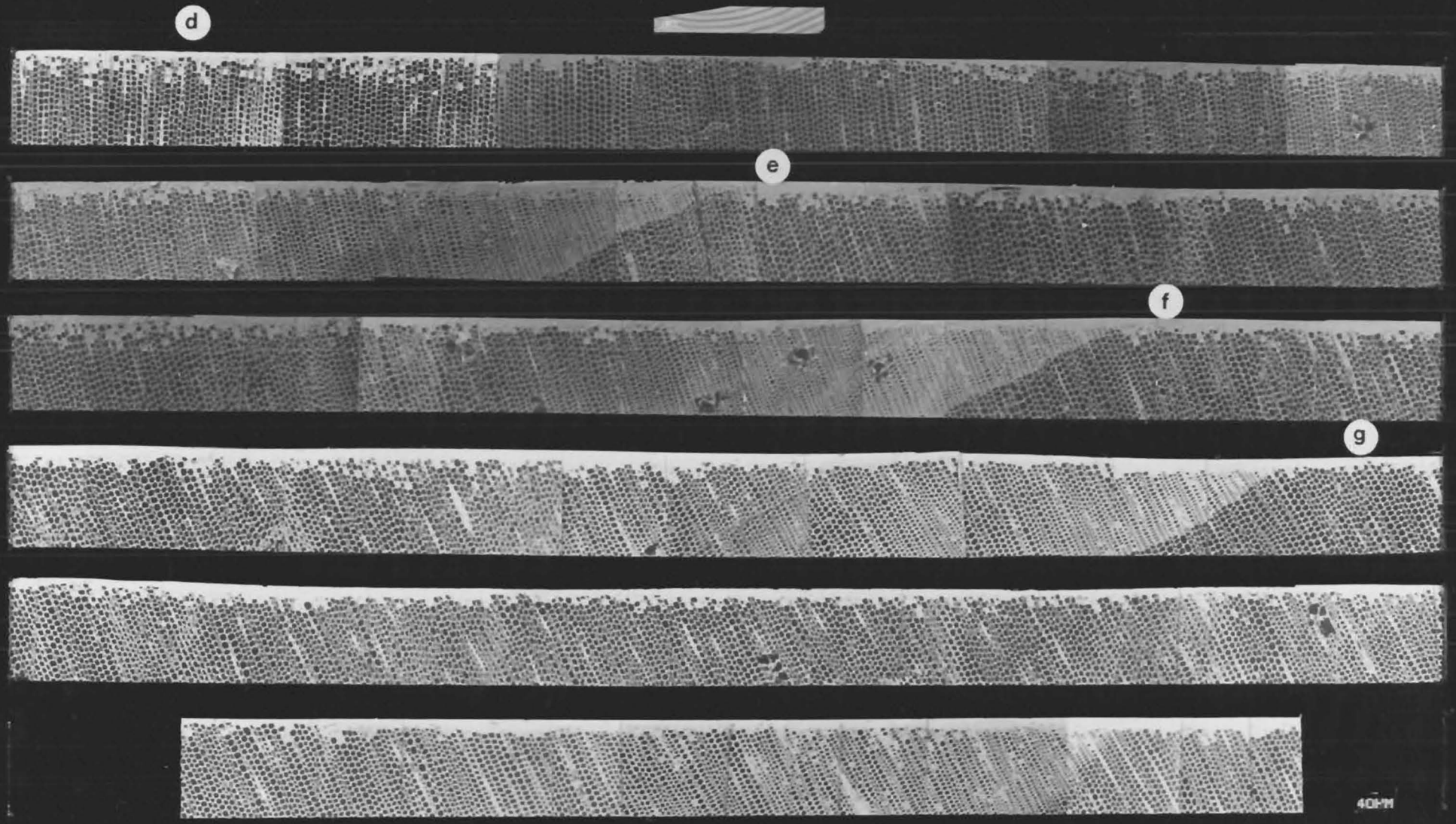

Figure 49.4 Pinus radiata Backscattered Electron Image SEM

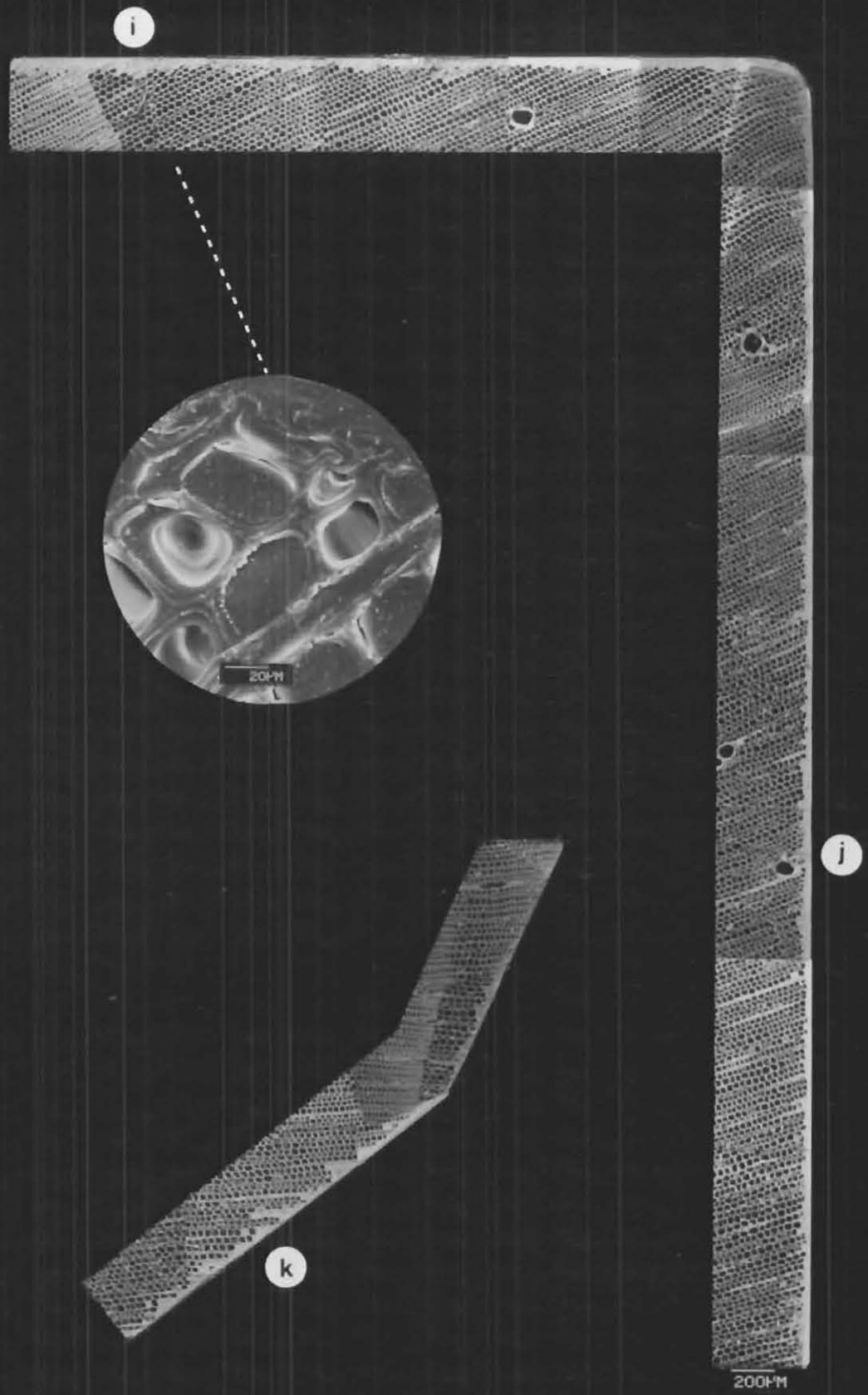

SEM

Backscattered Electron Image

Pinus radiata

Figure 49.5

FIGURE 50.1

A cross-section showing a "n"-type growth ring pattern cut through a Pinus radiata (radiata pine) weatherboard coated with TiO_2 tagged Wattyl Estapol Exterior Clear.

The entire length of this weatherboard section was photographed under the S E M and the individual micrographs pieced together such that figures 50.2 to 50.5 depict the sequence from left to right in an enlarged form.

"Left" and "right" refer to the edges of the weatherboard as presented in figure 50.1, and the white spots lettered a to k are reference markers to facilitate matching positions on figure 50.1 with figures 50.2 to 50.5.

The dashed lines point to positions on the weatherboard where magnifications to show details have been made.

fig 50.2 - left edge
fig 50.3 - top edge
fig 50.4 - top edge
fig 50.5 - right edge

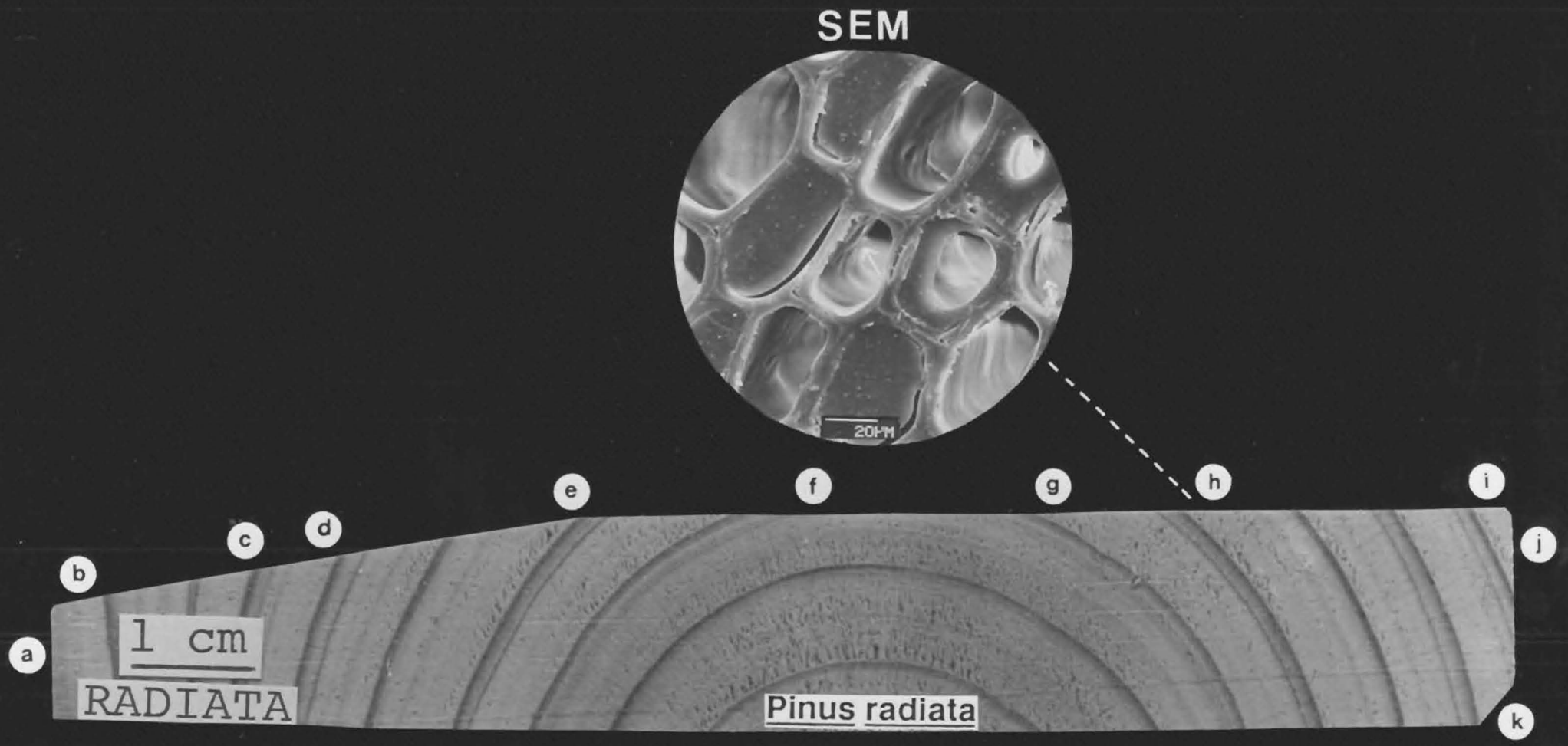

Figure50.1

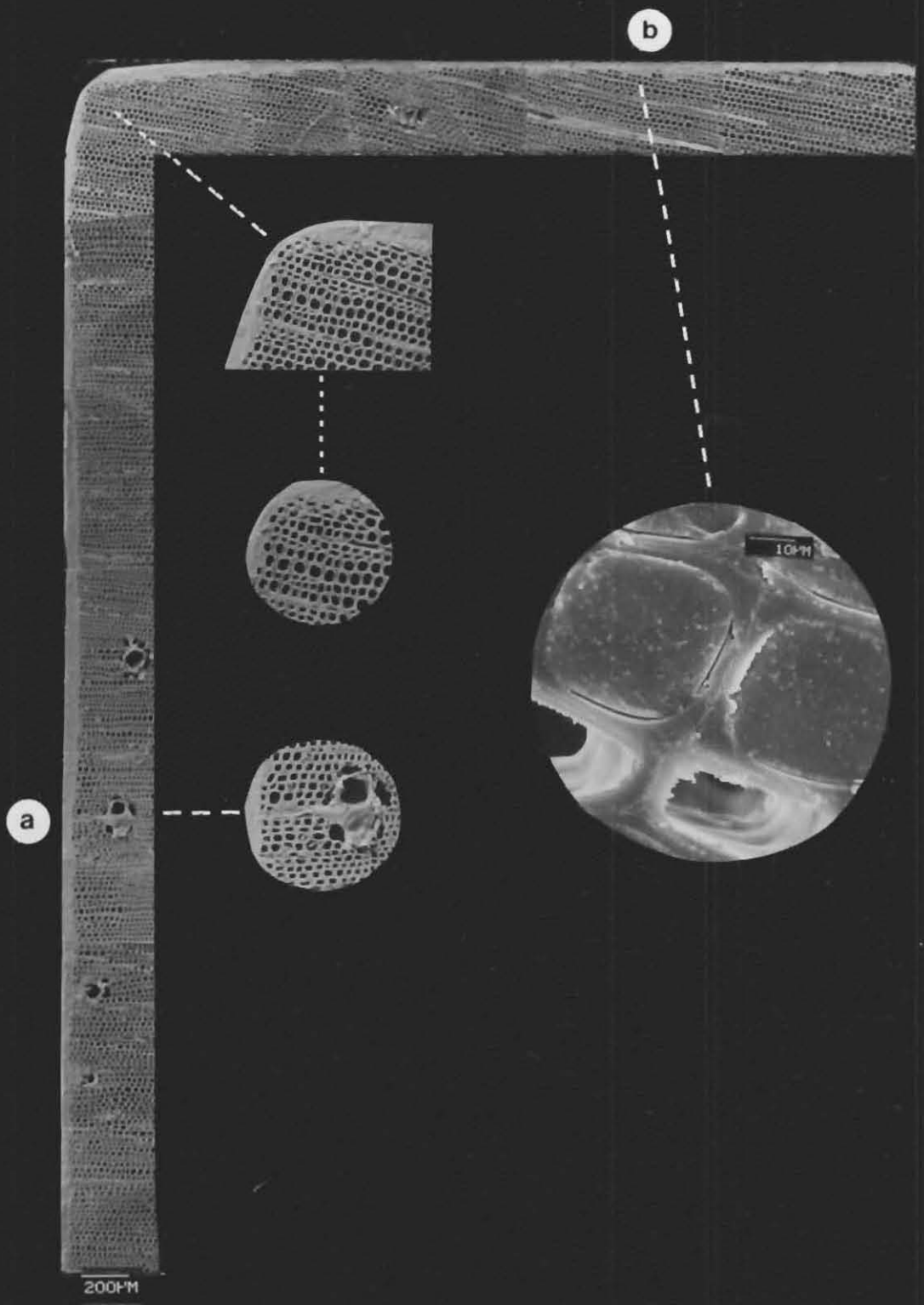

SEM

Backscattered Electron Image

Pinus radiata

Figure 50.2

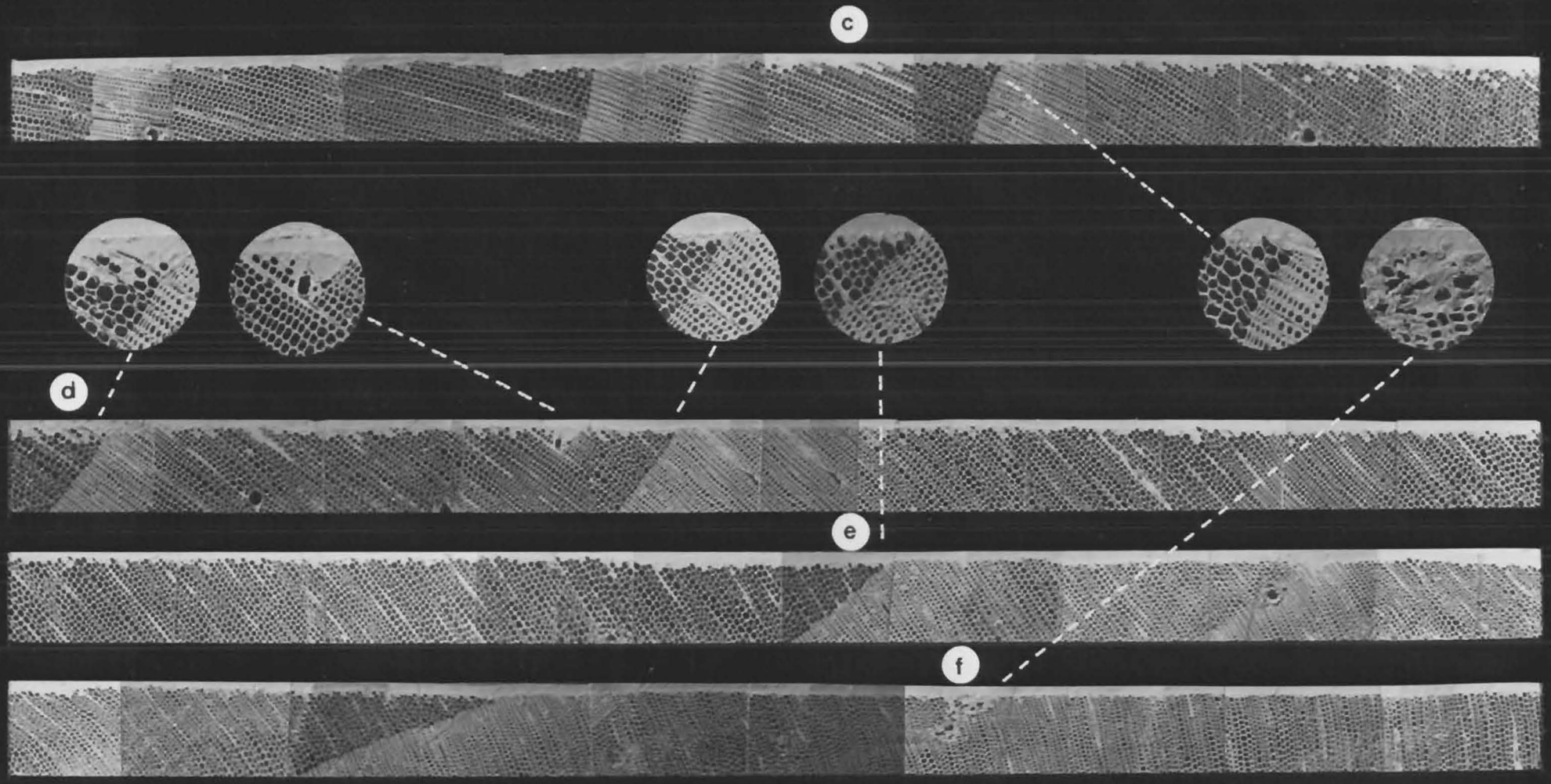

Figure 50.3 Pinus radiata

Backscattered Electron Image SEM

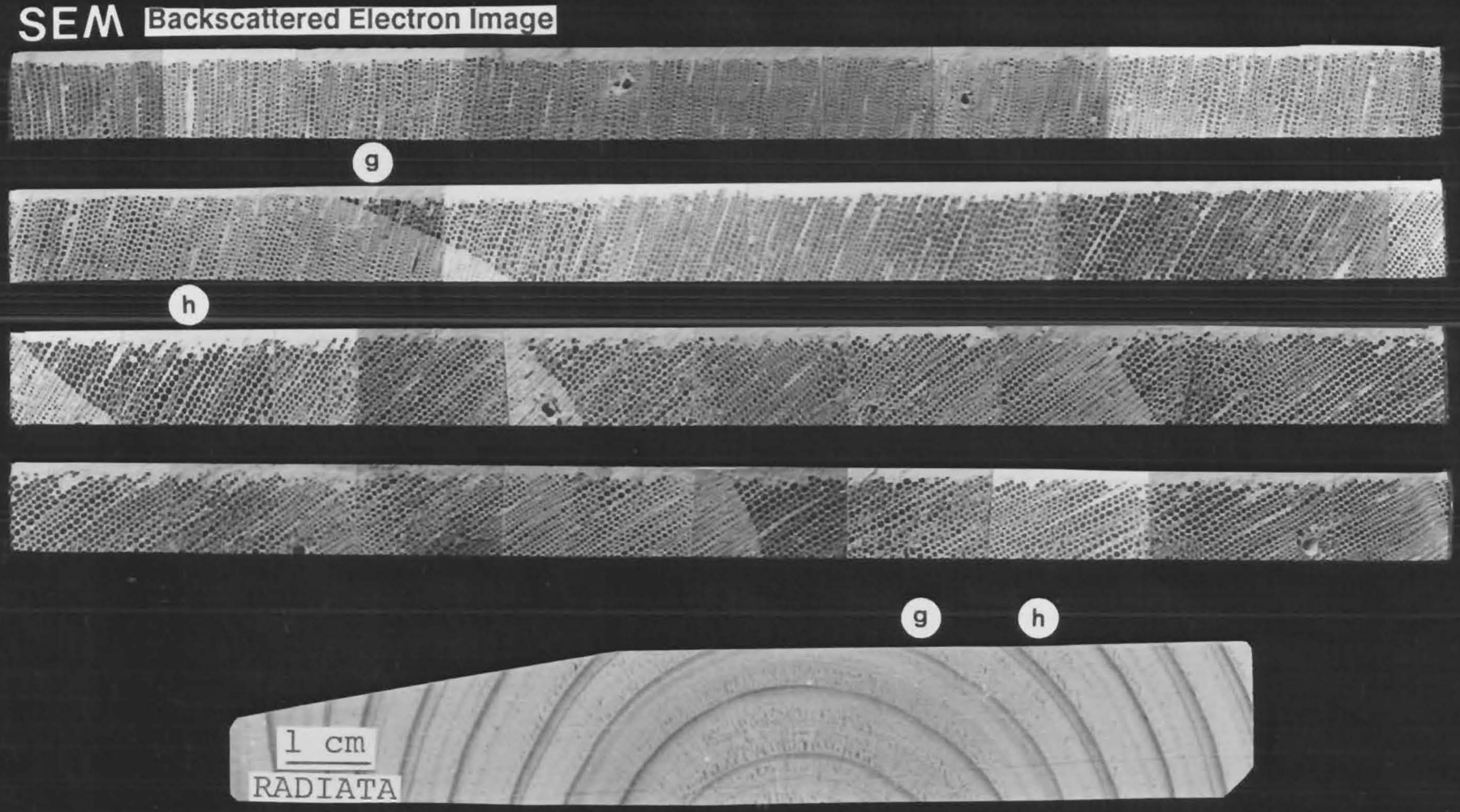

Figure 50.4 Pinus radiata

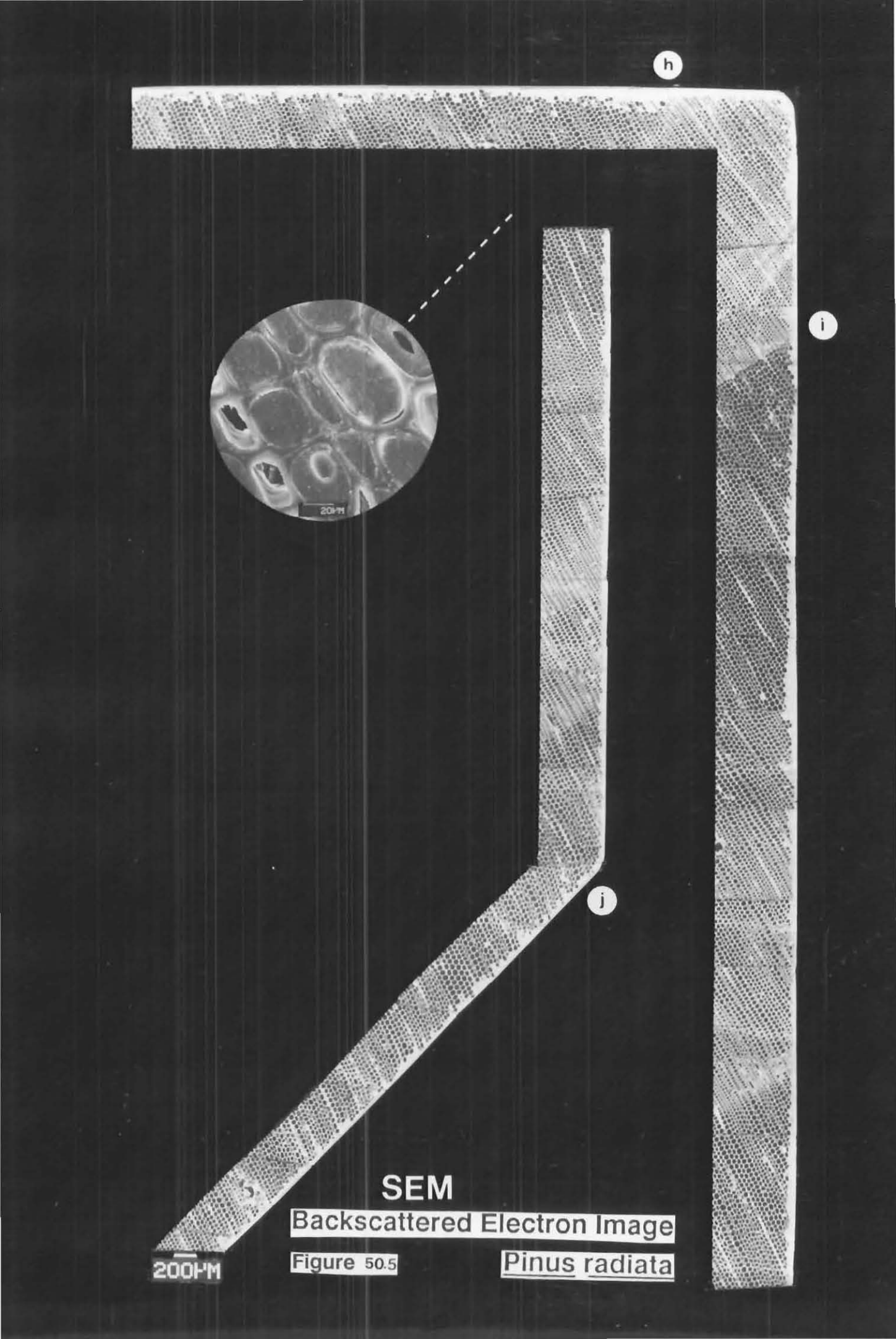

SEM

Backscattered Electron Image

Figure 50.5 Pinus radiata

Duncan's New Multiple Range test, which considers the 'span' involved in a comparison between two means taken from a larger group of means, was selected as the *a posteriori* test.

A regression analysis was employed to determine whether a functional relationship between the variables under study exists; ie. to describe the dependence of the y variable on the independent x variable.

The ANOVA for depth of penetration along the 14 cm length of the board is recorded in Table 2.1.1. Significant variation exists among taxa. The calculated F value of 3.91 exceeds the critical F value given in statistical tables at P=0.05, therefore the null hypothesis is rejected. The probability of obtaining such an F value by chance is 0.0001 indicating a significant treatment effect exists.

Duncan's New Multiple Range Test is given in Table 2.1.2, and shows that not only is there no significant difference among the means for depth of penetration recorded for *D. cupressinum* and *P. dacrydioides* but the difference among both 'u'-type and 'n'-type profiles for these two endemic taxa is also insignificant. However, the mean depth of penetration recorded for *P. radiata* weatherboards exhibiting the 'n'-type cut is significantly different from the latter two taxa. Although the mean depth of penetration in 'u'-type *P. radiata* boards is not significantly different from *D. cupressinum* and *P. dacrydioides* 'u'-type boards, it is significantly different from *D.cupressinum* 'n'-type boards.

The means and ranges for each taxon and the associated board profiles are recorded in appendix 4.2. The maximum penetration depth over the 14 cm interval was nine cells in both 'u' and 'n'-type *D. cupressinum* boards; six cells for 'u'-type and thirteen cells for 'n'-type *P. dacrydioides* boards and shallower in *P. radiata*, being eight cells in 'u'-type boards and six cells in 'n'-type boards.

The depth of coating penetration on the two edges (sides) of each board is also recorded in appendix 4. The terms 'left' and 'right' used here are merely for descriptive convenience. The analysis of variance is presented in Table 2.2.1. The calculated F value of 22.9 exceeds the critical F value at P=0.05, therefore, the null hypothesis is rejected. The probability of obtaining such an F value by chance is 0.0001.

Duncan's New Multiple Range Test in Table 2.2.2, indicates that the left and right edges of *D. cupressinum* 'u' and 'n'-type boards are significantly different from each other. This phenomenon is also statistically suggested in *P. dacrydioides* boards but there appears to be no significant difference between the left and right edges of *P. radiata* 'u' and 'n'-type boards. If the means for individual left and right sides are compared among taxa, some similarity exists, for example, all the right 'u'-type boards for the three taxa are not significantly different. The individual measurements for coating penetration as seen on the left and right edges show that the maximum penetration was significantly deeper on the sides than the top edge for both *D. cupressinum* and *P. dacrydioides*. Maximum penetration depth as seen on the edges of *P. radiata* boards was not significantly different to that observed along the 14 cm interval across the top edge. Twenty-seven cells was the maximum

TABLE 2

DEPTH OF COATING PENETRATION MEASURED ON THE TRANSVERSE FACE OF WEATHERBOARDS (refer appendix 4)

'u' - type and 'n' - type board profiles.

Coating : TiO_2 tagged Wattyl Estapol .

TABLE 2.1.1 ANALYSIS OF VARIANCE - ONE WAY ANOVA

SOURCE	df	SS	MS	F	P>F
AMONG TAXA	5	27.62	5.52	3.91	0.003
WITHIN	78	110.22	1.41		
TOTAL	83	137.84			

TABLE 2.1.2

DUNCAN'S NEW MULTIPLE RANGE FOR THE COMPARISON OF MEANS AT THE P=0.05 LEVEL.

THE MEANS WHICH ARE NOT SIGNIFICANTLY DIFFERENT (n.s) ARE GROUPED TOGETHER. THE MEANS ARE RANKED FROM HIGHEST TO LOWEST.

TAXA	BOARD PROFILE	DUNCAN GROUPING
Dacrydium cupressinum	'n' - type	n.s.
Dacrydium cupressinum	'u' - type	n.s.
Podocarpus dacrydioides	'u' - type	n.s.
Podocarpus dacrydioides	'n' - type	
Pinus radiata	'u' - type	
Pinus radiata	'n' - type	

TABLE 2.2.1

DEPTH OF COATING PENETRATION MEASURED ON THE TRANSVERSE FACE OF WEATHERBOARDS (refer appendix 4)

LEFT edge and RIGHT edge of board.
'u' - type and 'n' - type board profiles.
Coating : TiO_2 tagged Wattyl Estapol .

ANALYSIS OF VARIANCE - ONE WAY ANOVA

SOURCE	df	SS	MS	F	P>F
AMONG TAXA	11	3071.16	279.19	22.9	0.0001
WITHIN	108	1316.80	12.19		
TOTAL	119	4387.96			

TABLE 2.2.2

DUNCAN'S NEW MULTIPLE RANGE FOR THE COMPARISON OF MEANS AT THE P=0.05 LEVEL.

THE MEANS WHICH ARE NOT SIGNIFICANTLY DIFFERENT (n.s) ARE GROUPED TOGETHER. THE MEANS ARE RANKED FROM HIGHEST TO LOWEST.

TAXA	EDGE	BOARD PROFILE	MEAN	DUNCAN GROUPING
Dacrydium cupressinum	left	' u ' - type	17.8	n.s.
Podocarpus dacrydioides	left	' u ' - type	13.3	n.s.
Dacrydium cupressinum	right	' n ' - type	8.3	n.s.
Podocarpus dacrydioides	left	' n ' - type	8.1	
Dacrydium cupressinum	left	' n ' - type	4.7	n.s.
Dacrydium cupressinum	right	' u ' - type	4.5	
Podocarpus dacrydioides	right	' n ' - type	3.0	
Pinus radiata	left	' u ' - type	2.3	
Podocarpus dacrydioides	right	' u ' - type	1.9	
Pinus radiata	left	' n ' - type	1.6	
Pinus radiata	right	' u ' - type	1.5	
Pinus radiata	right	' n ' - type	1.2	

TABLE 2.3.1

REGRESSION ANALYSIS :

DEPTH OF COATING PENETRATION MEASURED ON THE TRANSVERSE FACE OF WEATHERBOARDS, TAXA, PROFILE AND POSITION ALONG BOARD (refer appendix 4)

PREDICTOR (independent variables)	REGRESSION COEFFICIENT	SD	t - RATIO
D. cupressinum	3.57	0.17	21.12
P. dacrydioides	2.97	0.17	17.59
P. radiata	2.30	0.17	13.62
'u'-TYPE PROFILE	0.08	0.12	0.67
POSITION (cm) INTERVALS	0.02	0.02	1.50

TABLE 2.3.2 ANALYSIS OF VARIANCE

SOURCE	df	SS	MS
Regression	5	8625.7	1725.1
Error	835	2681.3	3.2
Total	840	11307.0	

penetration depth recorded for both *D. cupressinum* and *P. dacrydioides* compared to a maximum depth of only four cells in *P. radiata.*

A regression analysis was made to determine the functional relationship between the dependent variable DEPTH and the independent variables - TAXA, PROFILE and POSITION (cm) along the board. The regression equation is :

DEPTH = 3.57 D.cupressinum + 2.97 P.dacrydioides + 2.30 P.radiata + 0.08 'u' type PROFILE + 0.02 POSITION

Table 2.3.1 shows that because the calculated t ratio is greater than the critical value of t, given in statistical tables, at the 95% confidence limit, the relationship between depth and taxa is significant. Because the t ratios associated with profile and position are less than the critical values of t at 95% confidence limits, depth is not dependent on profile or position interval along the board Table 2.3.2 shows that the variation accounted for by the regression equation is 8625.7 thus the regression accounts for 76% of the variation [SS].

5.2 COATING/SUBSTRATE-TRACHEID CELL INCLINATION

The slope of the wood grain away from the board face plays a role in the conduction of freshly applied coating into the wood. The slope controls the extent and length each tracheid wall is opened by machining. The angle made by the tracheid cell length and substrate face (coating interface) was quantitatively measured at intervals along the entire width of each weatherboard and the average and range for each class interval is shown in appendix 5. Statistical analyses were performed for each taxon.

The ANOVA for coating substrate tracheid cell inclination angle is recorded in Table 3.1.1. Significant variation exists among taxa. The calculated F value of 9.69 exceeds the critical F value in the statistical tables at P=0.05, therefore the null hypothesis is rejected. The probability of obtaining such an F value by chance is 0.0001.

Duncan's New Multiple Range Test is given in Table 3.1.2, it shows that with regard to cut there is no significant difference among the means for both *P. radiata* and *D. cupressinum* 'u'-type boards and *P. dacrydioides* 'n'-type boards; but significant difference between *P. dacrydioides* 'u'-type boards. *D. cupressinum* and *P. radiata* 'n'-type boards are significantly different from the other taxa types. In general 'u'-type boards exhibit a greater mean angle than 'n'-type boards with *P. dacrydioides* 'u'-type boards possessing the greatest mean angle of 6.55 degrees and *P. radiata* the smallest mean angle of 2.94 degrees. The angle ranges for each taxon and associated board profiles is shown in appendix 5. The maximum angles for 'u' and 'n'-type boards is 9 degrees and 7 degrees

TABLE 3

COATING SUBSTRATE TRACHEID CELL INCLINATION ANGLE

(refer appendix 5)

TABLE 3.1.1 ANALYSIS OF VARIANCE - ONE WAY ANOVA

SOURCE	df	SS	MS	F	P>F
AMONG TAXA	5	113.82	22.76	9.69	0.0001
WITHIN	78	183.15	2.34		
TOTAL	83	296.97			

TABLE 3.1.2

DUNCAN'S NEW MULTIPLE RANGE FOR THE COMPARISON OF MEANS AT THE P=0.05 LEVEL.

THE MEANS ARE RANKED FROM HIGHEST TO LOWEST.
THE MEANS WHICH ARE NOT SIGNIFICANTLY DIFFERENT (n.s) ARE GROUPED TOGETHER.

TAXA	BOARD PROFILE	DUNCAN GROUPING
Podocarpus dacrydioides	'u' - type	I n.s.
Pinus radiata	'u' - type	I
Podocarpus dacrydioides	'n' - type	I n.s.
Dacrydium cupressinum	'u' - type	I
Dacrydium cupressinum	'n' - type	I
Pinus radiata	'n' - type	I n.s

TABLE 3.2.1

COATING SUBSTRATE TRACHEID CELL INCLINATION ANGLE (refer appendix 5)

LEFT edge and RIGHT edge of board

'u' - type and 'n' - type board profiles.

Coating : TiO_2 tagged Wattyl Estapol.

ANALYSIS OF VARIANCE - ONE WAY ANOVA

SOURCE	df	SS	MS	F	P>F
AMONG TAXA	10	112.98	11.29	5.91	0.0001
WITHIN	49	93.60	1.91		
TOTAL	59	206.58			

TABLE 3.2.2

DUNCAN'S NEW MULTIPLE RANGE FOR THE COMPARISON OF MEANS AT THE P = 0.05 LEVEL.

THE MEANS WHICH ARE NOT SIGNIFICANTLY DIFFERENT (n.s) ARE GROUPED TOGETHER. THE MEANS ARE RANKED FROM HIGHEST TO LOWEST.

TAXA	EDGE	PROFILE	MEAN	DUNCAN GROUPING
Dacrydium cupressinum	right	'u' - type	6.4	
Dacrydium cupressinum	right	'n' - type	6.2	n.s.
Podocarpus dacrydioides	left	'u' - type	5.6	
Pinus radiata	left	'u' - type	5.0	n.s.
Pinus radiata	left	'n' - type	4.2	
Dacrydium cupressinum	left	'n' - type	4.0	n.s.
Dacrydium cupressinum	left	'u' - type	3.8	
Podocarpus dacrydioides	right	'n' - type	3.8	n.s.
Podocarpus dacrydioides	right	'u' - type	3.2	
Pinus radiata	right	'u' - type	2.6	n.s.
Pinus radiata	right	'n' - type	2.6	
Podocarpus dacrydioides	left	'n' - type	2.2	

TABLE 3.3.1 REGRESSION ANALYSIS

COATING SUBSTRATE TRACHEID CELL INCLINATION ANGLE, TAXA, PROFILE AND POSITION ALONG BOARD (refer appendix 5)

PREDICTOR (independent variables)	REGRESSION COEFFICIENT	SD	t - RATIO
D. cupressinum	3.03	0.24	12.72
P. dacrydioides	4.56	0.24	19.14
P. radiata	2.92	0.24	12.27
'u' - TYPE PROFILE	1.73	0.17	9.91
POSITION (cm) INTERVALS	0.04	0.02	1.72

TABLE 3.3.2 ANALYSIS OF VARIANCE

SOURCE	df	SS	MS
Regression	5	9620.4	1924.1
Error	415	1324.6	3.2
Total	420	10945.0	

for *D. cupressinum*; 12 degrees and 8 degrees for *P. dacrydioides* and 9 degrees and 5 degrees for *P. radiata* respectively.

The tracheid cell inclination angles as measured on the two edges of each board are also recorded in appendix 5. The analysis of variance is shown in Table 3.2.1. The calculated F value of 5.91 exceeds the critical F value at P=0.05, therefore the null hypothesis is rejected. The probability of obtaining such an F value by chance is 0.0001.

Duncan's New Multiple Range Test in Table 3.2.2 indicates that the left and right edges of *D. cupressinum* boards are significantly different from each other but there is no significant difference between the left edges of 'u' and 'n'-type boards and the right edges of 'u' and 'n'-type boards. This phenomenon is also statistically suggested for *P. dacrydioides* boards, except there is a significant difference with regard to the left edges of both 'u' and 'n'-type boards. Statistically there is very little difference between the left and right edges of *P. radiata* boards, although Duncan's Test separates the left edge 'u'-type boards from the other combinations.

A regression analysis was made to determine the functional relationship between the dependent variable ANGLE and the independent variables - TAXA, PROFILE and POSITION (cm) along the board.

The regression equation is :

ANGLE = 3.03 *D.cupressinum* **+ 4.56** *P.dacrydioides* **+ 2.92** *P.radiata* **+ 1.73** 'u' type **PROFILE + 0.03 POSITION**

Table 3.3.1 shows that because the calculated t ratio is greater than the critical value of t, given in statistical tables at 95% confidence limits, the relationship between tracheid cell inclination angle and taxa is significant. The relationship between tracheid cell inclination angle and board profile is also significant. However, because the calculated t ratio associated with position was less than the critical value of t, given in statistical tables at 95% confidence limits, tracheid cell inclination angle is not dependent on position along the board.

Table 3.3.2 shows that the variation accounted for by the regression equation is 9620.4 thus the regression accounts for 87% of the variation [SS].

5.3 TRACHEID CELL ROW GROWTH DIRECTIONS AND THE COATING INTERFACE

Growth ring pattern, age and position in the wood controls the radiating direction of the tracheid rows from the pith. Cell wall pitting occurs predominantly on the radial walls with the exception of some tangential pitting in latewood cells. The angular presentation of pits to the coating obviously plays a part in the movement path of liquids into the wood. In each board, tracheid pit positions vary from parallel to oblique and perpendicular to the coating interface. Tracheid cell row

TABLE 3.4.1

COATING / SUBSTRATE TRACHEID CELL INCLINATION ANGLE AND TRACHEID CELL GROWTH DIRECTION

CORRELATION ANALYSIS

VARIABLES.	INCLINATION ANGLE.	CELL DIRECTION.
INCLINATION ANGLE.	1.00 0.00	0.25 0.26
CELL DIRECTION.	0.25 0.26	1.00 0.00

TABLE 3.5.1

DEPTH OF COATING PENETRATION AND TRACHEID CELL GROWTH DIRECTION

CORRELATION ANALYSIS

VARIABLES.	PENETRATION DEPTH.	CELL DIRECTION.
PENETRATION DEPTH.	1.00 0.00	-0.08 0.63
CELL DIRECTION.	-0.08 0.63	1.00 0.00

growth direction angles viewed on the transverse face of weatherboards for both "u" and "n"-type cuts were measured and the results are presented in diagramatic form in appendix 6.

Statistical analyses were performed to determine whether the variables: coating penetration depth and tracheid cell row growth direction are interdependent or vary together. A correlation analysis was chosen to establish the strength of the relationship between the variables. Pearson's product moment correlation coefficient or 'r', is a number that ranges from -1.0 to + 1.0, indicating a negative or positive relationship; if it is zero, no relationship is suggested. The correlation coefficient is the ratio of the covariance to the product of the standard deviation of the two variables. The correlation matrix presented in table 3.4.1 shows that the correlation coefficient is -.08. A negative correlation coefficient indicates that as one variable goes up the other goes down, however, because the value is very close to zero it can be inferred that the two variables are unrelated. A test of significance for the correlation coefficient 'r' showed that the probability PROB > r under Ho:Rho=0 is 0.63 at the 0.05 level. It is concluded that there is no relationship between coating penetration depth and tracheid cell row growth direction with regard to all three taxa.

A correlation analysis was also chosen to determine the strength of the relationship between coating/substrate tracheid cell inclination angle and tracheid cell row growth direction. The correlation matrix presented in table 3.5.1 shows that the correlation coefficient is 0.25. A positive correlation coefficient indicates that the values of both variables increase together. A test of significance PROB > r under Ho : Rho=0 showed that the probability is 0.26 at the 0.05 level. It is concluded that the relationship between coating/substrate tracheid cell inclination angle and tracheid cell row growth direction is not significant for all three taxa studied.

5.4 COATING PENETRATION - A SEM STUDY.

The longitudinal views of coated boards depicted in figures 51 to 54 are typical examples of the gross nature of the coating on *D. cupressinum, P. dacrydioides* and *P. radiata* weatherboards. A comparison of figures 51 [A] to [C] suggests that the TiO_2 tagged Wattyl Estapol does not fill the entire space available in each cell. " Air pockets " and extractives and other deposits present in the cell lumens at the time of coating application are attributed to have disrupted the flow of the coating. This "air pocket " phenomenon is more obvious in boards coated on the radial face (compare figures 51 [B] and [C]); and this may be related to pit aperture orientation presented to the coating on entry. During the process of splitting the coating film away, to expose the cells beneath, the first few microns of the interface are removed thus a true cast/mould effect is difficult to produce. However, alternative techniques of serial sectioning were employed to obtain a complete " picture " of the coating/interface but in side view (compare figures 52 [C] and [D]).

Microscopic evidence suggests that gross penetration of the coating into ray parenchyma cells is minimal in *D. cupressinum* and *P. dacrydioides* compared to *P. radiata.* Figures 52 [A] and [B] depict tangential views of a *D. cupressinum* board showing the presence of coating in ray cells. Figures 52 [E], [F] and [G] provide evidence that the extent of gross penetration is shallow. The " air pocket " effect, previously mentioned, is more apparent in *P. dacrydioides* and *P. radiata* than in *D. cupressinum* (compare figures 51 [B], 52 [B] & [D] and 54 [A], [D] & [E]).

The zig zag path of coating flow into the wood is controlled partly by the gross structure of the wood and anatomical features exposed by machining on the longitudinal faces. The number, distribution and size of pits exposed controls the direction path too. Pit membranes destroyed during weatherboard manufacture and treatment processess, provide entry points for the coating. The exact percentage of open pits cannot be estimated as wood preparation for electron microscopy often damages the delicate pit membranes even though the greatest care is taken with unembedded wood samples. The electron beam is capable of destroying membranes. The backscattered electron images depicting the coating lining the cell lumens in the " air pocket " zones reveals empty pit apertures. After curing, the coating contracted in the lumens and the tangential views seen in figure 53 [A] and [D] show remnants of coating plugging the pit chambers (compare this with the radial views in figure 54 [A] and [D]).

The penetration path can be traced inwards through several cell rows (figure 52 [C] to [G]). The coating is visible through " pit windows " in the tracheids behind the exposed lumens of adjacent tracheids (figure 52 [D]). The simple pit membrane of ray cells is more " robust " and uniform in nature and less likely to allow coating through the cross-fields from adjacent tracheids. Figure 52 [G] shows the coating filling horizontal ray parenchyma cells. Note the deflected pit membrane in the

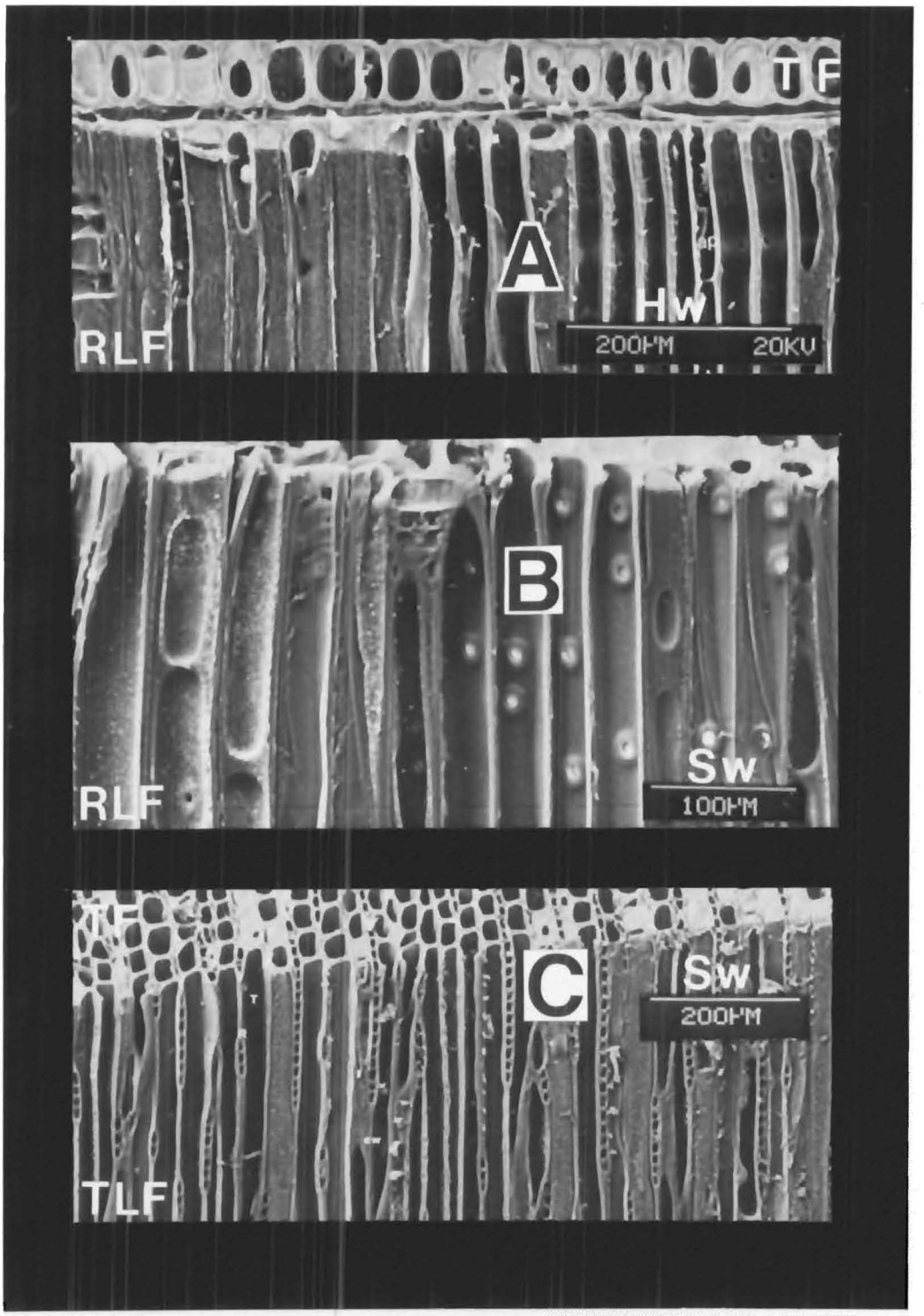

FIGURE 51

Transverse and longitudinal faces of (A) *D.cupressinum* (rimu), (B) *P.radiata* and (C) *P.dacrydioides* (kahikatea) wood coated with TiO_2 tagged Wattyl Estapol .

Note the coating covering the longitudinal face has been stripped off to reveal the cells beneath. The degree of penetration can be seen on the transverse face.(BSEI).

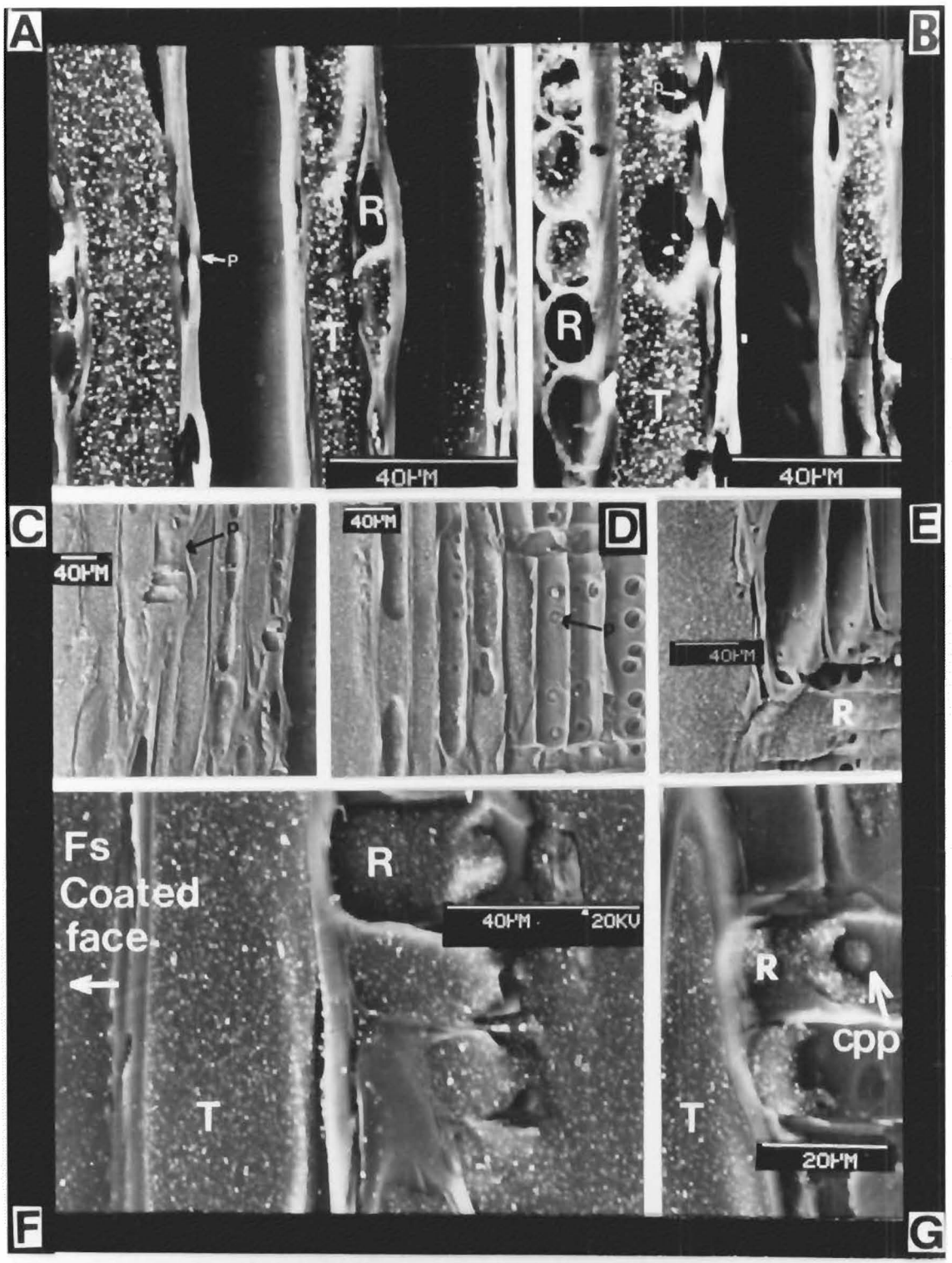

FIGURE 52

LONGITUDINAL VIEWS OF *D.cupressinum* (RIMU) COATED WITH TiO_2 TAGGED WATTYL ESTAPOL.

A. & B. The coating which was applied to the tangential face has been stripped away to reveal the partially filled ray cells and the "air pocket" regions (arrowed) where the coating has pulled away from the pit-pair. (Compare views in fig.C. and D.).

C. - G. Profile views of coated boards showing the degree of penetration in tracheids and ray cells. The coating was applied to the tangential longitudinal face of the board shown here at the extreme left of each micrograph. (BSEI)

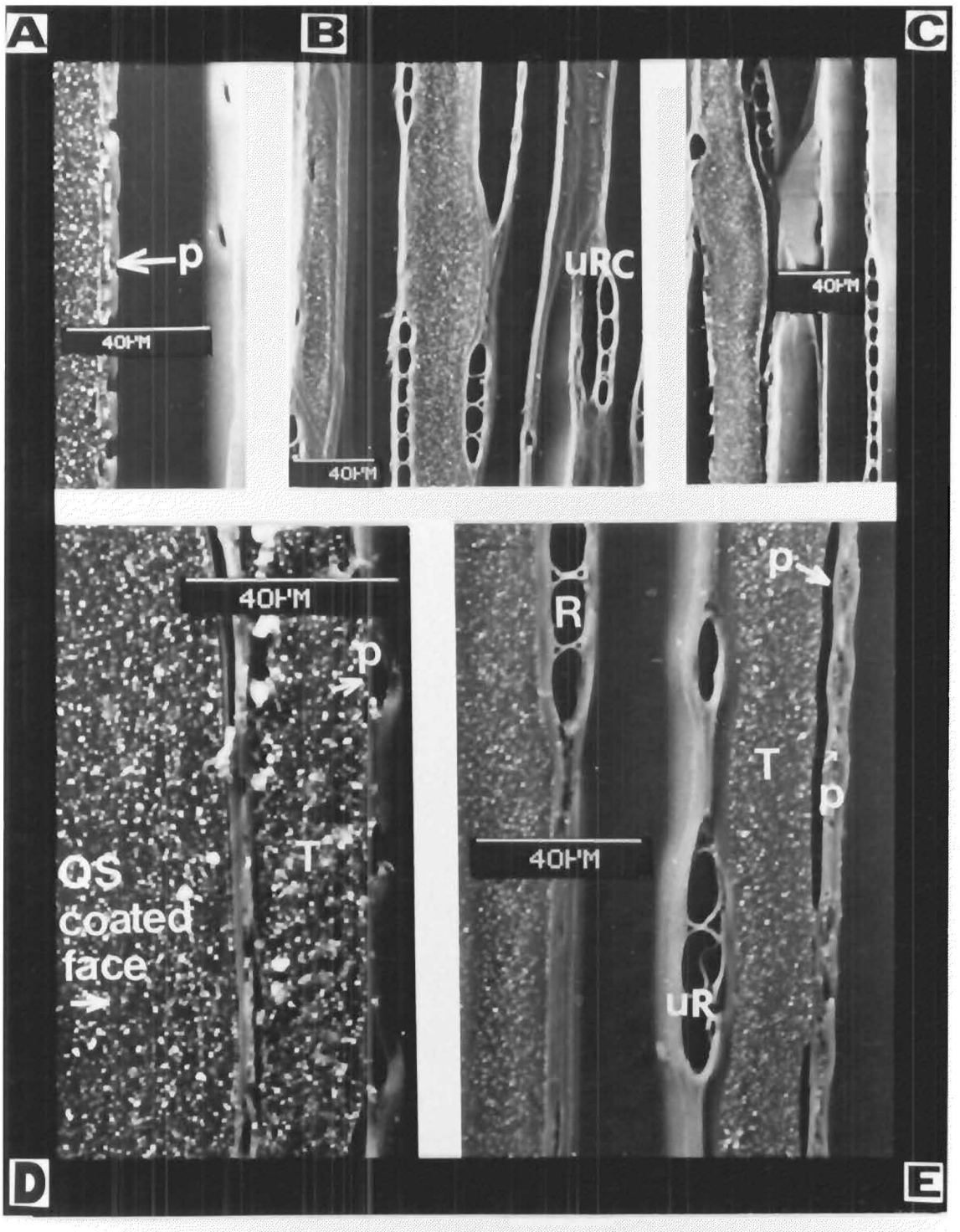

FIGURE 53

LONGITUDINAL VIEWS OF *P.dacrydioides* (KAHIKATEA) COATED WITH TiO_2 TAGGED WATTYL ESTAPOL .

A.- E. The coating was applied to the radial longitudinal face. (Extreme left of the micrographs; see Fig.D.).
Note the coating has pulled away from the tracheid wall in Fig.E.

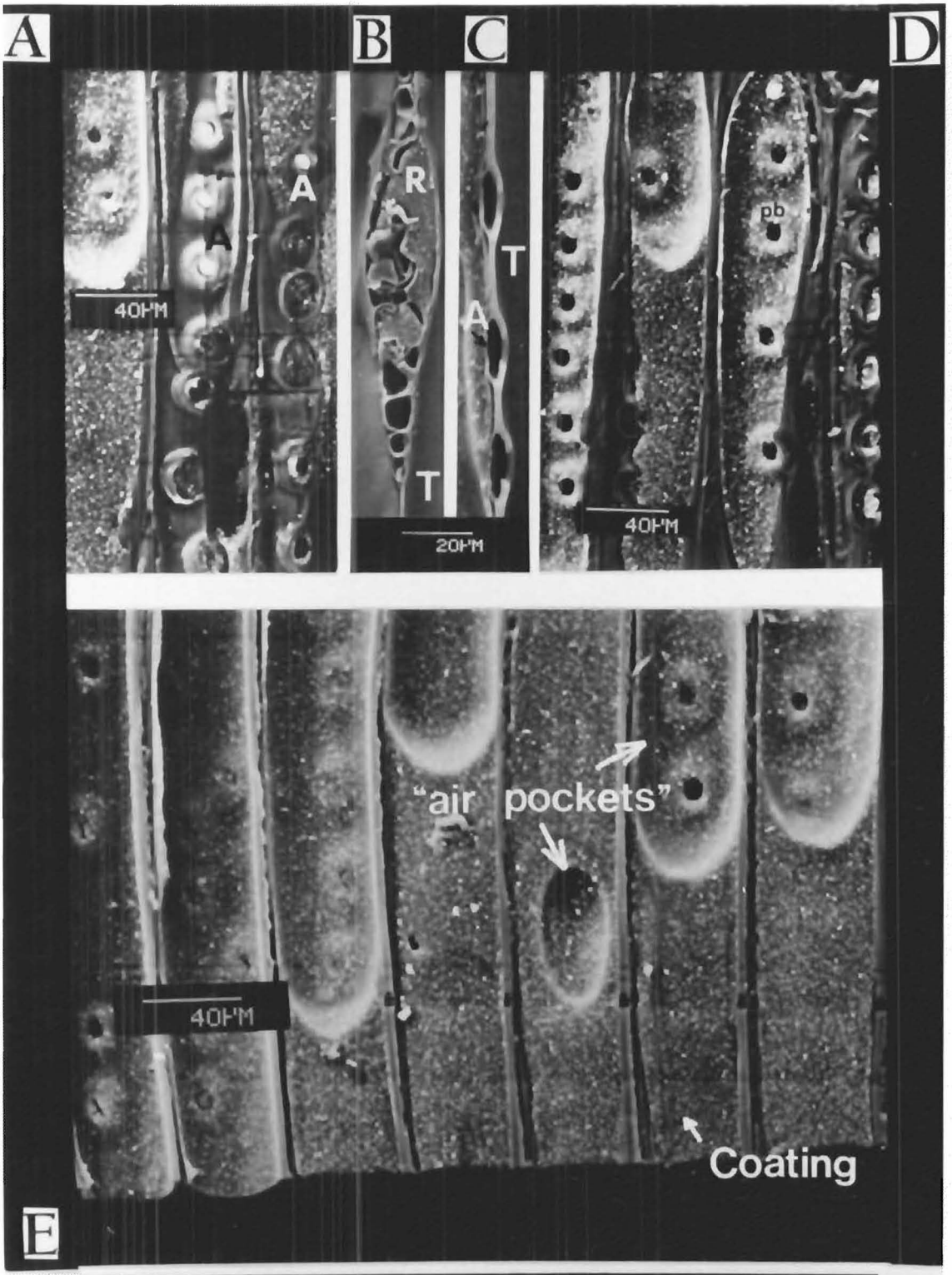

FIGURE 54

LONGITUDINAL VIEWS OF *P. radiata* COATED WITH TiO_2 TAGGED WATTYL ESTAPOL .

A. - E. The coating has been stripped away to reveal the cells beneath. Note the "air pocket" areas, aspirated pits and coating filling the margo / torus region.

B. Detail of a partially filled ray cell. (BSEI).

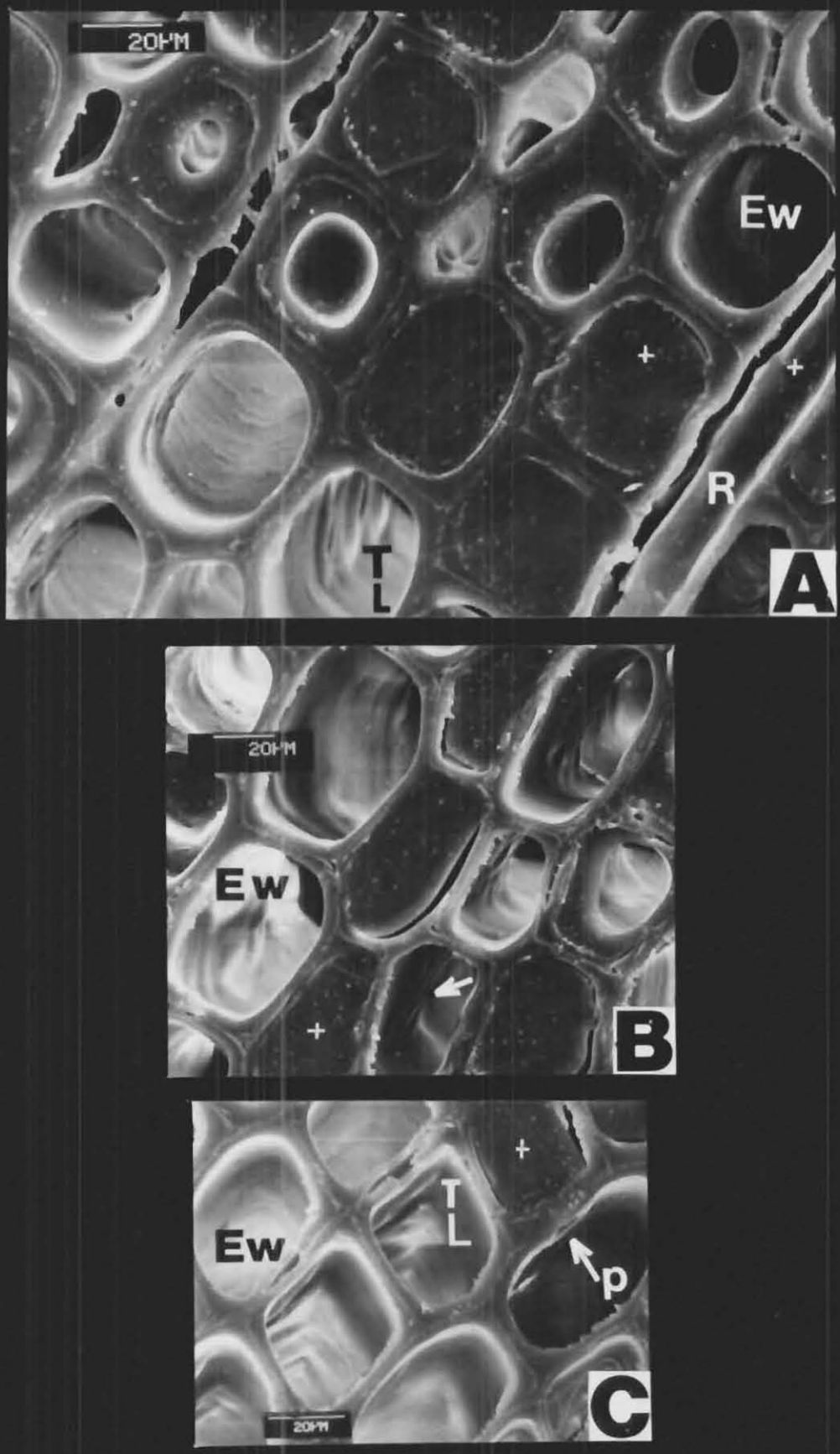

FIGURE 55

P.radiata COATED WITH TiO_2 TAGGED WATTYL ESTAPOL.
Transverse view showing the depth of penetration.
The coating was applied to the tangential longitudinal face. (SEM)

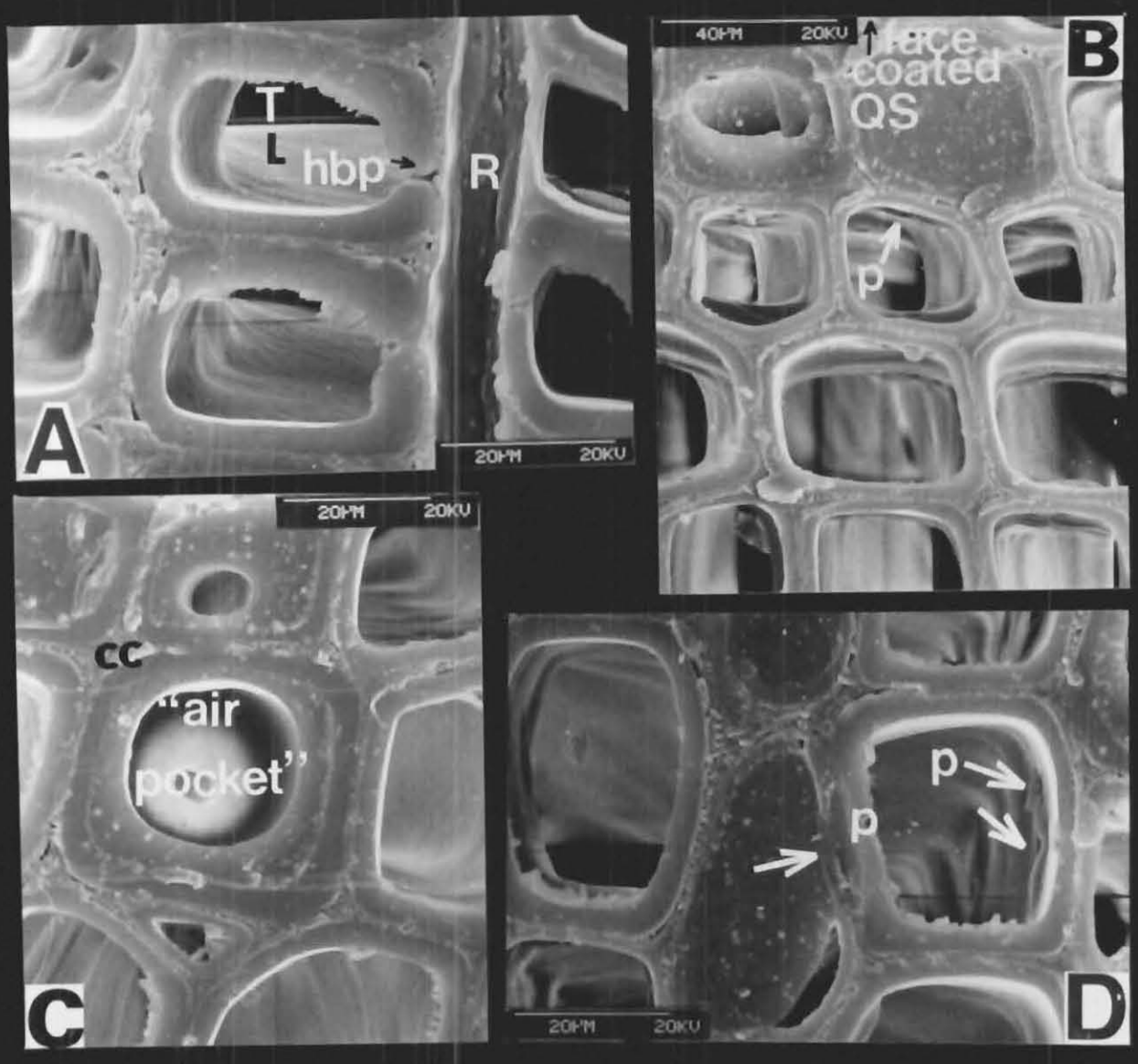

FIGURE 56

P.dacrydioides (KAHIKATEA) COATED WITH TiO_2 TAGGED WATTYL ESTAPOL .

A. - D. Transverse views showing the coating / pits and cell wall interface. (SEM).

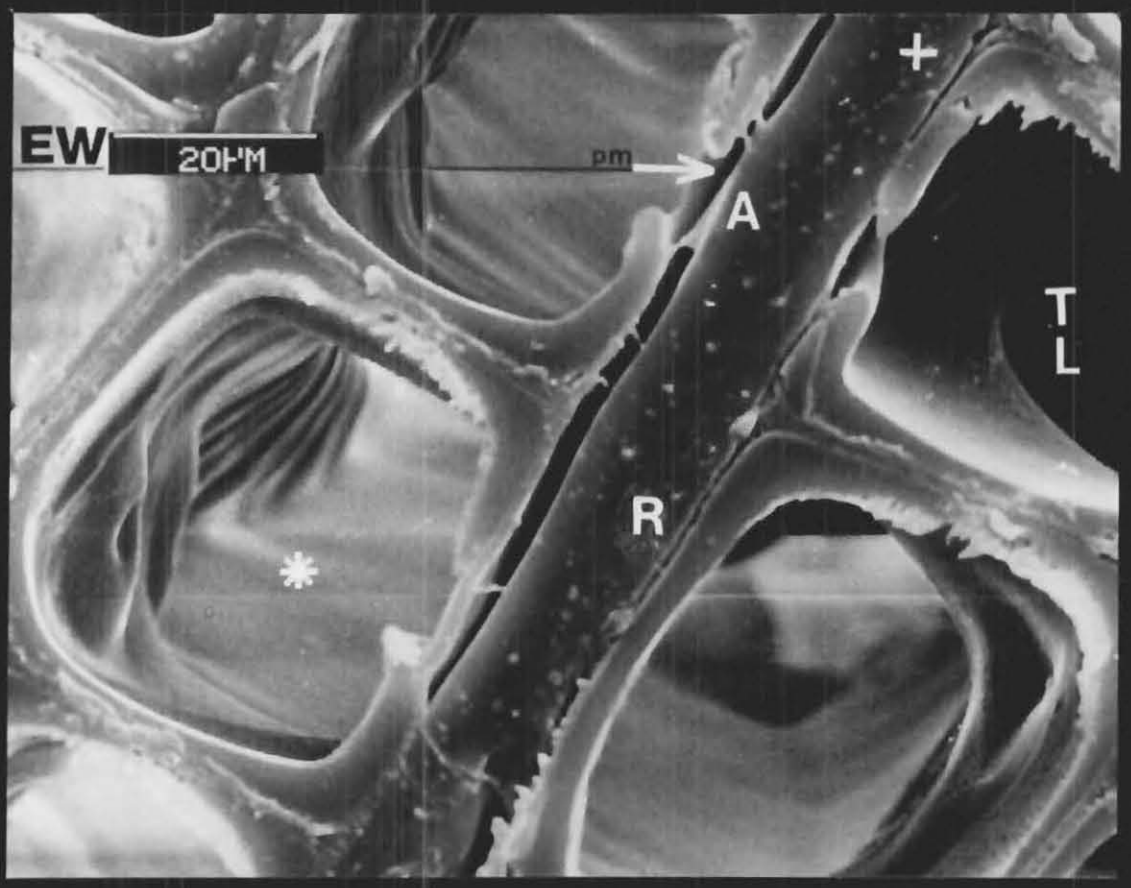

FIGURE 57

(T.F.) P.radiata COATED WITH TiO_2 TAGGED WATTYL ESTAPOL.

Detailed transverse view showing coating penetration along a ray cell and the aspirated pit membranes of adjacent tracheids. (SEM).

adjacent tracheid cell preventing the coating from bursting through into the ray cell. Aspirated pit membranes are depicted in figure 54 [A].

In order to envisage a hypothetical complex three-dimensional model of gross penetration, movement and coating retention, all three weatherboard faces must be imagined. Figures 55 to 57 are secondary electron images of typical transverse views of the coating in the taxa studied. Whereas the coating texture is enhanced in the backscattered electron images of the previous micrographs, here the texture of TiO_2 tagged Wattyl Estapol coating appears superficially smooth. Peering down into the *P. radiata* tracheids shown in figures 55 to 56, it is visually evident that aspirated pits prevent intertracheid penetration. Figure 57 is a characteristic example of coating filling a ray cell. The arrow points to the membrane adhering tenaciously to the coating and constricting entry into the adjacent tracheid cell through the half bordered cross-field pit apertures. Normally sap, ascending the trunk of a living tree, passes from one tracheid to the next along a zig zag route upwards and flows through the pit aperture of one tracheid into the pit chamber, through the medianly suspended pit membrane and out into the pit chamber of an adjoining tracheid and into the cell lumen and so on. However, the model for bulk coating movement in weatherboards is more complex. Firstly, it is important to remember that the weatherboards are coated/primed on the longitudinal face and the end grain is usually sealed, preventing coating entry. The initial entry point is therefore not from the base of the tracheid 'cylinders' upwards but from the excised sides of the tracheids and also through fissures, cracks and any opening caused by machining.

5.5 DISCUSSION

The wood substrate and its relationship to coatings, dyes, resins and preservatives all have one topic in common and that is penetration. Morphological factors relating to the penetration of solutions both into the cell wall and through the pit membrane have been extensively investigated. Penetration is not solely influenced by wood structure but by the molecular size and type of particles present in the coating fluid. As background and for comparative purposes, some diffusion studies documented in the literature are briefly outlined here.

Through a series of experiments, Wardrop & Davies (1961) were able to trace concentric rings of diffusion in *P. radiata* tracheid cell walls. They found that the middle lamella and cell corners, both areas of greatest lignin concentration, were the last regions to react with the reagents. The nature of the secondary wall is important in controlling movement of materials. The S_3 layer is the first layer that materials entering the cell must pass through from the lumen. Experimental evidence has indicated that of all the three secondary wall layers the S_2 layer is the most porous. In a study of the S_3 lignin concentration, Donaldson (1987) concluded that *P. radiata* tracheids have a highly lignified S_3 layer. He interpreted that lignin concentration determined porosity and suggested that

the observed low porosity in the S_3 layer is a consequence of high lignin concentration which acts as a barrier to diffusion. Ultrastructural studies of wood cellulose substrates from *P. radiata* led Donaldson (1988) to postulate that both the S_3 and S_1 layers of the secondary wall are barriers to enzyme penetration and that access to the S_2 layer is restricted. SEM X-ray microanalyses of tracheid cell walls of southern yellow pine treated with water based formulations of pentachlorophenol were made by de Groot & Kuster (1986). They found greater amounts of the preservative in the earlywood than in the latewood cells and proportional increases in the S_3 layer but by contrast the loadings in the S_2 layer were disproportionately low.

In their review of the history of coatings research, Harada & Wardrop (1960) and Wardrop & Davies (1961) noted that a range of aqueous solutions, including carbon black suspensions, Congo red dye, titanium oxide particles and metal salt solutions, have been employed to demonstrate the nature of the capillary system in the cell wall. The existence of a heterocapillary system was confirmed by Frey-Wyssling (1937) who estimated that the width of the larger capillaries between the microfibrils was greater than 100 nm whereas those within the microfibrils were around 1.0 nm. They also noted that large molecules of dyes were capable of penetrating the larger capillaries. As part of an investigation of pulping liquors into wood cells, using the electron microscope, Davies (1968) observed, under the electron microscope, silver nitrate particles deposited in the cell wall and believed that the particle diameters provided some indication of the diameter of the cell wall capillaries. More recent research has revealed that although direct visual measurement of the diameter of cell wall capillaries is not yet microscopically possible, indirect observations suggest that they are 3.2-100 nm in diameter (Smith et al, 1985). Capillary size is species dependent. Vinden (1984) developed and refined a diffusion model for wood with reference to Scots pine (*Pinus sylvestris*) and Norway spruce (*Picea abies*). The model depicted the interaction of the total void volume, lumen volume, cell wall void volume, permanent capillaries (macro and micro) and transient capillaries. Although Vinden's work relates directly to preservative studies it provides considerable insight to the types of movement operating within the cells.

As in all softwoods, liquid penetration in *D. cupressinum*, *P. dacrydioides* and *P. radiata* proceeds from tracheid to tracheid via the bordered pits. Wardrop & Davies (1961) provided a diagramatic representation of a section through a bordered pit to illustrate their theory that during pit border formation the initially formed pit border is distinct from the S_1 layer that partially overlies it. This border layer prevents reagents in the pit chamber from penetrating the secondary cell wall, instead they are forced through the pit aperture and out into the adjacent tracheid where they are allowed access to the inner layer of the cell wall. Yata (1981) traced the diffusion depth of chromium inwards from the surface of the tracheid cell wall adjacent to the pit chamber of bordered pits and found it was less than that inwards from the lumen entry point.

Morphological variation in bordered pit membranes in gymnosperms is discussed by Bauch et al (1972) and illustrated with reference to New Zealand woods by Meylan & Butterfield (1978) and Butterfield & Meylan (1980). Barnett (1977) discovered paracrystalline osmiophilic material in the developing bordered pits of *P. radiata* and obtained evidence that this material penetrates the torus during development via ectoplasmic strands. The pit membrane is unlignified (Imamura et al, 1974). Provided the pit membrane (torus) is suspended in the median position, articles of a certain size can move through the openings between the supporting strands comprising the margo (Côté, 1981). In the case of aspirated pit membranes, free passage of smaller particles suspended in the fluid is restrained although the actual liquid volume may be permitted through the membrane by diffusion processes (Côté, ibid).

Of the two main types of penetration distinguished - gross penetration of the eight coating systems and in particular the TiO_2 tagged Wattyl Estapol is obvious. Intracellular penetration, however, is more difficult to ascertain microscopically and discern whether preferential migration or localization of coating components actually occurs or whether the film composition remains constant throughout the entire level of penetration. Many types of interactions happen as soon as a coating is applied to wood and evidence and supporting theories require the collaboration of several methods of detection. The remainder of this discussion considers old and new concepts for a variety of coating systems and softwood substrate species. Current theories may be applicable in elucidating the behaviour of coated *D. cupressinum, P. dacrydioides* and *P. radiata* weatherboards. When interpreting the behaviour of a coating it is useful not only to view the system as a whole but to deal with the individual components such as the solvents and binders separately.

In a discussion on the physical and chemical nature of wood and coatings, Gatslick (1963) stressed the role of the extraction of chemicals from the wood substrate. Softwoods have a high level of extractives which tend to bulk the cell walls and restrict the migration of coating components. It is believed that the coating composition can change either as a result of the migration of wood extractives into the coating or the migration of fractions of the coating component out into the wood. Bleeding of resin through paint films occurs in some species but is infrequent in *P. radiata* (Sinclair, 1965). For years it was thought that the penetration of the binder was essential to securing good coating adhesion and in order to maintain a constant pigment/binder ratio in the dry primer a certain proportion of polymerised oil was incorporated into the system. The oil penetrated only to a depth of two to three cells (Sinclair, ibid). Mirams (1965) noted excessive absorption of paint oils in the dense summerwood bands of *P. radiata* and Miniutti (1963, 1965) deduced that paint oils penetrate deeper in the summerwood, reasoning that the pits were more likely to be open between adjacent summerwood cells than springwood cells. Deep penetration of paint oils robs the coating of film forming material (Miniutti, ibid).

A number of common variables are involved in the initial adhesion processes of both film forming coatings and adhesives on wood. Microscopic evidence of wood/adhesive interface relationships on Douglas fir (*Pseudotsuga menziesii*) were recorded by Nearn (1965). Because conventional white light and staining techniques were unable to show the presence of alkaline phenol formaldehyde resin in the cell walls, Nearn resorted to fluorescence microscopy to detect the total depth of penetration of the alkaline solvent and the lowest molecular weight material. He theorized that unlike adhesives, coatings do not form a two zoned interface instead an interlocking mechanism is formed.

Côté & Robison (1968) attempted to answer the question on whether only a component of a uralkyd clear coating system penetrated into the wood. Incident fluorescence and transmitted fluorescence microscopy suggested a superficial penetration of the non-volatile vehicle. This led them to speculate that the apparent coating penetration previously interpreted (Schneider & Côté, 1967) was not penetration of the uralkyd binder molecules but rather the solvent into the cell wall. To simplify the interpretation of the behaviour of the interface region of an alkyd coating on western white pine (*Pinus monticola*), Côté & Vasishth (1970)formulated coatings both with and without the presence of a mineral spirit solvent; and with the aid of several microscopic techniques were able to detect variation in porosity within the film itself which they interpreted as evidence of solvent penetration through wood cell lumens.

Further attempts were made by Schneider (1970) to substantiate and clarify the interaction phenomenon between coatings and wood cell walls. The direct carbon replica technique was employed in conjunction with electron microscopy to determine the presence, if any, of visible structural changes in the cell wall as a consequence of the interactions associated with the chemical components of the coating. Using specimens coated with a high viscosity, unpigmented uralkyd varnish and a low viscosity boiled linseed oil coating, Schneider deduced that infiltration of amorphous substances into the cell wall was subtle and to a shallow depth only. Autoradiography of a moisture cured urethane resin and oven dried wood indicated that cell wall penetration was minuscle (Schneider & Chang, 1971 unpub.report) and (Schneider, 1972).

Linseed oil is the simplest and oldest vehicle type and probably the most widely used drying oil (Clauser, 1984). The purpose of thermal bodying of oils is to increase their viscosity, adhesion, drying rate and water resistance (OCCA, 1969). In order to answer the question as to how much oil penetrates cell walls, Schneider (1979) conducted a series of experiments on white spruce (*Picea glauca* Moench.[Voss]) sapwood and with the aid of the scanning electron microscope was able to view the linseed oil deposits. The oil film covered the lumen interior surfaces but the distribution of oil within each sample was non uniform. Less than five percent of the oil appeared to be absorbed in the cell walls. A further series of experiments (Schneider, 1980) revealed that only the largest earlywood cell lumens nearest to the exposure surface were filled with oil and a few smaller earlywood lumens

were also filled. This led Schneider to suggest that capillarity is the main force of penetration. The occurrence of oil coated unfilled lumens further away from the exposure surface was explained by suggesting that they result from either oil spreading on the lumen surface or capillarity of cell walls after the oil has moved through open pits. A water-dilutable version of linseed oil manufactured by partially trans esterifying the oil with polyethylene glycol was examined by Vasishth (1983) who deduced that it remained water-leachable several weeks after deposition in the cell walls.

One of the earliest successful bulking agents to improve coating adhesion and wood stability was an unpolymerized phenol formaldehyde resin (Stamm, 1965) which appeared readily diffusible into the cell walls because of its high water solubility. However at the time it was still unknown whether the resin was chemically bonded to the wood or whether it was merely mechanically deposited within the walls. Research on bulking of wood and coatings adhesion have complemented each other in the quest for understanding and interpreting product behaviour. Using a sample of Douglas fir wood prepared with metabromophenol formaldehyde resin, Smith & Côté (1972) were able to demonstrate that under certain curing conditions the resin penetrated deeply into the cell walls.

As part of a research programme to produce water - borne clear coatings for wood, Vasishth (1983) discovered that for cell wall penetration to occur it was necessary to select a polymer that had a high proportion of molecules with molecular weight below 1000, because molecules greater than this either remained on the cell lumens or formed a film. Unlike the commonly used polymers which included water-dispersed polymers such as the acrylics, and solvent-based alkyds, Vasishth found that a certain class of polymers referred to as water-borne alkyds (also known as water-dilutable or water-reducible alkyds) behaved differently. Aqueous solutions of these water-borne alkyds swell wood irreversibly. In the presence of driers such as calcium, manganese or cobalt naphthenates, these water-borne alkyds polymerize on exposure to air and become water insoluble. The penetration of Eastern white pine (*Pinus strobus* L.) wood cell walls by a novel water-borne alkyd resin which was allowed to polymerize *in situ* was investigated by Smulski & Côté (1984). Because the majority of the uncured alkyd constituent oligomers were less than 50 nm in size and forty percent were smaller than 5 nm in size, they believed that the molecules were small enough to enter transient cell wall capillaries. The resin was prepared without metallic driers thus was present in the cell wall in a non-bonded and leachable form. Negative alkyd resin cast replicas of the pit openings and tracheid cell wall surfaces provided evidence of gross penetration and also transverse flow of the resin via ray parenchyma cells.

What happens to the volatile solvent portion of the coating is crucial in understanding coating/substrate relationships. It is now known that the solvent plays a dual role; it is responsible for the swelling of cell wall capillaries and subsequently provides an attractive medium which avoids chromatographic separation of coating components by the cell wall (Lucas & Smith, 1985). While water is able to swell the cell walls, latex particles, in latex coatings for example, are too large to penetrate even the most swollen cell walls (Middleton, 1985). In traditional organic coatings such as

varnishes, the solvent facilitates coating penetration into the cell lumens but neither the resin molecules nor the solvent show affinity for the cellulose component of the cell wall (Lucas & Smith, ibid). By contrast, water-borne solution coatings containing an organic co-solvent and low molecular weight resin molecules exhibit the requirements considered necessary for resin deposition within the wall. In testing their theory, Lucas & Smith compared a clear water-borne alkyd resin with the same resin dissolved in organic solvents. Interactions of several water-soluble organic co-solvents and water-borne polymer systems and Eastern white pine wood were investigated by Smith et al (1985) with the intention of tracing the penetration and swelling of cell wall capillaries. Ethylene glycol monobutyl ether, diethylene glycol monobutyl ether and ethylene glycol were the organic solvents they used to demonstrate that when applied in aqueous solution not only do they both penetrate and swell cell wall capillaries but they are prone to entrapment. Alkyd, acrylic and drying oil resins and polyethylene glycol were the water-borne polymer systems they used to demonstrate that cell wall capillary penetration is controlled by the molecular size and water solubility of the polymer. In a study of coating behaviour on Australian timbers, Drewe (1986) deduced that the uniformity of paint composition is changed by a filtration effect which, although minor, prevents certain pigments from entering the cells. However, fluorescence microscopy revealed only tentative evidence of vehicle penetration (predominantly the solvent) into the cell walls.

As some of these reviewed theories do not involve film forming coatings on wood, experiments were not performed to test them. However, they are useful in demonstrating penetration effects in situations involving wood cell walls. Some of them may provide support to any speculations made in this study on the macro and micro penetrations of the TiO_2 tagged Wattyl Estapol coating. In developing any theory, the chemical composition of the coating must first be considered. Approximately fifty-two percent of the solid fraction of the TiO_2 tagged Wattyl Estapol consists of 65% Soya Oil alkyd (unpub.data) and 2,2' dihydroxy-4-methoxy benzophenone, cobalt naphthenate, lead naphthenate, calcium naphthenate, organic rheological modifier, soya lecithin, rutile titanium dioxide and an acrylic dispersing resin comprises the remaining fourteen percent of solids present. The non-yellowing property of soya oil makes it suitable for clear coatings and white paints. The volatile portion contains approximately thirty percent White Spirit and less than three percent toluene, xylene, 1-methoxy-2-propyl acetate and methyl ethyl ketoxime. White spirit is composed mainly of hydrocarbons with a complex paraffin component. White Spirit has the following specification: density at 15^{oc} 0.78, distillation range 150-200^{oc} and an aromatic content of 18% w/w. White spirit is capable of dissolving long oil alkyds and modified phenolic resins. (O.C.C.A., 1969).

Does intracellular penetration occur in the TiO_2 tagged Wattyl Estapol coating when applied to *D. cupressinum*, *P. dacrydioides* and *P. radiata* weatherboards? As in all coating systems the degree of intracellular penetration depends on the molecular size of components and it is believed that it should be deeper for raw than for bodied oils. Microscopic evidence supports the premise that metal

salts and other preservative solutions penetrate the cell wall but highly magnified electron images were unable to show and account for all the coating components. X-ray microanalysis does not give clear indication on whether coating components detected in the three taxa cell walls are permanently fixed or subject to redistribution, migration and/or disintegration. Controversy still exists in the literature as to the existence of micro-capillaries, within cell walls, which are microscopically invisible.

The rate of curing may affect coating penetration and movement within cell voids. Soya Oil is a slow drying oil on its own. On curing the soya alkyd present in the TiO_2 tagged Wattyl Estapol undergoes a complex oxidation reaction which is catalysed by the metal naphthenate driers. Preferential migration of certain microscopically visible coating components, such as titanium dioxide, to a specific part of the coating film or into the substrate voids is demonstrated. Evidence that the solvent and/or vehicle penetrates the wood and migrates out or diffuses back into the paint film is tentative and not yet demonstrated microscopically. Solvent based coatings are capable of dissolving extractives in the wood and this is probably true for the TiO_2 tagged Wattyl Estapol.

There is consensus of opinion in the literature that all the ingredients of a coating can enter fissures, cavities and excised cell lumens but only the liquid portion of suitable molecular size can pass through the pit membranes through to adjoining cells. The pigment volume concentration is important in determining gross penetration into wood. In the case of the primer survey recorded in chapter 4, microscopic evidence suggests some degree of pigment/particle segregation in those tracheid cell lumens cut and exposed by machining (refer figures 23 [D] and 30 [A]). This phenomenon is also evident in the film layer lining the board surface. Larger angular " fragments " appear to have been denied entry into the cells below. Careful examination shows that the size of the particles present in the lumens of cells below the surface is smaller and more uniform. This may be due to the dimensions of the tracheids opened by machining and presented that way to the coating for entry. Some of the tracheids are partially flattened along their length, others exhibit tapering, undulating and twisted form. It is notable that the unembedded Toluidine blue stained sections photographed under the light microscope (refer figure 36 [C]) appear to possess a " porous " film layer above the cell tops; this recalls the observation by Côté & Vasishth (1970) of film porosity after deposition. An alternative and more probable explanation is that the larger particles were loosened during section preparation. If the scanning electron micrographs taken of the TiO_2 tagged Wattyl Estapol are compared with the primer micrographs, it becomes obvious that macro-particle segregation is absent. The more uniform distribution of coating particles could facilitate entry into the machine opened tracheids. Another important factor is that the percentage of rutile titanium dioxide in this novel coating system is less than that in the primers and this surely plays a role in gross penetration. Although electron microscope evidence supports the premise that the titanium particles remain randomly distributed once deposited in the cell lumen some tiny unidentifiable particles appeared to line the cell lumens, particularly in *P. radiata*.

The number of tracheids emerging on the weatherboard surface determines the number and location of possible tracheids presented to the coating across the board. Depth of gross penetration is also influenced by inclination of tracheid elements, the orientation of pits relative to the board surface, the surface area occupied by early and latewood zones, the figure and the grain of the wood. "Figure" refers to the pattern produced on the longitudinal wood surface, while "grain" refers to the direction of the major wood elements relative to the board edge (Harris, 1979). Tracheids act as capillary tubes for the conduction of the liquid portion of the TiO_2 tagged Wattyl Estapol coating. Within tree variation exists and changes in wood density and tracheid dimensions in *D. cupressinum*, *P. dacrydioides* and *P. radiata* are dependent on tree age rather than stem diameter. The largest tracheids occur about a third of the way up a stem. The longest tracheids occur in the outerwood and may be up to four times longer than the shortest tracheids which occur towards the central core zone. Hence the extent of tracheid lumens filled with the TiO_2 tagged Wattyl Estapol may be influenced by the tracheid dimensions present in each weatherboard piece. The presence of coating in adjacent tracheids in the upper regions of the board nearest to the film face is interpreted as having entered along separated tracheids or through pit membranes destroyed previously during preservative treatment of the wood. It is unlikely that the TiO_2 tagged Wattyl Estapol burst through the intact pit membranes; electron microscope evidence supports this idea.

Permanent structural changes occur in the wood during seasoning. Conventional pressure treatments can cause gross overloadings in the cells and the number of aspirated pits and damaged pit membranes may account partly for the variation pattern in the gross penetration observed. Pit aspiration, as a result of vacuum and pressure type treatments, affect subsequent rates of diffusion in the cell walls even though the actual solvent filled void volumes may remain the same (Vinden, 1984).

In softwoods, approximately ninety-five percent of the total volume of wood consists of tracheids (Harris, 1981), thus the influence of ray parenchyma cells on coating gross penetration is minor.

CHAPTER 6

A STUDY OF WEATHERED COATING/SUBSTRATES

6.1 ACCELERATED WEATHERING TESTS ON TIO_2 TAGGED WATTYL ESTAPOL ON *D. cupressinum, P. dacrydioides* AND *P. radiata* WEATHERBOARDS.

The natural environment is infinitely changing with respect to time, topography and meterology and therefore effects of natural exposure on materials will vary accordingly. The major natural environmental elements which cause the breakdown of coatings and substrates are: solar radiation (which includes the type and intensity of radiation), temperature, oxygen (and ozone), humidity, precipitation, wind, biological agents and atmospheric impurities. The term durability of a coating is synonymous with its economic life (Fullard, 1965) but no single factor can be isolated as the key to good durability (Wilkinson, 1987). The durability of a coating/finish refers to its ability to withstand the combined factors which exert an influence on it while it is exposed to the elements and is performing the functions of protection and decoration of the substrate.

Variables determining the performance of an exterior coating include : nature of the coating system, number of coats applied to the substrate, surface phenomena (including the degree of gloss), degree of exposure, timber species, grade and moisture content, substrate/film interactions and internal film reactions. Film breakdown involves both chemical and physical changes, although many of the latter are physical manifestations of the former (Ball, 1982). The chief causes of film breakdown are due to the failure of the pigment component and the vehicle; which ultimately results in the loss of adhesion of the film from the substrate.

Artificial weathering tests developed out of the need to shorten the time in evaluating product performance. Film breakdown could be conveniently speeded up to a fraction of the time it would normally take under outdoor natural exposure conditions. Ball (1982) traced the history of weathering tests and noted that by 1937 the American Society for Testing Materials (ASTM) held a symposium to determine how accurately artificial weathering tests could be correlated with each other and with natural weathering tests. Although accelerated weathering tests are claimed to simulate as closely as possible natural weathering, they cannot be equated with any natural exposure tests and correlation must be treated with caution. Therefore, no attempt was made in this study to relate to any other weathering trials. Artificial weathering tests are incapable of duplicating the complex

environmental elements and their interactions which occur naturally. In accelerated weathering tests, only a limited number of natural weathering factors can be simulated.

Weather-Ometers which use the xenon arc and carbon arc systems, represent recent developments in accelerated weathering equipment designed to meet the standards outlined by the ASTM. The emission spectrum of the xenon arc more closely resembles sunlight in the ultraviolet region of the spectrum than the carbon arc. Natural and accelerated weathering tests both have advantages and disadvantages, however, accelerated weathering tests are universally used to predict the performance of certain materials under certain conditions. Any product subject to photodegradation, outdoor exposure, fading and photochemical reactions may be tested under controlled laboratory conditions on a repetitive basis. Birchenough (1986) stressed that accelerated weathering tests are used as a quality assurance procedure to ensure the reliability and durability of a product.

A distinction must be made between deterioration (which refers to the result of exposure due to the effects of ultraviolet radiation, temperature and moisture) and degradation (which is the result of the effects of mechanical stresses and chemical changes such as oxidation).

The aim of this study was to evaluate the effect of accelerated weathering trials on uncoated weatherboards representing the three taxa and on the performance of TiO_2 tagged Wattyl Estapol coated weatherboards. Uncoated weatherboards were artifically weathered (refer method 2.14) for a period of three thousand hours. In order to determine whether the number of coats applied to the substrate showed any difference after weathering, boards with one coat of finish were weathered for two thousand hours and compared to boards with two coats of finish. For this trial, two thousand hours was chosen as it is in between one and three thousand hours. In another series of experiments, boards with two coats of finish were weathered for one thousand, two thousand and three thousand hours to assess the role of the time. Incidently, three thousand hours is approximately equal to a four and a half month period of continuous testing.

6.2 EDAX BULK ANAYLSIS OF THE WEATHERED COATING.

The spectral distribution of the elements detected in unweathered TiO_2 tagged Wattyl Estapol coating is presented in appendix 1.8. The key elements present after three thousand hours accelerated weathering tests are shown in appendix 7. The analytical data are expressed as intensity (counts per second), background (counts per second) and peak height to background. The slight increase in the proportion of TiO_2 in the coating suggested by the EDAX technique is in accordance with the observed decrease in the intensity of carbonyl group peaks indicated in the infrared spectra obtained for the coating (refer figures 66 to 68), which reflects incipient chemical breakdown of one of the organic components of the coating.

6.3 $L^* a^* b^*$ COLOUR SYSTEM

The Hunter Labscan Spectrocolorimeter tristimulus colour analyser for measuring reflective colours of surfaces was used to make absolute chromatic measurements of uncoated, coated, unweathered and weathered *D. cupressinum, P. dacrydioides* and *P. radiata* weatherboards. Four different colour systems for measuring absolute chromaticity; namely $L^* a^* b^*$, $L^* C^* H^*$, CIE Y x y and Dx Dy Dz (refer method 2.15) were used. Table 4 records the mean values for the three taxa obtained with the Hunter Labscan. Duplicate measurements were made with the Minolta Chroma-Meter and the mean values are shown in appendix 8 for comparison. Only the mean values for the L* a* b* and CIE Y x y systems were plotted to obtain three dimensional diagrams.

Figures 58 to 60 feature L* a* b* diagrams for coated and uncoated, weathered *D. cupressinum, P. dacrydioides* and *P. radiata* boards. Colour space is defined as a three dimensional geometric representation defining a range of colour dimensions which are hue, saturation and lightness (Standards Association of Australia, 1983, 1985). The term colour solid refers to that part of a colour space diagram which is occupied by surface colours (CIE, 1970). Regarding the symbols used in figures 58 to 60, it is important to note that each symbol has been spaced slightly further away from its neighbour to avoid superimposed pictorial clustering of symbols which is visually difficult to interpret. Therefore, to obtain the exact position, reference should be made to the numerical values for L* a* b* given in table 4 (4.1 to 4.3).

There is no internationally agreed system for colour names although a universal American colour language system has been published. The main advantage of using colour names is to provide a verbal description, however, colour is more precisely specified by other means such as the CIE L* a* b* and CIE Colorimetric systems which specify colour by three numerical values. The visual colour of the novel TiO_2 tagged Wattyl Estapol studied here could be verbally described as "off white" or "cream" compared to the "pure white" colour of the primers studied. The purpose of using spectrocolorimetric techniques in this study of weathered coatings/substrates was to obtain supplementary quantitative information on subtle changes invisible to the naked eye.

In the L* a* b* colour space diagram L* is the metric lightness factor expressed as a percentage. Thus white equals one hundred percent and black equals zero percent. Hue and chroma (saturation) are represented by a* and b*. Figures 58 [A], 59 [A] and 60 [A] depict L* a* b* plots for boards representing the three taxa, which received two applications of the TiO_2 tagged Wattyl Estapol coating and were artifically weathered for one thousand, two thousand and three thousand hours. The original unweathered coating has a mean value of approximately L* 89 a* -2 b* +12, thus when plotted on the diagram the coating position would lie two percent towards the green region and twelve percent towards the yellow region with an eighty nine percent lightness factor. Slight variation within the three taxa was noted in the individual L* a* b* values for the two coat

TABLE 4.1

COMPARISON OF DIFFERENT COLOUR SYSTEMS FOR MEASURING THE REFLECTIVE COLOURS OF THE SUBSTRATES.

The values are the averages obtained with the Hunter Labscan Spectrocolorimeter tristimulus colour analyser for Dacrydium cupressinum. Pinus radiata and Podocarpus dacrydioides weatherboards.

WEATHERBOARD SAMPLES	TAXA		
	Dacrydium cupressinum	Podocarpus dacrydioides	Pinus radiata
UNCOATED BOARD UNWEATHERED.	L* a* b* 63.35 +10.03 +25.59 X Y Z 33.10 32.01 18.46 Y x y 32.01 0.396 0.382	L* a* b* 74.94 + 7.26 +29.66 X Y Z 48.31 48.42 27.59 Y x y 48.42 0.389 0.388	L* a* b* 77.92 + 5.72 +23.16 X Y Z 52.49 53.08 35.88 Y x y 53.08 0.371 0.375
UN COATED BOARD WEATHERED 3000 HOURS.	L* a* b* 48.53 +18.69 +38.58 X Y Z 19.87 17.26 5.17 Y x y 17.26 0.470 0.407	L* a* b* 52.54 +16.82 +37.71 X Y Z 23.10 20.64 7.00 Y x y 20.64 0.455 0.406	L* a* b* 55.78 +16.19 +39.28 X Y Z 26.21 23.72 8.10 Y x y 23.72 0.451 0.408

TABLE 4.2

COMPARISON OF DIFFERENT COLOUR SYSTEMS FOR MEASURING THE REFLECTIVE COLOURS OF THE SUBSTRATES.

The values are the averages obtained with the Hunter Labscan Spectrocolorimeter tristimulus colour analyser for Dacrydium cupressinum. Pinus radiata and Podocarpus dacrydioides weatherboards.

WEATHERBOARD SAMPLES	TAXA		
	Dacrydium cupressinum	Podocarpus dacrydioides	Pinus radiata
COATED BOARD 1 COAT TiO_2 TAGGED WATTYL ESTAPOL EXTERIOR CLEAR WEATHERED 2000 HOURS.	L* a* b* 85.72 −0.10 +7.83 X Y Z 63.82 67.42 64.46 Y x y 67.42 0.328 0.346	L* a* b* 82.85 +3.33 +13.87 X Y Z 60.09 61.89 51.55 Y x y 61.89 0.346 0.356	L* a* b* 85.55 +1.87 +10.71 X Y Z 64.44 67.09 59.60 Y x y 67.09 0.337 0.351

TABLE 4.3

COMPARISON OF DIFFERENT COLOUR SYSTEMS FOR MEASURING THE REFLECTIVE COLOURS OF THE SUBSTRATES.

The values are the averages obtained with the Hunter Labscan Spectrocolorimeter tristimulus colour analyser for Dacrydium cupressinum. Pinus radiata and Podocarpus dacrydioides weatherboards.

WEATHERBOARD SAMPLES	TAXA		
	Dacrydium cupressinum	Podocarpus dacrydioides	Pinus radiata
COATED BOARD 2 COATS TiO_2 TAGGED WATTYL ESTAPOL EXTERIOR CLEAR UNWEATHERED	L* a* b* 89.51 -2.86 +11.10 X Y Z 70.01 75.24 66.87 Y x y 75.24 0.330 0.354	L* a* b* 89.64 -1.76 +12.20 X Y Z 70.80 75.53 65.87 Y x y 75.53 0.333 0.355	L* a* b* 89.46 -1.86 +12.38 X Y Z 70.38 75.15 65.29 Y x y 75.15 0.333 0.356
COATED BOARD 2 COATS TiO_2 TAGGED WATTYL ESTAPOL EXTERIOR CLEAR WEATHERED 1000 HOURS	L* a* b* 89.49 -2.68 +9.89 X Y Z 70.06 75.20 68.28 Y x y 75.20 0.328 0.352	L* a* b* 90.57 -1.79 +12.17 X Y Z 72.67 77.55 67.78 Y x y 77.55 0.333 0.355	L* a* b* 89.91 -1.45 +11.61 X Y Z 71.49 76.11 67.09 Y x y 76.11 0.333 0.354
COATED BOARD 2 COATS TiO_2 TAGGED WATTYL ESTAPOL EXTERIOR CLEAR WEATHERED 2000 HOURS	L* a* b* 87.90 -1.50 +7.96 X Y Z 67.45 71.85 67.31 Y x y 71.85 0.326 0.347	L* a* b* 88.07 -0.12 + 9.72 X Y Z 68.41 72.20 65.61 Y x y 72.20 0.331 0.350	L* a* b* 88.20 -0.02 +10.14 X Y Z 68.75 72.50 65.37 Y x y 72.50 0.332 0.350
COATED BOARD 2 COATS TiO_2 TAGGED WATTYL ESTAPOL EXTERIOR CLEAR WEATHERED 3000 HOURS	L* a* b* 87.96 -1.61 +8.60 X Y Z 67.52 71.99 66.72 Y x y 71.99 0.327 0.349	L* a* b* 89.05 -1.02 +10.21 X Y Z 69.96 74.27 67.00 Y x y 74.27 0.331 0.351	L* a* b* 88.34 -0.65 +9.95 X Y Z 68.71 72.78 65.88 Y x y 72.78 0.331 0.350

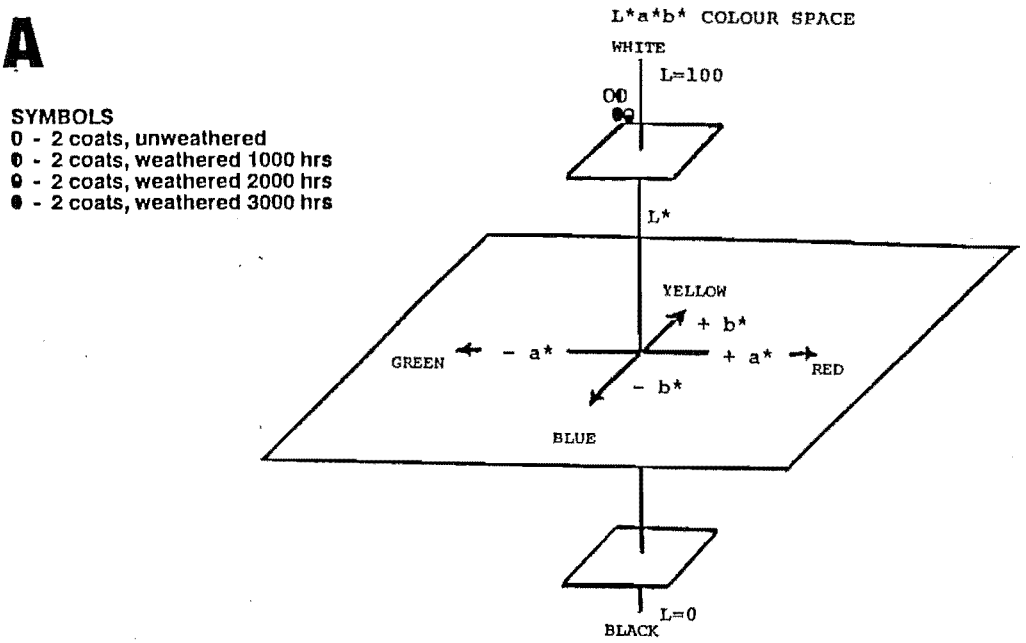

FIGURE 58(A)

L* a* b* plots for coated Dacrydium cupressinum (rimu) weatherboard before and after weathering measured with the Hunter Labscan Spectrocolorimeter. (refer table 4)
Coating - 2 coats, TiO_2 tagged Wattyl Estapol Exterior Clear.

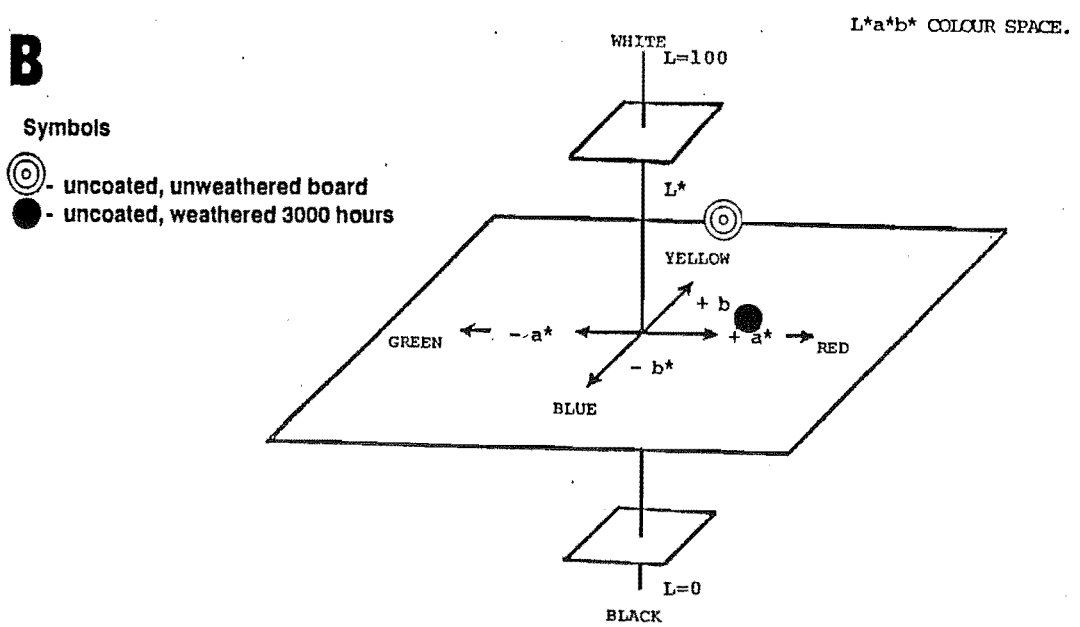

FIGURE 58(B)

L* a* b* plots for uncoated Dacrydium cupressinum (rimu) weatherboard, before and after weathering, measured with the Hunter Labscan Spectrocolorimeter. (refer table 4).

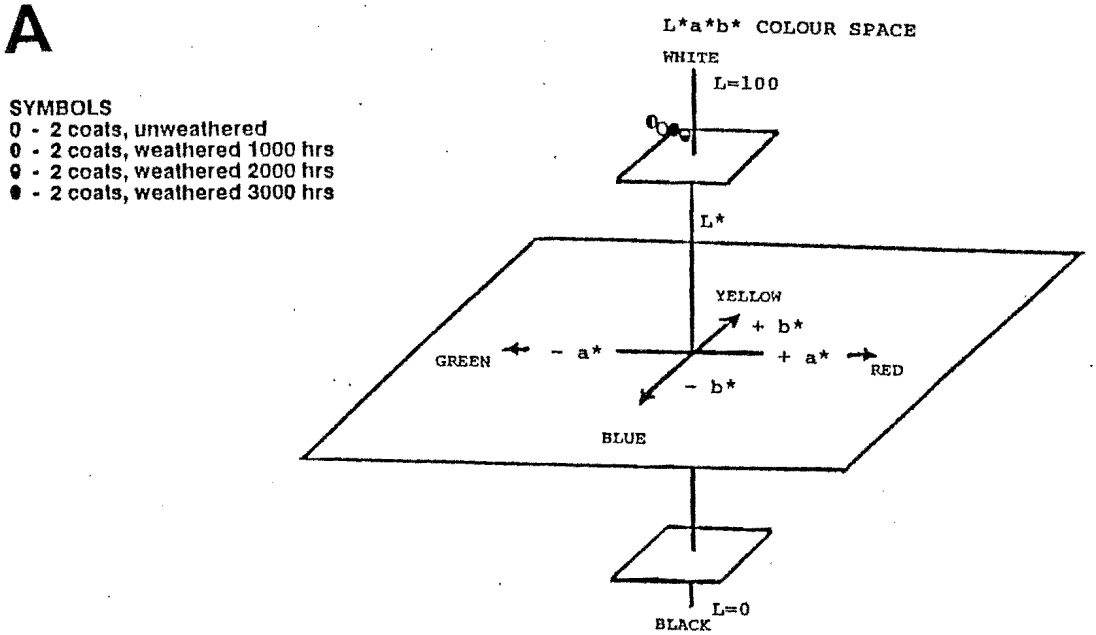

FIGURE 59(A)

L* a* b* plots for coated Podocarpus dacrydioides (kahikatea) weatherboard before and after weathering measured with the Hunter Labscan Spectrocolorimeter. (refer table 4)
Coating - 2 coats, TiO_2 tagged Wattyl Estapol Exterior Clear.

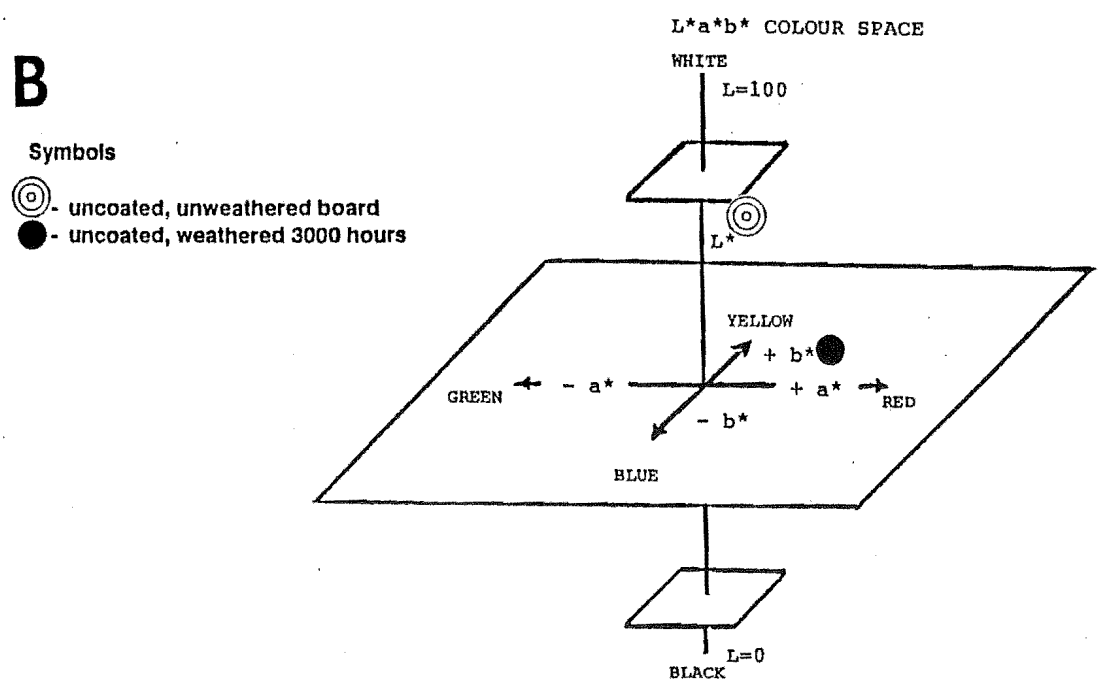

FIGURE 59(B)

L* a* b* plots for uncoated Podocarpus dacrydioides (kahikatea) weatherboard, before and after weathering, measured with the Hunter Labscan Spectrocolorimeter. (refer table 4).

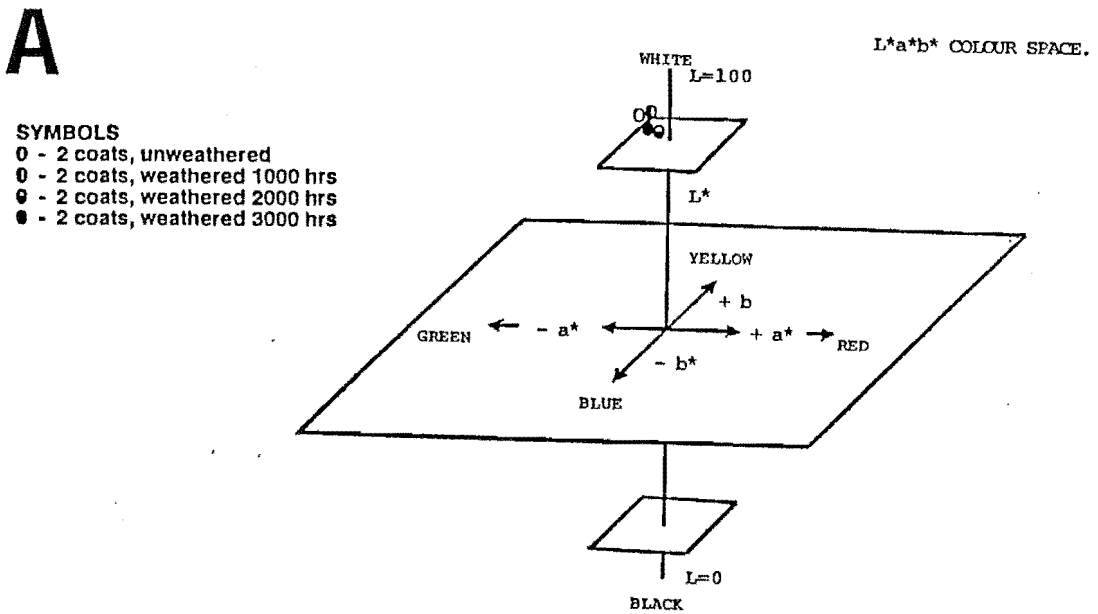

FIGURE 60(A)

L* a* b* plots for coated Pinus radiata (radiata pine) weatherboard before and after weathering measured with the Hunter Labscan Spectrocolorimeter. (refer table 4)
Coating - 2 coats, TiO_2 tagged Wattyl Estapol Exterior Clear.

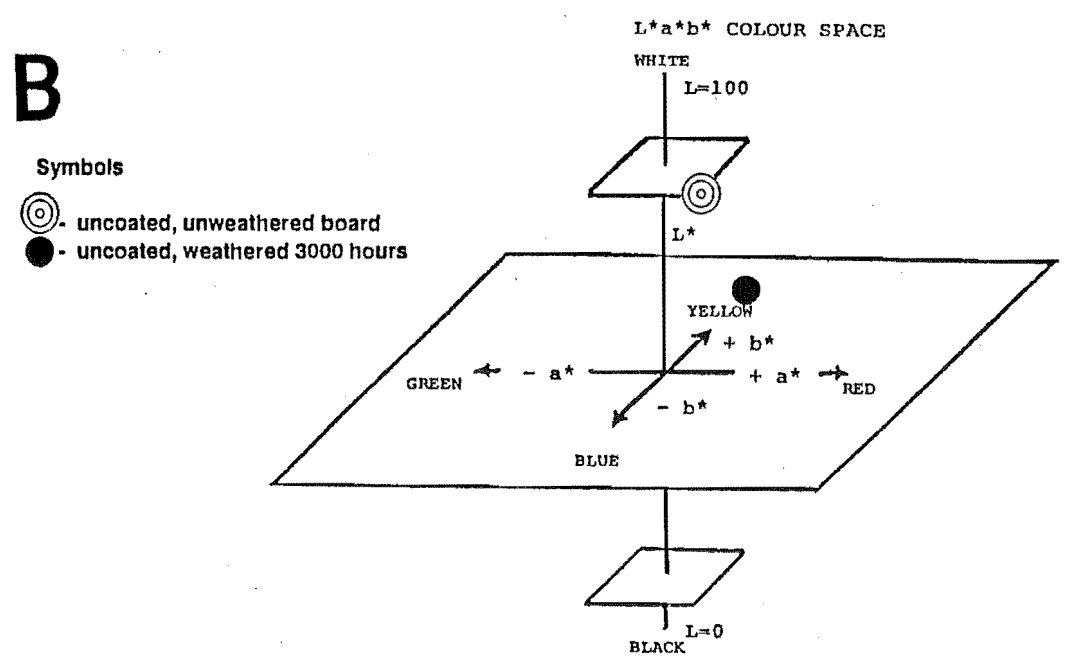

FIGURE 60 (B)

L* a* b* plots for uncoated Pinus radiata (radiata pine) weatherboard, before and after weathering, measured with the Hunter Labscan Spectrocolorimeter. (refer table 4).

applications and this was probably due to variation in coating penetration which resulted in subtle differences in surface phenomena. After one thousand hours weathering the metric lightness factor was eighty nine percent; by two thousand hours there was only a one to two percent drop; and when three thousand hours had been reached, the coating exhibited approximately eighty seven percent metric lightness. The coating on *D. cupressinum* showed a three percent decrease in lightness factor. Inconsistant values recorded for *P. dacrydioides* may be attributed to the slightly warped nature of the boards caused by moisture changes during the weathering cycle. It is notable that by three thousand hours the change in hue and chroma (saturation) for all three taxa was greater than the change in the lightness factor. For example, the mean values for *D. cupressinum* after three thousand hours were approximately L* 87 a -1 b* +8 indicating that visually the surface colour had become more "greenish blue" and less "yellow" with age.

The colour changes that occurred in weathered wood were recorded for the three taxa and are plotted in figures 58 [B], 59 [B] and 60 [B]. Unweathered *D. cupressinum* wood is much "redder" than the other two taxa. The average lightness factor values for *D. cupressinum, P. dacrydioides* and *P. radiata* were 63%, 74% and 77% respectively. After three thousand hours weathering there was a significant decrease in the metric lightness mean values. A fifteen percent decrease was recorded for *D. cupressinum* and twenty two percent decrease for both *P. dacrydioides* and *P. radiata* suggesting that the latter two substrates are more prone to change. Visually all three taxa exhibited the yellowing-browning effect characteristic of the initial stages of weathering of wood. After three thousand hours the plot positions shifted towards the yellow region for *D. cupressinum* and *P. radiata* but towards the red region for *P. dacrydioides*. It is concluded that the machined surface of *D. cupressinum* wood possesses the lowest metric lightness values compared to *P. radiata* board surfaces which have the highest.

6.4 CHROMATICITY

A definition of chromaticity is given in appendix 9 which also contains a modified version of the CIE chromaticity diagram showing the position of the standard illuminant D_{65} which represents daylight with a correlated colour temperature of 6500 kelvin units. Defining equations for the colour systems are given in method 2.15.

Figures 61 to 64 depict chromaticity diagrams for coated, uncoated, weathered and unweathered boards. Refer to table 4 for the mean values for each taxon. In the Y x y colour system, Y is the lightness factor expressed as a percentage based on a perfect reflectance of a hundred percent. Figure 61 shows the chromaticity diagram for one coat applications of TiO_2 tagged Wattyl Estapol on *D. cupressinum, P. dacrydioides* and *P. radiata* boards weathered for two thousand hours. The mean Y values were 67%, 61% and 67% respectively (table 4.2) and if these values are compared

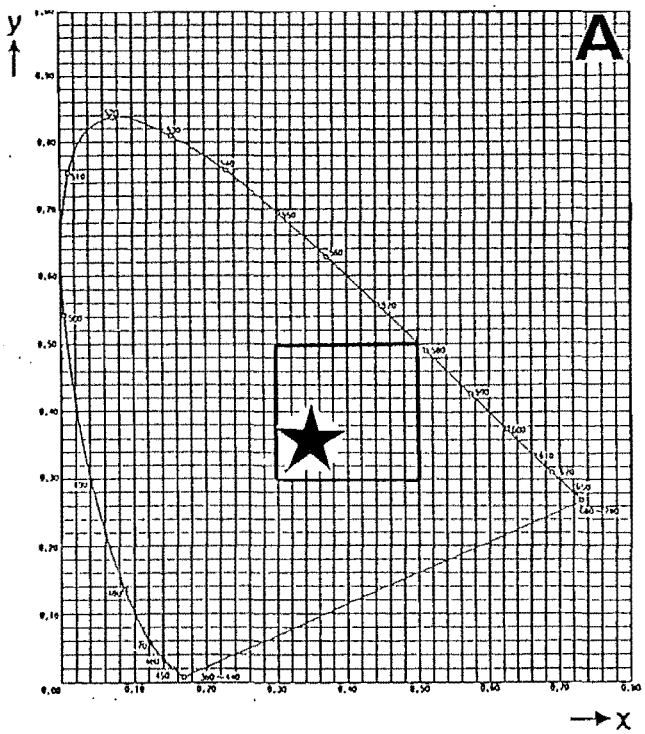

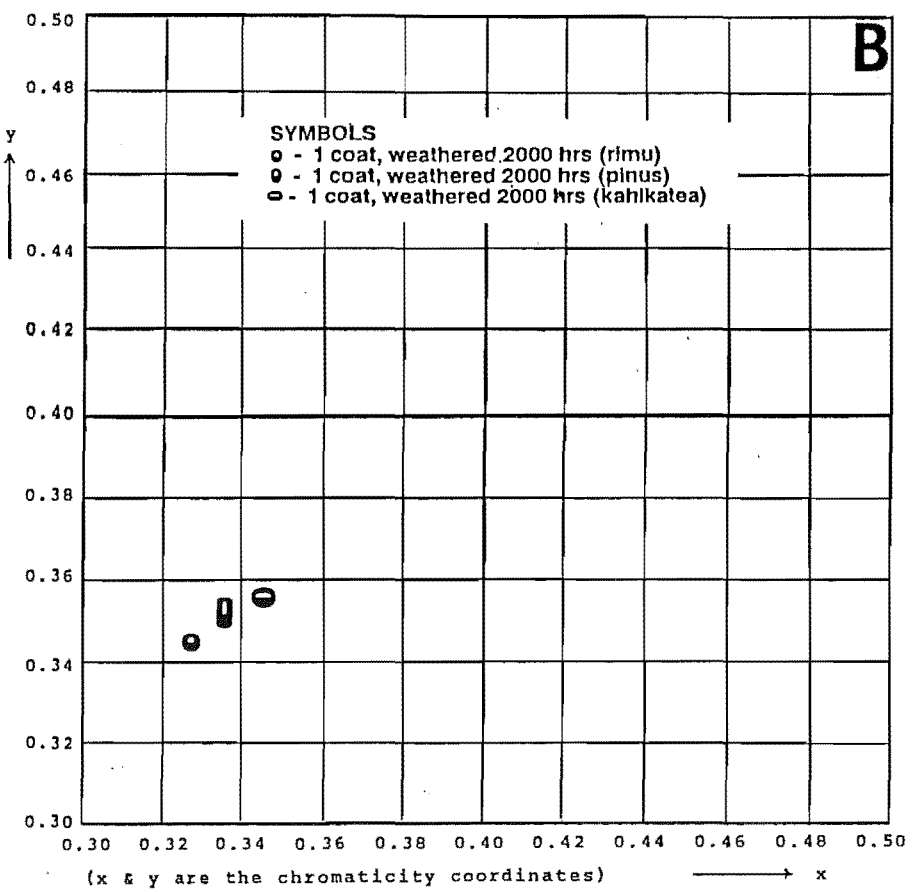

FIGURE 61 CHROMATICITY DIAGRAM

The star in graph A marks the position where weathered and coated Dacrydium cupressinum (rimu), Pinus radiata (radiata pine) and Podocarpus dacrydioides (kahikatea) boards plot on the chromaticity diagram. Grid square B is an enlargement of area ★
Measurements were made on the Hunter Labscan Spectrocolorimeter (see Table 4). Coating - TiO_2 tagged Wattyl Estapol Exterior Clear.

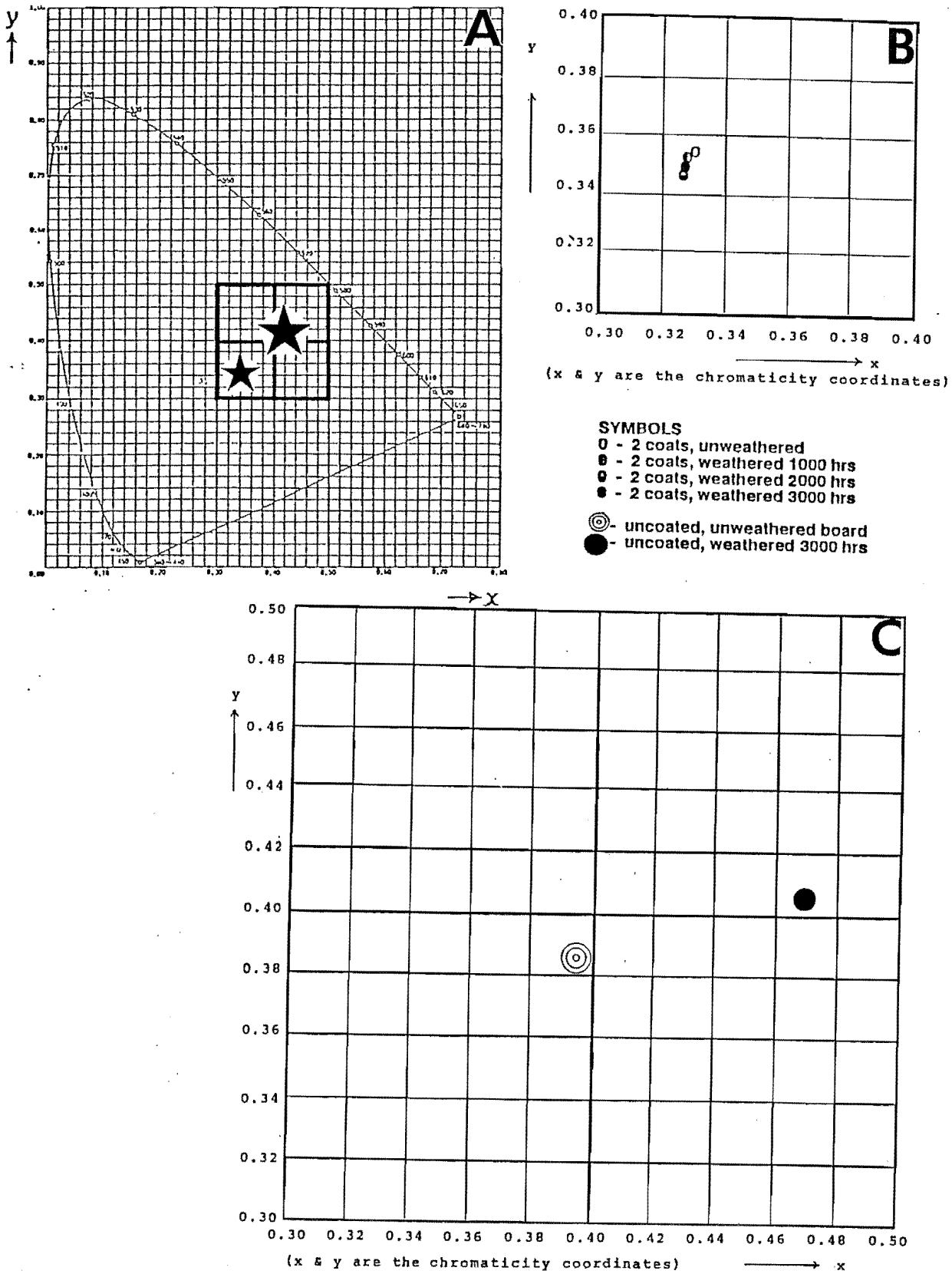

FIGURE 62 CHROMATICITY DIAGRAM .

The stars in graph A mark the position where both weathered and unweathered coated and uncoated Dacrydium cupressinum (rimu) weatherboard plot on the chromaticity diagram.

Grid square B is an enlargement of area ★
Grid square C is an enlargement of area ★
Measurements were made on the Hunter Labscan Spectrocolorimeter (see Table 4)
Coating - TiO_2 tagged Wattyl Estapol Exterior Clear.

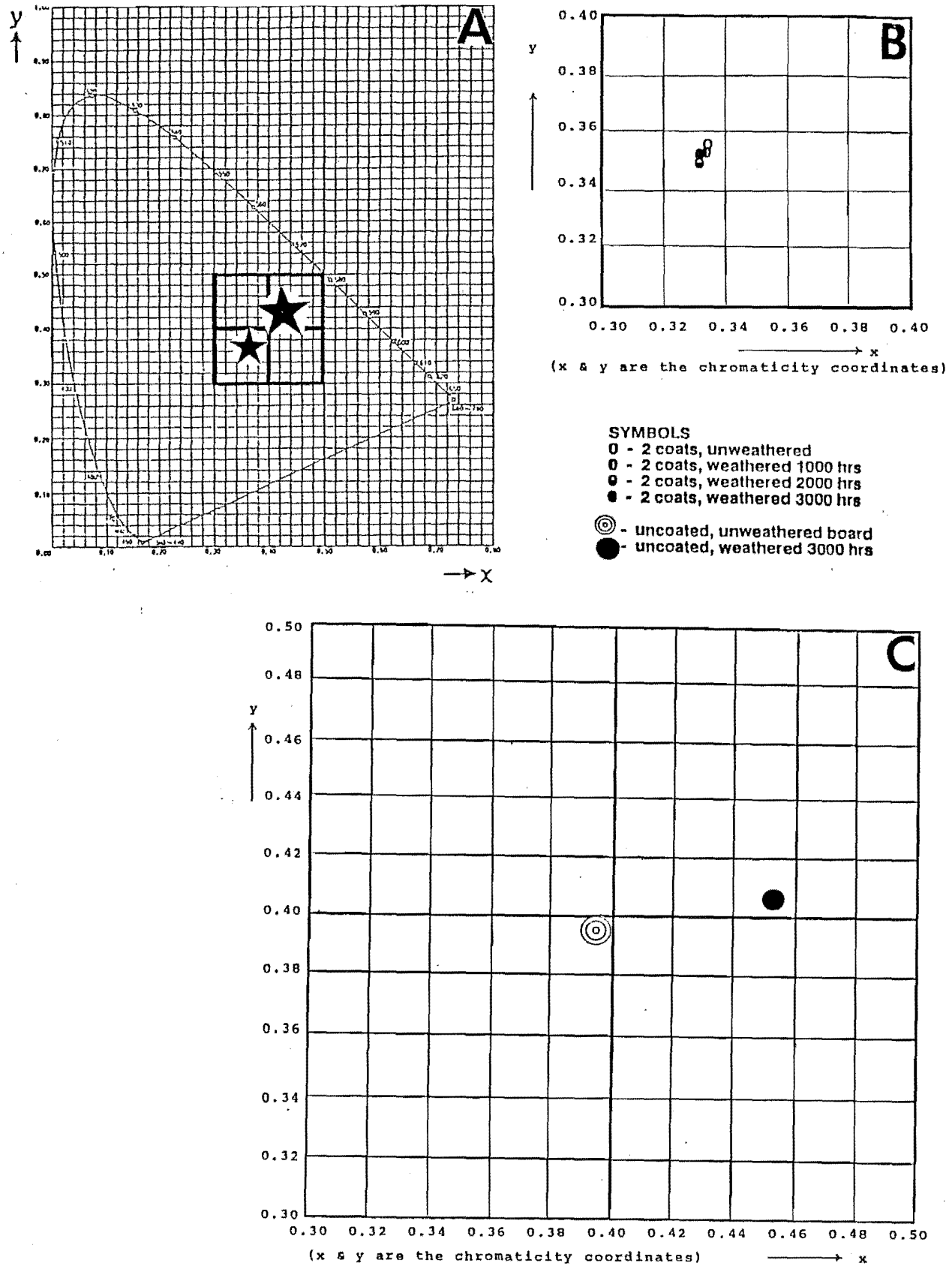

FIGURE 63 **CHROMATICITY DIAGRAM .**

The stars in graph A mark the position where both weathered and unweathered coated and uncoated Podocarpus dacrydioides (kahikatea) weatherboard plot on the chromaticity diagram.

Grid square B is an enlargement of area ★
Grid square C is an enlargement of area ★
Measurements were made on the Hunter Labscan Spectrocolorimeter (see Table 4) Coating - TiO_2 tagged Wattyl Estapol Exterior Clear.

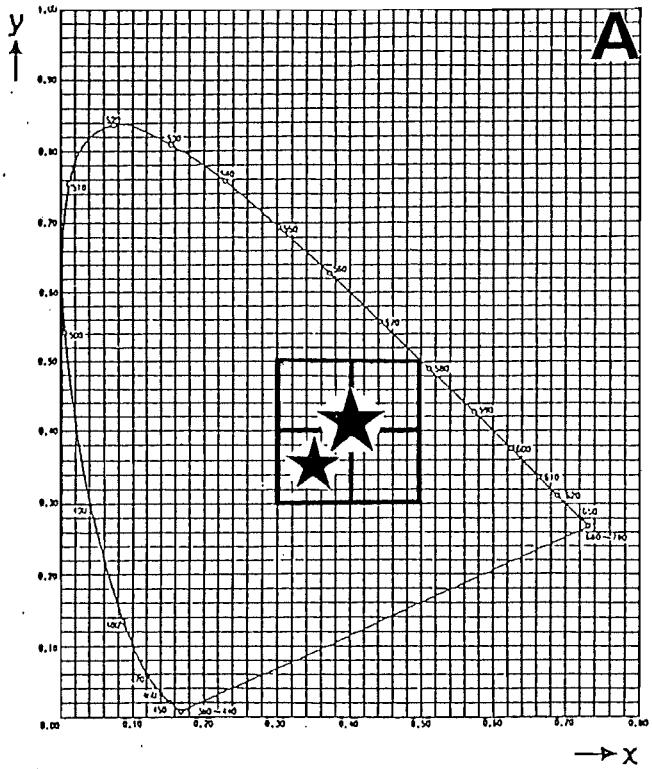

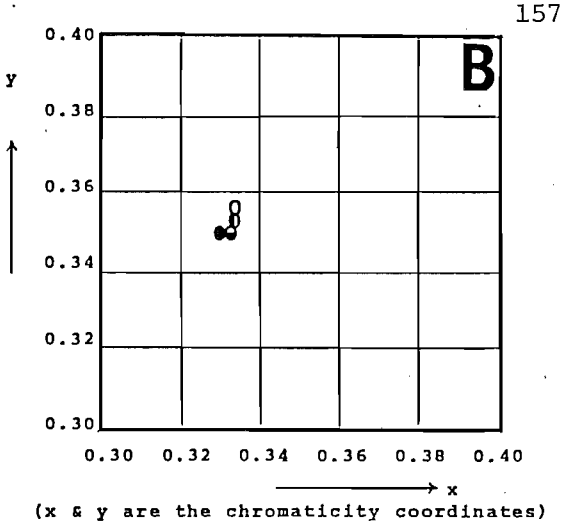

SYMBOLS
- 0 - 2 coats, unweathered
- 0 - 2 coats, weathered 1000 hrs
- 0 - 2 coats, weathered 2000 hrs
- ● - 2 coats, weathered 3000 hrs
- ◎ - uncoated, unweathered board
- ● - uncoated, weathered 3000 hrs

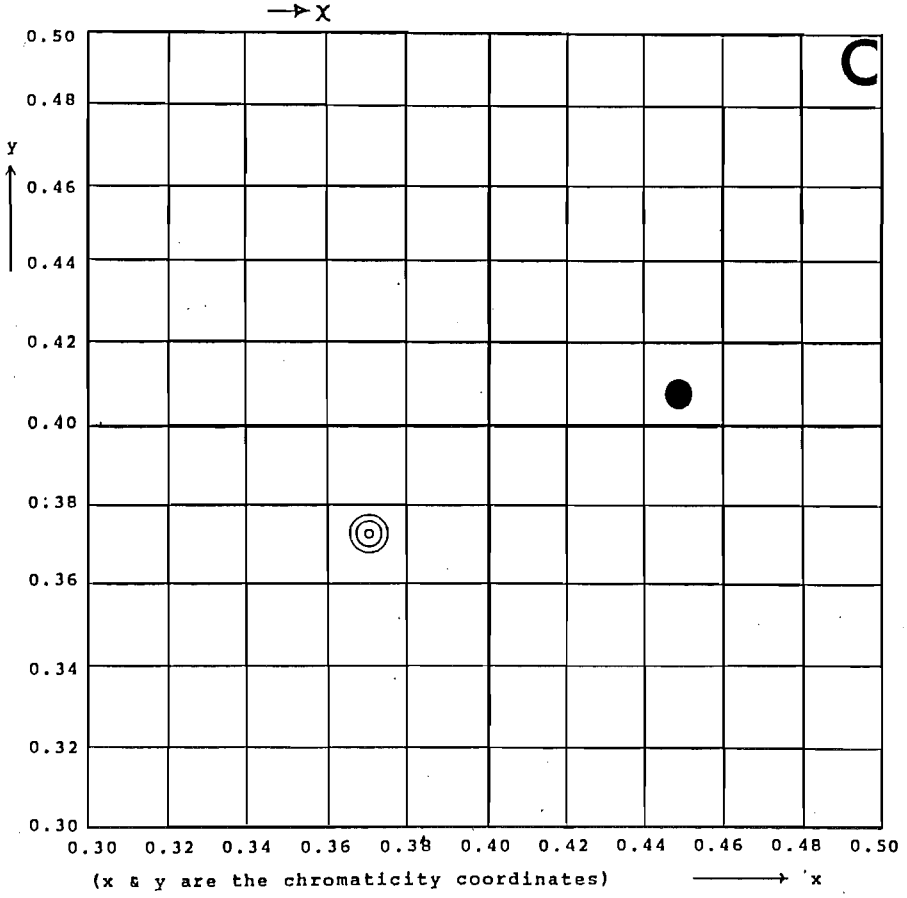

FIGURE 64 CHROMATICITY DIAGRAM .

The stars in graph A mark the position where both weathered and unweathered coated and uncoated Pinus radiata (radiata pine) weatherboard plot on the chromaticity diagram.

Grid square B is an enlargement of area ★
Grid square C is an enlargement of area ★
Measurements were made on the Hunter Labscan Spectrocolorimeter (see Table 4) Coating - TiO_2 tagged Wattyl Estapol Exterior Clear.

to those obtained for the two coat applications, weathered for the same period of time, the lightness factor Y values were 71%, 72% and 72% respectively (table 4.3). It is interpreted that the number of coats applied to the substrate determines the degree of reflectance and that weathering lowers the percentage of light that is reflected. Thinner films are more prone to loss of reflectance.

Figures 62 [B], 63 [B] and 64 [B] are details of chromaticity diagrams for two coat applications weathered for one thousand, two thousand and three thousand hours (refer table 4.3). The mean lightness factor Y value for the unweathered coating is 75%; after three thousand hours weathering the mean values had dropped to 71%, 74% and 72% respectively for *D. cupressinum, P. dacrydioides* and *P. radiata* coated boards. The x and y chromaticity values were plotted on the diagrams for comparison among taxa. Similar conclusions can be inferred from the results obtained with the Chromaticity Y x y colour system and with the L* a* b* system; i.e. as the process of weathering proceeds, the percentage of luminous reflectance is lowered and there is a change in chromaticity.

Figures 62 [C], 63 [C] and 64 [C] are details of chromaticity diagrams for uncoated, unweathered and weathered *D. cupressinum, P. dacrydioides* and *P. radiata* wood (refer table 4.1). The percentage light reflectance (Y values) decreased from 32%, 48% and 53% to 17%, 20% and 23% respectively for the three taxa, indicating that by three thousand hours the reflectance was approximately half the original value. It is notable that *P. radiata* wood still possessed the highest reflectance value after three thousand hours accelerated weathering. The numerical values plotted on the chromaticity co-ordinates x and y increased slightly for all three taxa after three thousand hours confirming the colour change associated with weathering processes.

There is a tendancy in the literature to assess visual changes in the properties of weathered coatings such as surface disfigurement, discolouration, colour change, gloss retention, qualitatively either with the aid of photographic standards or rated according to a ten point index system. The Glossgard system is a more accurate method enabling quantitative comparisons to be made for gloss evaluation. The loss of gloss after two thousand hours weathering is recorded for both two coat and one coat applications in appendix 10. The mean values for *D. cupressinum, P. dacrydioides* and *P. radiata* boards are compared with those for coated, unweathered boards. The results suggest that the wood substrate influences the original gloss level of the coating. *D. cupressinum* coated (two coats) unweathered boards retained the full gloss level of the coating whereas there was a slight decrease in gloss level after the coating was applied to *P. dacrydioides* and *P. radiata* wood. After two thousand hours weathering, the gloss level for all three taxa with two coats remained in the "gloss" range. But boards with only one coat exhibited further loss of gloss, with *P. dacrydioides* falling into the "semi-gloss" range. Thus it is concluded that gloss retention is affected by accelerated weathering conditions and the substrates.

6.5 FOURIER TRANSFORM INFRARED (FTIR).

To determine whether any chemical changes occurred in the coating during the three thousand hour weathering trials, infrared spectroscopy was considered a suitable method [Nakanishi, 1962; Miller & Stage, 1972; and Krishnan, 1984], (refer methods 2.16 and 2.17).

Infrared radiation in the 4000-666 cm^{-1} range is absorbed by organic molecules in varying amounts and characteristic frequency bands produced as a result of molecular vibration (stretching and bending) and rotation. Band position in infrared spectra are presented here as wavenumbers (unit cm^{-1}) and are directly proportional to the energy of vibration. Band intensities are expressed either as transmittance or absorbance [$\log_{10}$ reciprocal transmittance]. Shifts in absorption position and changes in intensity of bands may suggest chemical structural changes which in this study would be a result of weathering. Consultation of tables of "characteristic frequencies" published in the literature (Silverstein et al, 1981) were used here to assign names to the peaks in the spectral printouts. The two regions deemed important for preliminary examination of a spectrum are 4000-1300 cm^{-1} and 909-650 cm^{-1}. Characteristic 'stretching frequencies' of O-H, N-H and C=O functional groups occur in the higher frequency portion and aromatics in the lower frequency region. The intermediate section of the spectrum, 1300-909 cm^{-1} is known as the "fingerprint" region and commonly has a complex absorption pattern arising from interacting vibrational modes of C-O and C-H stretches.

Both FTIR and ATR spectra were obtained in this study. FTIR is a more sensitive technique as it scans deeper into the substrate and the corresponding spectra is more detailed. Compare figure 65 [A] and [B]. The TiO_2 tagged Wattyl Estapol is a long soya oil alkyd. The resin is produced by converting the soya oil to the monoglyceride form by the addition of glycerol to soya oil and then polymerising the monoglyceride with phthalic anhydride to form the alkyd. Direct comparison with the spectra of known structures is useful in interpretation. For example, the standard spectrum for soya bean oil, as depicted in the published spectral atlas, resembles that of this coating, in particular the carbonyl region; while the standard spectrum for rutile titanium dioxide echoes that observed in the 700 to 400 cm^{-1} region. Not all bands in a spectrum can be readily assigned and it is usual to define only the most prominent peaks and locate any other peaks associated with them. The characteristic carbonyl band occurs near 1725 cm^{-1} and it is noted that in the unweathered coating the FTIR spectrum has a strong band in the carbonyl region at 1735.9. Justification in accepting this band as a carbonyl band lies in the established fact that carbonyl bands are known to display high intensity and this part of most infrared spectra is generally free from other absorptions. The band peaking at 1616.3 may be assigned to C-H stretching frequencies. The bands peaking at 1465.9 to 1346.3 are of doubtful value for diagnostic purposes, however it is noted that the band peaking at 1465.9 may be due to CH_2 deformations. The band of high intensity at 1265.3 can probably be assigned to the C-O stretching frequency while the band peaking at 1118.7 is probably a C-C stretching

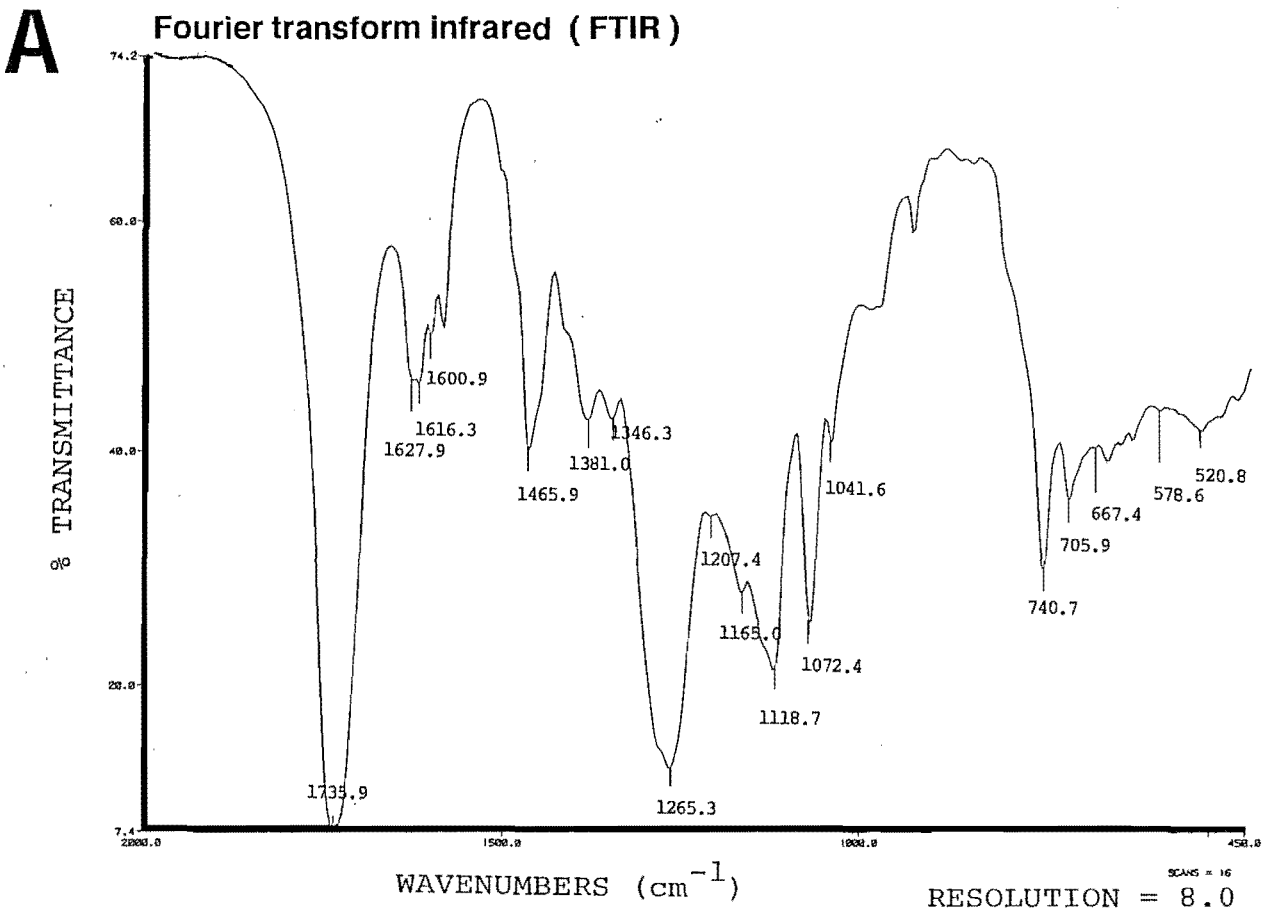

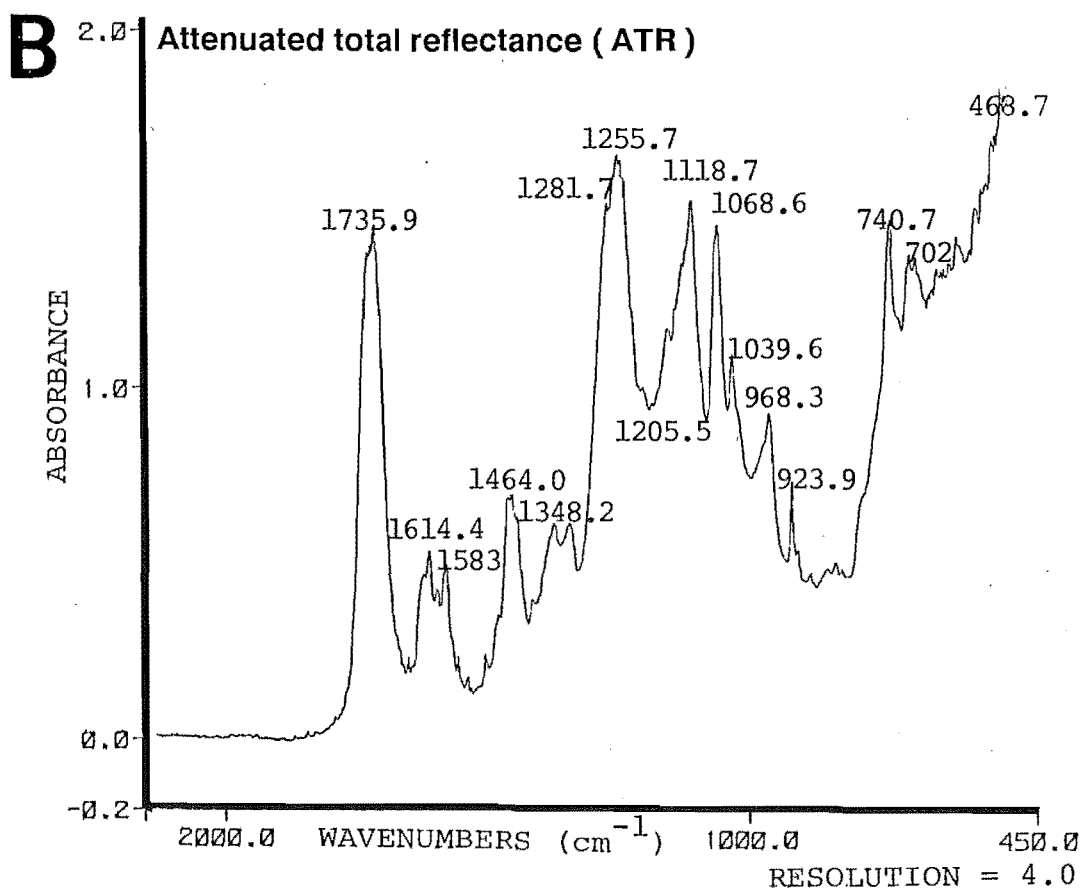

Figure 65 FTIR and ATR spectra of unweathered TiO_2 tagged Wattyl Estapol .

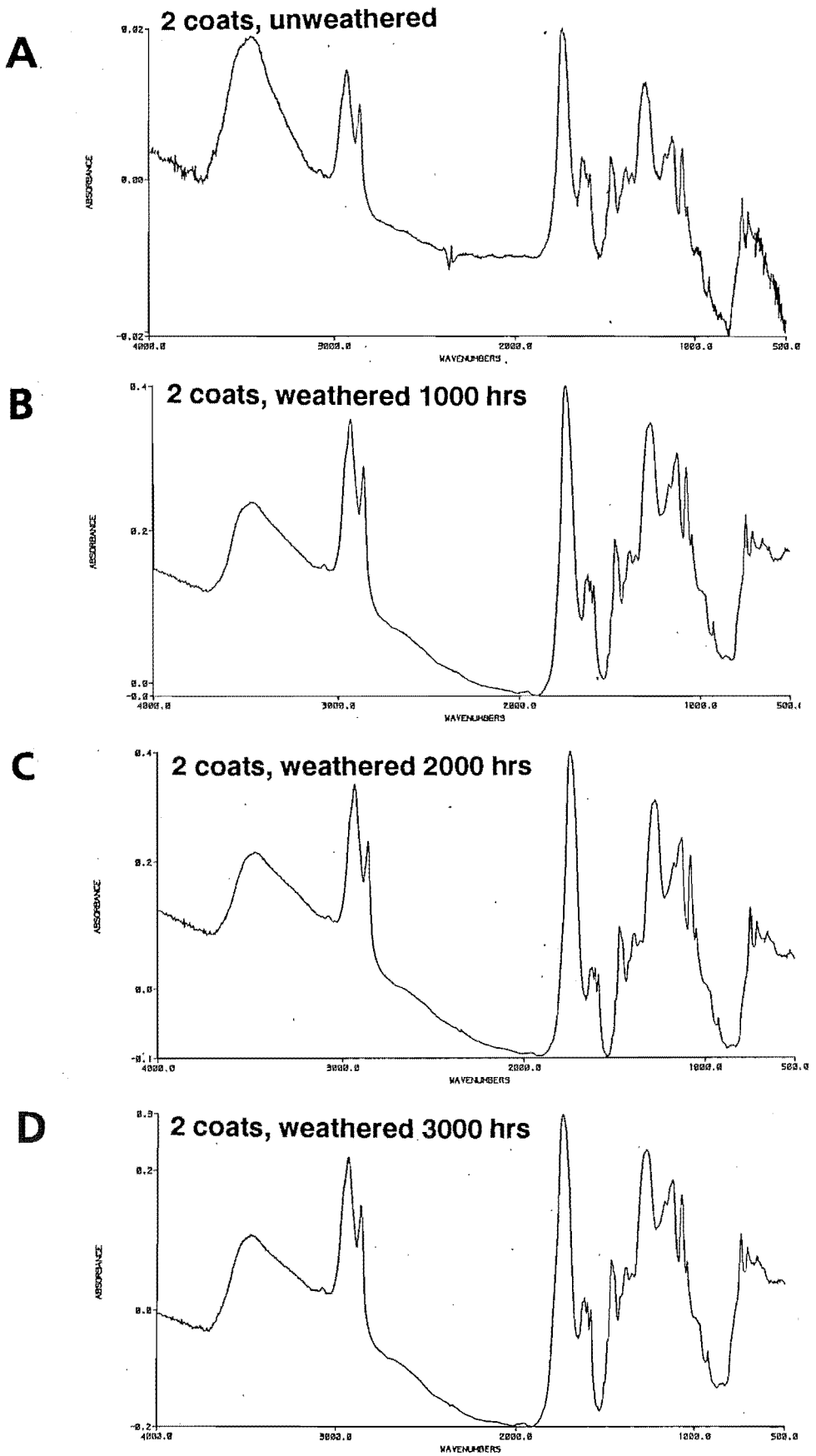

Figure 66 **FOURIER TRANSFORM INFRARED (FTIR) spectra.**

<u>Dacrydium cupressinum</u> **COATED WITH WATTYL TiO_2.TAGGED ESTAPOL.**

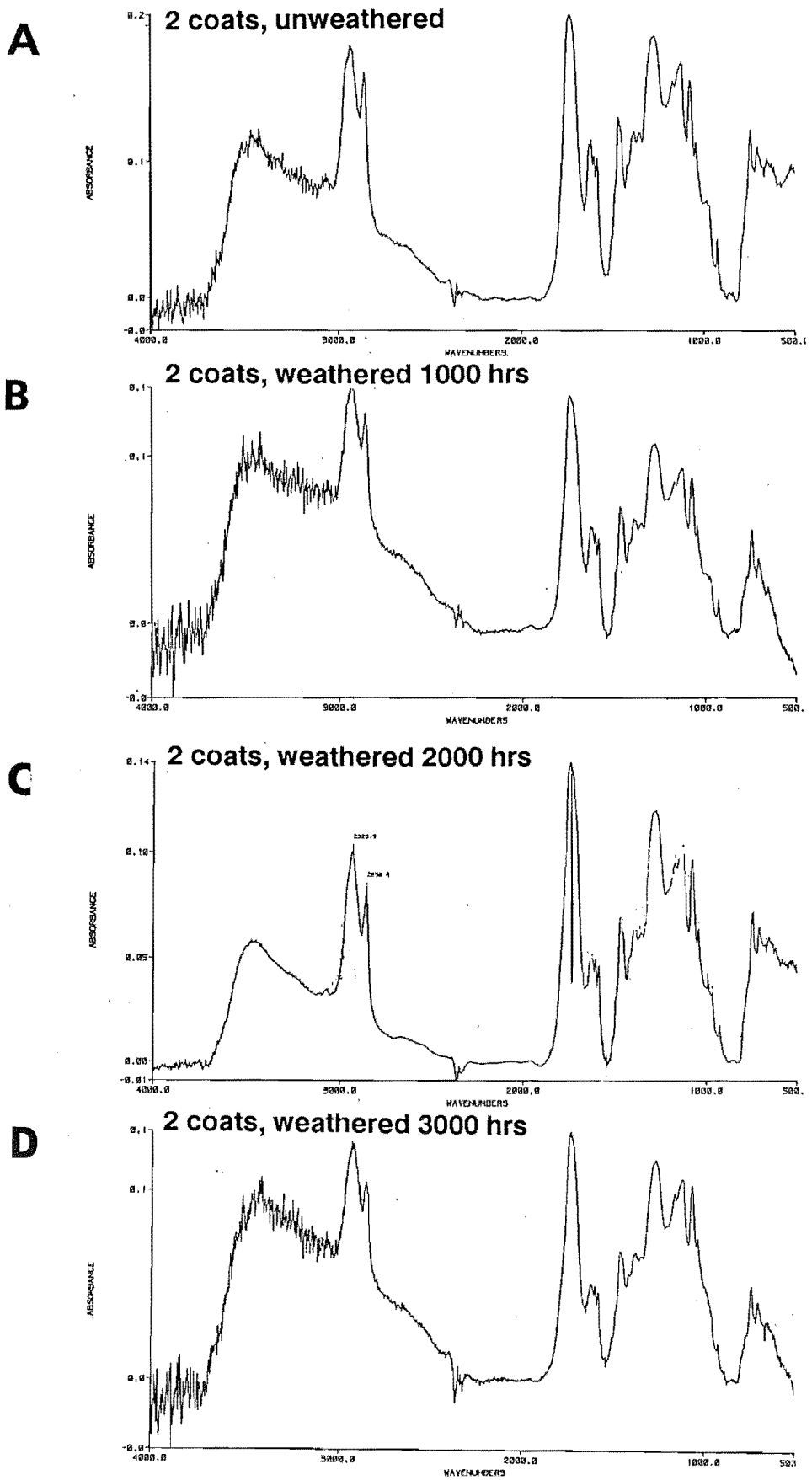

Figure 67 Fourier transform infrared (FTIR) spectra.

Podocarpus dacrydioides COATED WITH TiO_2 TAGGED WATTYL ESTAPOL.

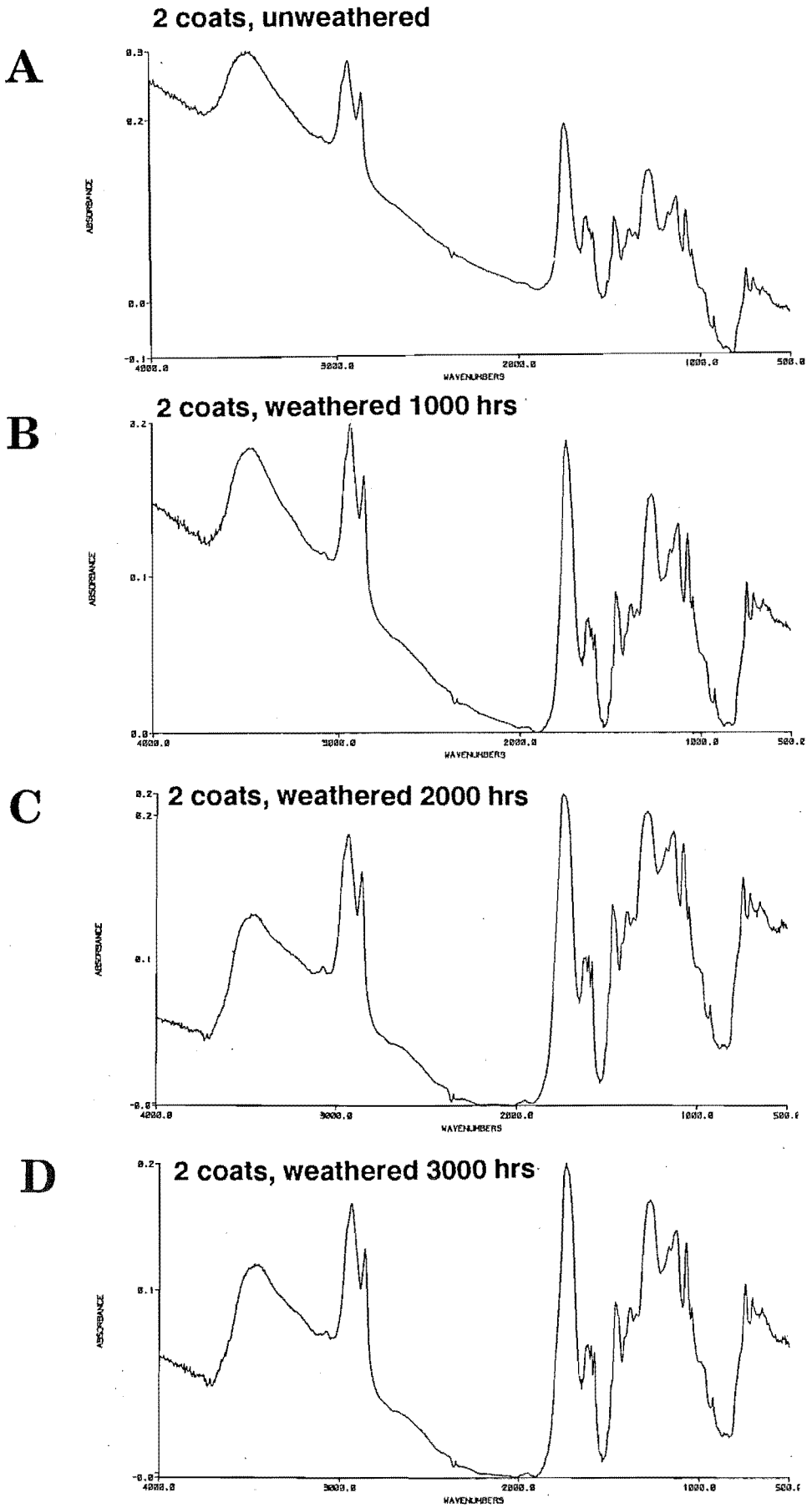

Figure 68 Fourier transform infrared (FTIR) spectra.

Pinus radiata COATED WITH WATTYL TiO_2 TAGGED ESTAPOL.

frequency. The band pattern of aromatic compounds is normally sufficiently well defined to permit at least tentative conclusions to be reached. Numerous bands between 600-400 cm^{-1} are indicative of the aromatics.

Figures 66 to 68 depict spectra of the coating on *D. cupressinum*, *P. dacrydioides* and *P. radiata* weatherboards after one thousand, two thousand and three thousand hours artificial weathering. Spectra of the unweathered coating applied to the three weatherboard taxa is included for comparison for slight variation may exist in the original coating/substrate interaction.

Band intensities of FTIR spectra are given as absorbance and can be directly compared with the ATR spectra. Frequencies in the 4000-500 cm^{-1} region are presented. The peaks in the 3600-3250 cm^{-1} region are due to the H_2O absorbed into the KBr pellet. The peaks at 2929.9 and 2856.6 may be assigned to C-H stretching frequencies.

The FTIR spectra for coated *D. cupressinum*, *P. dacrydioides* and *P. radiata* after three thousand hours weathering is essentially the same. The absorbance base lines have been normalized to zero in figures 66 [A & B] and 68 [C & D] and show virtually identical spectral patterns for two thousand hours and three thousand hours.

6.6 ATTENUATED TOTAL REFLECTANCE (ATR)

Figure 65 [B] shows the ATR spectra of the unweathered coating. ATR spectra of the coating on *D. cupressinum*, *P. dacrydioides* and *P. radiata* weatherboards after one thousand, two thousand and three thousand hours of artificial weathering are presented in figures 69 to 71. The ATR spectra for all three taxa after three thousand hours weathering is essentially the same. However, slight trends not detected by the FTIR technique are visible because the ATR technique is able to detect surface changes. Peak height of certain groups such as the carbonyl band at 1735.9 cm^{-1} show a decrease in intensity and the rutile titanium peak a corresponding increase with weathering.

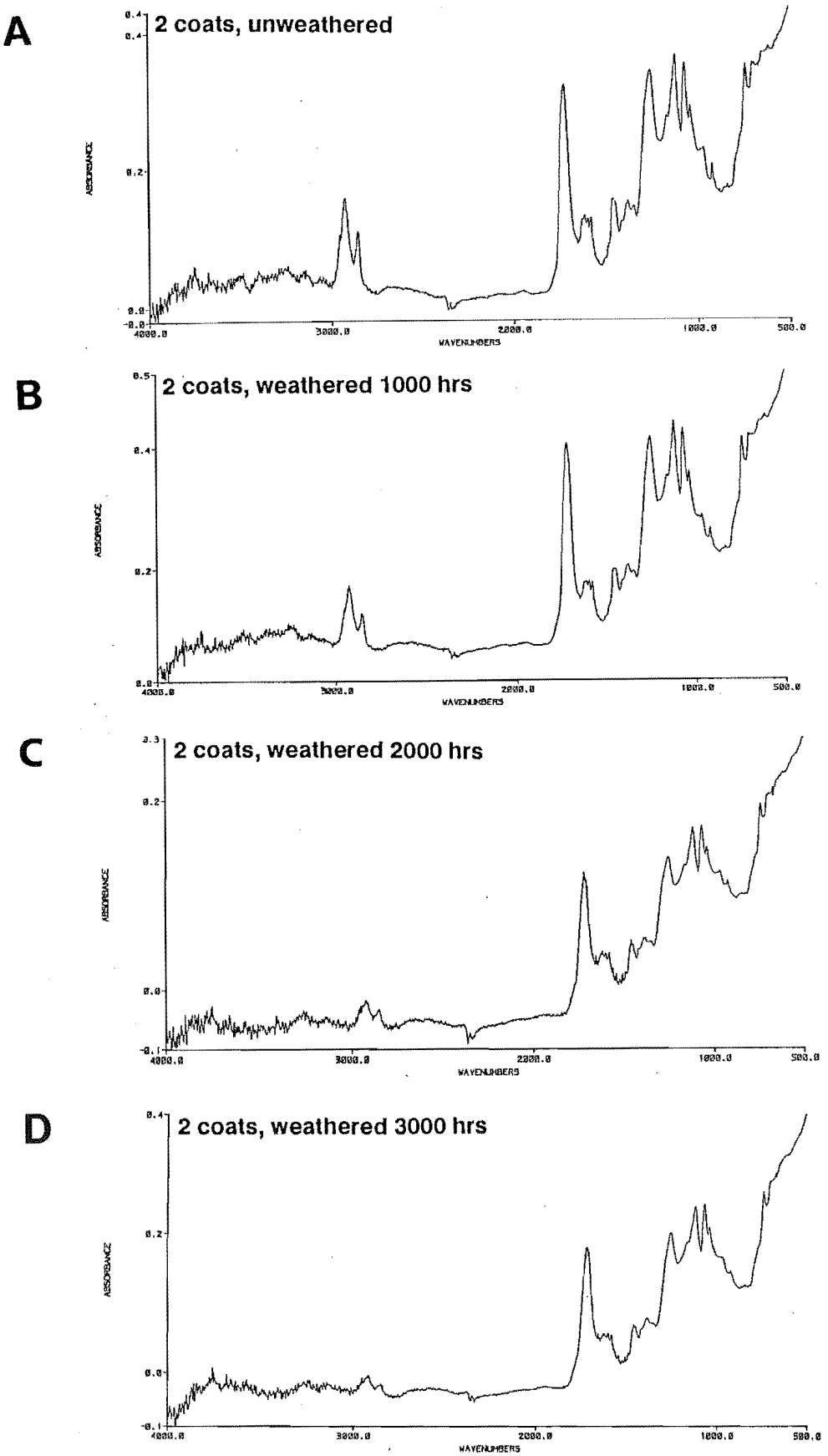

FIGURE 69 Attenuated total reflectance (ATR) spectra.

Dacrydium cupressinum **COATED WITH TiO_2 TAGGED WATTYL ESTAPOL .**

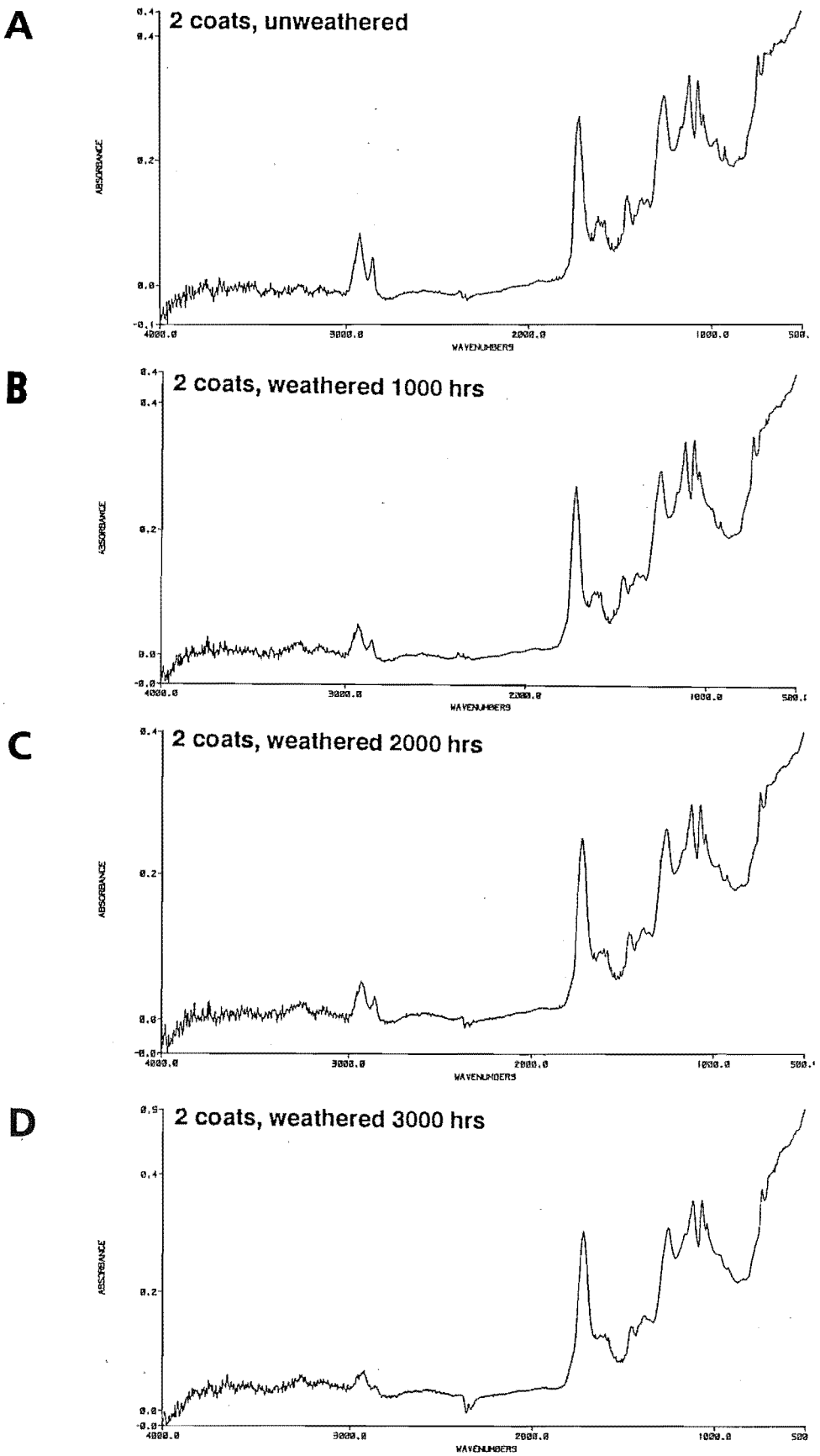

FIGURE 70 Attenuated total reflectance (ATR) spectra.

Podocarpus dacrydioides **COATED WITH TiO_2 TAGGED WATTYL ESTAPOL.**

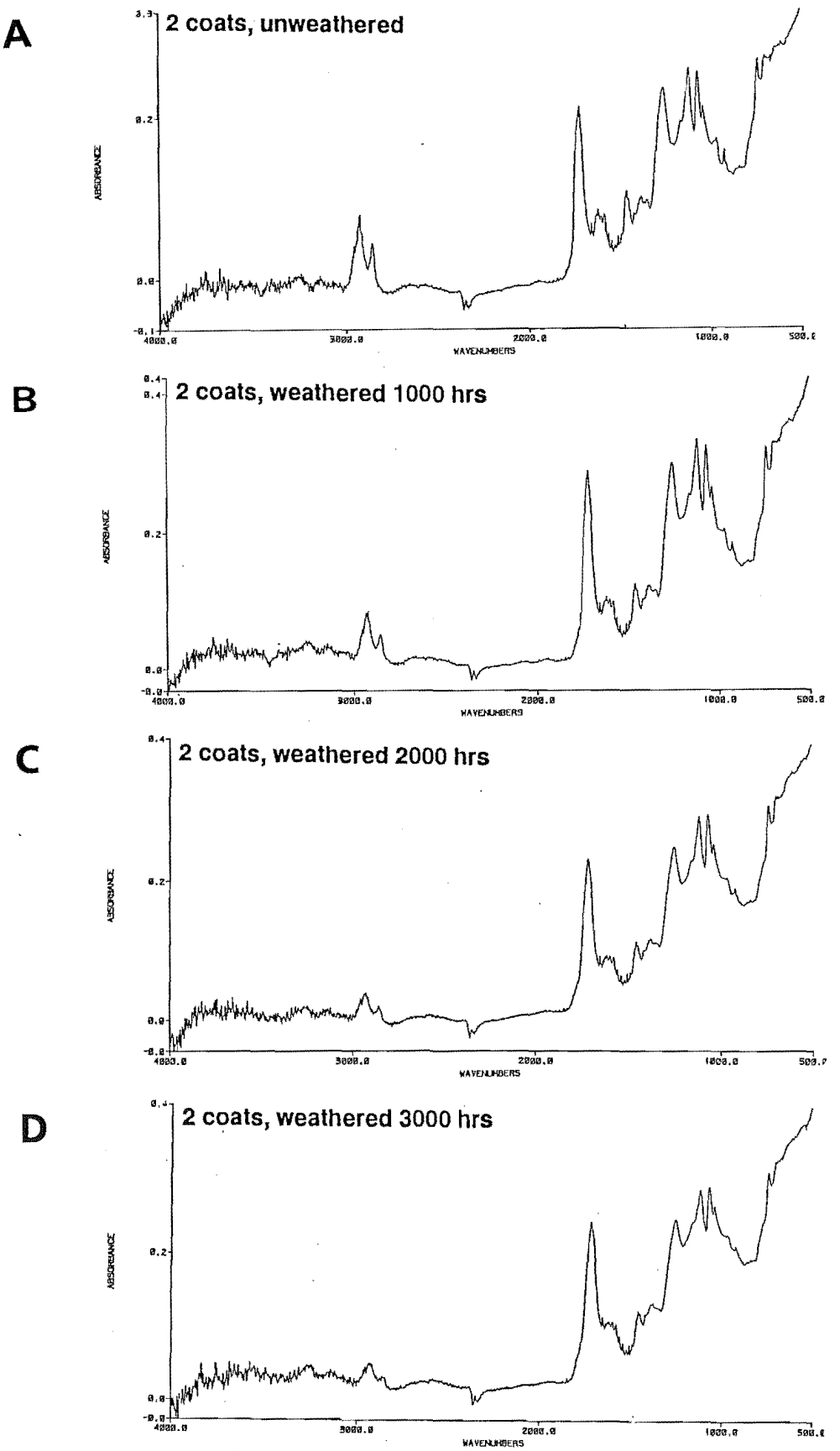

FIGURE 71 Attenuated total reflectance (ATR) spectra.

Pinus radiata **COATED WITH TiO_2 TAGGED WATTYL ESTAPOL.**

6.7 SCANNING ELECTRON MICROSCOPE STUDY OF WEATHERED COATING/SUBSTRATES.

Figure 72 compares *D. cupressinum*, *P. dacrydioides* and *P. radiata* weatherboards before and after accelerated weathering tests. The upper three sets of micrographs compare unweathered, uncoated boards with boards that have undergone weathering for a duration of three thousand hours, being the maximum period of weathering performed in this study. The top set of three micrographs represents typical examples of the quality of machining received by the three taxa during board preparation. Intertracheid bordered pits and tracheid to ray cross-field pits are visible on the unmodified cell walls. After three thousand hours the wood has changed significantly. *P. radiata* has the softest wood and so exhibits the greatest change. If the pith is present in a board, weathering will cause it to shrink within the timber and it will eventually fall out (Thorpe et al , 1987). The second and third trio of micrographs are increasing magnifications which accentuate the structural changes that have occurred.

During the course of weathering, wood becomes rough, the grain lifts, the resin canals separate from the surrounding elements, checks develop, grain loosens, failure occurs parallel to the grain, boards cup and warp and eventually the wood splits due to the loss of surface coherence. Close examination of the electron micrographs shows that by three thousand hours the cell wall layers have separated and cell voids and lumens have enlarged, particularly in the thin walled earlywood tracheids and ray parenchyma cells. The strength of the cell wall bonds is destroyed near the surface of the board where intercellular and intracellular cracks and checks have been produced. The earlywood and latewood boundaries are areas of greatest weakness and have started to move apart. The formation of longitudinal checking between walls of adjacent tracheids in the vicinity of the middle lamella region is evident in the third set of micrographs. Intercellular failure is characterized by the separation of cells at the middle lamella junctions; it appears to be initiated in the vicinity of rays and proceeds above and below them. As weathering proceeds the arch-like skeletal pattern produced will become more pronounced. In some cases the earlywood middle lamella remained intact during the early stages of weathering; in other cases the middle lamella appears more susceptible to degradation than the secondary wall. Weakening of intercellular bonding is greatest at the cell corner middle lamella region. Intrawall breakdown occurs in the secondary wall and is associated with S_1, S_2 and S_3 layer separation. The microfibrils, which are the most stable components, are still intact after three thousand hours of weathering.

The pit chamber of bordered pits in the wall of earlywood tracheids occupies a larger area of the wall and hence earlywood pits are more prone to kinking (Harris, 1981) during deformation. After three thousand hours of weathering, it is evident that the apertures of the bordered pits in the radial

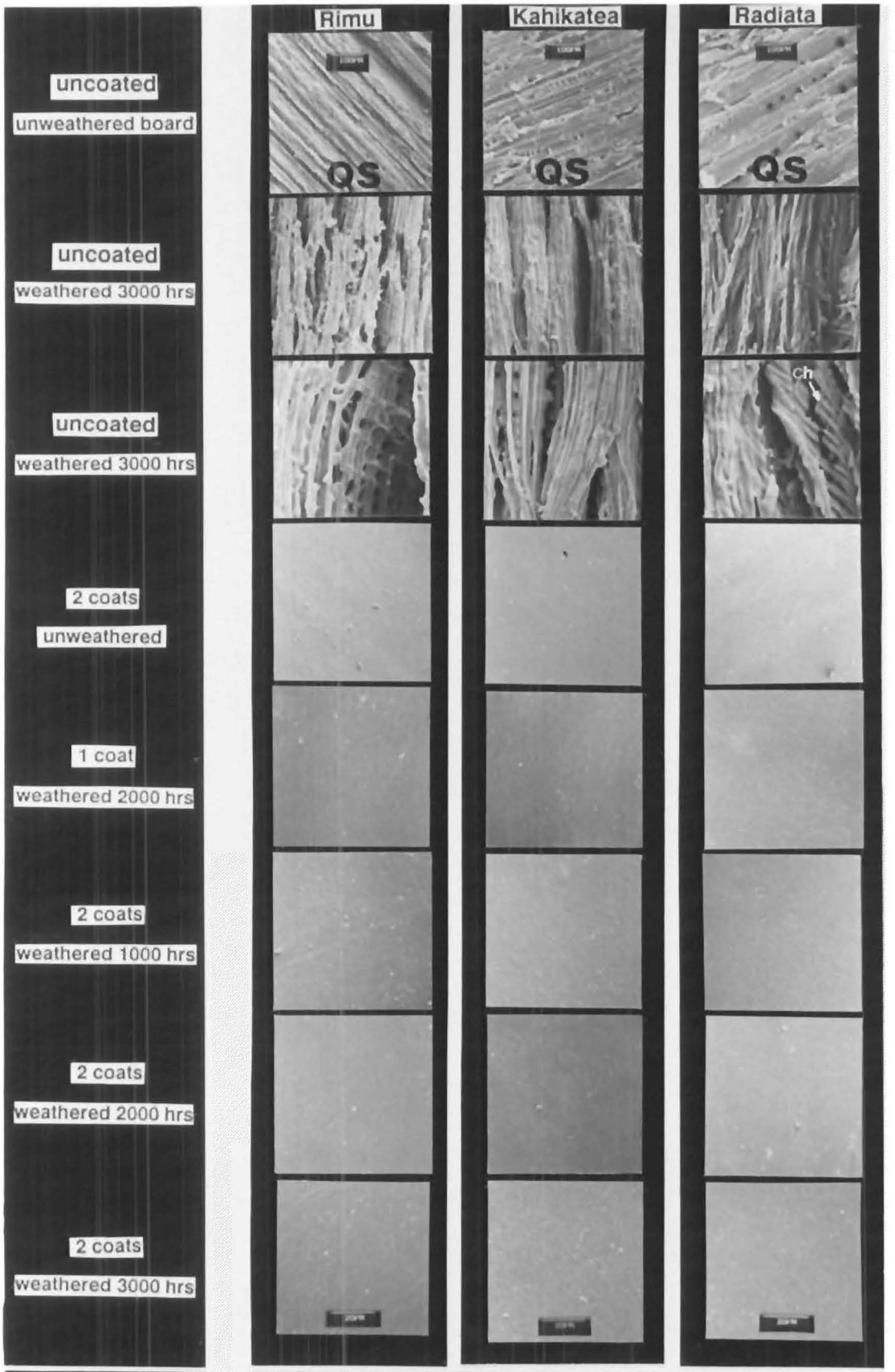

FIGURE 72

The effect of accelerated weathering on uncoated dressed boards and boards coated with TiO_2 tagged Wattyl Estapol.

walls of tracheids have enlarged almost to the limit of the pit chambers. The circular bordered pits may be more resistant to stresses than the elliptical half bordered cross-field pits. Diagonal microchecks, exhibiting a comb-like structure, pass through the bordered pits suggesting that the microchecks originate at the fibril angles of the S_2 wall layer and may be a consequence of local variations in concentrations of tensile strength. Cross-field pit apertures coalesce with continued exposure. It is notable that after three thousand hours of weathering, profile views of boards coated with two coats of finish revealed no evidence of loss of adhesion. The wood structure underneath appeared unaffected and resembled that of unweathered wood, indicating the protective nature of the two coats was still functional.

The fourth photographic set depicts the three taxa with two coats of finish in an unweathered state. A comparison of sets five and six show that after two thousand hours of accelerated weathering, the presence of one or two coat systems did not visually reveal any structural changes on the coating surface. This indicates that a longer period of weathering is therefore required for structural changes to manifest themselves. Sets six, seven and eight show the effect of weathering on boards with two coats of finish after one thousand hour, two thousand hour and three thousand hour intervals. From these observations it is concluded that microscopically there is no visual change on the coating surface after three thousand hours weathering.

As part of the recommended procedure for painting weatherboards it is important that care is taken in the painting of the edges. Some weatherboard manufacturers produce boards with sharp arrises while others produce boards with rounded arrises. Rounded arrises are preferred because paint tends to shrink away further from a sharp arris and leave only a thin film. (B.R.A.N.Z., 1978). Paint failure in the early stages occurs at the arris (Cassens & Feist, 1980), however, in this study the coating was still intact along the board edges after three thousand hours of accelerated weathering.

6.8 DISCUSSION

Worldwide, considerable research has been done on the exterior durability and performance of an immense range of coating systems, usually related to specific brands, many of which are now obsolete, and to coatings formulated to suit the timber species used in that particular country. Haslam & Wertham (1931), amongst others, recognised that not only was coating composition significant in determining the life of a coating but the macro and microstructure of the wood substrate was important as well. Compared to the amount of research on coating service life, much less has been reported on the changes that occur within the substrate during the process of aging. As well as within and between tree species variability, seasonal variation present in the wood substrate controls wood quality and affects performance. In New Zealand, Sinclair & Chamberlain (1959), Jessop (1965), Kerr (1965), Preston & Chittenden (1978), B.R.A.N.Z. (1978), Blakeney (1979), Plackett et al

(1984), Jensen & Whitney (1986) and others have contributed to our understanding of paint performance by performing natural and artificial weathering tests on a variety of timber substrates including *P. radiata*, the most widely used species. Detailed descriptions of wood anatomical changes as a consequence of aging, however are lacking. Jessop (1956) studied the durability of both pigmented and clear coatings used in New Zealand and concluded that the cause of paint failure was due more to the nature of the wood than to the paint film. With reference to moisture studies, Haagden (1977) also arrived at a similar conclusion that wood was the determining partner. These theories, are subject to debate, and there is as yet no consensus of opinion as to whether the coating or the substrate has greater influence, or whether both are equally important.

Visual assessment of discolouration of coatings and wood substrates provides qualitative information on the state of the product. Light fastness refers to the ability to withstand colour change on exposure to light; and fading refers to the colour change that involves a lightening or weakening of colour and may involve a change in hue. Jessop (1956), noted that sunlight and temperature cause *P. radiata* wood to turn brown in the absence of moisture and grey under moisture cycling conditions. The actual initial colour changes that occur depends on the original colour exhibited by the wood substrate species. Feist & Hon (1984) described the yellowing or browning and eventual greying of Ponderosa pine and southern yellow pine wood as weathering proceeds and attributed it to the chemical decompositon of lignin and increase in cellulose content in the cells near the surface of the board. Visible light has been estimated to penetrate wood up to 200μm but ultraviolet light can only penetrate wood to a maximum depth of 75μm (Feist & Hon, ibid). They noted that usually the grey colour of weathered wood only extends to a depth of 0.10 to 0.25 mm and the dark brown layer immediately underneath extends to a depth of 2.5 mm. During natural weathering processes, exposed wood undergoes photodegradation and photooxidative degradation. Degradation reactions are a surface phenomenon.

The primary function of a primer is to bond, the secondary function is to seal the surface of the wood and reduce the rate of change of moisture content (Jensen, 1986). Subsequent coats fill minor imperfections and should bond with the film underneath. A coating protects the timber from excessive expansion and contraction and associated dimensional changes. The performance of a coating is dependant on the wood substrate remaining dry during service (Miller, 1983). Haagden (1977) stressed that the form of the horizontal profile of weatherboards determines the wood behaviour. Cassens & Feist (1980) pointed out that coatings perform better on quarter sawn boards than on flat sawn boards.

The lower density earlywood bands shrink and swell at a greater rate than the denser latewood bands. Growth ring boundaries are areas of high stress. In the early stages of a coatings life it is soft and elastic; it can move sympathetically with the timber and is capable of adjusting to the change in moisture content in the wood on which it was applied; but with age it becomes more brittle. It has

been suggested that oil based coatings are more impermeable to the uptake and loss of moisture (Blakeney, 1979). Plackett & Blakeney (1987) reported that oil based primers exhibit a greater tendency to embrittlement and will eventually crack due to wood expansion and contraction. They noted that clear finishes based on epoxy resins were not as flexible as acrylic clear finishes. Miniutti (1963) argued that coating in the cavities of cells below the surface does not prevent movement of water from cell to cell and that if water entered through the back of the board or via cracks in the coating film the swelling of wood cells would not be prevented.

For years it was thought that oil based primers, which were formulated with up to sixty to seventy percent oil content, mechanically anchored the film to the substrate (OCCA, 1974). But subsequent research disproved this showing that an oily primer can vary in composition across a substrate of differing porosity and is ultimately subject to adhesion problems (OCCA, ibid). Haslam & Werthan (1931) deduced that deep penetration of the coating did not prevent the loss of film adhesion with time. They noted that although the depth and irregularity of penetration could be increased by the addition of mineral spirits, which decreased the viscosity of the vehicle, "dry spots" were produced in those areas suffering from film composition depletion. Underhaug et al (1983) also concluded that coating adhesion was not improved by good penetration in spruce (*Picea abies*). Whether coating penetration is crucial to the service life of the film is still the subject of much speculation.

In evaluating coating performance, numerous variables must be considered with reference to the purpose and conditions of the service of the coating. In the past, coating aging phenomena was assessed qualitatively by scales, ranking methods and accompanying descriptions. Later diagrams of standard features were published in several languages (Talen, 1963) to facilitate interpretation of results and aid comparisons. However it was not until quantitative techniques were devised, that accurate assessment of subtle yet invisible changes could be made. Zichermann & Thomas (1972) used the SEM to examine in detail macroscopic changes that occurred on the surface of coated loblolly pine (*Pinus taeda*) boards. Because after three thousand hours weathering, the TiO_2 tagged Wattyl Estapol coating did not display any visual changes such as chalking, cracking, checking, blistering, flaking, waterspotting and other features commonly associated with film aging, these phenomena will not be further elaborated.

Schneider & Côté (1967) speculated that if the film composition remained constant throughout the entire level of penetration in the wood, then its performance would be dependant on its formulation but if preferential migration of coating components occurred then the original function is limited. Ball (1980) postulated that the interactions of the components of a coating are often responsible for its breakdown. Present day research in the coatings industry is focused on the topic of photodegradation (Hedley, 1987). Ultraviolet stabilizers are added to clear coatings to protect

them against the effect of ultraviolet light. Williams (1983) stressed that the photochemical stability of the surface beneath a coating was critical for coating durability.

Because the novel coating system studied here had TiO_2 added to the formulation it was altered from a "clear finish" to an opaque coating thus any comparison made to coating behaviour is made with reference to pigmented systems rather than clear finishes.

Titanium dioxide constitutes a major part of pigmentation and its photoactivity contributes to the weathering performance of the finish. Moisture content is essential to the photocatalytic processes involving titanium dioxide, hydroxyl ions adsorbed on the pigment surface react with electrons released by ultraviolet radiation (Blakey, 1985). Accelerated weathering tests tend to reproduce only those wavelengths present in the sunlight that are crucial for deterioration of coatings (Birchenough, 1986).

Each pigment and the binding medium present in a coating has its own characteristic absorption spectra. Titanium dioxide in a coating acts as an internal filter (Neville, 1963). Depending on the coating system, film failure is either caused by chalking in which the binder is totally decomposed and the pigments and extenders are consequently lost, or by embrittlement caused by further polymerization of the binder and eventual cracking of the film. Hoffmann & Saracz (1969, 1970) assessed the weathering performance of selected paint films and concluded that the radiation band causing total decomposition depended on the pigment used. Both anatase and rutile titanium dioxide particles have different wavelengths. In general, the wavelengths that caused total decomposition lay between 300 and 400 nm. They found that under natural and accelerated weathering conditions, the rate of chalking of mixtures of anatase with rutile titanium dioxide decreased exponentially as the proportion of rutile titanium dioxide increased.

There are two main ultraviolet radiation induced mechanisms which contribute to coating breakdown : (i) photochemical degradation and (ii) photocatalytic degradation. In photochemical degradation, ultraviolet radiation acts directly on the binder without influence from the pigment. For example, in oil modified alkyds, the aromatic part of the alkyd is rapidly degraded by radiation below 250 nm but if radiation is above 295 nm then the aliphatic components are more susceptible to degradation (Blakey, 1985). Thus in natural sunlight, which contains only a small portion of ultraviolet below 300 nm, degradation is most likely to be initiated in the aliphatic component. The ultraviolet stabilizer incorporated into the TiO_2 tagged Wattyl Estapol coating is 2,2' dihydroxy-4-methoxy benzophenone. Whether photochemical or photocatalytic degradation activity predominates depends on the ratio of pigment photoactivity to ultraviolet absorption by the resin. Degradation by whatever mechanism will ultimately result in the loss of gloss as the pigment particles are exposed at the surface of the film.

CHAPTER 7

Conclusion

Schneider (1972) wrote that although there is clear evidence about the nature of wood/coating interactions "...much remains in the realm of speculation and untested theory..."

Gooch (1980) postulated that "...the successful coating of timber starts with the forester with his sylvicultural methods. It continues at the timber mill with the method of cutting the logs. The timber treater plays his part as does the designer of the timber profiles. The care of the timber then passes into the hands of the builder, the carpenter and finally the painter. All must play their parts conscientiously..."

Harris (1974) predicts that "...wood in one form or another will long continue to provide a substrate for surface coatings..."

and Talen (1963) stated that "...there is no single method for the prediction of paint performance..."

The complex interaction of coating systems and wood substrates is environmentally, physically, chemically and biologically controlled. The variables are numerous and some of the important factors determining the behaviour are : coating formulation, composition, pigmentation, pigment volume concentration, solvent choice, rheology, viscosity, thixotropy, contact angle, application treatment, wetting ability, penetration ability, substrate adhesion, number of coats, bonding of subsequent coats, curing method, drying time, timber species, wood density, wood grain, texture, growth ring boundary pattern, heartwood/sapwood, earlywood/latewood, age of wood, wood anatomy, wood ultrastructure, wood porosity, presence of knots, resin canals, extractives, machining quality, substrate orientation, rough sawn or dressed timber, flat sawn or quarter sawn, chemical stability of the wood, seasoning, wood moisture content, untreated or preservative treated, depth of penetration of coating, gross and/or intracellular penetration, migration of coating and/or wood components, extraction, aging phenomena, weathering phenomena, deterioration, degradation, effect of temperature, ultraviolet light, oxygen, moisture, diurnal and seasonal changes.

Some of the more salient features deduced from this investigation are summarized here.

The survey of the seven primer systems on *D. cupressinum, P. dacrydioides* and *P. radiata* weatherboards revealed no significant difference in penetration depth among taxa and that gross penetration of the coating was limited to three cells deep. Because of their larger dimensions, earlywood tracheid cell lumens are more easily filled than the smaller lumened latewood cells.

Mean contact angles ranged between 20-28 degrees and were statistically shown to be significantly different among the eight coating systems. Although Duncan's New Multiple Range Test was not sensitive enough to distinguish major differences at the P=0.05 level, it singled out Epiglass 1st coat wood primer, Epiglass G.P.182 oil based alkyd primer and Taubmans wood primer as of greater significance than the other five coating systems studied.

Coating viscosity and contact angle alone did not control depth of penetration. It is postulated that coating composition, pigment grade and particle size may limit depth of entry. Paint film structure and pigment dispersion in the final product depends on the intrinsic particle shape and the concentration of pigment particles in the medium. Pigment milling, whether dry grinding or wet grinding, may cause aggregation, agglomeration or air flocculation of particles. Although it is not yet possible to examine liquid paints directly with an electron microscope, to determine whether the clusters of pigments seen in a cured dry film were also present or whether they only develop during drying, other analytical methods have been adopted by the coating industry. For example, liquid nitrogen freezing techniques have demonstrated that although the state of dispersion and individual particle separation is incomplete in a dried film, the small clusters of pigment particles behave as separate entities of high stability. Certain pigments may be associated with high molecular polymer regions of the coating film.

The three water based primers and the four solvent based primers all exhibited similar behaviour on the wood substrates, by contrast, the TiO_2 tagged Wattyl Estapol showed good penetration potential. The percentage of rutile titanium dioxide was greater in the primers than in the Wattyl Estapol alkyd. Backscattered electron images showed that the texture of the cured primers was much coarser than that of the TiO_2 tagged Wattyl Estapol coating. Normally Wattyl Estapol is manufactured as a clear finish and thus contains all the attributes of a clear film forming coating but the addition of rutile titanium dioxide altered it into an opaque coating.

The quality of timber machining, substrate orientation (tangential and radial longitudinal faces), the slope of the tracheid files relative to the board surface, type of weatherboard mounting chosen (whether 'u'-type or 'n'-type profiles) were all considered as important features determining coating/substrate relationships. All the upper rows of coating filled cells in the vicinity of the coating/substrate interface would have either been opened by machining or emerged at some point on the board surface to produce tube-like structures possessing the ability to facilitate liquid conduction into the wood.

Interspecific variation in wood anatomy of the three taxa was not significant with reference to the observed film forming behaviour of the primer systems, however interspecific variation was influential in the penetration pattern exhibited by the TiO_2 tagged Wattyl Estapol coating.

Both *D. cupressinum* and *P. dacrydioides* have longer, narrower tracheid cells compared to *P. radiata* which has shorter, wider tracheids.

Mean gross penetration depth was statistically shown to be significantly different among taxa. Duncan's New Multiple Range Test indicated that with regard to cut, the mean depth of penetration in both 'u' and 'n'-type boards is not significantly different between *D. cupressinum* and *P. dacrydioides*. By contrast mean penetration depth for *P. radiata* 'n'-type boards is significantly different from the latter two taxa. The mean penetration depth of *P. radiata* 'u'-type boards is not significantly different from the two endemic taxa with the same profile cut but significantly different from *D. cupressinum* 'n'-type boards.

The maximum gross penetration depth recorded across the top surface for *D. cupressinum* 'u' and 'n'-type boards is nine cells; the maximum penetration depth for *P. dacrydioides* is six cells in 'u'-type boards and thirteen cells in 'n'-type boards. Penetration depth is shallower for *P. radiata* weatherboards, with the maximum depth being eight cells for 'u'-type boards and six cells for 'n'-type boards. Extreme maximum penetration occurred on the sides of the boards as seen in profile view. Individual measurements showed that maximum penetration depth varied between samples. Electron microscope evidence revealed that variation in gross penetration depth was related to growth ring pattern and symmetry with reference to 'pith' position along the board when viewed on the transverse face.

The mean angle made by the tracheid cell length and the substrate face (coating interface) was statistically shown to be significantly different among taxa. Duncan's New Multiple Range Test showed that with regard to cut, there was no significant difference among the means for *D. cupressinum* and *P. radiata* 'u'-type boards and *P. dacrydioides* 'n'-type boards but significant difference between *P. dacrydioides* 'u'-type boards. *D. cupressinum* and *P. radiata* 'n'-type boards are significantly different from the other taxa types. 'U'-type boards exhibit a greater mean tracheid cell inclination angle than 'n' -type boards.

The presence of axial parenchyma showed little effect on liquid conduction. Gross penetration along ray parenchyma cells was variable both among and within taxa. Deep penetration appeared to be associated with ray parenchyma cells widened and separated from adjacent cells during the process of machining, to yield fissures permitting coating entry. The presence of coating in tracheid lumens located a considerable distance below the coating interface were often associated with adjacent ray parenchyma cells whose cross-field pit apertures may have been opened as a consequence of mechanical stress. Of the three taxa, the wood of *P. radiata* is most easily distorted during machining and the rays of this taxon exhibited the longest penetration distance. If the angle of the ray cell is at right angles to the coating interface then bulk coating entry into the "tubes" is made more accessible than into "tubes" lying at oblique angles to the surface.

The chief function of a solvent in a pigment/film-former/solvent combination, is to adjust the viscosity of the suspension and evaporate at a later stage. Solvents not only thin the coating and help "wet" the wood surface, but contribute to lumen penetration phenomena.

Scanning electron and transmission electron microscope evidence of tracheid cell walls are in accordance with previous reports that wood preservatives are distributed within the cell wall and may line the cell lumens as well.

Energy dispersive X-ray analysis of the key elements present in the coatings confirmed microscopic observations that the smallest sized titanium dioxide and other pigment particles present in the coating, accumulate along any irregularities on the cell wall, such as warts and thickenings.

To establish the extent of intracellular wall penetration, migration, or localisation of coating components and whether the coating film composition is constant throughout the entire level, techniques such as X-ray microanalysis are required in addition to electron microscopy.

All the components of the coatings appear to enter the cell cavities but only the liquid portion of suitable molecular size are capable of passing through the intertracheid pits. There is still unresolve d debate on the porosity of the secondary wall. The S_3 cell wall layer is believed to be an area of low porosity due to the high lignin concentration present and thus thought to act as a barrier to diffusion.

The intertracheid bordered pits in all three taxa are predominantly distributed along the tracheid wall in uniseriate fashion. If the torus is still suspended in the normal median position then the coating particles of certain molecular size can pass between the radiating microfibrillar mesh of the margo. Pit aspiration inhibits penetration. It is theorized that the presence of deep penetration may be attributed to the number of ruptured pit membranes previously destroyed during board preparation thus enabling bulk movement. The observed presence of adjacent coated cells separated by walls containing pits with intact pit membranes is thought to be the result of separate flow routes. The coating path into the wood is not only controlled by the number of opened pits but the orientation and angle of the substrate, i.e., whether tangential, oblique or radial faces are presented to the coating.

Statistical analyses indicated that correlations between coating penetration depth and tracheid cell row growth direction; and between coating/substrate tracheid cell inclination angle and tracheid cell row growth direction were insignificant.

The size of cross-field pits varies along the tracheid length when viewed on the tracheid lumen face and this depends on the timber species and whether it is taxodioid, cupressoid or pinoid type. Both *D. cupressinum* and *P. dacrydioides* may possess large taxodioid cross-field pits between ray parenchyma and tracheid cells. It has been observed in *D. cupressinum* that narrow bordered cross-field pits with very wide apertures are located near the tips of tracheid files. Therefore it is postulated that if these pit membranes were broken during timber processing, then they represent accessible entrances.

Several schools of thought on intracellular coating penetration have been discussed.

Accelerated weathering tests were performed on the wood substrates.

Scanning electron microscopy revealed macro and micro structural changes in the wood and showed that *P. radiata* was most prone to aging phenomena. Visually observed changes in the wood of all three taxa were confirmed quantitatively by spectrocolorimetric techniques and the results are in agreement with that expected for early stages of weathering. It is notable that *P. radiata* wood retained the highest light reflectance value after three thousand hours artificial weathering. The durability of the TiO_2 tagged Wattyl Estapol coating was evaluated after three thousand hours. Its satisfactory performance is attributed to the incorporation of ultraviolet stabilizers into the coating formulation and the addition of rutile titanium dioxide. As expected, the number of coats applied to the substrate is affected by weathering. One coat applications showed the greatest changes with regard to reflectance, chromaticity and gloss retention, compared to two coat applications. The wood morphology and structure underneath the coating remained unaltered after three thousand hours weathering. Chromaticity studies indicated that two applications of coating on *P. radiata* wood retained higher light reflectance values than those of *D. cupressinum* and *P. dacrydioides* with two coats, that were weathered for three thousand hours. Scanning electron microscope examination of the surfaces of boards which received two applications of the TiO_2 tagged Wattyl Estapol coating revealed that after three thousand hours weathering, there was no significant difference between the three taxa; the coating was still intact and surface changes were absent.

FTIR and ATR spectroscopic techniques showed that the changes detected in the intensities of the major functional groups present in the coating were very minor.

To conclude, the TiO_2 tagged Wattyl Estapol alkyd exhibited good penetration ability and performed well in the standard weathering tests; but the high cost of producing this special coating for exterior use will restrict its commercial viability.

REFERENCES

AMERICAN SOCIETY FOR TESTING MATERIALS 1987 Annual Book of ASTM Standards:General Methods and Instrumentation *USA, ASTM.* **14.02:** 1343p

BALL, P. 1982 Accelerated weathering : A feasible proposition. *Australian Oil and Colour Chemists Association Proceedings and News* 10-18

BANOV, A. 1982 Paints and Coatings Handbook for Contractors, Architects, Builders and Engineers *2nd ed.* New York, McGraw- Hill 432p

BARNETT, J.R. 1977 Tracheid differentiation in Pinus radiata. *Wood Science and Technology* **II :** 83-92

BARNETT, J.R. & HARRIS, J.M. 1975 Early stages of bordered pit formation in radiata pine. *Wood Science and Technology* **9 :** 233-241

BAUCH, J. LIESE, W. & SCHULTZE, R. 1972 The morphological variability of the bordered pit membranes in Gymnosperms. *Wood Science & Technology* **6 :** 165-184

BIRCHENOUGH, D. 1986 Accelerated weathering tests. Why is it necessary to perform accelerated weathering. *European Coatings Journal* pp46-54

BLACKENEY, M.R. 1979 Timber and its relationship to the Paint Industry. *New Zealand Painter & Decorator* 14-24

BLAKEY, R.R. 1985 Evaluation of paint durability; natural and accelerated. *Progress in Organic Coatings* **13:** 279-296

BOOKER, R.E. 1989 Hypothesis to explain the characteristic appearance of aspirated pits. *Proceedings of the 2nd Pacific Regional Wood Anatomy Conference.* Forest Products Research and Development Institute. Los Banos.(College), Philippines. 17p.

BUILDING RESEARCH ASSOCIATION OF N.Z. 1978 Wood Primers. *Building Information Bulletin.* 208p

BUTTERFIELD, B.G. & MEYLAN, B.A. 1980 Three-dimensional structure of wood : an ultrastructural approach. London, Chapman and Hall Ltd. 103p.

CASSENS, D.L. & FEIST, W.C. 1980 Wood finishing-selection and application of exterior finishes for wood. *U.S.A. North Central Regional publication on Wood Finishing* **135 :** 1-8

CHANDLER, J.A. 1977 X-ray microanalysis in the electron microscope. *In* **Practical Methods in Electron Microscopy. A.Glauert (ed),** North Holland-Elsevier. 547p

CHANDLER, J.A. 1983 Principles of X-ray microanalysis in Biology. *In* **Basic Methods in Biological X-ray microanalysis. G.M.Roomans and J.D.Shelburne (eds)** *U.S.A. Scanning Electron Microscopy Inc.***pp** 1-12

CHOU, C.K., CHANDLER, J.A., & PRESTON, R.D. 1973 Microdistribution of metal elements in wood impregnated with a copper-chrome-arsenic preservative as determined by analytical electron microscopy. *Wood Science and Technology* **7 :** 151-160

CLAUSER, H.R.(ed) 1984 Encyclopedia/Handbook "Materials, Paints and Finishes" Pennsylvania, Technomic Publishing Co. Inc. 564p

COMMISSION INTERNATIONAL DE L'ECLAIRAGE (C.I.E.) 1970 International Lighting Vocabulary No.17 (E 1.1) *3rd ed.* Paris, Bureau Central de la CIE. 359p

CÔTÉ, W.A. 1965 Cellular ultrastructure of woody plants. *Proceedings Advanced Science Seminar. Pinebrook Conference Centre,New York.* Syracuse University Press. **603p**

CÔTÉ, W.A. 1981 Ultrastructure-critical domain for wood behaviour: Its origins, current concepts, future potential. *Wood Science and Technology* **15 :** 1-29

CÔTÉ, W.A. 1983 Wood as a substrate for coatings. *Journal of Coatings Technology* **55 (699) : 25-35**

CÔTÉ, W.A. & KRAHMER, R.L. 1962 The permeability of coniferous pits demonstrated by electron microscopy. *TAPPL*, **45 :** 119-122

CÔTÉ, W.A. & ROBISON, R.G. 1968 A comparative study of wood; wood coating interaction using incident fluorescence and transmitted microscopy. *Journal of Paint Technology* **40 (525):** 427-432

CÔTÉ, W.A. & VASISHTH, R.C. 1970 Light and electron microscopic studies of wood/wood coating systems. *Proceedings Xth Fatipec Congress,Montreux, Switzerland.* pp57-65

DAVIES, G.W. 1968 Electron microscopy and cell wall porosity. *Appita* **21** (4) : 117-130

de GROOT, R. & KUSTER, T.A. 1986 S.E.M. X-ray microanalysis of tracheid cell walls in Southern Pine sapwood treated with water dispersible pentachloro phenol. *Wood and Fiber Science* **18 (1) :** 58-67

DESAI, R.L. & COTE, W.A. 1976 Use of SEM/EDXA in characterizing water-based surface treatments for wood. *Journal of Coatings Technology* **48 (614) :** 33-37

DONALDSON, L.A. 1983 Anatomy of root wood in Araucariaceae and some Podocarpaceae indigenous to New Zealand. *New Zealand Journal of Botany* **21 :** 221-227

DONALDSON, L.A. 1987 S_3 lignin concentration in radiata pine tracheids. *Wood Science and Technology* **21 :** 227-234

DONALDSON, L.A. 1988 Ultrastructure of wood cellulose substrates during enzymatic hydrolysis. *Wood Science and Technology* **22 :** 33-41

DREWE, R.1986 Australian timbers and their inherent coating problems. *Surface Coatings Australia 27th Convention N.S.W.* 26-27

EXLEY, R.R., BUTTERFIELD, B.G., & MEYLAN, B.A. 1973 The preparation of wood specimens for the scanning electron microscope. *Journal of Microscopy* **101 :** 21-30

EXLEY, R.R., MEYLAN, B.A., & BUTTERFIELD, B.G. 1977 A technique for obtaining clean cut surfaces on wood samples prepared for the scanning electron microscope. *Journal of Microscopy* **110 :** 75-78

FEIST, W.C. & HON, D.N.S. 1984 Chemistry of weathering and protection. *In* **The Chemistry of Solid Wood Advances in Chemistry series 207 E.Rowell (ed)** Washington D.C. *American Chemical Society* pp401-451

FREY-WYSSLING, A. 1937 *Protoplasma* **27 :** 372

FREY-WYSSLING, A., BOSSHARD, H.H & MUHLETHALER, K 1956 Die submikroskopische Entwicklung der Hoftupfel. *Planta* **47 :** 115-126

FULLARD, J.E. 1969 Exterior durability of coatings. *Journal of the Oil and Colour Chemists Association.* **52 :** 334-346

GATSLICK, H.B. 1963 Physical and chemical characteristics of wood. *Official Digest.* **35 :** 781-792

GOOCH, C. 1980 Applied finishes for timber in exterior situations in New Zealand. *Journal of the Oil and Colour Chemists Association.* **63 (12) :** 492-495

GRAY, V.R. 1961 The wetting, adhesion and penetration of surface coatings on wood. *Journal of the Oil and Colour Chemists Association* **44 :** 756-783

HAAGDEN, H. 1977 Wood protection by coatings. *Forschungsinstitut fur Pigmente und Lacke.* **Lecture Transcript.**

HALL, J.L. (ed) 1978 Electron Microscopy and Cyto Chemistry of Plant Cells. Netherlands, Elsevier. 444p

HARADA, H. & CÔTÉ, W.A. 1967 Cell wall organization in the pit border region of softwood tracheids *Holzforschung* **21 :** 81-85

HARADA, H. & WARDROP, A.B. 1960 Cell wall structure of ray parenchyma cells of a softwood Cryptomeria japonica. *Mokuzai Gakkai Shi* **6 (1) :** 34-41

HARRIS, J.M 1974 The future for Wood : a look towards 2000. *Journal of the Oil and Colour Chemists Association* **57 :** 339-341

HARRIS, J.M. 1979 Wood as a substrate for surface coatings. *Chemistry and Industry in New Zealand. December 1979.* New Zealand Forest Service Reprint **No 1283.** ODC 829.1.

HARRIS, J.M. 1981 Wood quality of radiata pine. *Appita* **35 (3) :** 211-215

HASLAM, J.H. & WERTHAN, S. 1931 Studies in the painting of wood : influence of wood structure on paint behaviour. *Industrial and Engineering Chemistry 23 (2) :* 226-233

HAYAT, M.A. 1975 Positive Staining for Electron Microscopy. New York, van Nostrand Reinhold Company. 361p

HEDLEY, M.E. 1987 Surface Coatings for Timber. *New Zealand Engineering* **42 (7) :** 65-66

HOFFMANN, E. & SARACZ, A. 1969 Weathering of Paint Films:II Chalking caused by anatase titanium dioxide in latex paints *Journal of the Oil and Colour Chemists Association* **52 :** 1130-1144

HOFFMANN, E. & SARACZ, A. 1972 Weathering of Paint Films: IV Influence of the radiation intensity on chalking of latex paints. *Journal of the Oil and Colour Chemists Association* 55 : 101-113

I.A.W.A. 1964 Multilingual Glossary of Terms used in Wood Anatomy. *International Association of Wood Anatomists* Switzerland, Konkordia Winterthur 186p

IMAMURA, Y., HARADA, H. & SAIKI, H. 1974 Further study on the development of the bordered pit in Coniferous tracheids. *Journal Japan Wood Research Society* 20 (4): 157-165

JANSEN, M.L. & WHITNEY, R.S. 1986 Performance testing of wood primers.*Journal of the Oil and Colour Chemists Association* 69 (5): 117-128

JESSOP, A.S. 1965 Prospects in terms of service life for (a) Pigmented coatings, (b) Colour coatings.*New Zealand Timber Development Association - Paint and Protection Coatings for Wood Symposium. November 1965* Auckland. 1-10

KAEISER, M. 1954 Microstructure of Wood *Podocarpus. Phytomorphology* 4 : 39-47

KERR, C.J. 1965 The Paint Timber System with Special Reference to Weatherboards. *Proceedings New Zealand Timber Development Association - Paint and Protective Coatings for Wood Symposium November 1965* Auckland

KERR, A.J. & GORING, D.A.I. 1975 The ultrastructural arrangement of the wood cell wall. *Cellulose Chem.Technology.* 9 : 563-573

KININMONTH, J.A. & WILLIAMS, D.H. 1972 Measuring the moisture content of wood. *New Zealand Journal of Forestry Science* No.60, ODC 812.211 12p

KRISHNAN, K 1984 Different Accessories - Main Applications and Handling Techniques. In *Fourier Transform Spectrosopy.* T.Theophanides, ed. D.Reidel Pub.Co 139-158

LAMBOURNE, R.(ed) 1987 Paint and Surface Coatings; Theory and Practice.(Ellis Horwood Series) In *Applied Science and Industrial Technology* Chichester, Ellis Horwood Ltd Pub. 696p

LARKIN, P.A. 1979 Handbook of elementary statistical tests. University of British Colombia. 161p

LEWIS, P.R. & KNIGHT, T.D.P 1977 Staining methods for sectioned material. In *Practical Methods in Electron Microscopy.* A.M.Glauers, ed **North Holland** 311p

LIESE, W. 1965 The fine structure of bordered pits in softwoods. In *Cellular ultrastructure of Woody Plants.* W.A.Cote ed, Syracuse University Press 603p

LUCAS, P. & SMITH, L. 1985 Effect of solvent choice on water-based coating/wood interactions. *Journal of Coatings Technology* 57 (726) : 65-70

McQUIRE, A.J. 1975 Effect of wood density on preservative retention in fence posts. *New Zealand Journal of Forestry Science* 5 (1) : 105-109

McQUIRE, A.J., BUTCHER, J.A., HEDLEY, M.E., CROSS, D.J., PRESTON, A.F & CUMMINS, N.H.O. 1975 Current wood preservation research at F.R.I. *New Zealand Wood Preservers Association Inc.Conference, Rotorua. 2nd October 1975* 11p

McQUIRE, A.J., BUTCHER, J.A., HEDLEY, M.E. & VINDEN, P. 1979 Wood preservation for the farmer. Part 4 Preparation, treatability and durability. *New Zealand Farmer* 100 (21) : 25-31

MEYLAN, B.A. & BUTTERFIELD, B.G. 1978 The Structure of New Zealand Woods. *New Zealand Department of Scientific & Industrial Research Bulletin*. 222 : 250p

MIDDLETON, T.M. 1985 Vessels of stem wood in New Zealand (Nothofagus). M.Sc (First Class Honours) Thesis. University of Canterbury, Christchurch. 203p

MILLER, E.R. 1983 Prediction of performance of exterior wood coatings. *Journal of the Oil and Colour Chemists Association* 66 (10) : 308-315

MILLER, R.G. & STAGE, B.C. 1972 Laboratory Methods in Infrared Spectroscopy. 2nd ed. New York, Heyden & Son Ltd. 375p

MILLS, P.E. & McQUIRE, A.J. 1976 Performance of radiata pine sash units over eight years exposure. *Wood Working Industry* 1 (3) : 30-31

MINIUTTI, V.P. 1963 Properties of softwoods that affect the performance of exterior paints. *Official Digest* 35 : 451-471

MINIUTTI, V.P. 1965 Microscale changes in cell structure of softwood surfaces. *Official Digest* 37 : 692-697

MIRAMS, R.V. 1965 The painting of radiata pine. *Proceedings New Zealand Timber Development Association - Paint and Protective Coatings for Wood Symposium, November 1965*, Auckland.

MORGANS, W.M. 1984 Outlines of Paint Technology : vol 1.Materials; vol 2.Finished Products. High Wycombe, Griffin & Co. Ltd. 236p

MURMANIS, L. & RIVERS, B.H. 1986 Surface and substrate characteristics related to abrasive planing conditions. *Wood and Fiber Science* 18 (1) : 107-117

MURMANIS, L. & SACHS, I. 1969 Seasonal development of secondary xylem in Pinus strobus L. *Wood Science and Technology* 3 : 177-193

NAKANISHI,K. 1962 Infrared Absorption Spectroscopy - Practical. San Francisco, Holden-Day Inc. 233p

NASIR, M.J. 1976 X-ray analysis without the need for standards. *Journal of Microscopy* 108 : 79-87

NEARN, W.T. 1965 Wood-Adhesive Interface Relations. *Official Digest* 37 : 720-733

NEVILLE, G.H.J. 1963 Some observations on the weathering of titanium dioxide pigment paint films. *Journal of the Oil and Colour Chemists Association* 46 (9) : 753-778

N.Z.P.M.A. 1978 How to prepare timber weatherboards for painting. *New Zealand Painter and Decorator* pp27-29

NUNN, R.E. 1970 Electron Microscopy : microtomy, staining and specialized techniques. London, Butterworths. 58p

OIL AND COLOUR CHEMISTS ASSOCIATION (G.B.) Paint Technology Manuals. Part 2 Solvents, Oils, Resins and Driers. (1969) 2nd ed 268p **& Part 3 Convertible Coatings (1966) 2nd ed** 318p. London, Chapman & Hall.

OIL AND COLOUR CHEMISTS ASSOCIATION 1974 Surface Coatings : a complete handbook of paint technology. *N.S.W.University Press.* 486p

OIL AND COLOUR CHEMISTS ASSOCIATION of AUSTRALIA 1984 Surface Coatings : vol 1. Raw Materials and their Usage; vol 2. Paints and their Application. Australia, Randwick.

ORMAN, H.R. & REID, J.S. 1946 Wood anatomy of New Zealand Dacrydium species. *New Zealand Journal of Forestry* **5 (3) :2-7**

PAGE, D.H. 1976 A note on the Cell Wall Structure of Softwood Tracheids. *Wood and Fiber* **7 : 246-248**

PATEL, R.N. 1967 Wood anatomy of Podocarpaceae indigenous to New Zealand. 1. Dacrydium. *New Zealand Journal of Botany* **5** 171-184

PATEL, R.N. 1967 Wood anatomy of Podocarpaceae indigenous to New Zealand. 2. Podocarpus. *New Zealand Journal of Botany* **5(3)** : 307-321

PATEL, R.N. 1970 Anatomy of stem and root wood of Pinus radiata.D.Don. *New Zealand Journal of Forestry Science* **1 (1)** : 37-49

PIERCE, P.E. & SCHOFF, C.K. 1988 Coating film defects. Federation series on coatings technology. Philadelphia. *Federation of Societies for Coating Technology.* 25p

PLACKETT, D.V. & BLACKENEY, M. 1987 Exterior surface finishes for timber. *New Zealand Ministry of Forestry* Trees and Timber, Wood Properties and Uses 7 : 1-8

PLACKETT, D.V., CHITTENDEN, C.M. & PRESTON,A.F. 1984 Exterior weathering trials on Pinus radiata roofing shingles. *New Zealand Journal of Forestry Science* **14 (3)** : 368-381

PLINY (GAIUS PLINIUS SECUNDUS)-PLINY THE ELDER. Natural History. vols IV & IX; Books 16 & 35 (trans. H.Rackham),*Massachusetts, Harvard University Press.*556p & 421p

PRESTON, A.F. & CHITTENDEN, C.M. 1978 Accelerated tests of weather resistant natural finishes for Pinus radiata. *Journal of Coating Technology* **50 (637)** : 59-61

REID, J.S. 1961 New Zealand Building Timbers, How, Where and When to use them 3rd ed Wellington, Owen Govt. Printer. 74p

REID, N. 1975 Ultramicrotomy: Practical Methods in Electron Microscopy. North Holland, American Elsevier. 353p

PARHAM, R.A & BAIRD, W.M. 1973 The bordered pit membrane in differentiating Balsam fir. *Wood and Fiber* **5 :** 80-86

ROBARDS, A.W. 1978 Scanning Electron Microscopy. In *Electron Microscopy and Cytochemistry of Plant Cells.* J.L. Hall ed North Holland, Elsevier-Biomedical Press. 444p

ROLAND, J.C. 1978 General Preparation and Staining of Thin Sections. p.1-62 **In** *Electron Microscopy and Cytochemistry of Plant Cells* **J.L.Hall ed** North Holland - Biomedical Press. 444p

ROOMANS, G.M. & SHELBURNE, J.D. eds 1983 Basic Methods in Biological X-ray microanalysis. U.S.A., Scanning Electron Microscopy Inc. 283p

RUEL, K., BARNARD, F. & GORING, D.A.I. 1978 Lamellation in the S_2 layer of softwood tracheids as demonstrated by scanning transmission electron Microscopy. *Wood Science and Technology*. **12** : 287-291

RUSS, J.C. 1983 Analysis of Elemental Ratios in "Thin" Samples. In *Basic Methods in Biological X-ray Microanalysis*. **G.M.Roomans & J.D.Shelburne eds.** Scanning Electron Microscopy Inc U.S.A. pp261-270

RYAN, K.G. 1986 Preparation techniques for X-ray Analysis in the transmission electron microscope of wood treated with copper-chrome-arsenate. *Material und Organismen* **21** : 223-234

RYAN, K.G. & FLOWER, N.E. & PRESLAND, M.R. 1984 Specimen holder design for X-ray microanalysis of thin films in the T.E.M. reduction of spurious X-rays. *Journal of Microscopy* **134** : 281-289

SCHNEIDER, M.H. 1970 Coating penetration into wood substance studied with electron microscopy using Replica Techniques. *Journal Paint Technology* **42 (547):** 457-460

SCHNEIDER, M.H. 1972 Wood Coating Interactions - A Review. *Journal of Paint Technology* **44 (564)** : 108-110

SCHNEIDER, M.H. 1979 Scanning electron microscope study of a coating component deposited from solution into wood. *Journal of Oil and Colour Chemists Association* **62** : 441-444

SCHNEIDER, M.H. 1980 Microscopic distribution of linseed oil after application to wood surface. *Journal of Coatings Technology* **52 (665)** : 64-67

SCHNEIDER, M.H. & CÔTÉ, W.A. 1967 Studies of wood and coating interactions using fluorescence microscopy and pyrolysis gas-liquid chromotography. *Journal of Paint Technology* **39 (511)** : 465-471

SILVERSTEIN, R.M., CLAYTON-BASSLER, G., MORRILL, T.C. 1981 Spectrometric identification of Organic Compounds 4th ed New York, John Wiley & Sons 442p

SINCLAIR, R.M. 1962 Painting of treated timber. *Proceedings New Zealand Wood Preservers Association* 21-37

SINCLAIR, R.M. 1965 Research into the performance of paints on timber in New Zealand. *Proceedings Paint and Protective Coatings for Wood Symposium November.1965 Auckland.* New Zealand Development Association

SINCLAIR, R.M.& CHAMBERLAIN, G. 1959 Paint durability on radiata pine. *New Zealand Department of Scientific and Industrial Research Publication* **1-4**

SMITH, L.A. & CÔTÉ, W.A. 1972 Resin penetration into wood cell walls. *Journal of Paint Technology* **44 (564) :** 71

SMITH, W.B., CÔTÉ, W.A., SIAU, J.F. & VASISHTH, R.C. 1985 Study of interactions between wood and water-soluable organic solvents . *Journal of Coatings Technology* **57 (727) :** 83-90

SMITH, W.B., CÔTÉ, W.A., SIAU, J.F. & VASISHTH, R.C. 1985 Interactions between water-borne polymer systems and the wood cell wall. *Journal of Coatings Technology* **57 (729):** 27-35

SMULSKI, S. & CÔTÉ, W.A. 1984 Penetration of wood by a water-borne alkyd resin. *Wood Science and Technology* **18 :** 59-75

SOKAL, R.R. & ROHLF, F.J. 1981 Biometry : the Principles and Practice of Statistics in Biological Research. San Francisco, W.H.Freeman. 859p

STAMM, A.J. 1965 Wood and cellulose-water relationships and their effect upon finishes. *Official Digest* **37 :** 654-669

STAMM, A.J. 1965 Modification of wood for improved finishing. *Official Digest.* **37 :** 707-719

STANDARDS ASSOCIATION OF AUSTRALIA 1975 Method 214.1 Consistency of Paints measured by the Krebs-Stormer Viscometer. AS 1580 : 1-4

STANDARDS ASSOCIATION OF AUSTRALIA 1983 Guide to the Specification of Colours. AS 2633 : 1-19

STANDARDS ASSOCIATION OF AUSTRALIA 1985 Colour Standards for General Purposes. AS 2700 : 8-11

TALEN, H.W. 1963 The Requirements for the prediction of paint performance. *Journal of the Oil and Colour Chemists Association* **46 (11) :** 940-972

THOMAS, R.J. 1968 The development and ultrastructure of the bordered pit membrane in the Southern Yellow Pines. *Holzforschung* **22 :** 38-44

THOMAS, R.J. 1970 Origin of bordered pit margo microfibrils. *Wood and Fiber* **2 :** 285-287

THORPE, T., COLLINS, M., PLACKETT, D., HEDLEY, M., & TURNER, J. 1987 Weatherboards. *Ministry of Forestry Trees and Timber, Wood Properties and Uses* **5 :** 11p

TIMBER DEVELOPMENT ASSOCIATION OF AUSTRALIA 1968 Painting of Timber; Opaque Pigmented Finishes. *Technical Timber Guide Timber Development of Australia* **7 :** 1-8

UNDERHAUG, A., LUND, T.J. & KLEIVE, K. 1983 Wood protection - the interaction between substrate and product and the influence on durability. *Journal of Oil and Colour Chemists Association,* **16 (1) :** 345-350

VASISHTH, R.C. 1983 Importance of depositing polymers in wood-cell walls for wood treatment. *Proceedings American Wood Preservers Association 79th Annual Meeting* **79 :** 129-136

Van STEVENINCK, R.F.M. & Van STEVENINCK, M.E. 1978 Ion Localization. In *Electron Microscopy and Cytochemistry of Plant Cells* .187-234 J.L.Hall, ed. North Holland, Elsevier. 444p

VINDEN, P. 1984 The effect of raw material variables on preservative treatment of wood by diffusion processes. *Journal of the Institute of Wood Science* **10** : 31-41

WARDROP, A.B. 1954 The Fine Structure of the conifer tracheid. *Holzforschung* **8** : 12-29

WARDROP, A.B. & DADSWELL, H.E. 1957 Variations in the cell wall organization of tracheids and fibres. *Holzforschung* **11 (2)** : 33-41

WARDROP, A.B. & DAVIES, G.W. 1961 Morphological factors relating to the penetration of liquids into wood. *Holzforschung* **15** : 129-144

WARDROP, A.B., LIESE, W. & DAVIES, G.W. 1959 The nature of the wart structure in conifer tracheids. *Holzforschung* **13** : 115-120

WILKINSON, M. 1987 Surface coatings and wood substrates. *Proceedings Institute Wood Science Conference March 1987 High Wycombe* pp1-6

WILLIAMS, R.S. 1983 Effect of grafted U.V. stabilizers on wood surface erosion and clear coating performance. *Journal Applied Polymer Science* **28** : 2093-2103

YATA, S., MUKUDAI, J. & KAJITA, H. 1978 Morphological Studies on the Movement of Substances into the Cell Wall of Wood. I : Methods for microscopical detection of diffusing substances in the cell wall. *Mokuzai Gakkaishi* **24** : 591-597

YATA, S., MUKUDAI, J. & KAJITA, H. 1979 Morphological Studies on the Movement of Substances into the Cell Wall of Wood. II : Diffusion of copper compounds into the cell wall. *Mokuzai Gakkaishi* **25 (3)** : 171-176

YATA, S., MUKUDAI, J. & KAJITA, H. 1981 Morphological Studies on the Movement of Substances into the Cell Wall of Wood. III : Diffusion of zinc compounds into the cell wall. *Mokuzai Gakkaishi* **27 (12)** : 821-827

YATA, S., MUKUDAI, J. & KAJITA, H. 1981 Morphological Studies on the Movement of Substances into the Cell Wall of Wood. IV.: Diffusion of hexavalent chromium into the cell wall. *Mokuzai Gakkaishi* **27 (12)** : 821-827

YATA, S., MUKUDAI, J., & KAJITA, H. 1982 Morphological Studies on the Movement of Substances into the Cell Wall of Wood. V Distribution of chromium in the Cell Wall. *Mokuzai Gakkaishi* **28 (1)** : 10-16

YATA, S. & NISHIMOTO, K. 1983 Application of SEM-EDXA technique to the study of metal distribution in preservative treated wood. *Wood Research* **69** : 71-79

YATA, S. & NISHIMOTO, K. 1983 Distribution of metal elements in wood impregnated with aqueous solutions of metal salts as determined by SEM-EDXA. *Wood Research* **69** : 80-88

YOUNG, G. 1988 Machining properties : How does radiata pine shape up? *What's New in Forest Research. New Zealand Ministry of Forestry - Forest Research Institute* **163** : 1-4

YOUNG, O.A. & SERVICE, M.J. 1971 Slow viscous flow and the organization of the cell wall in conifer tracheids. *Wood Science and Technology* **5 : 1-5**

ZICHERMAN, J.B. & THOMAS, R.J. 1972 Scanning electron microscopy of weathered coatings on wood. *Journal of Paint Technology* **44 : 88-94**

APPENDIX 1.1

DULUX PRIMERCRYL 100 % ACRYLIC.

(**A**) *ELEMENTS PRESENT IN THE COATING.(CAMBRIDGE SEM/EDXA)*

* ABBREVIATIONS *
(CPS - counts per second; P/B - Peak to Background)
(ZAF - Atomic number,Absorption & Fluoresence corrections)

Energy range 0 - 20 keV.

ELEMENTS	INTENSITY (CPS)	BACKGROUND (CPS)	P/B RATIO
P K	12.248	194.173	0.063
S K	4.866	42.271	0.115
Ca K	198.262	153.922	1.288
Ti K	599.551	84.194	7.121
Zn K	52.069	229.393	0.227

ELEMENTS	ATOMIC % RELATIVE CONC.
P K	0.032
S K	0.011
Ca K	0.315
Ti K	0.842
Zn K	0.079

ZAF CORRECTION ELEMENTS	K	Z	A	F
P K	0.017	1.040	0.217	1.022
S K	0.006	1.070	0.264	1.034
Ca K	0.212	1.065	0.701	1.131
Ti K	0.678	0.979	0.574	1.005
Zn K	0.086	0.968	0.682	1.000

ELEMENTS	ATOMIC % ELEMENTS
P K	7.905
S K	2.224
Ca K	21.134
Ti K	61.995
Zn K	6.743

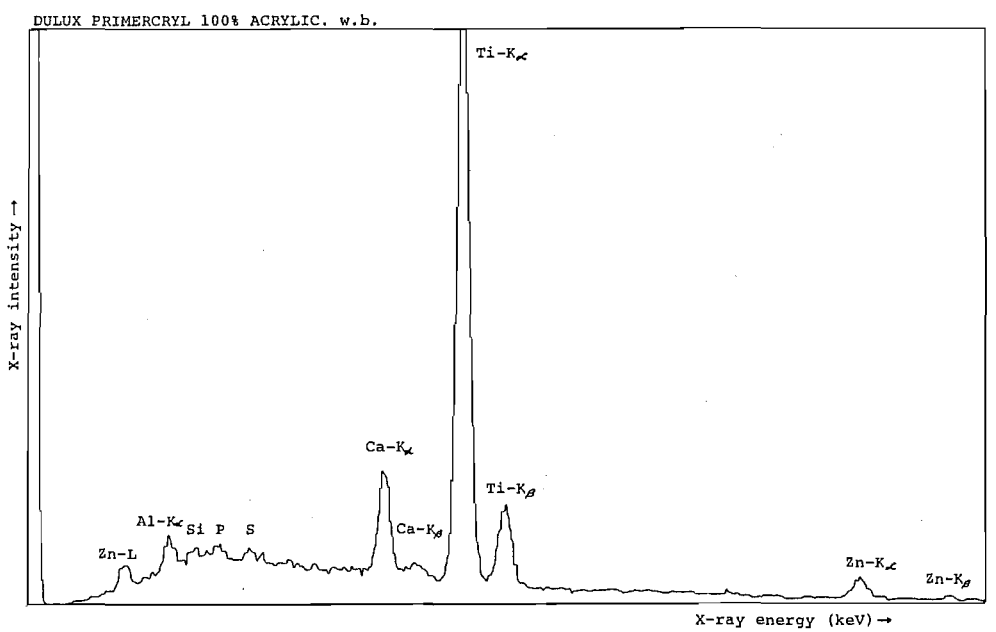

(**B**) *EDXA SPECTRUM OF ELEMENTS IN THE COATING.*
(JEOL JSM - 35 SEM / LINK 290 EDXA).

APPENDIX 1.2

EPIGLASS WATER BASED WOOD PRIMER.

(**A**) *ELEMENTS PRESENT IN THE COATING.(CAMBRIDGE SEM/EDXA)*

Energy range 0 - 20 keV.

ELEMENTS	INTENSITY (CPS)	BACKGROUND (CPS)	P/B RATIO
Al K	43.020	47.456	0.907
Si K	57.785	25.607	2.257
S K	59.755	61.063	0.979
K K	23.869	108.817	0.219
Ti K	758.575	107.311	7.069

ELEMENTS	ATOMIC % RELATIVE CONC.
Al K	0.037
Si K	0.036
S K	0.026
K K	0.008
Ti K	0.202

ZAF CORRECTION ELEMENTS	K	Z	A	F	ELEMENTS	ATOMIC % ELEMENTS
Al K	0.078	1.015	0.200	1.016	Al K	22.303
Si K	0.078	1.048	0.158	1.012	Si K	25.227
S K	0.066	1.045	0.202	1.017	S K	15.859
K K	0.023	1.014	0.373	1.062	K K	2.687
Ti K	0.755	0.956	0.638	1.000	Ti K	33.925

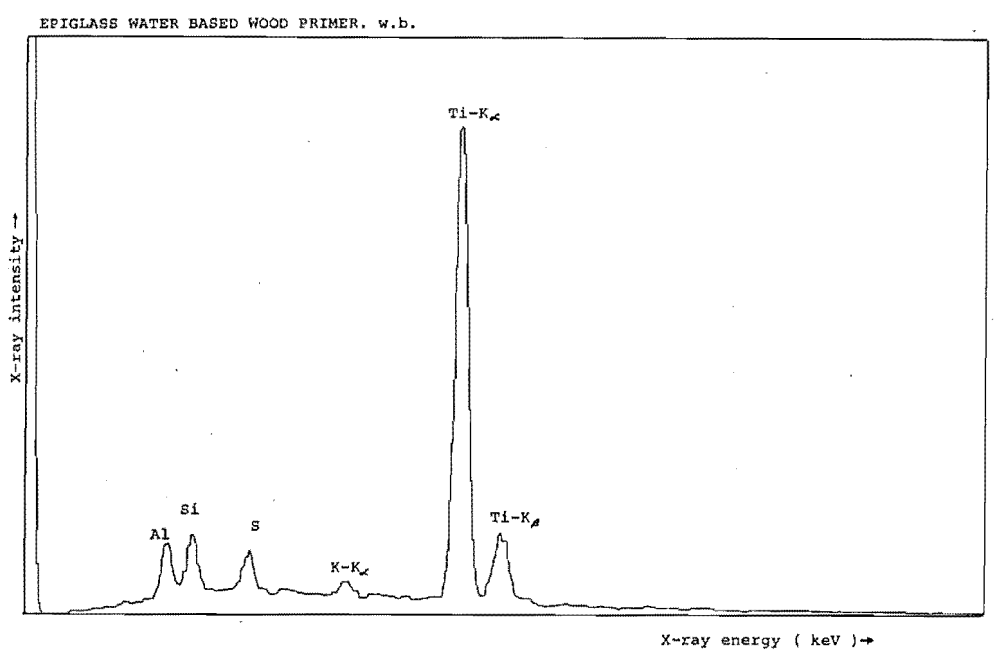

(**B**) *EDXA SPECTRUM OF ELEMENTS IN THE COATING.*
(JEOL JSM - 35 SEM / LINK 290 EDXA).

APPENDIX 1.3

TAUBMANS PREMIUM FAST COAT WOOD PRIMER.

(**A**) *ELEMENTS PRESENT IN THE COATING.(CAMBRIDGE SEM/EDXA)*

Energy range 0 - 20 keV.

ELEMENTS	INTENSITY (CPS)	BACKGROUND (CPS)	P/B RATIO
Al K	6.931	49.778	0.139
Si K	2.288	22.965	0.100
P K	4.858	23.778	0.204
Ca K	98.710	111.328	0.887
Ti K	565.479	63.408	8.918
Zn K	31.057	202.808	0.153

ELEMENTS	ATOMIC % RELATIVE CONC.
Al K	0.037
Si K	0.008
P K	0.015
Ca K	0.222
Ti K	1.080
Zn K	0.064

ZAF CORRECTION ELEMENTS	K	Z	A	F
Al K	0.015	1.040	0.094	1.008
Si K	0.004	1.073	0.113	1.012
P K	0.007	1.040	0.172	1.019
Ca K	0.134	1.065	0.685	1.149
Ti K	0.778	0.979	0.659	1.004
Zn K	0.062	0.967	0.697	1.000

ELEMENTS	ATOMIC % ELEMENTS
Al K	17.041
Si K	3.171
P K	3.961
Ca K	12.399
Ti K	59.015
Zn K	4.413

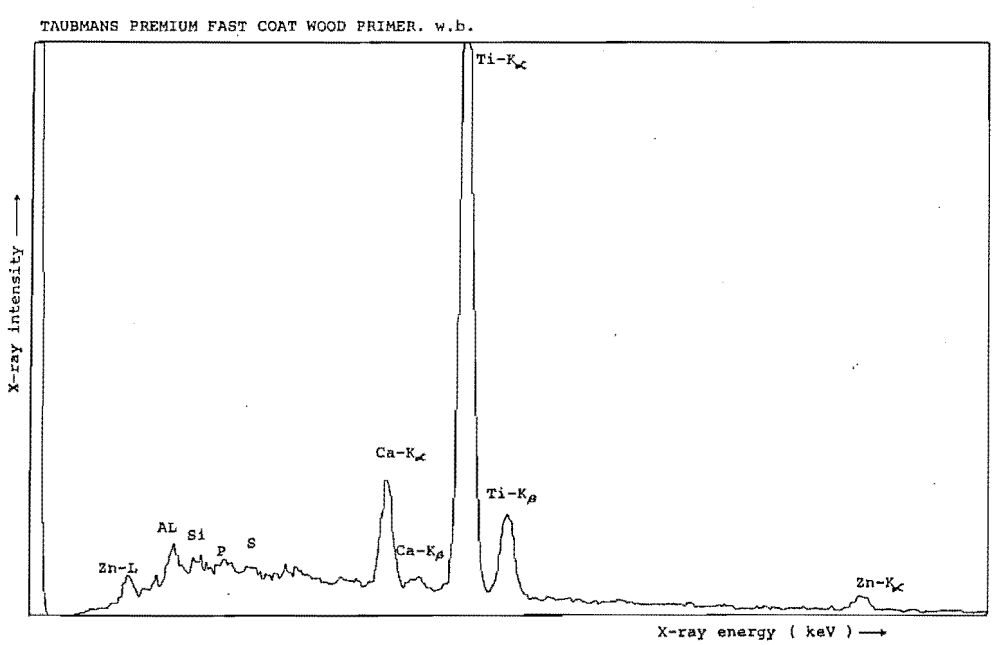

(**B**) *EDXA SPECTRUM OF ELEMENTS IN THE COATING.*
(JEOL JSM - 35 SEM / LINK 290 EDXA).

APPENDIX 1.4

DULUX WUNDERPRIME.

(**A**) *ELEMENTS PRESENT IN THE COATING.(CAMBRIDGE SEM/EDXA)*

Energy range 0 - 20 keV.

ELEMENTS	INTENSITY (CPS)	BACKGROUND (CPS)	P/B RATIO
Mg K	4.455	33.107	0.135
Al K	114.707	28.619	4.008
Si K	157.933	33.123	4.768
P K	7.917	36.568	0.216
S K	56.625	42.199	1.342
Ca K	9.026	168.516	0.054
Ti K	548.094	79.115	6.928

ELEMENTS	ATOMIC % RELATIVE CONC.
Mg K	0.041
Al K	0.612
Si K	0.603
P K	0.025
S K	0.155
Ca K	0.017
Ti K	0.905

ZAF CORRECTION ELEMENTS	K	Z	A	F
Mg K	0.012	1.029	0.178	1.019
Al K	0.196	1.002	0.261	1.018
Si K	0.201	1.034	0.153	1.009
P K	0.009	1.003	0.101	1.013
S K	0.059	1.031	0.147	1.009
Ca K	0.008	1.027	0.412	1.054
Ti K	0.515	0.944	0.601	1.000

ELEMENTS		ATOMIC % ELEMENTS
Mg	K	3.454
Al	K	26.444
Si	K	32.834
P	K	3.682
S	K	13.465
Ca	K	0.606
Ti	K	19.515

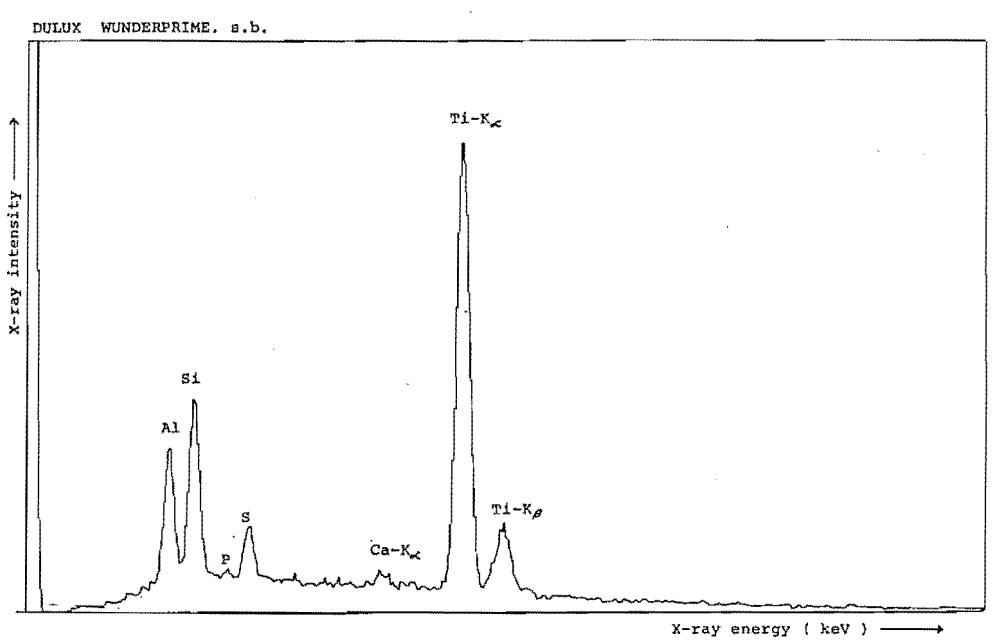

(**B**) *EDXA SPECTRUM OF ELEMENTS IN THE COATING.*
(JEOL JSM - 35 SEM / LINK 290 EDXA).

APPENDIX 1.5

EPIGLASS 1ST COAT WOOD PRIMER.

(**A**) *ELEMENTS PRESENT IN THE COATING.(CAMBRIDGE SEM/EDXA)*

Energy range 0 - 20 keV.

ELEMENTS	INTENSITY (CPS)	BACKGROUND (CPS)	P/B RATIO
Al K	19.365	41.251	0.469
Si K	95.152	24.074	3.952
P K	5.090	27.257	0.187
S K	19.133	32.115	0.596
Ca K	78.323	140.647	0.557
Ti K	665.497	76.997	8.643

Elements	Atomic % concentration.
Al K	0.037
Si K	0.131
P K	0.006
S K	0.019
Ca K	0.052
Ti K	0.394

ZAF CORRECTION ELEMENTS	K	Z	A	F
Al K	0.038	1.014	0.187	1.019
Si K	0.139	1.046	0.197	1.010
P K	0.007	1.014	0.121	1.015
S K	0.023	1.043	0.175	1.018
Ca K	0.080	1.039	0.511	1.090
Ti K	0.714	0.955	0.604	1.000

ELEMENTS	ATOMIC % ELEMENTS
Al K	13.126
Si K	34.923
P K	3.297
S K	7.170
Ca K	6.528
Ti K	34.056

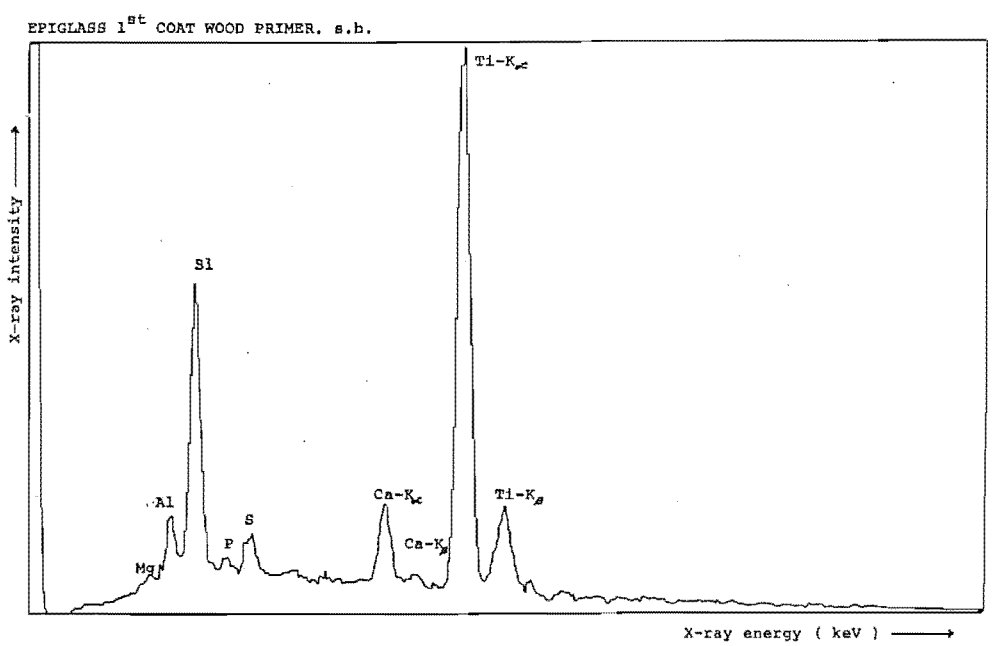

(**B**) *EDXA SPECTRUM OF ELEMENTS IN THE COATING. (JEOL JSM - 35 SEM / LINK 290 EDXA).*

APPENDIX 1.6

EPIGLASS G.P.182 OIL BASED ALKYD PRIMER.

(**A**) *ELEMENTS PRESENT IN THE COATING.(CAMBRIDGE SEM/EDXA)*

Energy range 0 - 20 keV.

ELEMENTS	INTENSITY (CPS)	BACKGROUND (CPS)	P/B RATIO
Al K	33.534	65.384	0.513
Si K	126.623	39.709	3.189
Ca K	57.409	274.496	0.209
Ti K	664.966	85.313	7.794
Fe K	10.039	198.562	0.051

ELEMENTS	ATOMIC % RELATIVE CONC.
Al K	0.037
Si K	0.100
Ca K	0.022
Ti K	0.228
Fe K	0.003

ZAF CORRECTION ELEMENTS	K	Z	A	F
Al K	0.063	1.013	0.197	1.019
Si K	0.178	1.046	0.168	1.006
Ca K	0.056	1.038	0.526	1.093
Ti K	0.690	0.955	0.648	1.002
Fe K	0.012	0.967	0.539	1.000

ELEMENTS	ATOMIC % ELEMENTS
Al K	19.247
Si K	43.009
Ca K	4.381
Ti K	32.603
Fe K	0.760

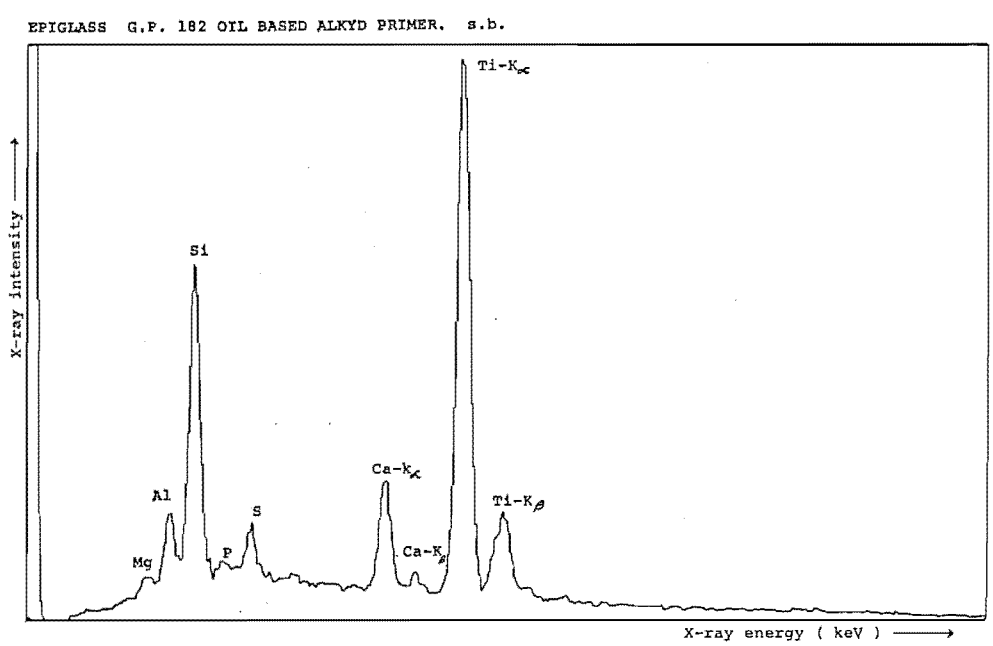

(**B**) *EDXA SPECTRUM OF ELEMENTS IN THE COATING.*
(JEOL JSM - 35 SEM / LINK 290 EDXA).

APPENDIX 1.7

TAUBMANS WOOD PRIMER.

(**A**) *ELEMENTS PRESENT IN THE COATING.(CAMBRIDGE SEM/EDXA)*

Energy range 0 - 20 keV.

ELEMENTS	INTENSITY (CPS)	BACKGROUND (CPS)	P/B RATIO
Al K	8.341	57.777	0.144
Si K	5.627	35.037	0.161
S K	6.024	73.434	0.082
Ca K	521.503	146.554	3.558
Ti K	334.649	103.854	3.222

ELEMENTS	ATOMIC % RELATIVE CONC.
Al K	0.037
Si K	0.010
S K	0.014
Ca K	0.811
Ti K	0.460

ZAF CORRECTION ELEMENTS	K	Z	A	F
Al K	0.018	1.015	0.129	1.010
Si K	0.009	1.048	0.157	1.016
S K	0.008	1.045	0.322	1.044
Ca K	0.575	!.040	0.703	1.070
Ti K	0.390	0.956	0.396	1.000

ELEMENTS	ATOMIC % ELEMENTS
Al K	12.463
Si K	4.923
S K	1.809
Ca K	41.208
Ti K	39.597

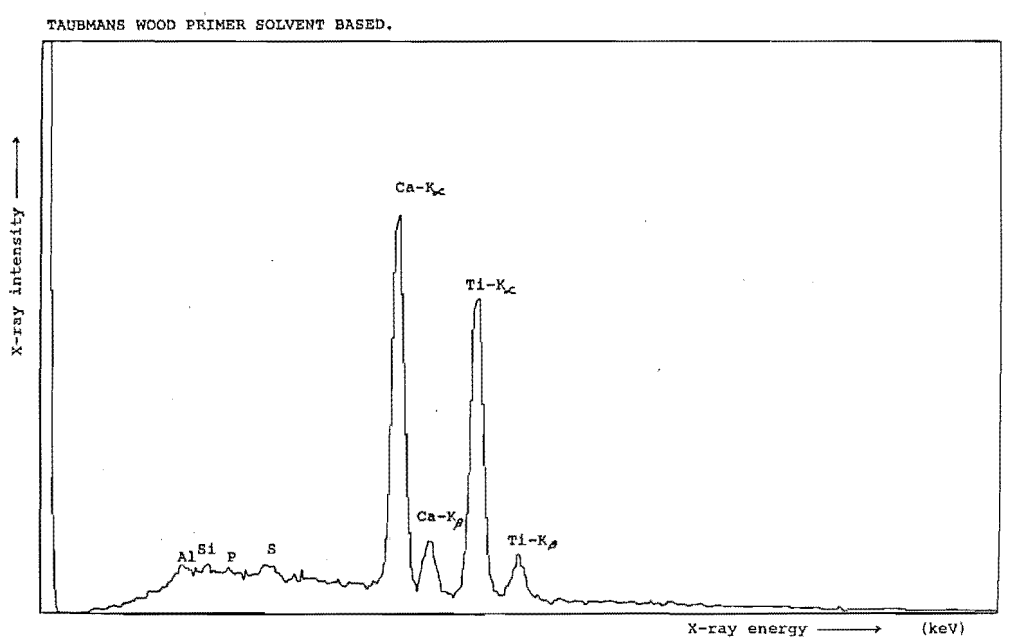

(**B**) *EDXA SPECTRUM OF ELEMENTS IN THE COATING. (JEOL JSM - 35 SEM / LINK 290 EDXA).*

APPENDIX 1.8

WATTYL ESTAPOL EXTERIOR CLEAR TiO_2 TAGGED.

(**A**) *ELEMENTS PRESENT IN THE COATING. (CAMBRIDGE SEM/EDXA)*

Energy range 0 - 20 keV.

ELEMENTS	INTENSITY (CPS)	BACKGROUND (CPS)	P/B RATIO
Al K	1.529	12.887	0.119
S K	7.545	36.624	0.206
Ca K	3.945	80.612	0.049
Ti K	341.090	27.041	12.614
As K	7.857	113.193	0.069

ELEMENTS	ATOMIC % RELATIVE CONC.
Al K	0.265
S K	1.189
Ca K	0.803
Ti K	86.985
As K	10.758

ZAF CORRECTION ELEMENTS	K	Z	A	F	ELEMENTS	ATOMIC % ELEMENTS
Al K	0.003	1.093	0.415	1.003	Al K	0.568
S K	0.012	1.126	0.753	1.016	S K	1.345
Ca K	0.008	1.100	0.948	1.140	Ca K	0.659
Ti K	0.870	1.005	0.981	1.000	Ti K	85.846
As K	0.108	0.921	0.983	1.000	As K	11.582

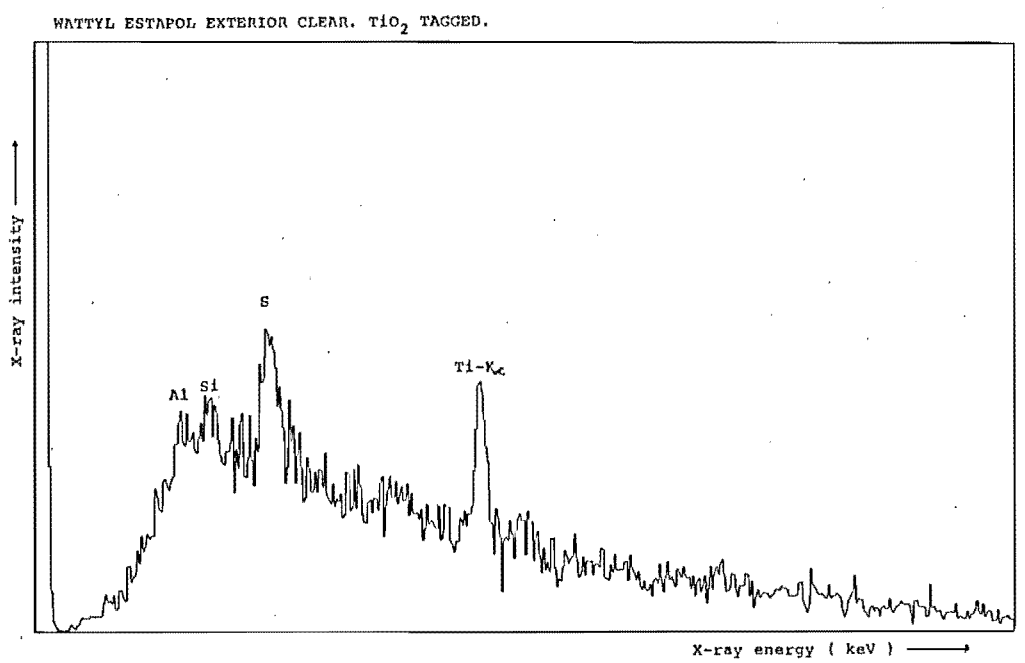

(**B**) *EDXA SPECTRUM OF ELEMENTS IN THE COATING. (JEOL JSM - 35 SEM / LINK 290 EDXA).*

APPENDIX 1.9

RIMU WEATHERBOARD (UNCOATED). *Dacrydium cupressinum.*

(**A**) *ELEMENTS PRESENT IN THE WOOD.(CAMBRIDGE SEM/EDXA)*

Energy range 0 - 20 keV.

ELEMENTS	INTENSITY (CPS)	BACKGROUND (CPS)	P/B RATIO
Al K	1.804	12.112	0.149
Si K	9.349	13.701	0.682
S K	3.508	17.970	0.195
Cl K	1.456	19.310	0.075
K K	26.656	26.723	0.998
Ca K	19.426	30.512	0.637
Cr K	1.721	31.339	0.055
Fe K	7.429	31.323	0.237
Cu K	1.919	28.013	0.069
Zn K	4.650	26.028	0.179

ZAF CORRECTION ELEMENTS	K	Z	A	F	ELEMENTS	WEIGHT % ELEMENTS
Al K	0.016	1.035	0.421	1.005	Al K	3.038
Si K	0.071	1.065	0.540	1.005	Si K	10.379
S K	0.028	1.065	0.704	1.015	S K	3.107
Cl K	0.012	1.017	0.770	1.025	Cl K	1.304
K K	0.254	1.018	0.882	1.025	K K	23.366
Ca K	0.199	1.041	0.824	1.007	Ca K	19.513
Cr K	0.027	0.949	0.917	1.033	Cr K	2.514
Fe K	0.148	0.950	0.951	1.026	Fe K	13.578
Cu K	0.062	0.920	0.967	1.000	Cu K	5.906
Zn K	0.183	0.921	0.975	1.000	Zn K	17.294

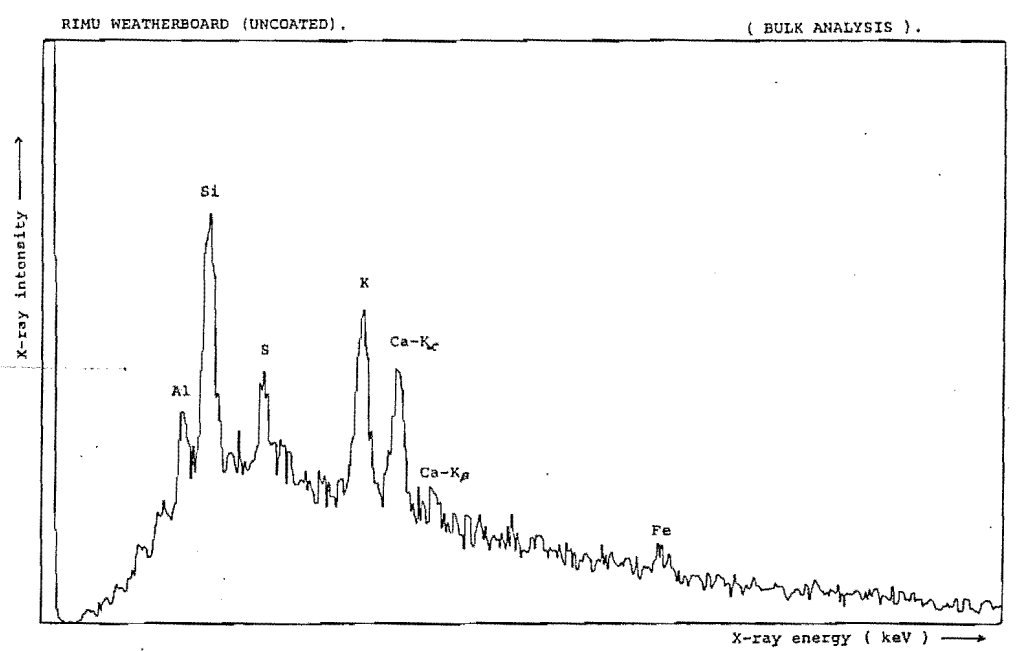

(**B**) *EDXA SPECTRUM OF ELEMENTS IN THE WOOD.*
(JEOL JSM - 35 SEM /LINK 290 EDXA).

APPENDIX 1.10

KAHIKATEA WEATHERBOARD. (UNCOATED). *Podocarpus dacrydioides.*

(**A**) *ELEMENTS PRESENT IN THE WOOD.(CAMBRIDGE SEM/EDXA).*

Energy range 0 - 20 keV.

ELEMENTS	INTENSITY (CPS)	BACKGROUND (CPS)	P/B RATIO
Si K	2.597	19.652	0.132
S K	2.432	25.127	0.097
Cl K	3.044	26.533	0.115
K K	11.546	32.621	0.354
Ca K	8.337	34.672	0.240
Cr K	26.666	33.481	0.796
Cu K	11.695	27.642	0.423
As K	7.427	27.460	0.270

ZAF CORRECTION ELEMENTS	K	Z	A	F	ELEMENTS	WEIGHT % ELEMENT
Si K	0.013	1.128	0.360	1.002	Si K	2.876
S K	0.012	1.136	0.589	1.006	S K	1.698
Cl K	0.016	1.083	0.681	1.009	Cl K	2.050
K K	0.070	1.082	0.819	1.016	K K	7.241
Ca K	0.055	1.105	0.840	1.016	Ca K	5.371
Cr K	0.264	1.009	0.948	1.021	Cr K	24.989
Cu K	0.241	0.982	0.971	1.035	Cu K	22.633
As K	0.328	0.932	0.979	1.000	As K	33.142

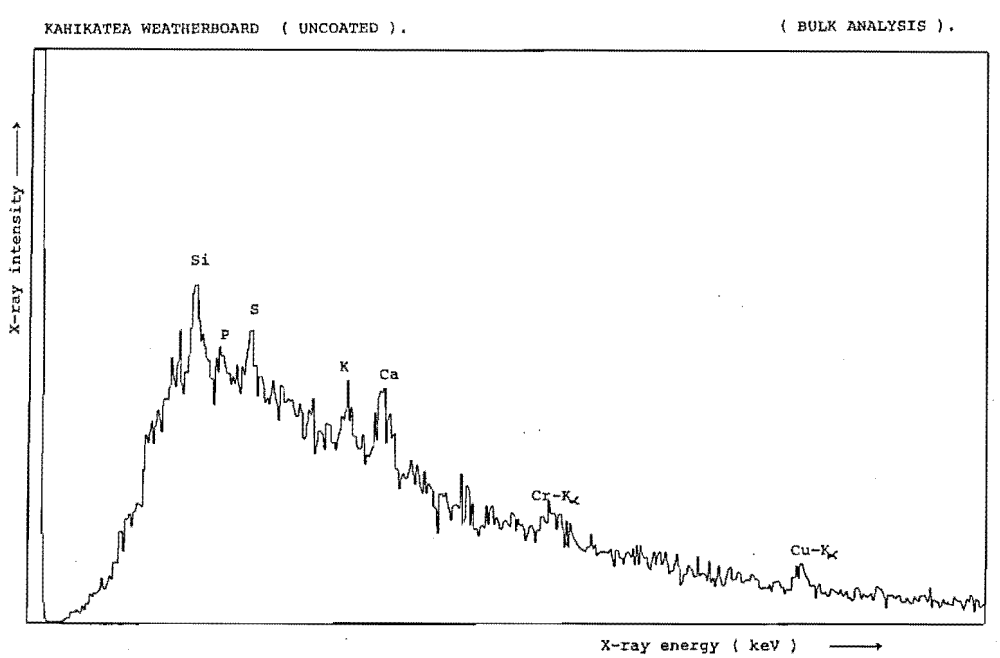

(**B**) *EDXA SPECTRUM OF ELEMENTS IN THE WOOD.*
(JEOL JSM - 35 SEM / LINK 290 EDXA).

APPENDIX 1.11

RADIATA PINE WEATHERBOARD. (UNCOATED). *Pinus radiata.*

(**A**) *ELEMENTS PRESENT IN THE WOOD.(CAMBRIDGE SEM/ EDXA)*

Energy range 0 - 20 keV.

ELEMENTS	INTENSITY (CPS)	BACKGROUND (CPS)	P/B RATIO
Al K	1.363	18.428	0.074
Si K	1.577	21.138	0.075
Cl K	1.314	55.611	0.024
K K	4.484	33.800	0.133
Ca K	2.365	34.359	0.069
Cr K	11.349	33.045	0.343
Cu K	6.619	57.369	0.115
Zn K	1.018	25.671	0.040
As K	4.287	26.607	0.161

ZAF CORRECTION ELEMENTS	K	Z	A	F	ELEMENTS	WEIGHT % ELEMENTS
Al K	0.014	1.099	0.251	1.001	Al K	4.680
Si K	0.015	1.131	0.332	1.001	Si K	3.480
Cl K	0.013	1.087	0.662	1.006	Cl K	1.677
K K	0.052	1.085	0.808	1.011	K K	5.266
Ca K	0.029	1.109	0.839	1.014	Ca K	2.811
Cr K	0.212	1.012	0.952	1.026	Cr K	19.378
Cu K	0.258	0.985	0.977	1.039	Cu K	23.319
Zn K	0.049	0.987	0.984	1.057	Zn K	4.279
As K	0.358	0.935	0.979	1.000	As K	35.110

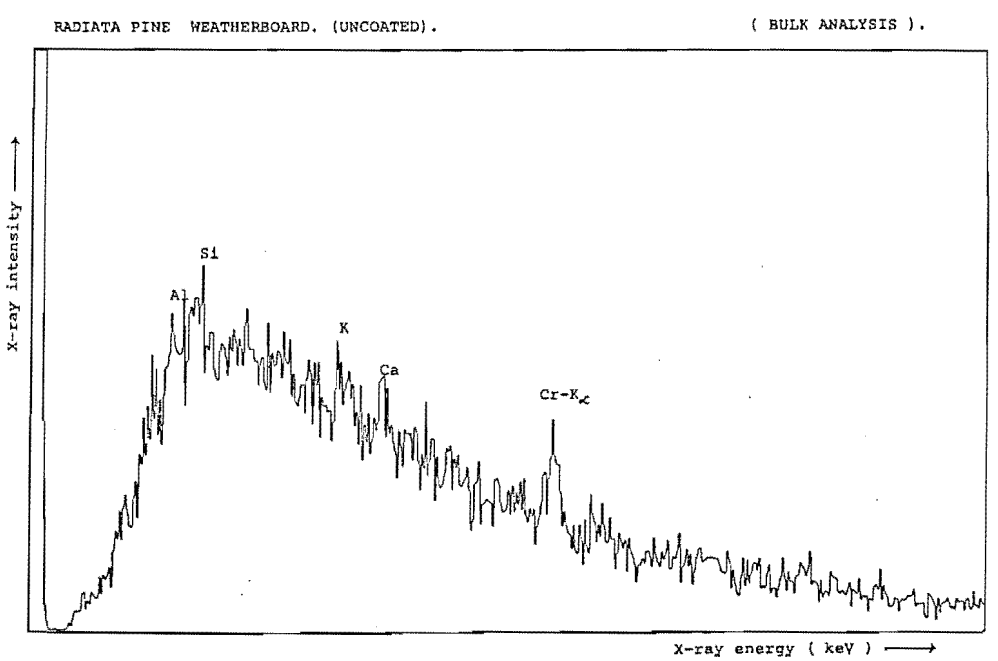

(**B**) *EDXA SPECTRUM OF ELEMENTS IN THE WOOD.*
(JEOL JSM - 35 SEM / LINK 290 EDXA).

APPENDIX 2

VISCOSITY RANGES IN KREBS UNITS OF COATINGS MEASURED AT 24^{OC}

The viscosity was measured on the Rotating Paddle Viscometer (Stormer Krebs type) and the Rotothinner viscometer.

BRAND	COATING	KREB UNITS (KU)
DULUX	PRIMERCRYL 100% ACRYLIC	61
EPIGLASS	WATER BASED WOOD PRIMER	74-76
TAUBMANS	PREMIUM FAST COAT WOOD PRIMER	74-76
DULUX	WUNDERPRIME	64-65
EPIGLASS	FIRST COAT WOOD PRIMER	70-72
EPIGLASS	G.P.182 OILBASED ALKYD PRIMER	70-72
TAUBMANS	WOOD PRIMER	67-69
WATTYL	TiO_2 TAGGED ESTAPOL EXTERIOR CLEAR	72

Viscosity is the resistance to flow (O.C.C.A,1984)

When a liquid is stirred the rate at which it flows is directly proportional to the force applied (Morgans,1984)

FORCE APPLIED (SHEAR STRESS) = CONSTANT x RATE OF FLOW (SHEAR).

APPENDIX 3

TABLE

AVERAGE CONTACT ANGLES OF COATINGS

(Ten measurements of contact angle were made for each coating, [refer Method 2.13.])

BRAND COATING	mean (degrees)	S D	M S	range (degrees)
DULUX PRIMERCRYL 100% ACRYLIC	28.3	3.36	11.28	24 - 34
EPIGLASS WATER BASED WOOD PRIMER	25.8	1.87	3.49	23 - 28
TAUBMANS PREMIUM FAST COAT WOOD PRIMER	26.8	3.19	10.17	23 - 31
DULUX WUNDERPRIMÉ	26.5	2.41	5.80	23 - 30
EPIGLASS 1st COAT WOOD PRIMER	20.8	2.57	6.60	19 - 26
EPIGLASS G P 182 OIL BASED ALKYD PRIMER	22.3	3.33	11.08	19 - 29
TAUBMANS WOOD PRIMER	24.5	3.10	9.61	21 - 29
WATTYL TiO_2.TAGGED ESTAPOL EXTERIOR CLEAR	27.6	3.77	14.21	20 - 34

APPENDIX TABLE 4

DEPTH OF COATING PENETRATION MEASURED ON THE TRANSVERSE FACE OF WEATHERBOARDS

Coating - TiO_2 tagged Wattyl Estapol Exterior Clear.
The number of filled cells were counted along rows of tracheids inwards from the coating/substrate interface.

Ten measurements were made at 1 cm intervals along the top edge of each weatherboard.
Ten measurements were also made on the "left" and "right" edges for comparison.

TAXA	Dacrydium cupressinum		Podocarpus dacrydioides		Pinus radiata	
CLASS INTERVAL cm	GROWTH RING PATTERN PRODUCED CUT					
	RIMU "u" - type	RIMU "n" - type	KAHIKATEA "u" - type	KAHIKATEA "n" - type	RADIATA "u" - type	RADIATA "n" - type
1	2,2,2,3,1,5,2,2,1,2	5,4,7,6,3,8,1,4,3,5	2,1,5,3,2,5,5,5,5,3	5,1,8,2,9,1,6,1,11,6	4,2,1,2,3,3,2,3,3,2	2,4,3,1,1,1,2,2,2,1
2	2,1,3,4,2,3,2,3,2,1	6,1,1,4,2,4,2,3,3,3	5,5,4,5,5,4,5,2,5,5	5,2,4,3,2,3,8,3,5,2	3,2,5,3,5,3,8,5,5,3	3,3,2,4,2,3,5,1,4,5
3	1,2,1,2,2,2,2,3,1,1	1,4,2,3,2,2,3,3,5,7	4,2,2,6,5,6,6,4,3,3	3,2,4,2,1,3,1,1,1,4	2,2,4,3,3,5,2,4,2,3	4,2,2,1,4,6,4,3,2,3
4	3,2,1,3,2,2,2,4,3,2	4,3,2,1,3,1,8,5,5,5	4,3,3,2,6,1,3,4,5,4	2,3,1,1,4,2,2,3,2,3	2,3,4,5,5,4,2,2,2,3	5,1,1,1,3,4,3,3,3,3
5	3,4,3,3,3,2,1,1,3,4	1,6,2,3,5,1,2,5,3,2	3,2,5,6,5,4,4,3,4,4	3,1,2,1,1,1,2,1,1,2	2,4,4,5,4,3,5,3,4,4	1,1,1,2,2,3,2,1,1,1
6	2,3,3,1,3,1,2,4,4,1	2,7,6,3,6,6,3,2,3,7	3,2,2,2,1,2,2,2,2,1	1,3,1,1,1,4,1,2,1,5	1,4,2,4,1,1,3,4,5,3	1,1,2,1,1,2,1,3,2,2
7	6,2,5,1,1,3,4,2,3,5	2,2,5,3,3,3,2,7,4,7	3,3,3,2,2,3,1,1,2,2	1,6,2,4,2,1,2,1,2,4	5,1,3,2,2,2,4,3,1,2	1,1,1,1,2,2,1,1,1,1
8	6,5,5,5,5,4,4,4,3,4	1,2,6,3,3,5,3,4,5,5	5,1,3,5,6,2,6,2,5,5	6,13,9,8,10,2,6,8,9,6	4,5,2,3,3,2,3,3,2,1	2,1,2,1,1,1,1,2,1,1
9	3,5,3,2,4,4,3,6,3,1	4,4,8,2,9,4,4,7,4,7	3,4,2,2,3,2,1,4,3,2	3,4,3,6,1,7,7,6,6,5	3,3,1,1,1,4,3,3,3,3	5,2,3,2,2,1,6,4,2,2
10	5,6,9,3,9,7,3,7,3,6	5,5,4,2,2,1,4,4,1,5	4,5,2,3,1,1,4,3,3,4	3,2,2,3,4,1,6,3,4,1	3,4,1,1,4,5,2,2,3,6	2,1,2,1,1,1,1,3,1,2
11	5,6,2,3,7,2,4,5,4,6	3,4,3,3,5,5,6,5,1,2	4,2,4,4,4,2,3,2,4,3	2,1,3,2,4,3,2,3,3,3	2,3,1,3,1,1,2,1,2,1	1,2,2,1,1,2,2,1,1,2
12	6,6,6,4,2,5,2,4,4,7	4,7,2,5,4,3,3,6,6,7	4,5,4,5,5,4,2,4,4,5	2,1,1,2,1,1,1,1,1,2	2,4,3,5,4,5,6,5,4,2	2,1,3,1,4,2,3,4,4,4
13	7,7,5,6,6,3,3,7,8,2	5,1,7,5,2,6,2,1,8,2	3,3,2,2,2,1,2,2,2,2	1,2,1,1,2,1,2,2,1,1	3,1,2,1,1,1,1,2,2,1	2,2,3,5,2,2,3,1,3,1
14	3,7,7,4,4,8,2,5,4,4	3,5,9,5,6,6,7,4,6,7	1,2,1,3,2,1,2,2,2,1	9,5,3,4,3,4,7,5,4,3	1,2,3,3,3,2,3,3,1,4	2,1,3,3,4,4,2,2,3,3
left edge	23,17,9,21,19,15,27,14,16,17.	5,4,2,8,7,11,4,1,1,4	2,3,10,12,17,15,9,24,27,14,14.	11,15,3,9,9,10,3,3,11,7	2,1,1,2,2,3,4,3,3,2	1,1,1,2,3,1,1,3,1,2
right edge	5,2,4,6,5,4,2,5,6.	14,9,5,14,2,8,8,5,8,10.	3,1,2,1,3,1,3,1,3,1	1,1,2,3,10,3,1,1,1,7	1,1,1,2,2,2,1,2,2,1.	1,1,2,2,1,1,1,1,1,1

APPENDIX TABLE 4.2 DEPTH OF COATING PENETRATION MEASURED ON THE TRANSVERSE FACE OF WEATHERBOARDS

Coating - TiO_2 tagged Wattyl Estapol Exterior Clear.
The number of filled cells were counted along rows of tracheids inwards from the coating/substrate interface.

The means and ranges for each class interval is presented.

TAXA	Dacrydium cupressinum								Podocarpus dacrydioides								Pinus radiata							
CLASS INTERVAL	GROWTH RING PATTERN PRODUCED CUT																							
	"u" - type				"n" - type				"u" - type				"n" - type				"u" - type				"n" - type			
cm	MEAN	SD	MS	RANGE	MEAN	SD	MS	RANGE	MEAN	SD	MS	RANGE	MEAN	SD	MS	RANGE	MEAN	SD	MS	RANGE	MEAN	SD	MS	RANGE
1	2.2	1.1	1.21	1-5	4.6	2.1	4.41	1-8	4.6	1.4	1.96	1-5	6.8	2.8	7.84	1-11	2.4	1.0	1.00	1-4	2.0	0.9	0.81	1-4
2	2.3	1.0	1.00	1-4	2.9	1.5	2.25	1-6	4.8	1.1	1.21	2-5	3.6	1.1	1.21	2-8	4.6	1.6	2.56	2-8	3.1	1.3	1.69	1-5
3	1.7	0.7	0.49	1-3	3.1	1.7	2.89	1-7	3.6	1.6	2.56	2-6	2.0	1.3	1.69	1-4	2.5	1.1	1.21	2-5	2.8	1.0	1.00	1-6
4	2.4	0.7	0.49	1-4	3.9	1.8	3.24	1-8	4.1	1.2	1.44	1-6	2.3	1.0	1.00	1-4	2.9	1.2	1.44	2-5	3.0	1.2	1.44	1-5
5	2.7	0.9	0.81	1-4	3.0	1.4	1.96	1-6	4.0	0.8	0.64	2-6	1.7	0.6	0.36	1-3	3.8	0.8	0.64	2-5	1.7	0.8	0.64	1-3
6	2.4	0.7	0.49	1-4	4.5	1.8	3.24	2-7	1.8	0.6	0.36	1-3	2.2	1.2	1.44	1-5	2.4	1.5	2.25	1-5	1.4	0.7	0.49	1-3
7	3.2	1.7	2.89	1-6	3.8	1.7	2.89	2-7	2.2	0.7	0.49	1-3	1.8	0.4	0.16	1-6	2.5	1.3	1.69	1-5	1.2	0.4	0.16	1-2
8	4.5	0.9	0.81	3-6	3.8	1.6	2.56	1-6	5.0	1.8	3.24	1-6	7.3	3.4	11.5	2-13	2.8	0.8	0.64	1-5	1.5	0.5	0.25	1-2
9	3.6	1.1	1.21	1-6	5.6	2.3	5.29	2-7	2.4	0.8	0.64	1-4	4.9	2.2	4.84	1-7	2.5	1.1	1.21	1-4	2.6	2.7	7.29	1-6
10	5.8	2.6	6.76	3.9	3.0	1.7	2.89	1-5	2.8	1.3	1.69	1-5	3.8	1.0	1.00	1-6	2.7	1.0	1.00	1-6	1.8	0.7	0.49	1-3
11	4.1	1.4	1.96	2-7	3.7	1.7	2.89	1-5	3.8	0.9	0.81	2-4	2.8	0.8	0.64	1-4	1.6	0.5	0.25	1-3	1.4	0.4	0.25	1-2
12	4.6	2.0	4.00	2-7	4.7	1.8	3.24	2-7	3.8	1.0	1.00	2-5	1.2	0.4	0.16	1-2	4.0	1.2	1.44	2-6	3.2	1.0	1.00	1-4
13	5.0	1.8	3.24	2-8	4.0	2.1	4.41	1-8	2.0	0.6	0.36	1-3	1.5	0.5	0.25	1-2	1.7	0.7	0.49	1-3	1.9	0.7	0.49	1-5
14	4.8	1.4	1.96	2-7	5.6	1.8	3.24	3-9	1.6	0.6	0.36	1-3	4.8	1.8	3.24	3-9	2.1	0.7	0.49	1-4	2.8	0.9	0.81	1-4
left edge	17.8	5.0	25.0	9-27	4.7	3.1	9.6	1-11	13.0	7.6	57.7	2-27	8.1	4.0	16.0	3-11	2.3	0.9	0.81	1-4	1.4	0.7	0.49	1-3
right edge	4.3	1.5	2.25	2-6	7.3	3.8	14.4	2-14	2.5	0.8	0.64	1-3	3.0	3.0	9.0	1-10	1.4	0.5	0.25	1-2	1.2	0.4	0.16	1-2

APPENDIX 5

TABLE

COATING SUBSTRATE TRACHEID CELL INCLINATION ANGLE

The angle made by the tracheid cell length and the sawn substrate/coating interface was measured at 1 cm intervals across the entire width of each weatherboard including the sides. (see figures 45 – 50). The mean angle and range for each class interval is presented.

TAXA

Dacrydium cupressinum Podocarpus dacrydioides Pinus radiata

GROWTH RING PATTERN PRODUCED CUT

CLASS INTERVAL	RIMU								KAHIKATEA								RADIATA							
	"u" - type				"n" - type				"u" - type				"n" - type				"u" - type				"n" - type			
cm	MEAN	SD	MS	RANGE	MEAN	SD	MS	RANGE	MEAN	SD	MS	RANGE	MEAN	SD	MS	RANGE	MEAN	SD	MS	RANGE	MEAN	SD	MS	RANGE
1	3.6	0.5	0.3	3-4	6.0	0.7	0.5	5-6	6.0	1.0	1.0	5-7	7.0	0.0	0.0	7-7	3.0	0.7	0.5	2-4	2.2	0.8	0.7	1-3
2	4.2	1.3	1.7	2-5	4.4	0.9	0.8	3-5	8.8	1.9	3.7	9-11	7.0	1.6	2.5	5-8	4.0	1.6	2.5	2-6	3.8	0.4	0.2	3-4
3	4.0	1.2	1.5	2-5	1.8	0.5	0.2	1-2	6.0	0.7	0.5	5-7	5.0	0.7	0.5	4-8	5.2	1.3	1.7	4-7	4.8	0.4	0.2	4-5
4	3.4	1.1	1.3	2-5	4.0	0.7	0.5	3-5	3.8	1.1	1.2	3-5	3.6	1.7	2.8	2-6	4.6	0.9	0.8	4-6	4.0	0.7	0.5	3-5
5	3.6	1.1	1.3	2-5	2.8	0.5	0.2	2-3	5.0	1.6	2.5	3-6	2.4	0.9	0.8	2-4	4.2	0.8	0.7	3-5	1.4	0.6	0.3	1-2
6	4.2	0.4	1.2	4-5	5.2	1.3	1.7	4-7	4.4	2.2	4.8	2-8	2.4	1.3	1.8	1-4	7.0	2.0	4.0	4-9	3.8	1.3	1.7	2-5
7	5.0	1.2	1.5	3-6	3.0	1.2	1.5	2-5	6.6	1.1	1.3	5-8	3.0	0.7	0.5	2-4	7.4	0.5	0.3	7-8	2.8	0.8	0.7	2-4
8	8.0	0.7	0.5	7-9	2.2	0.8	0.7	1-3	5.2	1.1	1.2	4-7	2.6	0.5	0.3	2-3	4.2	1.3	1.7	3-6	3.6	1.7	2.8	1-5
9	4.8	1.3	1.7	3-6	2.2	0.5	0.2	2-3	7.6	2.9	8.3	3-10	6.0	0.0	0.0	6-6	6.6	1.2	1.3	5-8	2.4	1.3	1.8	1-4
10	4.4	0.5	0.3	4-5	4.8	1.1	1.9	4-6	9.6	0.9	0.7	8-10	5.2	0.8	0.7	4-6	5.4	0.5	0.3	5-6	4.2	0.8	0.7	3-5
11	6.0	1.0	1.0	5-7	4.0	1.0	1.0	3-5	8.4	1.1	1.3	7-10	5.6	0.9	0.8	5-7	6.0	1.4	2.0	5-8	2.6	0.5	0.3	2-3
12	4.4	1.1	1.3	3-6	3.8	0.8	0.7	3-5	3.4	0.9	0.8	2-4	5.4	0.9	0.8	4-6	6.0	1.0	1.0	5-7	2.8	1.1	1.2	1-4
13	5.0	1.2	1.5	3-6	3.2	0.5	0.2	3-4	7.0	1.0	1.0	6-8	7.4	1.3	1.8	5-8	6.0	1.6	2.3	4-8	1.6	0.5	0.3	1-2
14	6.4	0.5	0.3	6-7	2.0	0.7	0.5	1-3	10.0	1.8	3.5	9-12	5.0	1.0	1.0	4-6	2.8	0.4	0.2	2-3	1.2	1.3	1.7	0-3
left edge	3.8	1.3	1.7	2-5	4.0	1.9	3.5	2-6	5.6	0.9	0.8	5-7	3.8	1.6	2.7	2-7	5.0	0.7	0.5	4-6	3.2	1.8	3.2	0-4
right edge	6.4	1.1	1.3	5-8	6.2	1.5	2.2	4-8	2.2	1.8	3.2	1-5	2.6	0.6	0.3	2-3	4.2	0.4	0.2	4-5	2.6	1.5	2.3	1.4

APPENDIX 6

FIGURE – shows the tracheid cell row growth directions viewed on the transverse face of the weatherboard for both "n" and "u"-type patterned boards.
The angle made by the tracheid cell rows and the coating interface was measured at 1 cm intervals along the top edge of each weatherboard and also the "left" and "right" side edges for comparison.

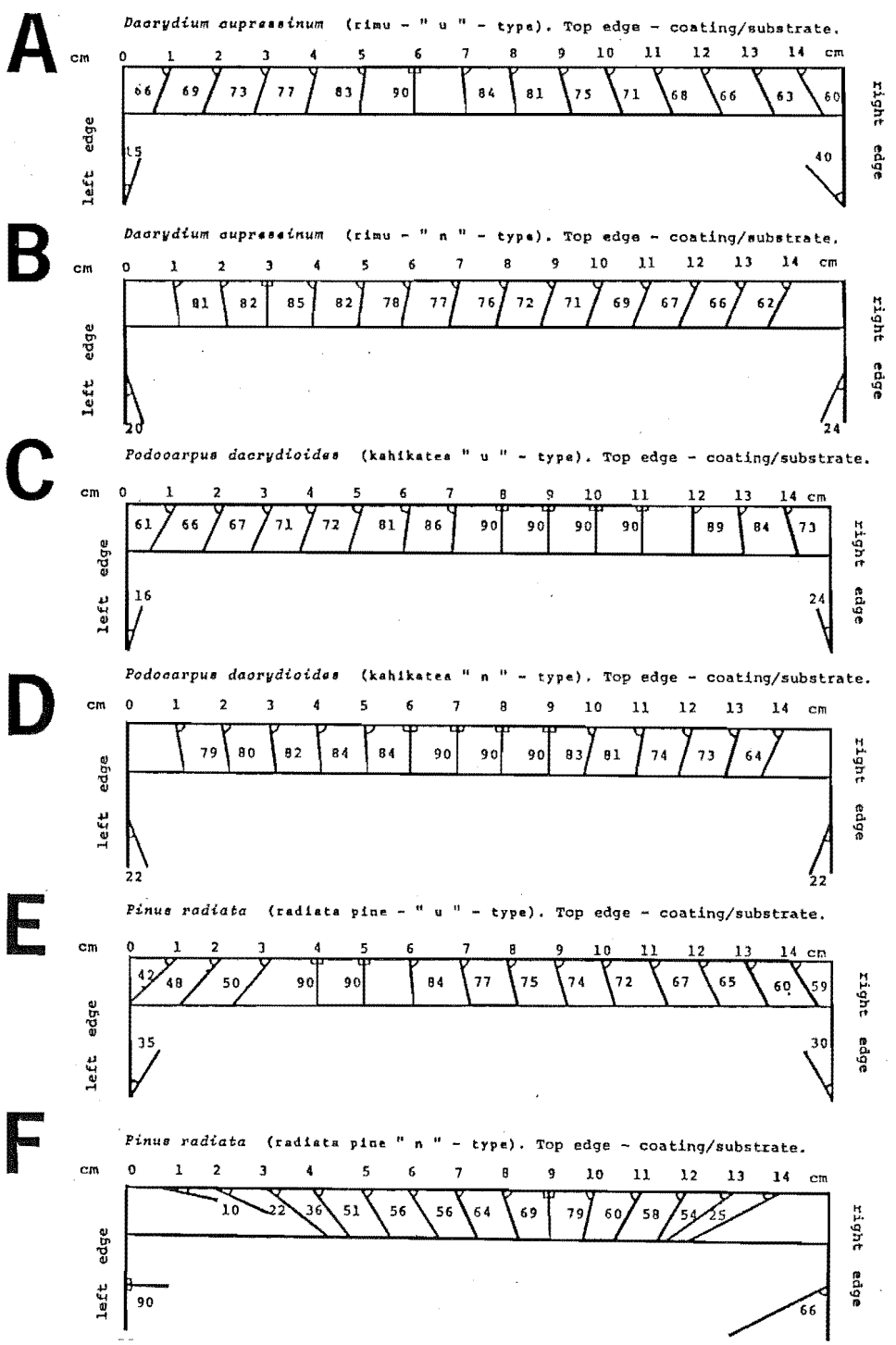

APPENDIX TABLE 7

ELEMENTS PRESENT IN TiO_2 TAGGED WATTYL ESTAPOL COATING AFTER 3000 HOURS ACCELERATED WEATHERING TESTS (CAMBRIDGE SEM/EDXA)

WEATHERBOARD SUBSTRATE TAXA	ELEMENTS	INTENSITY (CPS)	BACKGROUND (CPS)	P/B RATIO	WEIGHT % ELEMENT
D.cupressinum	AL K	11.26	99.00	0.11	2.74
	Si K	5.89	59.10	0.10	1.18
	S K	24.44	128.90	0.19	4.76
	Ca K	7.51	223.19	0.03	1.59
	Ti K	375.76	85.85	4.37	89.70
P.dacrydioides	Al K	3.41	35.55	0.09	0.63
	Si K	6.06	51.33	0.11	0.90
	S K	15.31	54.55	0.28	0.16
	K K	13.33	56.18	0.23	2.11
	Ca K	9.26	59.06	0.15	1.56
	Ti K	430.50	47.53	9.05	89.18
P.radiata	Si K	6.7	31.91	0.21	0.87
	S K	11.1	33.75	0.32	1.37
	Cl K	14.8	41.28	0.35	1.90
	K K	26.3	46.73	0.56	3.67
	Ca K	8.5	57.41	0.14	1.26
	Ti K	478.6	49.60	9.65	87.15

APPENDIX 8

TABLE 8.1

COMPARISON OF DIFFERENT COLOUR SYSTEMS FOR MEASURING THE REFLECTIVE COLOURS OF THE SUBSTRATES.

The values are the averages obtained with the Minolta Chroma-Meter CR200 tristimulus colour analyser for Dacrydium cupressinum, Pinus radiata and Podocarpus dacrydioides weatherboards.

WEATHERBOARD SAMPLES	TAXA *D.cupressinum*	*P.dacrydioides*	*P. radiata*
UNCOATED BOARD	L* 60.78 a* +7.77 b* +19.84	L* 77.84 a* +3.83 b* +22.20	L* 74.99 a* +5.53 b* +24.42
UNWEATHERED.	L* 60.78 C* 21.30 H° 68.70	L* 77.84 C* 22.57 H° 80.30	L* 74.99 C* 25.03 H° 77.30
	Dx 0.507 y 0.538 z 0.749	Dx 0.264 y 0.276 z 0.469	Dx 0.299 y 0.317 z 0.537
	Y 29.00 x .3791 y .3720	Y 52.95 x .3653 y .3737	Y 48.27 x .3745 y .3778
UN COATED BOARD	L* 48.46 a* +17.38 b* +36.32	L* 57.03 a* +13.42 b* +38.29	L* 53.40 a* +13.88 b* +36.35
WEATHERED 3000 HOURS.	L* 45.46 C* 40.26 H° 64.50	L* 57.03 C* 40.57 H° 70.80	L* 53.40 C* 38.90 H° 69.20
	Dx 0.745 y 0.928 z 1.375	Dx 0.549 y 0.603 z 1.075	Dx 0.610 y 6.669 z 1.141
	Y 14.88 x .4676 y .4067	Y 24.96 x .4407 y .4091	Y 21.42 x .4433 y .4071

TABLE 8.2

COMPARISON OF DIFFERENT COLOUR SYSTEMS FOR MEASURING THE REFLECTIVE COLOURS OF THE SUBSTRATES.

The values are the averages obtained with the Minolta Chroma-Meter CR200 tristimulus colour analyser for Dacrydium cupressinum, Pinus radiata and Podocarpus dacrydioides weatherboards.

WEATHERBOARD SAMPLES	TAXA *D.cupressinum*	*P.dacrydioides*	*P.radiata*
COATED BOARD 1 COAT	L* 84.75 a* +0.44 b* +5.81	L* 82.30 a* +3.33 b* +14.35	L* 85.85 a* +2.19 b* +10.44
	L* 84.75 C* 5.82 H° 85.70	L* 82.30 C* 14.73 H° 77.00	L* 85.85 C* 10.66 H° 78.20
TIO_2 TAGGED WATTYL ESTAPOL EXTERIOR CLEAR	Dx 0.183 y 0.184 z 0.228	Dx 0.206 y 0.216 z 0.331	Dx 0.163 y 0.170 z 0.250
WEATHERED 2000 HOURS.	Y 65.53 x .3246 y .3406	Y 60.87 x .3465 y .3561	Y 67.69 x .3360 y .3434

APPENDIX 8

TABLE 8.3

COMPARISON OF DIFFERENT COLOUR SYSTEMS FOR MEASURING THE REFLECTIVE COLOURS OF THE SUBSTRATES.

The values are the averages obtained with the Minolta Chroma-Meter CR200 tristimulus colour analyser for Dacrydium cupressinum, Pinus radiata and Podocarpus dacrydioides weatherboards.

WEATHERBOARD SAMPLES	TAXA *D.cupressinum*			*P.dacrydioides*			*P.radiata*		
COATED BOARD	L*	a*	b*	L*	a*	b*	L*	a*	b*
	89.38	−2.17	+8.84	89.19	−1.06	+10.03	89.17	−1.39	+10.10
2 COATS	L*	C*	H^o	L*	C*	H^o	L*	C*	H^o
	89.30	9.10	103.7	89.19	10.08	96.00	89.17	10.19	97.80
TiO_2 TAGGED WATTYL ESTAPOL EXTERIOR CLEAR	Dx	y	z	Dx	y	z	Dx	y	z
	0.133	0.126	0.191	0.131	0.128	0.202	0.132	0.128	0.203
UNWEATHERED.	Y	x	y	Y	x	y	Y	x	y
	74.81	.3259	.3479	74.59	.3298	.3494	74.54	.3294	.3498
COATED BOARD	L*	a*	b*	L*	a*	b*	L*	a*	b*
	89.10	−1.86	+7.63	90.80	−1.82	+9.85	90.01	−1.35	+9.29
2 COATS	L*	C*	H^o	L*	C*	H^o	L*	C*	H^o
	89.10	7.85	103.6	90.80	10.01	100.4	90.01	9.38	98.2
TiO_2 TAGGED WATTYL ESTAPOL EXTERIOR CLEAR	Dx	y	z	Dx	y	z	Dx	y	z
	0.134	0.129	0.185	0.113	0.108	0.179	0.122	0.118	0.186
WEATHERED 1000 HOURS.	Y	x	y	Y	x	y	Y	x	y
	74.40	.3241	.3453	78.07	.3281	.3494	76.33	.3278	.3481
COATED BOARD	L*	a*	b*	L*	a*	b*	L*	a*	b*
	86.98	−0.45	+5.73	87.86	+0.23	+8.12	87.21	+0.27	+6.97
2 COATS	L*	C*	H^o	L*	C*	H^o	L*	C*	H^o
	86.98	5.74	94.5	87.86	8.12	88.5	87.21	6.97	87.8
TiO_2 TAGGED WATTYL ESTAPOL EXTERIOR CLEAR	Dx	y	z	Dx	y	z	Dx	y	z
	0.157	0.155	0.198	0.144	0.144	0.205	0.152	0.152	0.204
WEATHERED 2000 HOURS.	Y	x	y	Y	x	y	Y	x	y
	69.98	.3229	.3408	71.80	.3203	.3449	70.44	.3263	.3427
COATED BOARD	L*	a*	b*	L*	a*	b*	L*	a*	b*
	88.56	−1.38	+6.79	89.02	−0.90	+8.16	89.66	−0.86	+8.69
2 COATS	L*	C*	H^o	L*	C*	H^o	L*	C*	H^o
	98.56	6.92	101.4	89.02	8.20	96.2	89.66	8.73	95.6
TiO_2 TAGGED WATTYL ESTAPOL EXTERIOR CLEAR	Dx	y	z	Dx	y	z	Dx	y	z
	0.139	0.135	0.185	0.132	0.130	0.190	0.124	0.122	0.186
WEATHERED 3000 HOURS.	Y	x	y	Y	x	y	Y	x	y
	73.25	.3234	.3434	74.23	.3266	.3457	75.58	.3275	.3466

APPENDIX 9

Simplified (CIE,1931) chromaticity diagram to show the position of the CIE standard illuminant condition D_{65} (6500^{o}k).

The visible spectrum extends from 380 nm (purplish blue) to 780 nm (red). Chromaticity is the colour quality of a colour stimulus definable by its chromaticity co-ordinates or by the dominant (or complimentary) wavelength and its purity taken together.(CIE,1970).
A chromaticity diagram is a plane diagram in which points specified by the chromaticity co-ordinates x and y represent the chromaticities of colour stimuli. (AS 2633 (1983)).

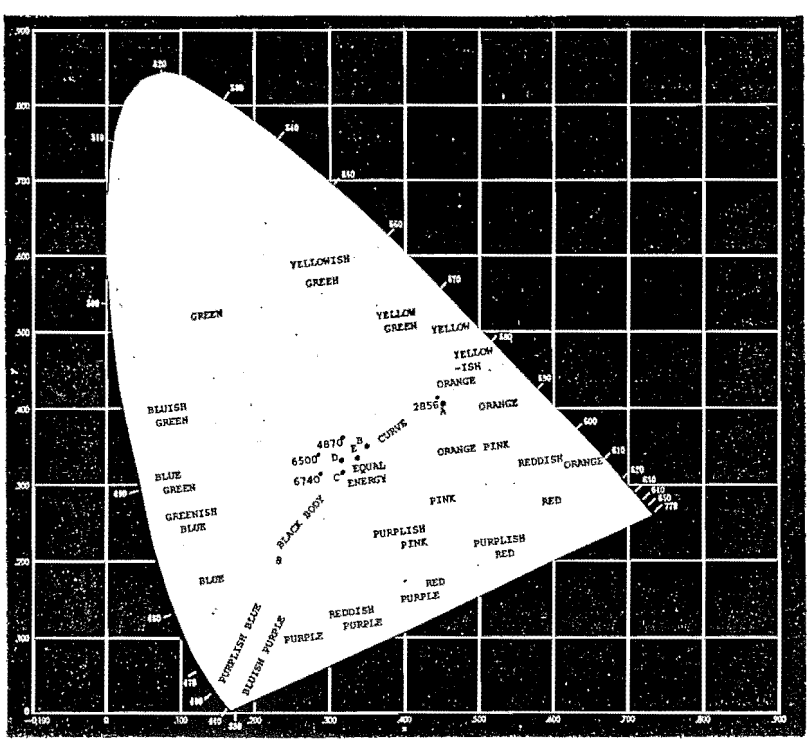

APPENDIX 10

The "GLOSSGARD SYSTEM 60" was used to obtain the 60 degree gloss measurements.

GLOSS is defined as the visual impression created by the reflection properties of a surface.

FULL GLOSS (FINISH) a surface with a specular gloss reading above 85 gloss units when the specular direction is 60 degrees.

GLOSS (FINISH) a surface with a specular gloss reading above 50 gloss units but not exceeding 85 gloss units when the specular direction is 60 degrees.

SEMI-GLOSS (FINISH) a surface with a specular gloss reading above 20 gloss units but not exceeding 50 gloss units when the specular direction is 60 degrees.

LOW GLOSS (FINISH) a surface with a specular gloss reading above 5 gloss units but not exceeding 20 gloss units when the specular direction is 60 degrees.

FLAT (FINISH) a surface with a specular gloss reading below 5 gloss units when the specular direction is 60 degrees.

TABLE

THE EFFECT OF WEATHERING ON THE SURFACE GLOSS APPEARANCE OF TiO_2 TAGGED WATTYL ESTAPOL CLEAR COATED WEATHERBOARDS.

(GLOSSGARD SYSTEM 60).
Comparison of the loss of gloss on boards with 1 coat and 2 coats after weathering for 2000 hours.

TAXA	Dacrydium cupressinum			Podocarpus dacrydioides			Pinus radiata		
Hours weathered	mean	S D	M S	mean	S D	M.S	mean	S.D	M S
2 coats unweathered	89.75	1.06	1.12	81.5	1.70	2.89	80.75	1.06	1.12
(2 COATS) 2000 hours	84.25	0.35	0.12	78.7	7.42	55.0	70.50	0.70	0.49
(1 coat) 2000 hours	80.0	1.41	1.98	35.5	6.36	40.4	54.25	3.88	15.05

PUBLICATIONS

MIDDLETON, T.M. 1985 Vessels of stem wood in New Zealand *(Nothofagus).* M.Sc. (First Class Honours) Thesis. University of Canterbury, Christchurch. 203p

MIDDLETON, T.M. 1987 Aggregate rays in New Zealand *Nothofagus* **(Fagaceae) stem wood and their influence on vessel distribution.** *International Association of Wood Anatomists Bulletin* n.s. **8 (1) :** 53-57

MIDDLETON, T.M. 1987 Perforation plates and vessel elements of the stem sapwood in New Zealand *Nothofagus* **Blume. (Fagaceae) with particular reference to their lengths.** *Mauri Ora* **14 :** 1-8

MIDDLETON, T.M. 1987 Vessel distribution, grouping and frequency in the stem wood of New Zealand *Nothofagus* **(Fagaceae) Taxa.** *Mauri Ora* 14 : 9-14

MIDDLETON, T.M. 1988 The 'Last Ray' in beech - as seen under the scanning electron microscope. *New Zealand Environment (Winter 1988)* **54 :** 14

MIDDLETON, T.M. 1988 Intervessel pits in the stem wood of New Zealand *Nothofagus* **(Fagaceae).** *International Association of Wood Anatomists Bulletin* n.s. **9 (4)** : 327-331

MIDDLETON, T.M. 1988 Ballooning in Wood. *New Zealand Environment (Summer 1988)* **60 :** 26-27

MIDDLETON, T.M. 1989 Modification of the latex paint infusion technique for the determination of vessel length in hardwoods. Wood Science and Technology (*Journal of the International Academy of Wood Science*) **23** : 299-302

MIDDLETON, T.M. & BUTTERFIELD, B.G. 1990 Vessel-length distribution in the stems of three New Zealand species of *Nothofagus*. Wood Science and Technology (*Journal of the International Academy of Wood Science*) **24** : (in press)

DONALDSON, L.A., HOLLINGER, D., MIDDLETON, T.M. & SOUTER, E.D. 1987 Effect of CO_2 enrichment on wood structure in *Pinus radiata* **D.Don.** *International Association of Wood Anatomists Bulletin* n.s. **8 (3) :** 285-289

PUBLICATIONS

MIDDLETON, T.M. 1985 Vessels of stem wood in New Zealand *(Nothofagus)*. M.Sc. (First Class Honours) Thesis. University of Canterbury, Christchurch. 203p

MIDDLETON, T.M. 1987 Aggregate rays in New Zealand *Nothofagus* (Fagaceae) stem wood and their influence on vessel distribution. *International Association of Wood Anatomists Bulletin* n.s. 8 (1) : 53-57

MIDDLETON, T.M. 1987 Perforation plates and vessel elements of the stem sapwood in New Zealand *Nothofagus* Blume. (Fagaceae) with particular reference to their lengths. *Mauri Ora* 14 : 1-8

MIDDLETON, T.M. 1987 Vessel distribution, grouping and frequency in the stem wood of New Zealand *Nothofagus* (Fagaceae) Taxa. *Mauri Ora* 14 : 9-14

DONALDSON, L.A., HOLLINGER, D., MIDDLETON, T.M. & SOUTER, E.D. 1987 Effect of CO_2 enrichment on wood structure in *Pinus radiata* D.Don. *International Association of Wood Anatomists Bulletin* n.s. 8 (3) : 285-289

MIDDLETON, T.M. 1988 The 'Last Ray' in beech - as seen under the scanning electron microscope. *New Zealand Environment (Winter 1988)* 54 : 14

MIDDLETON, T.M. 1988 Intervessel pits in the stem wood of New Zealand *Nothofagus* (Fagaceae). *International Association of Wood Anatomists Bulletin* n.s. 9 (4) : 327-331

MIDDLETON, T.M. 1988 Ballooning in Wood. *New Zealand Environment (Summer 1988)* 60 : 26-27

MIDDLETON, T.M. 1989 Modification of the latex paint infusion technique for the determination of vessel length in hardwoods. Wood Science and Technology (*Journal of the International Academy of Wood Science*) 23 : 299 - 302

MIDDLETON, T.M. & BUTTERFIELD, B.G. 1990 Vessel-length distribution in the stems of three New Zealand species of *Nothofagus*. Wood Science and Technology (*Journal of the International Academy of Wood Science*) 24 : 17-22

MIDDLETON, T.M. 1990 WOOD STRUCTURE AND COATINGS, AN ELECTRON MICROSCOPE STUDY OF *Dacrydium cupressinum*, *Podocarpus dacrydioides* and *Pinus radiata* WEATHERBOARD SUBSTRATES.

Ph.D. Thesis. University of Canterbury, Christchurch, New Zealand. 211 p.

PUBLICATIONS continued...

MIDDLETON, T.M. 1991 Perforation plates - ' ladders ' in beech wood under the electron microscope. New Zealand Tree Grower. vol. 12 (No. 4): p 25. (November 1991).

MIDDLETON, T.M. 1991 Wood substrates and coatings under the electron microscope. New Zealand Painter and Decorator. vol. 44 (No. 11): p. 16 - 17. (November / December 1991).

MIDDLETON, T.M. 1991 Fantastic Fibres - a magnified glimpse of New Zealand beech wood. New Zealand Environment. Number 68 : p. 14 - 15 . (December 1991).

MIDDLETON, T.M. 1992 'Rays' captured with the scanning electron microscope. New Zealand Tree Grower. vol. 13 (No. 1): p. 27. (February 1992).

MIDDLETON, T.M. 1992 Secrets behind the Bark - The inner secrets of a native beech tree. Growing Today. vol. 5 (No. 2): p.6 - 7 . (March 1992).

MIDDLETON, T.M. 1992 Timber and Paint. Terra Nova. Issue 15 : p. 51 - 52. (April 1992).

MIDDLETON, T.M. 1992 Rimu, kahikatea and radiata - an electron microscope study of coated weatherboards. New Zealand Forestry. vol. 37 (No. 1): p. 17 - 19 . (May 1992).

MIDDLETON, T.M. 1993 Coating/wood substrate behaviour in Dacrydium cupressinum, Podocarpus dacrydioides and Pinus radiata weatherboards. Wood Science and Technology (Journal of the International Academy of Wood Science). vol. 27 (5) : 357 - 371.

* Also have illustrations in N.Z. Geological Soc. booklets.

PUBLICATIONS continued ...

MIDDLETON, T.M. 1994 Focus on Torus - Tracheids under the electron microscope.
Surface Coatings Australia : Journal of the Surface Coatings Association Australia Inc. & the Surface Coatings Association New Zealand Inc. vol. 31 (No 7) July : 15.

MIDDLETON, T.M. 1994 Wood and coatings, an electron microscope study of anatomical features of Dacrydium cupressinum, Podocarpus dacrydioides, Pinus radiata and New Zealand Nothofagus taxa. Abstract. In: The Third Pacific Regional Wood Anatomy Conference 1994 Rotorua, N.Z. International Association of Wood Anatomists Journal (IAWA) vol.15 (3): 213 - 214.

MIDDLETON, T.M. 1996 An electron microscope study of coated weatherboards from three timber species.
Surface Coatings Australia : Journal of the Surface Coatings Association Australia Inc. & the Surface Coatings Association New Zealand Inc.
vol. 33 (3), March,: 26 - 30.

MIDDLETON T M 1997 "The performance of coated weatherboards"
Surface Coatings Australia : Journal of the Surface Coatings Association Australia Inc. & the Surface Coatings Association New Zealand Inc.
vol. 34 (11), November Page 25 – 27

ISSN 0815 — 709X
Surface Coatings Association Australia,
Vol. 31, No. 7

FOCUS ON TORUS
Tracheids Under the Electron Microscope

DR. T.M. Middleton, BA, BSc, MSc (First Class Honours), PhD, Department of Plant and Microbial Sciences, University of Canterbury, Christchurch, New Zealand

The transmission electron microscope is a superb instrument to obtain an 'eye-ball' examination of the torus; it is rather like targeting the bulls-eye of taurus! All those involved in the timber industry can now 'peer' deep into wood, and focus on some amazingly delicate structures.

Pinus radiata D.Don. (radiata) is of increasing importance in wood research worldwide, while *Podocarpus dacrydioides* A.Rich. (kahikatea), a native gymnosperm of New Zealand, is popular in the building and home renovating industry and is used in a variety of ways, including exterior cladding. These two timber species were chosen to illustrate the structure of wood. This particular study formed part of a research programme on coating behaviour and weatherboards. Select timbers and coating systems currently available on the New Zealand market were analysed before and after weathering and examined with the aid of the transmission electron microscope (Figure 1). The topic of coatings/wood structure has interested paint chemists, physicists, and engineers for years. However more information from the wood anatomist's point of view was deemed necessary (Middleton 1990, 1991, 1992a, b, 1993).

Tracheids are the long water (sap) conducting cells present in the wood of gymnosperms (softwoods). A variety of pits are present in tracheid walls depending on the adjacent cell types through which the sap flows. Inter-tracheid pits are bordered and possess over-arching walls referred to as pit borders. A bordered pit-pair in *Pinus radiata* wood is shown in Figure 2. The pit membrane consists of a central thickened area termed the torus surrounded by the margo, a radiating network of microfibrils like the spokes of a wheel. When viewed in cross-section, the pit membrane appears as a thin wavy line which is normally suspended in the median position. When pit aspiration occurs the torus and margo are deflected to one side against the pit aperture and the tracheid wall, and the flow of sap through into an adjacent tracheid is prevented. Tracheid walls are typically multi-layered and consist of the middle lamella, primary layer and a three layered secondary zone. In *Pinus radiata* a warty layer is present on the lumen surface as shown in Figure 2.

The importance of the torus and margo, and the tracheid cell wall in determining coating behaviour is stressed here. Bulk flow of the coating and gross penetration of conduits is readily demonstrated with the aid of the scanning and transmission electron microscopes, and confirmed by EDXA (energy dispersive X-ray analysis) techniques (Figure 3). However penetration of the cell wall by components of the coating of certain molecular particle size is the current topic of research worldwide. Titanium particles, present in the coating are too large to pass into the cell walls, and hence tend to line the tracheid lumens (Figure 4).

As new theories on penetration are tested and the torus and margo are targeted, the search for microcapillaries will advance, the mysteries will unfold, and the clues will come into focus!

AUTHOR

Dr T.M. Middleton completed BA, BSc, MSc (First Class Honours) and PhD degrees at the University of Canterbury, New Zealand, and was awarded a scholarship to study coatings and wood substrates.

This paper was submitted November 1993.

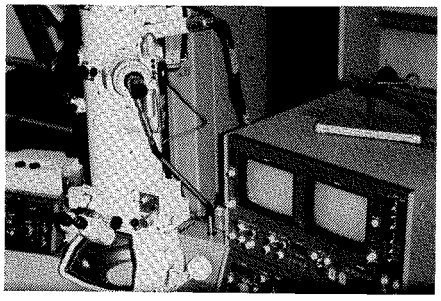

Figure 1. A transmission electron microscope.

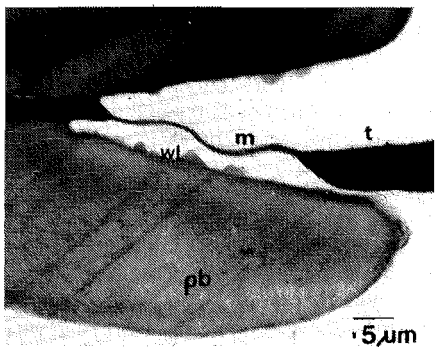

Figure 2. Magnified detail of a cross-section through a tracheid cell in Pinus Radiata *wood showing the warty layer (wl), pit border (pb), margo (m) and torus (t). (Bar scale in microns (µm)).*

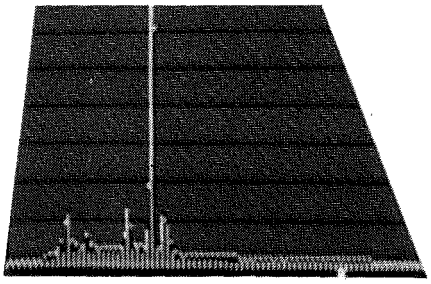

Figure 3. EDXA spectrum of a titanium rich coating used on the weatherboards.

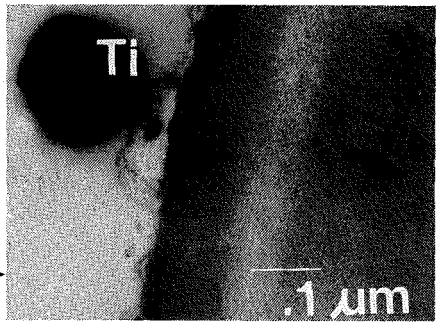

Figure 4. Detail of a coated Podocarpus dacrydioides *weatherboard showing a titanium particle (Ti) present in the coating.*

BIBLIOGRAPHY

1. *Middleton, T.M. 1990. "Wood structure and coatings — An electron microscope study of Dacrydium cupressinum, Podocarpus dacrydioides and Pinus radiata weatherboard substrates." Ph.D. Thesis. University of Canterbury, Christchurch, New Zealand 211 p.*
2. *Middleton, T.M. 1991. "Wood substrate and coatings under the electron microscope." New Zealand Painter and Decorator. 44 (11): 16-17.*
3. *Middleton, T.M. 1992 (a). "Timber and Paint". Terra Nova 15 : 51-52 (April).*
4. *Middleton, T.M. 1992 (b). "Rimu, kahikatea and radiata — an electron microscope study of coated weatherboards". New Zealand Forestry 37 (1) : 17-19. (May).*
5. *Middleton, T.M. 1993. "Coating/wood substrate behaviour in Dacrydium cupressinum, Podocarpus dacrydioides and Pinus radiata weatherboards". Wood Science and Technology. 27 (5) 357-371.*

NOV/DEC 1991
VOLUME 44
NO.11

NEW ZEALAND

Painter & Decorator

"Wood Substrates And Coatings Under The Electron Microscope"

Dr. T.M. Middleton
B.A.,B.Sc.,M.Sc,(First Class Honours), Ph.D.

Significant contribution to our knowledge of the wonderful world of wood has been provided by the electron microscope. Technical improvement both in technique and instrumentation methods have enabled scientists to visualize many aspects of wood anatomy at very high magnifications.

One of our earliest written evidence on the subject of wood is Pliny the elder (Gaius Plinius Secundus), a Roman scientist of the first century A.D. His works on natural history indicate that wood was not only painted for decorative purposes but the architects of the day recognised the need for surface protection of timber. He observed that timber was smeared with dung and dried to proof it against the action of the atmosphere. Thus for centuries it has been known that wood is a naturally durable material and yet it is one of the most variable of substrates. Within a single board major variations in density are apparent. Worldwide each country has its own history of the use of timber influenced by the distribution and availability of timber species.

How many tree lovers have had the opportunity to marvel at the structure of wood magnified thousands of times! This collection of micrographs featured in figure 1 depict an array of *Pinus radiata* weatherboards that have been painted with a titanium rich coating and cut transversely to reveal the depth and pattern of gross penetration of the coating and photographed under the scanning electron microscope.

The two major cell types in *Pinus radiata* are the water conducting tracheids (T), and the rays (R). Notice the primer has become locked in the tracheids and also penetrated the long ray. Gross penetration is facilitated by the number of cells opened during timber machining and also by the presence of cracks in the wood. Air pockets and extractives present in the cells can disrupt paint penetration.

This glimpse inside *Pinus radiata* provides painters and decorators with the special opportunity to marvel at the structure of wood. IF TREES COULD TALK! WHAT 'WOOD' THEY SAY?!!!

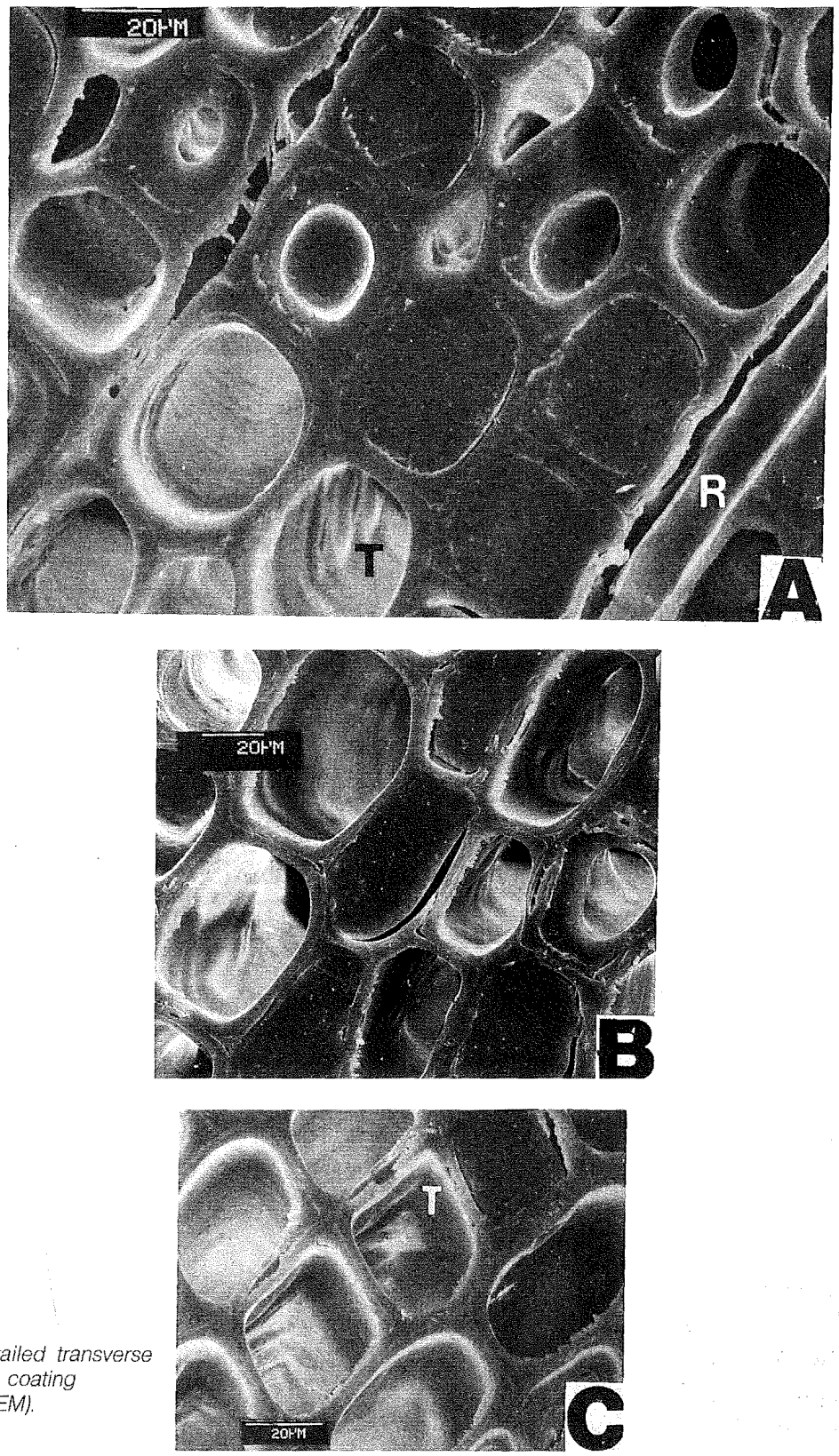

P. radiata Detailed transverse view showing coating penetration (SEM).

FIGURE 1

Fantastic Fibres — a magnified glimpse of New Zealand beech wood

T M Middleton

December 1991
ISSN 0110-6287 Number 68

The beauty of *Nothofagus*, New Zealand's native beech, is appreciated by many trampers, tree growers, toy makers, and tree lovers. This collection of images of beech wood (see facing page) photographed by scanning electron microscope gives readers the opportunity to understand more fully, and to marvel at, some of the fascinating anatomical features of beech fibres at fairly high magnifications.

Five taxa of *Nothofagus* grow endemically [1] in N.Z. forests: *Nothofagus menziesii* (silver beech, Tawhai), *N. fusca* (red beech, Tawhairaunui), *N. truncata* (hard beech, Tawhairaunui), *N. solandri* (black beech, Tawhairauriki) [2], and *N. solandri* var. *cliffortioides* (mountain beech, Tawhairauriki). Their wood, like most hardwoods, is composed predominantly of vessels, fibres, and ray cells. The bulk of beech wood is occupied by thick-walled fibre cells which provide strength. Anatomical differences exist between the taxa of beech, owing partly to their geographic distribution.

The figures depict respectively transverse and longitudinal views of fibres in mountain beech (fig. A) and red beech (figs. B & C). Notice the tiny slit-like pits (arrowed) in the walls of the fibres.

These micrographs illustrate superb cell shapes and cell wall textures. "Nice *Nothofagus*!" "Beautiful Beech!".

References

1. J T Salmon, *The Native Trees of New Zealand* Reed 1980, pp208–218.
2. (strictly, *N. solandri* var. *solandri*)

Dr T M Middleton did B.Sc., BA, MSc and PhD degrees at the University of Canterbury, has taken hundreds of electron micrographs of wood at Canterbury, and held a U.G.C. scholarship to study coatings and wood substrates.

New Zealand Environment
Number 68 Spring 1991

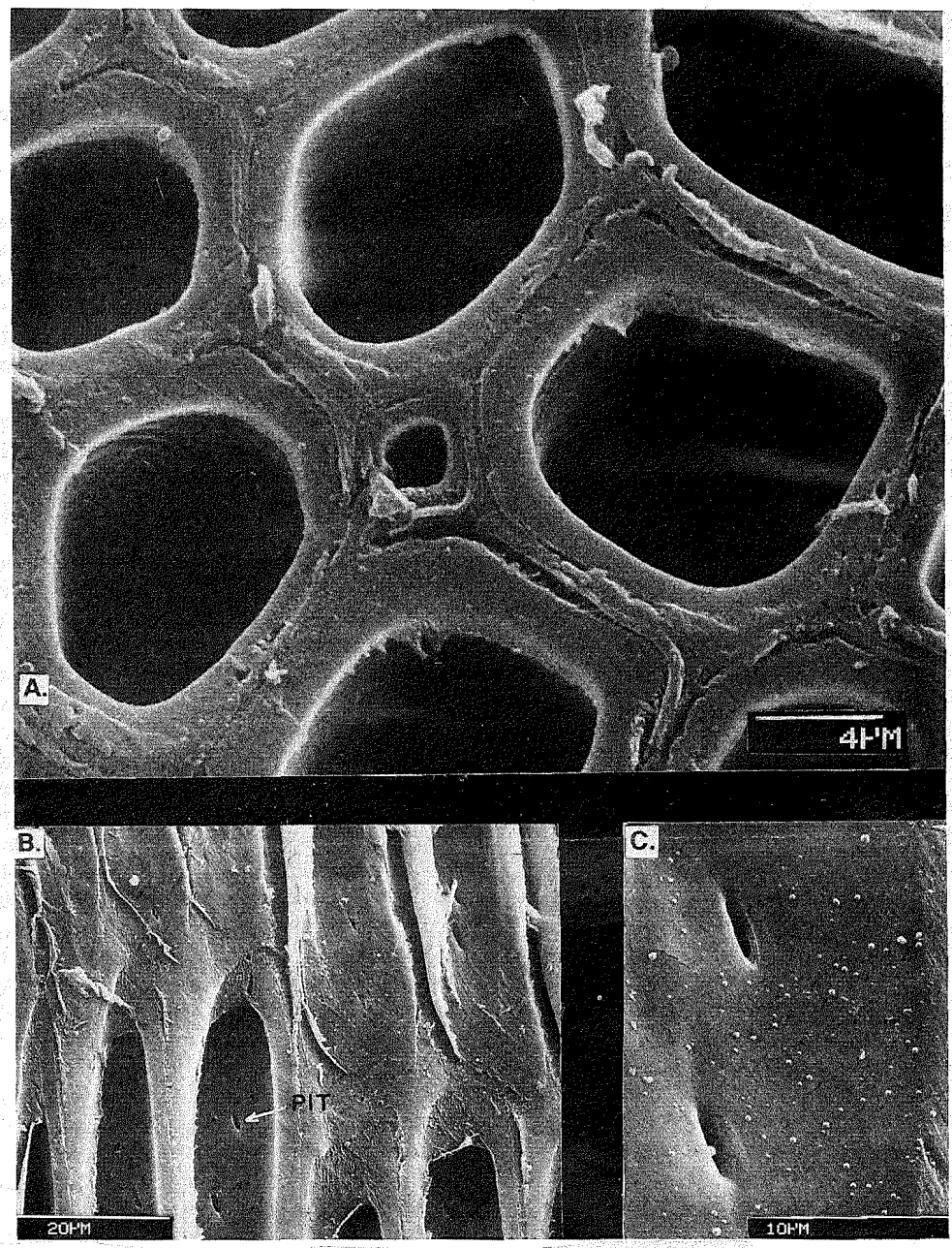

Rimu, kahikatea and radiata: an electron microscope study of coated weatherboards

Dr T.M. Middleton *

Abstract

Coating penetration behaviour in *Dacrydium cupressinum* (rimu) *Podocarpus dacrydioides* (kahikatea), both native softwood timbers, and *Pinus radiata* (radiata pine), an exotic softwood weatherboard timber, is briefly discussed.

Introduction

Weatherboard performance can be indirectly traced back to the forester with the silvicultural methods used and then continued onwards to the timber mill where cutting and timber treatment procedures play their role eventually to the final use of the product. It is well known that the complex interaction of wood substrates and coating systems is environmentally, physically, chemically and biologically controlled. The variables are numerous and include factors such as timber species, wood density, grain texture, wood anatomy, wood ultrastructure, seasoning and treatment of timber, machining quality, coating formulation and composition, viscosity, rheology, and wetting ability, to name a few.

Coating/substrate relationships have fascinated researchers for many years and this report provides a glimpse of the topic from the wood anatomist's view with the aid of the electron microscope. Now foresters and all those involved in the forest industry have the great opportunity to examine closely a selection of highly magnified images of three softwood species.

Dacrydium cupressinum (rimu), *Podocarpus dacrydioides* (kahikatea) and *Pinus radiata* (radiata pine) were chosen to illustrate wood behaviour, (Middleton, 1990). On the basis of wood anatomy rimu and kahikatea belong to the Podocarpaceae family, while radiata belongs to the Pinaceae family and is placed in the Ponderosa group of conifers. The anatomy of stem wood of the indigenous Podocarpaceae has been described in detail by Orman and Reid (1946), and Patel (1967 a & b) and *Pinus radiata* by Patel (1971). Tracheids and rays are the major cell types in all three taxa. The water conducting tracheid cell walls are pierced by a variety of pit types. Figure 1 is an ultrathin cross-section through a tracheid cell in radiata pine showing an intertracheid pit pair which has a border (pb) and possesses a torus (t) and margo (m) membrane. Several very highly magnified details of the image are shown. Figures 2 and 3 show cross-sections of rimu and kahikatea weatherboards and details of paint-filled cells and coating penetration photographed under the scanning electron microscope.

Materials

In this study good-quality, dressed, preservative-treated, bevel-back, flat-sawn and quarter-sawn weatherboards were primed with a specially formulated titanium rich coating (Middleton, 1990), in accordance with the New Zealand Paint Manufacturers Association guidelines.

* *Department of Plant and Microbial Sciences, University of Canterbury, Christchurch*

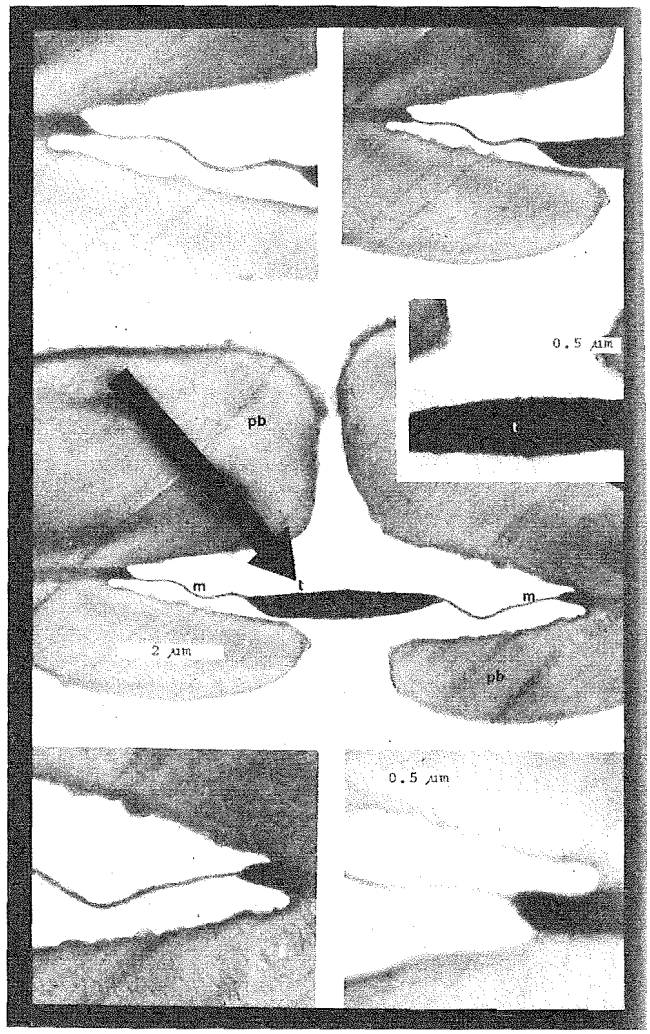

Figure 1 ***P. radiata*** **(radiata pine) wood; highly magnified cross-section through two adjacent tracheid cells to show details of the pit membrane at different magnifications.**

Results and Discussion

Two types of wood/coating interactions have been recognised: (a) Gross penetration where the coating fills the cell lumens; and (b) Cell wall penetration where components of the coating fill the inter-microfibrillar areas of the cell walls and possibly the amorphous regions within the cellulose microfibrils. If the film composition remains constant throughout the entire level of penetration into the wood then its performance at any point is dependent on its formulation; however, if a preferential migration of certain components of the coating exists to a specific part of the film or the wood substrate then the dependence of the original coating to performance is limited.

Figure 4 shows a collection of micrographs of coated kahikatea weatherboards. The degree of gross penetration is clearly visible in figure 4A. All the upper rows of coating filled cells in the vicinity of the coating/substrate interface would

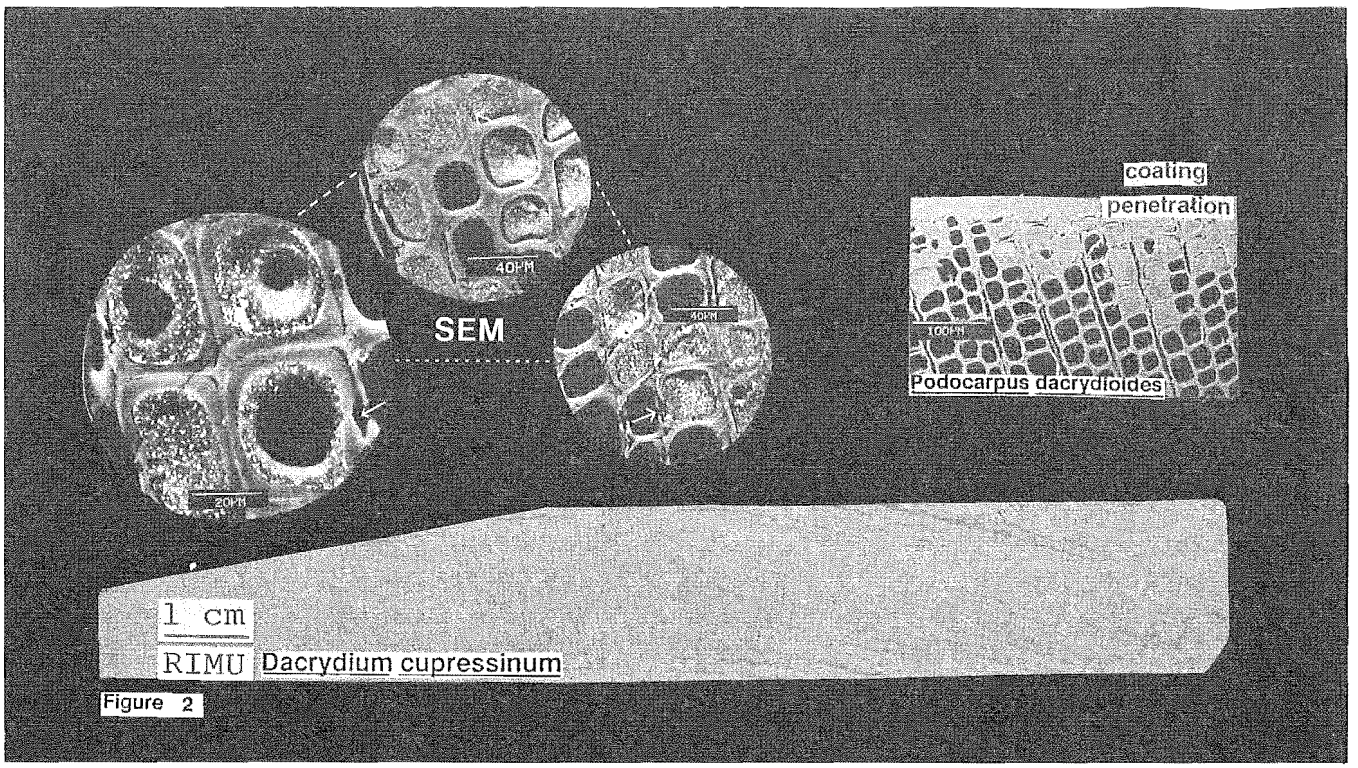

Figure 2 Cross-section through *D. cupressinum* (rimu) and *P. dacrydioides* (kahikatea) weatherboards, with highly magnified details showing paint penetration.

have either been opened by machining or emerged at some point on the board surface to produce tube-like structures with the ability to facilitate liquid conduction into the wood. The weatherboard in figure 4B was cut to expose the long tracheid cells filled with the coating. Air pockets, extractives, and other deposits present in the cell lumens at the time of coating application are attributed to have disrupted the flow of the coating.

Ultrathin sections of tracheid cells were examined at very high magnifications under the transmission electron microscope. Preparation of samples for ultrastructural studies is complex and involves staining of the cells with uranyl acetate and lead citrate for photographic purposes. Tracheid cell walls

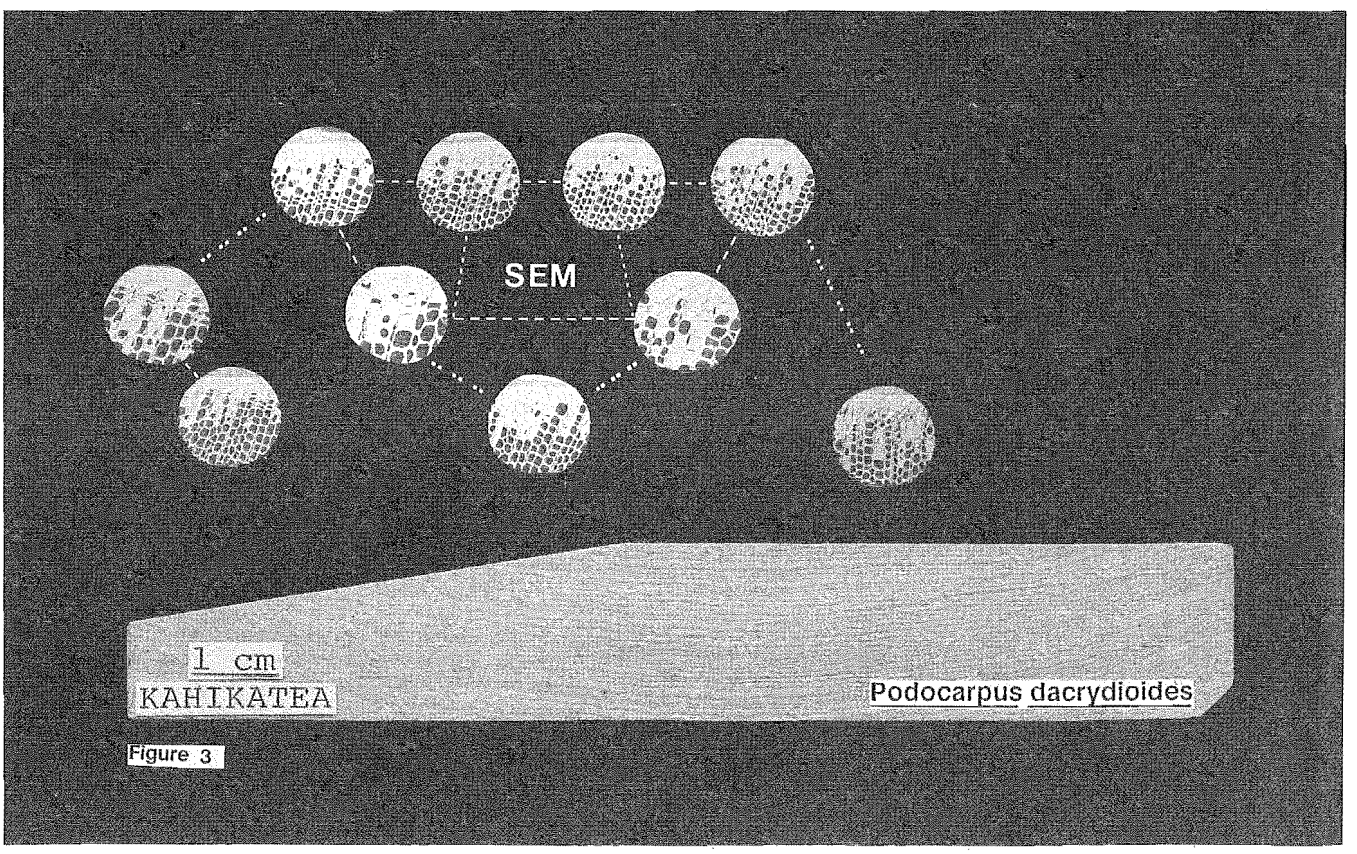

Figure 3 Cross-section through a *P. dacrydioides* (kahikatea) weatherboard; with highly magnified details of paint penetration.

Rimu, kahikatea and radiata: an electron microscope study of coated weatherboards (Dr T.M. Middleton) .....

New Zealand
Tree Grower
Tree Grower February 1992
Vol 13 No. 1 February 1992
ISSN 0111-2694

'Rays' captured with the scanning electron microscope

Dr T.M. Middleton

These incredible patterns found on the walls of the ray parenchyma cells in New Zealand *Nothofagus* (beech) wood magnified thousands of times were photographed with the aid of the Cambridge Stereoscan mark 250 scanning electron microscope. This collection of micrographs have been selected to provide viewers with a unique opportunity to marvel at the fascinating designs produced by nature.

The wood of *Nothofagus* is composed predominantly of water-conducting vessel elements, fibres and ray parenchyma cells. The radiating rays produce the spoke-like pattern on the surface of cut tree trunks. The anatomical structure of ray cells is readily distinguished under the electron microscope. The cell walls are pierced by numerous pits (arrowed). The pits are arranged along the length of the cell. Profile and frontal views are depicted here showing structural details.

By throwing a little "ray of light" onto imagination observers with an artistic eye may notice the resemblance of the fully preserved three dimensional ray cells to pastry rolls, crisp fork pricked pies and crusts! The external habit and form of beech trees growing in New Zealand has been appreciated by photographers, tourists, trampers, and tree lovers, yet hidden behind the bark is another world of beauty.

RAYS! 'Wood' you believe it!

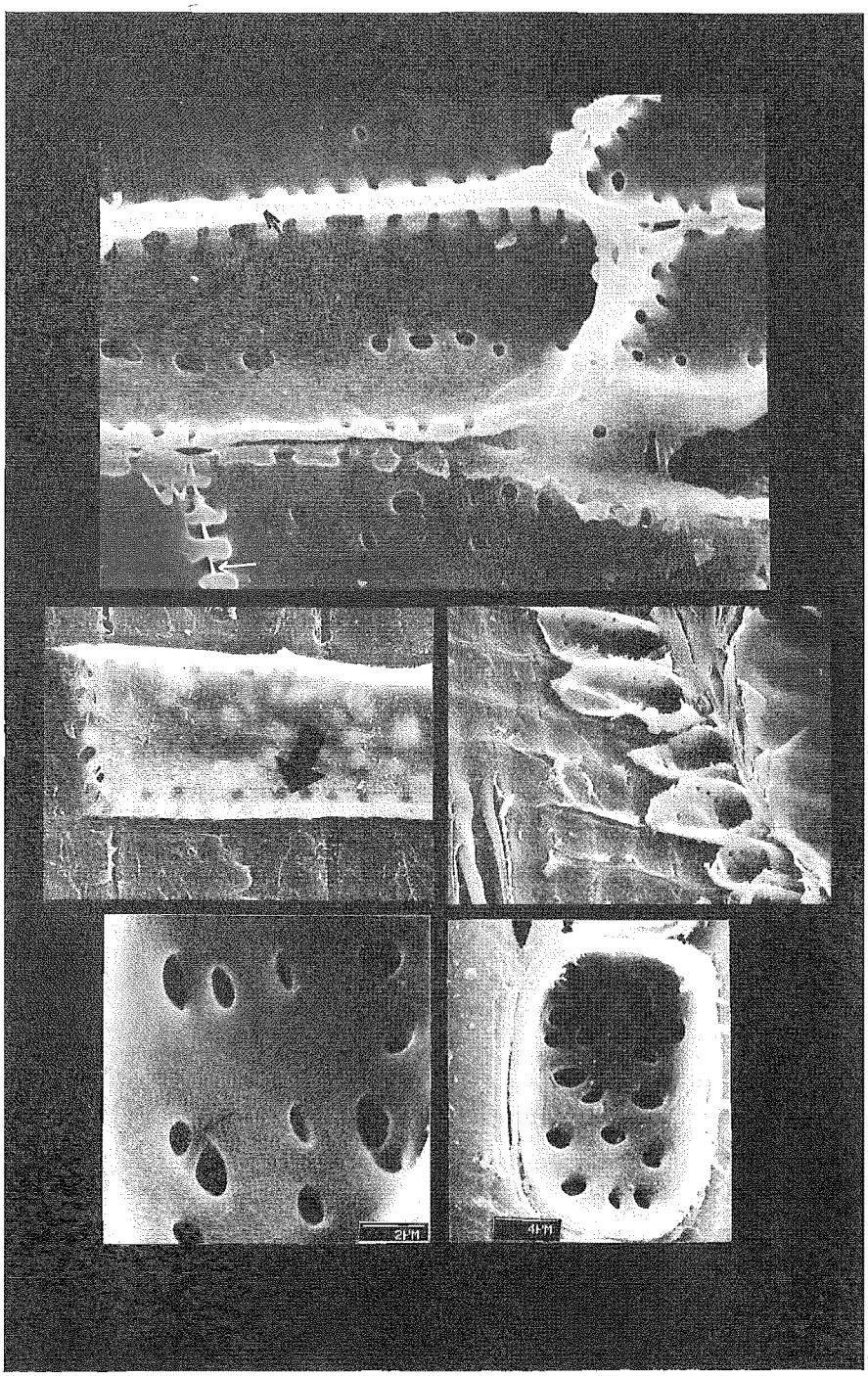

'Rays' captured with the scanning electron microscope (Dr. T.M. Middleton) .....

are multilayered and a detail of the secondary wall is depicted in figure 4C and 4D. The zoned rutile titanium particles present in the coating are very obvious as dark crystals. X-ray analysis was performed to detect key elements in the coating and their location and distribution. Figure 5 depicts a detail of two adjacent tracheid cells. Note the pit borders overarching the pit and the layered cell wall. The coating filled tracheid lumen and pit aperture is indicated by the dense distribution of titanium particles. The X-ray map in figure 5B of titanium has been superimposed onto the electron image shown in figure 5A. X-ray techniques have been successfully used to trace a number of elements present in the coating and establish the extent and localisation of certain coating components.

Conclusion

Technical improvement in both technique and instrumentation have enabled scientists to make a significant contribution to the field of wood ultrastructure. This selection of micrographs are superb examples of wood/substrate relationships as exemplified by rimu, kahikatea and radiata weatherboards and are presented here to enable readers to appreciate and marvel at the fascinating anatomy of wood.

References

Middleton, T.M. 1990 Wood structure and coatings, an electron microscope study of *Dacrydium cupressinum, Podocarpus dacrydioides* and *Pinus radiata* weatherboard substrates. Ph.D Thesis. University of Canterbury, Christchurch, N.Z. 211 p.

Orman H.R. and Reid J.S. 1946 Wood anatomy of New Zealand *Dacrydium* species. New Zealand Journal of Forestry. 5 (3): 2-7.

Patel, R.N. 1967a Wood anatomy of Podocarpaceae indigenous to New Zealand, 1 *Dacrydium*. New Zealand Journal of Botany 5: 171-184.

Patel, R.N. 1967b Wood anatomy of Podocarpaceae indigenous to New Zealand, 2 *Podocarpus*. New Zealand Journal of Botany 5: 307-321.

Patel, R.N. 1971 Anatomy of stem and root wood of *Pinus radiata* D.Don New Zealand Journal of Forestry Science. 1: (1): 37-49.

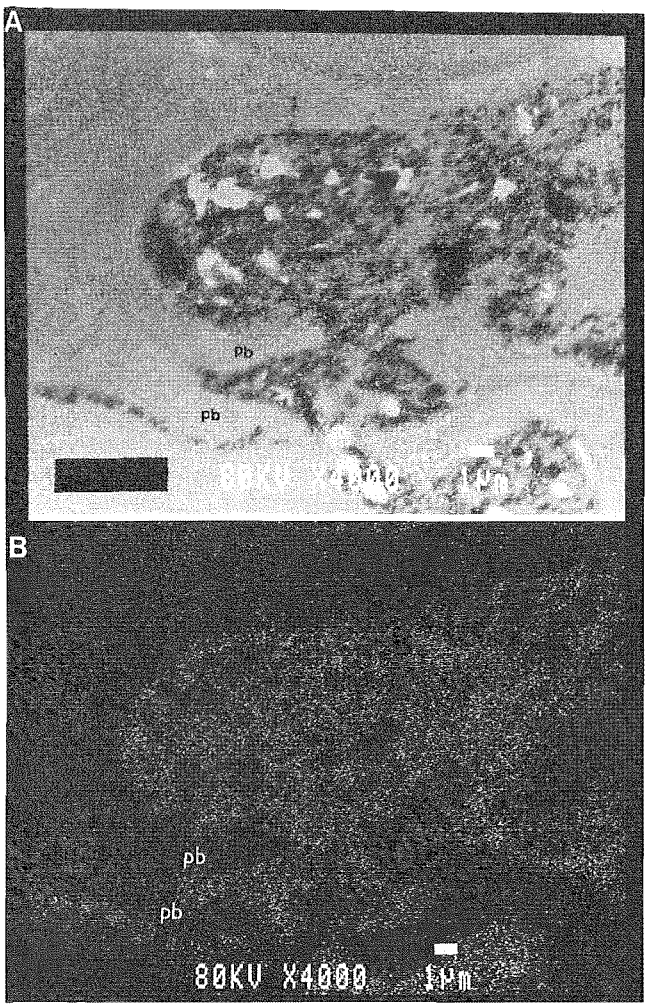

Figure 5 Transverse section of coated *P. radiata* (radiata pine) wood. 5A – Ultrathin section through intertracheid bordered pits. 5B – Corresponding element X-ray map for figure 5A.

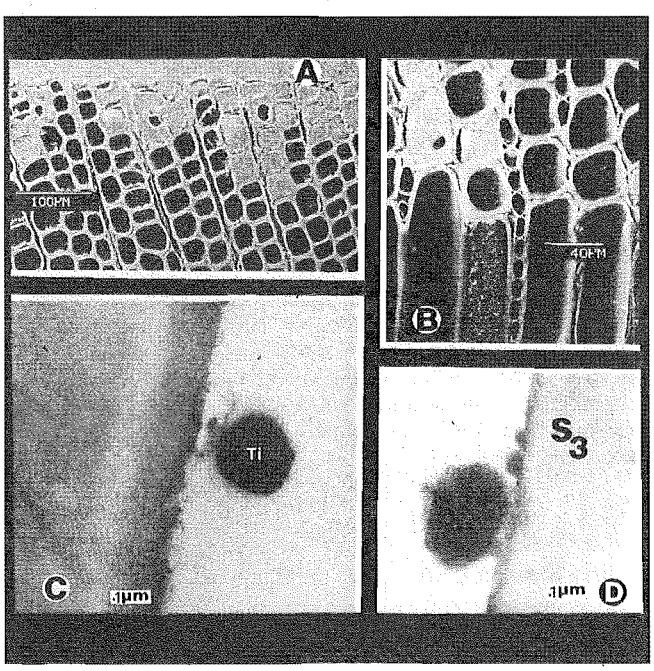

Figure 4 Transverse section of coated *P. dacrydioides* (kahikatea) wood. 4C & 4D – Ultrathin sections showing the coating / tracheid wall interface.

List of abbreviations used in the photographs

t – torus
m – margo
T – tracheid cell
R – ray cell
P – pit
S1, S2, S3 – layers of the secondary cell wall
Ti – titanium particle
pb – pit border
SEM/STEM – scanning/transmission electron microscope image
Bar scale shown in microns

VOLUME 37, NUMBER 1
MAY
1992

N.Z. INSTITUTE OF FORESTRY

ISSN 0112-9597

Wood Sci. Technol. 27:357–371 (1993)

Wood Science and Technology

Coating/wood substrate behaviour in *Dacrydium cupressinum*, *Podocarpus dacrydioides* and *Pinus radiata* weatherboards

T. M. Middleton*, Christchurch, New Zealand

Summary. An electron microscope study of the behaviour of *Dacrydium cupressinum* Lamb. (rimu), *Podocarpus dacrydioides* A. Rich. (kahikatea) and *Pinus radiata* D. Don. (radiata pine); two endemic timbers of New Zealand and one exotic timber coated with a specially formulated TiO_2 tagged long soya oil alkyd coating was made using both the scanning and transmission electron microscopes. The key elements present in the coating were detected by energy dispersive X-ray analysis and used to qualitatively trace coating penetration into wood. Quantitative information on the nature of the coating penetration was obtained by photographing the entire cross-sectional length of each weatherboard under the scanning electron microscope and counting the number of filled cells inwards from the coating interface. The performance of the coating and the three weatherboard taxa were tested using accelerated weathering techniques involving the Xenon-arc Weather-Ometer. Coated and uncoated boards were weathered for up to three thousand hours. Coating durability and substrate behaviour were qualitatively assessed microscopically. Fourier transform infrared and attenuated total reflectance methods were used to obtain quantitative information on coating performance and particular reference is made to these latter techniques.

Introduction

"... Apud nos materiae finduntur aliquae sponte; ob id architecti eas fimo inlitas siccari iubent ut adflatus non neceant..." ... (We have in our country (Rome) some timbers liable to split of their own, and architects consequently recommend that they should be smeared with dung and then dried, so as to make them proof against the action of the atmosphere.)...

[... Pliny, first century A.D.]

Pliny's works are one of our earliest written evidence that wood was not only painted for decorative purposes but that the architects recognised the need for surface protection of timber.

For centuries it has been known that wood is a naturally durable material and yet it is one of the most variable of substrates. Within a single board major variations in density are apparent.

The complex interaction of coating systems and wood substrates is environmentally, physically, chemically and biologically controlled. A greater understanding of the

* The author gratefully acknowledges Dr. B. G. Butterfield, Dr. L. M. H. Middleton, and the University Grants Committee for awarding the U.G.C. scholarship to carry out the research

topic of coatings and wood structure from the wood anatomists view was deemed necessary. Worldwide much research has been done by the paint chemistry, physics and engineering fields on coating durability and performance. In New Zealand Sinclair, Chamberlain (1959), Jessop (1965), Kerr (1965), Preston, Chittenden (1978), B.R.A.N.Z. (1978), Blackeney (1979), Jansen, Whitney (1986), Plackett, Blackeney (1987) and Hedley (1987) have contributed to the understanding of a variety of coating systems and timbers available on the local market.

Wood structure and its relationship to coatings, resins, dyes and preservatives share the common topic of penetration (Middleton, Butterfield 1990, Middleton 1991, 1992). Early works by Wardrop, Davies (1961) provided a basis for future studies on the penetration of liquids into cell walls and through pit membranes. Subsequent research by Schneider, Côté (1967), Côté, Robison (1968), Côté, Vasishth (1970), Schneider (1970, 1972, 1979, 1980), Desai, Côté (1976), Yata et al. (1978, 1983), Vinden (1984), Smith et al. (1985), and de Groot, Kuster (1986) and others have demonstrated that controversy still exists in the literature as to the existence of micro-capillaries within cell walls which are microscopically invisible. However there is consensus that gross penetration and bulk flow into lumens exists. The coating is capable of entering excised cells and fissures, but only the liquid portion of suitable molecular size can pass through the pit membranes through to adjacent cells. If the film composition remains constant throughout the entire level of penetration then its performance is dependent on its formulation, however if preferential migration of certain components of the coating into a specific part of the film or wood substrate occurs then the dependence of the original coating to performance is limited.

This study evolved from a detailed survey of coating systems on weatherboards (Middleton 1990). Unlike the other primers which exhibited an average gross penetration of 1–2 cells deep this specially formulated coating exhibited deep penetration in all three taxa examined. A detailed electron microscope study was made on *Dacrydium cupressinum* Lamb. (rimu), *Podocarpus dacrydioides* A. Rich. (kahikatea), and *Pinus radiata* D. Don. (radiata pine) weatherboards to determine their response to the solvent thinned long soya oil alkyd coating system which is normally manufactured as a clear coating for exterior use, but was tagged with rutile titanium dioxide (TiO_2) for research purposes. The wood anatomical and morphological features including measurements of cell dimensions have been described and recorded by Orman, Reid (1946), Patel (1967, 1970) and Donaldson (1983). Both *D. cupressinum* and *P. dacrydioides* have longer narrower tracheid cells compared to *P. radiata*.

The extent of coating penetration was examined. Coating durability and weatherboard performance were evaluated using accelerated weathering tests. Analytical methods including Fourier transform infrared and attenuated total reflectance were used to supplement microscopic interpretation of the results.

Materials and methods

Good quality, dressed, preservative treated, new bevel-back, flat and quarter sawn weatherboard representing the three taxa were prepared for painting as outlined in the New Zealand paint manufacturers guidelines. The long soya oil alkyd coating was tagged with TiO_2. 10% w/w of rutile TiO_2 dispersion was incorporated in the coating.

According to the paint manufacturers (pers. comm.) the dispersion contained 61.6% Du Pont Ti-Pure R902 grade which in turn contained a minimum of 91% rutile TiO_2. The chemical composition was disclosed by the manufacturers. Approximately 52% of the solid fraction consisted of 65% soya oil alkyd and 2.2' dihydroxy-4-methoxy benzophenone, cobalt naphthenate, lead naphthenate, calcium naphthenate, organic rheological modifier, soya lecithin, rutile TiO_2 and an acrylic dispersing resin comprised the remaining 14% of the solids. The volatile portion contained approximately 30% White Spirit and less than 3% toluene, xylene, 1-methoxy-2-propyl acetate and methyl ethyl ketoxime.

Qualitative bulk X-ray analysis only of the coating for the determination of key elements was determined with the Cambridge Stereoscan mark 250 scanning electron microscope (SEM) with an EDAX SW 9100/40 system and Dec PDP 11 computer with software supplied by EDAX, and also with the Jeol JSM-35 SEM fitted with a Link 290 EDAX system. Both microscopes were operated at the energy KeV most appropriate to each type of instrument to allow for positive identification of certain possible overlapping k and l characteristic lines. Graphite rod specimen holders were used to reduce the background radiation. Each analysis was performed during 60 live seconds. Intensity (CPS), background (CPS) and peak height to background (P/B) ratios were obtained. ZAF (atomic number, absorption and fluorescence) corrections were performed by computer methods. Care was taken during wood sample preparation to avoid redistribution and loss of elements by using sections of oven dried wood that was not dehydrated through any graded series of solvent.

Preparation and trimming of small blocks of weatherboards for SEM examination followed that described by Middleton (1985, 1987, 1990). Over 1,000 micrographs were studied. The backscatter detector was chosen to provide atomic number contrast as paint contains elements of higher atomic number than wood and emits more backscattered electrons (Middleton 1989).

Air dried specimens were dehydrated in two changes of 100% ethanol before infiltrating with 100% London resin (L. R. White – medium grade). The resin was either oven thermal cured at 70 °C or polymerized in a nitrogen environment. Other specimens were first air dried then oven dried for 1 hour at 70 °C and subsequently embedded directly into 100% Spurr's resin and left to polymerize at 70 °C. The embedded samples were trimmed into 'mesa' shapes on the LKB Pyramitome using glass knives. Ultra-thin sections were cut with a diamond knife on the LKB 2128 Ultrotrome iv Bromma Ultramicrotome system. The knife cutting angle was set at 3°. Ribbons of 70 nm sections were placed onto 100 mesh copper grids. Sections were stained with 1% uranyl acetate in 50% ethanol; washed in ethanol and subsequently stained in Sato's lead citrate which was prepared following Hayat's (1975) schedule. The stained sections were examined under the Jeol 1200 EX TEM operated with an accelerating voltage of 80 KeV and spot size of 2. Qualitative information of the location of certain elements present in the coating to scanning transmission mode (STEM). For this analysis unstained sections were contained in an EM-SR graphite specimen retainer in the SM-SCSH specimen holder to prevent extraneous background interference.

Methods of measuring coating contact angles followed those described by Pierce and Schoff (1988). The contact angle of 2 mm drops of coating on glass slides were measured with the aid of a camera lucida attached to an Olympus light microscope.

The Minitab and SAS packages for statistical analyses were used in conjunction with the IBM and UNISYS computer systems. Statistical analyses included analysis of variance, Duncan's new multiple range test, correlation and regression to determine whether there was any variation among the three taxa with regard to studies on coating penetration depth, tracheid file inclination angle and tracheid cell row growth direction.

Accelerated weathering tests were performed on the coating and wood substrates using the Atlas Xenon arc Weather O-meter model Ci 65 controlled irradiance exposure system. The test method used was ASTM G 26-83. The spectral irradiance selected was 0.55 W/m^2 at 340 nm when operated at 6,000 watts. Relative humidity was controlled by the use of a wet bulb depression circuit. The air temperature was set at 34 °C and conditioned water at 17 °C. Weatherboard specimens were positioned vertically on a rack and rotated at 1 ± 0.1 rpm during exposure. The cycle comprised 18 minutes continuous light and spray followed by 102 minutes light. Coated and uncoated boards were weathered for a period of 1,000 hours, 2,000 hours and 3,000 hours.

A Biorad Digilab FTS 60 was used to produce Fourier transform infrared (FTIR) spectra of unweathered and weathered coated boards. For each sample 1 mg of coating was scraped off the weatherboard and mixed with 100 mg dry potassium bromide powder and ground to a fine powder. The mixture was pressed in vacuo to produce a transparent pellet. The FTIR scans up to 100 µm in depth (Nakanishi 1962, Miller, Stage 1972, and Krishnan 1984).

The attenuated total reflectance (ATR) technique also known as multiple internal reflectance or internal reflection spectroscopy was chosen to supplement FTIR results. A Biorad Digilab FTS 60 was used. For each sample two thin 1 cm square shavings of coating were pressed against both sides of a K RS-5 crystal and clamped between rubber backed aluminum foil. A 45° crystal geometry was used and the spectra recorded at 4 cm^{-1} resolution. The ATR scans up to 5 µm in depth.

Spectrocolourimetric and spectroscopic techniques including the L* a* b* and chromaticity colour systems were used to obtain supplementary quantitative information on performance and are discussed in Middleton (1990).

Results

Figure 1 shows the EDAX spectra of the coating. The titanium peak is very obvious and according to the paint manufacturers (pers. comm.) the titanium was coated with Al_2O_3 and SiO_2 to improve coating dispersibility, performance and durability. H, C, O, Fe, Mg, and small concentrations of Ca, Pb, Co, Mn, Cl, S and N are also present in the coating, however the X-ray technique is incapable of detecting all these elements.

At 25 °C the coatings viscosity is 72 krebs units (ku) and the average contact angle of the coating with the substrate is 27 degrees compared to the viscosity of 70 ku and contact angle of 22 degrees for the solvent based alkyd primer system that was chosen for brief comparison (Middleton 1990).

Figures 2 A and B and 3 A–C depict sets of micrographs showing details of *D. cupressinum*, *P. dacrydioides* and *P. radiata* weatherboards cut to reveal depth of

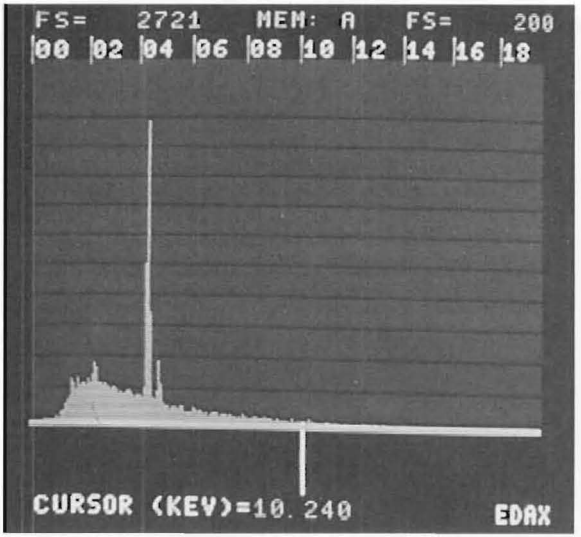

Fig. 1. EDXA spectrum of the TiO_2 tagged long soya oil alkyd coating

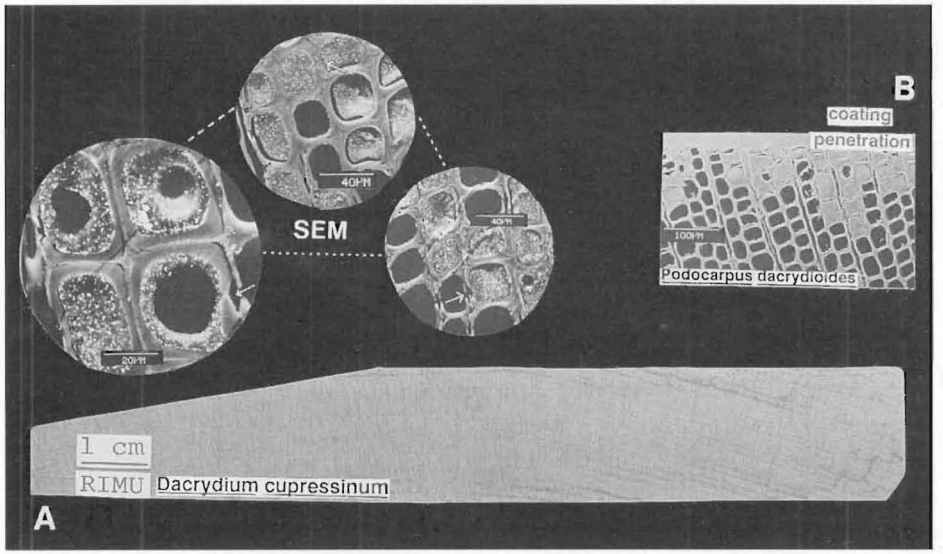

Fig. 2 A and B. Cross-section through (**A**) *D. cupressinum* and (**B**) *P. dacrydioides* weatherboards with magnified details showing coating penetration. (Pit-pairs arrowed). SEM

coating penetration. Intertracheid pitting on the radial wall are indicated by arrows. The mean gross coating penetration was 9 cells for *D. cupressinum*, 13 cells for *P. dacrydioides* and 8 cells for *P. radiata* (Middleton, ibid). Statistical analyses were also performed to determine whether the variables of coating penetration depth and tracheid cell row growth direction as measured in transverse view across the boards

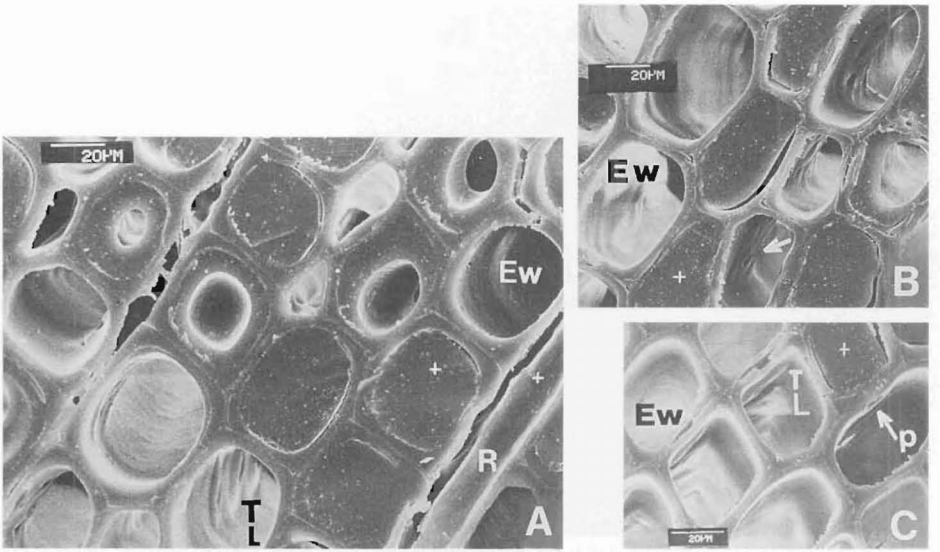

Fig. 3 A–C. Transverse views of *P. radiata* weatherboards showing coating (+) penetration into the earlywood (Ew) tracheid and ray (R) cells. Note the empty lumens (TL) and intertracheid bordered pits (P); (arrowed)

are interdependent or vary together. The correlation analysis indicated that both variables were unrelated and a test of significance for the correlation coefficients showed that the probability (PROB $> r$ under H_0: Rho = 0) was 0.03 at the 0.05 level indicating that the relationship is insignificant. Statistical analysis also indicated that the relationship between tracheid file inclination angle and tracheid cell row growth direction was insignificant for all three taxa (Middleton, ibid).

A detailed SEM study of coating/substrate behaviour confirmed statistical analyses. In contrast to the minimal gross penetration of 1–2 cells as exhibited by primers this TiO_2 tagged alkyd coating travelled into the wood of all three taxa for several millimetres. Highly magnified unstained ultra-thin sections provided evidence that the large titanium pigment particles were contained in the cell lumens. Figure 4 A shows a transverse section through coating filled tracheid and ray cells in *D. cupressinum*. An X-ray map of the Ti-k element (Fig. 4 b) was superimposed onto the electron image to confirm visual observation of titanium particle distribution. For comparison Fig. 5 A depicts an X-ray map of the Ti-k element in a tracheid in *P. radiata* coated with the primer. Bulk flow occurs through intertracheid pits whose membranes were broken by some process. Figure 5 B shows a group of titanium particles congreating along irregularities present on the S_3 layer of the tracheid secondary cell wall in *P. radiata*. The zonation pattern exhibited by titanium particles is illustrated in Fig. 6 A. It was observed that in *P. radiata* titanium particles were attracted to the warty layer (Fig. 6 B); however both *D. cupressinum* and *P. dacrydioides* lack a warty layer.

Coating penetration was deeper in the large earlywood cells than in the smaller lumens of latewood cells. Coating penetration into ray parenchyma was minimal in

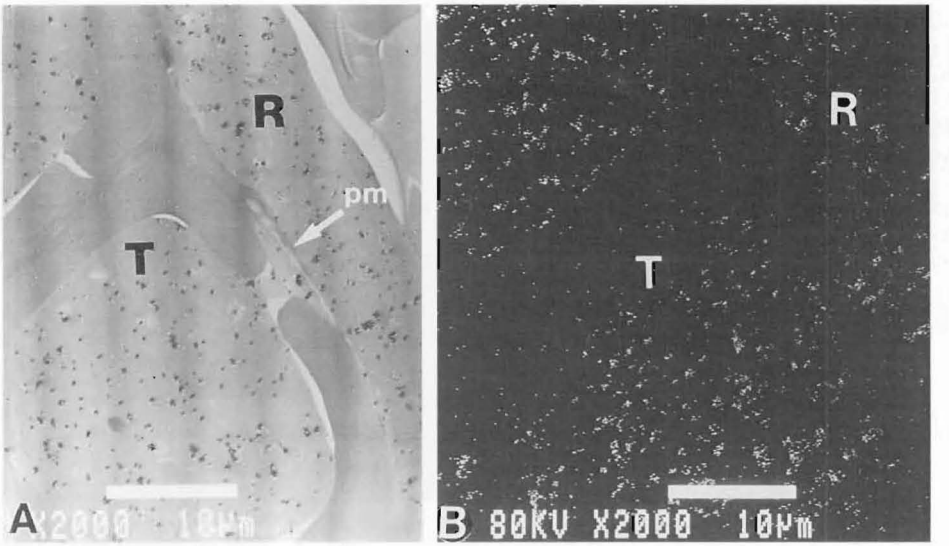

Fig. 4 A and B. **A**: Ultra-thin unstained transverse section through adjacent tracheid (T) and ray (R) cells. Note the intact pit membrane (pm) separating the coating filled cells. **B**: Corresponding EDXA element (Ti-k) X-ray map of Fig. **A**. (*D. cupressinum*)

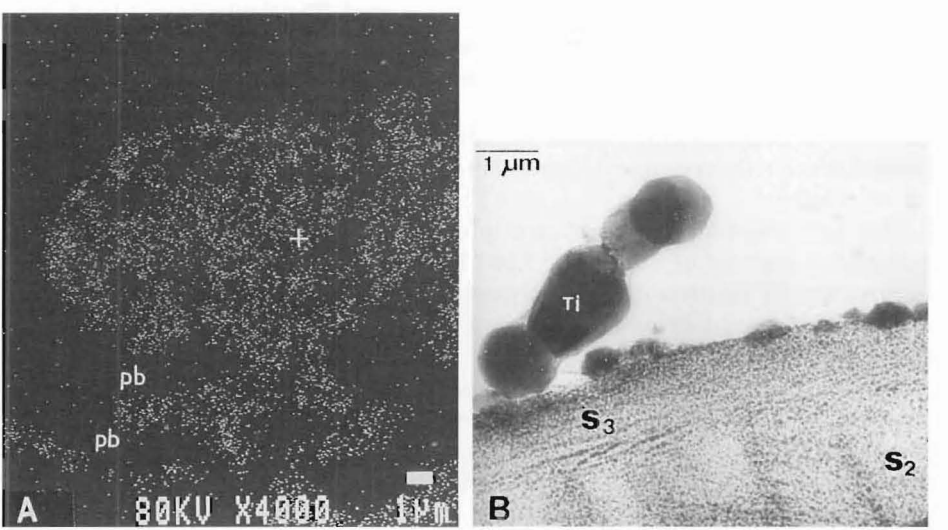

Fig. 5 A and B. **A**: EDXA element (Ti-k) X-ray map of an alkyd primer system (+) in a *P. radiata* tracheid. Note the bordered pit-pair (pb). **B**: Ultra-thin stained section showing titanium particles (Ti) at the coating/tracheid cell wall interface (*P. radiata*)

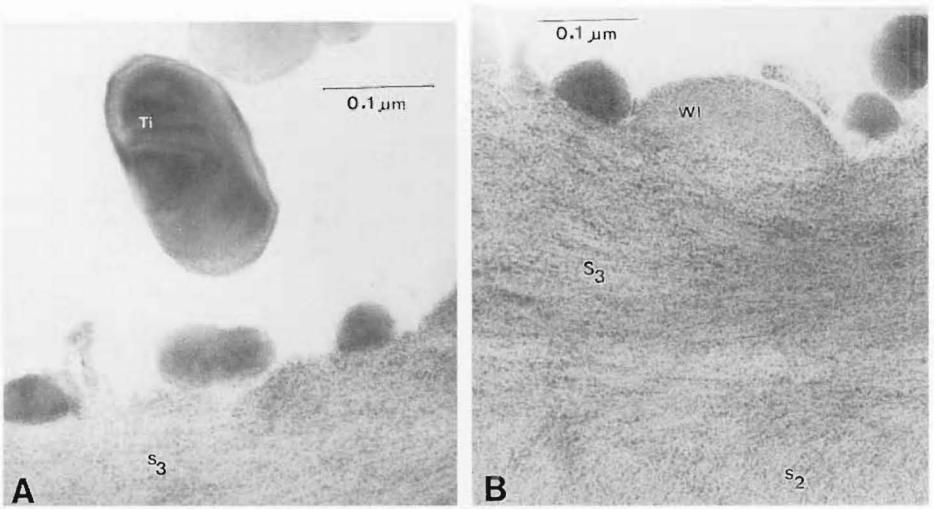

Fig. 6 A and B. Highly magnified details of coating/wood substrate behaviour at the secondary wall layer (S_3) and warty layer (wl) interface in *P. radiata*. Note the large titanium (Ti) particle exhibiting the characteristic zoning

D. cupressinum and *P. dacrydioides* compared to *P. radiata*. The rutile form of TiO_2 has a mean particle size of 0.2–0.3 µm and a refractive index of 2.71. Deposits of smaller particles lining the S_3 layer of the cell wall were also observed but were too small to be identified by the X-ray detector. These deposits appeared intact and not dragged across the section during microtoming.

The effect of accelerated weathering trials on uncoated boards representing the three taxa and on coating performance was evaluated. The results of an EDAX bulk analysis of weathered coating was compared with those obtained for unweathered coating (Middleton, ibid). The slight increase in the proportion of TiO_2 in the coating suggested by the EDAX technique is in accordance with the observed decrease in the intensity of carbonyl group peaks indicated by infrared spectra obtained for the coating which reflects incipient chemical breakdown of one of the organic component of the coating.

Infrared spectroscopy was chosen to determine whether any chemical changes occurred in the coating during the 3,000 hours weathering trials. Band position in infrared spectra are presented here as wave numbers (unit cm^{-1}). Band intensities are expressed either as transmittance or absorbance. Shifts in absorption position and changes in intensity of bands may suggest chemical structural changes, which in this study would be a result of weathering. Consultation of tables of "characteristic frequencies" (Silverstein et al. 1981) were used here to assign names to the peaks. The two regions deemed important for preliminary examination of the spectrum are the 4,000–1,300 cm^{-1} and 909–650 cm^{-1}. Characteristic 'stretching frequencies' of O–H, N–H, and C=O functional groups occur in the higher frequency portion and aromatics in the lower frequency region.

Figure 7 A and B depicts the FTIR and ATR spectra of the unweathered TiO_2 tagged long soya oil alkyd coating. During manufacture the resin is produced by

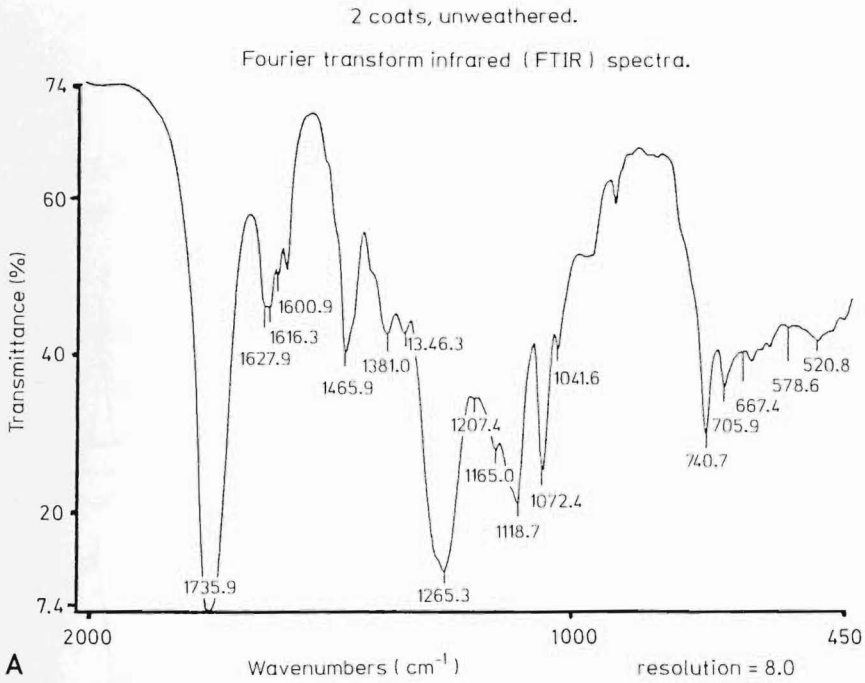

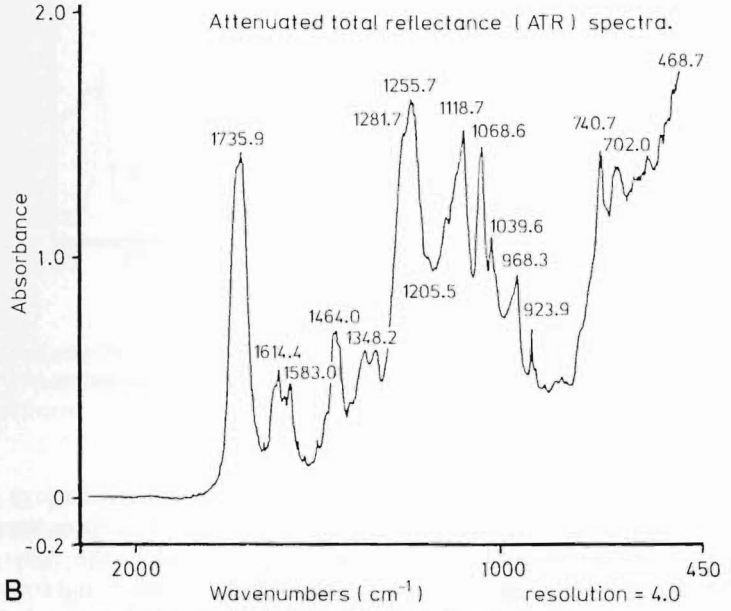

Fig. 7 A and B. Fourier transform infrared and attenuated total reflectance spectra for unweathered TiO_2 tagged long soya oil alkyd coating

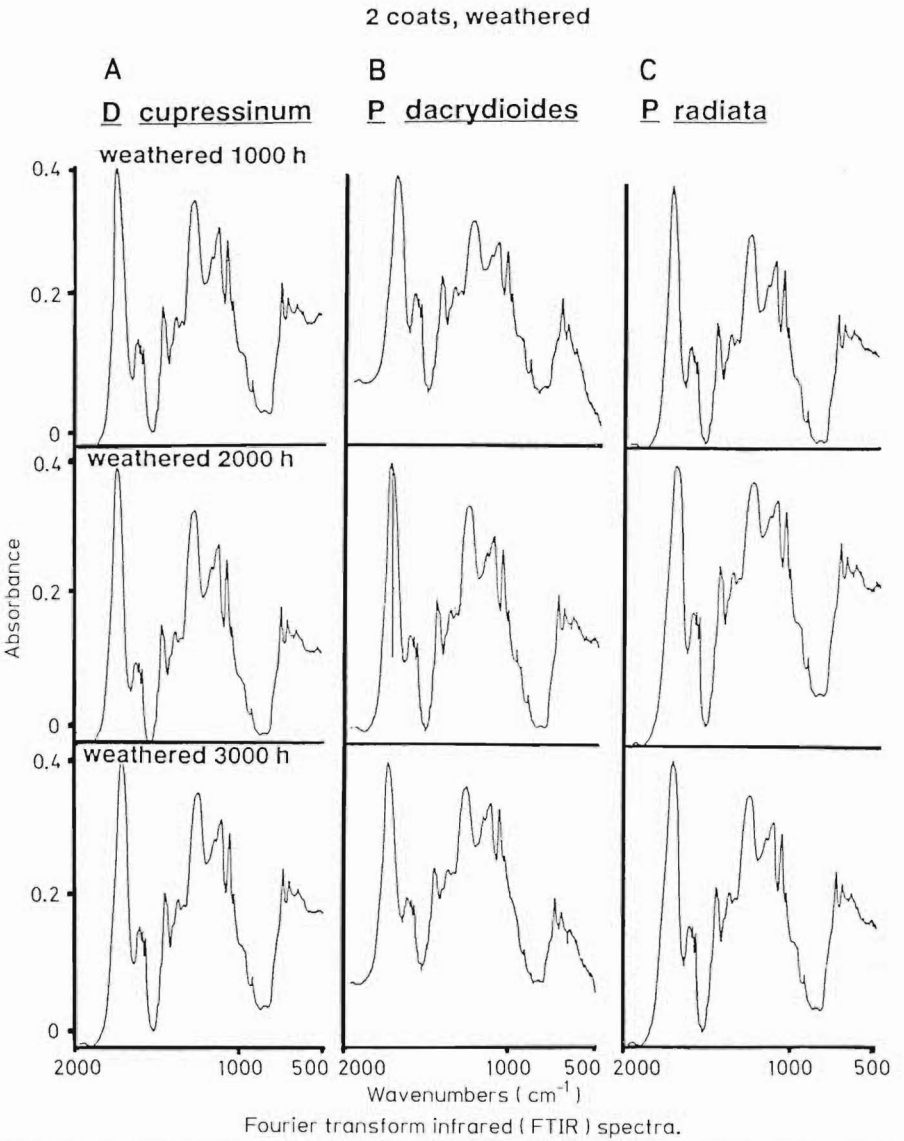

Fig. 8 A–C. Fourier transform infrared spectra for **A** *D. cupressinum*, **B** *P. dacrydioides* and **C** *P. radiata* weatherboards coated with 2 coats of TiO_2 tagged long soya oil alkyd coating and weathered on the Xenon-arc Weather-Ometer

converting the soya oil to the monoglyceride form by the addition of glycerol to soya oil and then polymerising the monoglyceride with phthalic anhydride to form the alkyd. The standard spectrum for rutile TiO_2 echoes that observed in the 700–400 cm^{-1} region. The characteristic carbonyl band occurs near 1725 cm^{-1} and it is noted that in the unweathered coating the FTIR spectrum has a strong band in the carbonyl region at 1735.9 cm^{-1}. The band peaking at 1616.3 cm^{-1} may be assigned

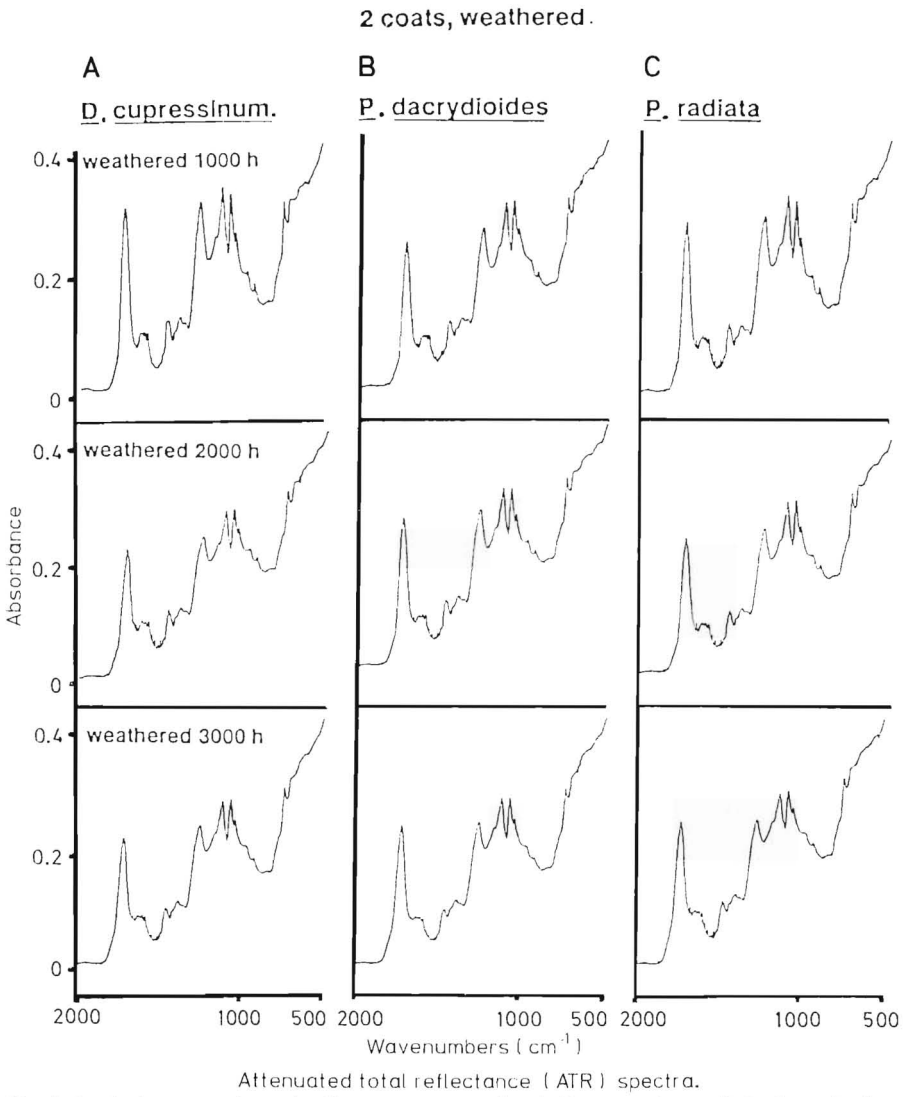

Fig. 9 A–C. Attenuated total reflectance spectra for **A** *D. cupressinum*, **B** *P. dacrydioides* and **C** *P. radiata* weatherboards coated with 2 coats of TiO_2 tagged long soya oil alkyd coating and weathered on the Xenon-arc Weather-Ometer

to C–H stretching frequencies. The bands peaking at 1465.9 cm^{-1} to 1346.3 cm^{-1} are of doubtful value for diagnostic purposes, however it is noted that the band peaking at 1465.9 cm^{-1} may be due to CH_2 deformations. The band of high intensity at 1265.3 cm^{-1} can probably be assigned to the C–O stretching frequency, while the band peaking at 1118.7 cm^{-1} is probably as C–C stretching frequency. Numerous bands between 600–400 cm^{-1} are indicative of the aromatics. Figures 8 A–C depict

FTIR spectra of the coating after 1,000 hours, 2,000 hours and 3,000 hours weathering, and show that after 3,000 hours the spectral patterns are essentially very similar. However slight trends not detected by the FTIR technique are visible in Figures 9 A–C because the ATR technique is able to detect surface changes. Peak height of certain groups such as the carbonyl band at 1735.9 cm^{-1} show a decrease in intensity and the rutile titanium peak a corresponding increase with weathering.

Discussion

The TiO_2 tagged long soya oil alkyd coating exhibited deeper penetration than primers. In most cases, particularly exemplified by the primer systems, coating penetration is limited to 1–2 cells deep which were either opened by machining or to that length of tracheid which due to the slope of the grain aided entry. All the upper rows of cell lumens observed filled with coating would have emerged at some point on the surface of the substrate to form tubes which facilitated the conduction of liquids. Feist (1984) observed improved performance of coatings on rough sawn timber which provides a greater surface area for the coating or finish and better mechanical adhesion. The TiO_2 tagged alkyd coating studied here was locked deep into the wood substrate of all three taxa, and behaved more like a penetrating finish than solely a film former. Normally the coating is manufactured as a clear coating so exhibited many of the attributes of clear coatings.

Quarter sawn weatherboards are more stable than flat sawn boards because timber shrinks less in the radial direction. The earlywood bands in *D. cupressinum* and *P. dacrydioides* are indistinct compared to those in *P. radiata* which is also more prone to distortion during machining. Most movement occurs at the growthring boundary and this is most obvious in *P. radiata*. Harris (1981) staed that in gymnosperms approx. 95% of the total volume of wood consists of tracheids.

Microscopic examination suggested that the slope of tracheid files relative to the board surface and coating interface, cell row growth direction, and board mounting could be important factors influencing coating behaviour. Statistical analyses however, showed that although significant differences were present among taxa the correlation between these variables was insignificant. Coating viscosity and coating contact angle alone were not statistically significant.

Coating behaviour is a result of a complex interaction of a range of variables (Neville 1963; Zicherman 1972; Underhaug et al. 1983). Blackeney (1979) deduced that the denser the wood, the poorer the paintability and that viscosity alone did not control paintability and substrate penetration. There is diverse opinion whether treated timber is amenable to painting. Plackett and Blackeney (1987) found that boron salts do not present painting problems and that light organic solvent preservative (LOSP) treated wood could be painted. The rate of curing may affect coating movement within cell voids soya oil is a slow drying oil on its own. On curing the soya alkyd present in the coating undergoes a complex oxidation reaction which is catalized by the metal naphthenate driers. The percentage of rutile TiO_2 was greater in the primer systems than in the TiO_2 tagged alkyd coating, and backscattered electron images showed that the texture of the cured primers were much coarser than the TiO_2 tagged alkyd coating. Preferentially migration of certain microscopically visible coat-

ing components such as the titanium particles to a specific part of the coating film or into the substrate voids and along cell wall irregularities is demonstrated. It is not yet possible to examine the paint in liquid form directly with the electron microscope to determine whether clusters of pigments seen in the cured form were also present in the liquid form or whether they only developed during drying.

As part of a research programme to produce water-borne clear coatings for wood Vasishth (1983) discovered that for cell wall penetration to occur it was necessary to select a polymer that had a high proportion of molecules with low molecular weight below 1,000 because molecules greater than this either remained on the cell lumen or formed a film. Drewe (1986) in a study of coating behaviour on Australian timbers deduced that uniformity of paint composition is changed by a filtration effect which although minor prevented certain pigments from entering the cells.

Artificial accelerated weathering tests demonstrated the coatings success in terms of performance and durability. The two main ultraviolet radiation induced mechanisms which contributed to coating breakdown are photochemical degradation and photocatalytic degradation. In oil modified alkyds the aromatic part of the alkyd is rapidly degraded by radiation below 250 nm but in radiation above 295 nm then the aliphatic components are more susceptible to degradation (Blakey 1985). The ultraviolet stabilizer incorporated into this TiO_2 tagged alkyd coating was 2.2'-dihydroxy-4-methoxy benzophenone. Degradation resulted in loss of gloss as the pigment particles are gradually exposed at the surface of the film. Subtle changes in gloss were quantitatively measured.

FTIR and ATR spectroscopic techniques showed that the changes detected in the intensities of the major functional groups present in the coating were very minor. EDXA techniques confirmed these results.

To conclude the TiO_2 tagged alkyd coating exhibited excellent penetration ability and performed well in the standard weathering tests, but the high cost of producing this coating for exterior use will restrict its commercial viability.

References

ASTM 1987: Annual book of ASTM standards: General methods and instrumentation. U.S.A. ASTM 14.02

Bauch, J.; Liese, W.; Schultze, R. 1972: The morphological variability of the bordered pit membranes in Gymnosperms. Wood Sci. Technol. 6: 165–184

Blackeney, M. R. 1979: Timber and its relationship to the Paint Industry. N.Z. Painter & Decorator. 14–24

Blakey, R. R. 1985: Evaluation of paint durability; natural and accelerated. Prog. in Organic Coatings. 13: 279–296

B.R.A.N.Z. 1978: Wood primers. Building Info. Bull. 208 p

Côté, W. A. 1981: Ultrastructure – critical domain for wood behaviour: Its origins, current concepts, future potential. Wood Sci. Technol. 15: 1–29

Côté, W. A.; Robison, R. G. 1968: A comparative study of wood; wood coating interactions using incident fluorescence and transmitted microscopy. J. Paint Technol. 40 (525): 427–432

Côté, A. A.; Vasishth, R. C. 1970: Light and electron microscopic studies of wood/wood coating systems. Proc. Xth Fatipec Cong. Montreaux, Switzerland, 57–65

de Groot, R.; Kuster, T. A. 1986: SEM, X-ray microanalysis of tracheid cell walls in Southern Pine sapwood treated with water dispersible pentachloro phenol. Wood Fiber Sci. 18 (1): 58–67

Desai, R. L.; Côté, W. A. 1976: Use of SEM/EDXA in characterizing water-based surface treatments for wood. J. Coating Technol. 48 (614): 33–37

Donaldson, L. A. 1983: Anatomy of root wood in Araucariaceae and some Podocarpaceae indigenous to New Zealand. N.Z.J. Bot. 21: 221–227

Drewe, R. 1986: Australian timbers and their inherent coating problems. Surface Coatings Aust. 27th Convention N.S.W. 26–27

Feist, W. C.; Hon, D. N. S. 1984: Chemistry of weathering and protection. In: Chemistry of Solid Wood. Advances in Chemistry Series 207. Rowell, E. (ed.). Am. Chem. Soc. 401–451, Washington D.C.

Harris, J. M. 1981: Wood quality of radiata pine. Appita 35 (3): 211–215

Hayat, M. A. 1975: Positive staining for electron microscopy. New York: van Nostrand Reinhold Co.

Hedley, M. E. 1987: Surface coating for timber. N.Z. Eng. 42 (7): 65–66

Jansen, M. L.; Whitney, R. S. 1986: Performance testing of wood primers. J.O.C.C.A. 69 (5): 117–128

Jessop, A. S. 1965: Prospects in terms of service life for (a) pigmented coatings, (b) colour coatings. Paint and Protection Coatings for Wood Symposium. N.Z.T.D.A. 1–10

Kerr, C. J. 1965: The paint timber system with special reference to weatherboard – Paint and protective coatings for wood symposium. Auckland, N.Z.T.D.A.

Krishnan, K. 1984: Different accessories – Main applications and handling techniques. In: Fourier Transform Spectroscopy. Theophanides, T. (ed.). pp. 139–158 Reidel Pub. Co.

Middleton, T. M. 1985: Vessels of stem wood in New Zealand (*Nothofagus*). M.Sc. (First Class Honours) Thesis. University of Canterbury, Christchurch, New Zealand, 203 p.

Middleton, T. M. 1987: Aggregate rays in New Zealand *Nothofagus* Blume. (Fagaceae) stem wood and their influence on vessel distribution. IAWA Bull. n.s. 8 (1): 53–57

Middleton, T. M. 1989: Modification of latex paint infusion technique for the determination of vessel-length in hardwoods. Wood Sci. Technol. 23: 299–302

Middleton, T. M.; Butterfield, B. G. 1990: Vessel-length distribution in the stem of three New Zealand species of *Nothofagus*. Wood Sci. Technol. 24: 17–22

Middleton, T. M. 1990: Wood structure and coatings – An electron microscope study of *Dacrydium cupressinum, Podocarpus dacrydioides* and *Pinus radiata* weatherboard substrates. Ph.D. Thesis. University of Canterbury, Christchurch, New Zealand, 211 p.

Middleton, T. M. 1991: Wood substrates and coatings under the electron microscope. N.Z. Painter & Decorator. 44 (11): 16–17, Nov./Dec.

Middleton, T. M. 1992: Timber and paint. Terra Nova 15: 51–52, April

Middleton, T. M. 1992: Rimu, kahikatea and radiata – an electron microscope study of coated weatherboards. N.Z. Forestry. 37 (1): 17–19, May

Miller, R. G.; Stage, B. C. 1972: Laboratory methods in infrared spectroscopy. 2nd ed. New York: Heyden & Son Ltd.

Nakanishi, K. 1962: Infrared absorption spectroscopy – practical. San Francisco: Holden Day Inc.

Neville, G. H. J. 1963: Some observations on the weathering of titanium dioxide pigment paint films. J.O.C.C.A. 46 (9): 753–778

Orman, H. R.; Reid, J. S. 1946: Wood anatomy of New Zealand *Dacrydium* species. N.Z.J. For. 5 (3): 2–7

Patel, R. N. 1967: Wood anatomy of Podocarpaceae indigenous to New Zealand. (1) *Dacrydium*, N.Z.J. Bot. 5 (3): 171–184

Patel, R. N. 1967: Wood anatomy of Podocarpaceae indigenous to New Zealand. (2) *Podocarpus*, N.Z.J. Bot. 5 (3): 307–321

Patel, R. N. 1970: Anatomy of stem and root wood of *Pinus radiata*, D. Don. N.Z.J. For. Sci. 1 (1): 37–49

Pierce, P. E.; Schoff, C. K. 1988: Coating film defects. Fed. Soc. Coating Technol., Philadelphia

Plackett, D. V.; Blackeney, M. 1987: Exterior surface finishes for timber. Trees & Timber, Wood Properties & Uses. N.Z.M.O.F. 7: 1–8

Pliny (Gaius Plinius Secundus)-Pliny the elder first century A. D. Natural History. Vols 1V & 1X Books 16 & 35 (Trans. H. Rackham) Massachusetts, Harvard Univ. Press

Preston, A. F.; Chittenden, C. M. 1978: Accelerated tests of weather resistant natural finishes for *Pinus radiata*. J. Coating Technol. 50 (637): 59–61
Schneider, M. H. 1970: Coating penetration into wood substance studied with electron microscopy using replica techniques. J. Paint Technol. 42 (547): 457–460
Schneider, M. H. 1972: Wood weatherboard interactions – a review. J. Paint Technol. 44 (504): 108–110
Schneider, M. H. 1979: Scanning electron microscope study of a coating component deposited from solution into wood. J.O.C.C.A. 62: 441–444
Schneider, M. H. 1980: Microscope distribution of linseed oil after application to wood surface. J. Coating Technol. 52 (665): 64–67
Schneider, M. H.; Côté, W. A. 1967: Studies of wood and coating interactions using fluorescence microscopy and pyrolysis gas-liquid chromatography. J. Paint Technol. 39 (511): 465–471
Silverstein, R. M.; Clayton-Bassler, G.; Morrill, T. C. 1981: Spectrometric identification of organic compounds. 4th ed. New York: John Wiley & Sons.
Sinclair, R. M.; Chamberlain, G. 1959: Paint durability on radiata pine. N.Z. D.S.I.R. publication 1–4
Smith, W. B.; Côté, W. A.; Siau, J. F.; Vasishth, R. C. 1988: Study of intersections between wood and water-soluble organic solvents. J. Coating Technol. 57 (727): 83–90
Smith, W. B.; Côté, W. A.; Siau, J. F.; Vasishth, R. C. 1988: Interactions between water-borne polymer systems and the wood cell wall. J. Coating Technol. 57 (729): 27–35
Underhaug, A.; Lund, T. J.; Kleive, K. 1983: Wood protection – the interaction between substrates and product and the influence on durability. J.O.C.C.A. 16 (1): 345–350
Vasishth, R. C. 1983: Importance of depositing polymers in wood cells for wood treatment. Proc. Am. Wood Pres. Assoc. 79th Annual Meeting 79: 129–136
Vinden, P. 1984: The effect of raw material variables on preservative treatment of wood by diffusion processes. J. Inst. Wood Sci. 10: 31–41
Wardrop, A. B.; Davies, G. W. 1961: Morphological factors relating to the penetration of liquids into wood. Holzforschung 15: 129–144
Yata, S.; Mukuda, J.; Kajita, H. 1978: Morphological studies on the movement of substances into the cell wall of wood. I: Methods for microscopic detection of diffusing substances in the cell wall. Mokuzai Gakkaishi 241: 591–597
Yata, S.; Nishimoto, K. 1983: Application of SEM-EDXA technique to the study of metal distribution in preservative treated wood. Wood Res. 69: 71–79
Zicherman, J. B.; Thomas, R. J. 1972: Scanning electron microscopy of weathered coatings on wood. J. Paint Technol. 44: 88–94

(Received November 28, 1991)

Dr. T. M. Middleton, B.A., B.Sc., M.Sc. (First Class Honours), Ph.D.
Wood Science Research Laboratory
Department of Plant and Microbial Sciences
University of Canterbury
Private Bag, Christchurch, Canterbury
New Zealand